

SYNTHESIS OF CHARGED RECEPTORS SELECTIVE FOR ANIONIC COMPONENTS OF
BACTERIAL MEMBRANES

A Dissertation by

Manjula B. Koralegedara

Master of Science, Wichita State University, 2008

Bachelor of Science, University of Peradeniya, 2000

Submitted to the Department of Chemistry
and the Faculty of the Graduate School of
Wichita State University
In Partial Fulfillment of
the Requirements for the Degree of
Doctor of Philosophy

August 2010

© Copyright 2010 by Manjula B.K.Koralegedara
All Rights Reserved

SYNTHESIS OF CHARGED RECEPTORS SELECTIVE FOR ANIONIC COMPONENTS OF
BACTERIAL MEMBRANES

The following faculty have examined the final copy of this dissertation for form and content, and recommended that it be accepted in partial fulfillment of the requirement for the degree of Doctor of Philosophy with a major in Chemistry.

Dennis H. Burns, Committee Chair

David M. Eichhorn, Committee member

Erach Talaty, Committee Member

William Groutas, Committee Member

William Hendry, Committee member

Accepted for the Fairmount College of Liberal Arts and Sciences

William D. Bischoff, Dean

Accepted for the Graduate School

J. David McDonald, Dean

DEDICATION

This dissertation is lovingly dedicated to my parents, who have raised me to be the person I am today.

ACKNOWLEDGEMENTS

I would like to express my gratitude to my advisor, Dr. Dennis Burns, for his support, patience, and encouragement throughout my graduate studies. His technical and editorial advice was essential to the completion of this dissertation and has taught me innumerable lessons and insights on the workings of academic research in general.

I am pleased to thank my committee members Dr. Talaty, Dr. Wimalasena, Dr. Groutas, Dr. Eichhorn and Dr. W. Hendry for their much needed guidance and support any time. Dr. Eichhorn, and Mr. John Bullinger from Wichita state university get my special thanks for X-ray crystallographic analysis.

Dr. Kevin Langenwalter and Amanda, thank you very much for your friendship and willingness to lend a hand whenever I needed it.

I owe my sincere gratitude to all my teachers who provided me the foundation for my education.

My parents, my brothers especially Tissa and their families receive my deepest gratitude for their faith in me and always encouraging me to finish this work. I would like to thank my little son Oshada, for being so patient with me and loving me, even at the times I was not the nicest mom in the world. His smile made me want to complete this work. Finally, and most importantly, I would like to thank my husband Ganganath. His support, encouragement, quiet patience, understanding and love during the past few years were undeniably what made this dissertation possible.

ABSTRACT

A receptor able to selectively bind a phosphatidylglycerol head group of a bacterial membrane phospholipid, PPG is an attractive synthetic target as a modular component of an antimicrobial therapeutic. The major challenge to the preparation of such receptors, able to exclusively recognize this bacterial membrane component, is to create a binding motif that will complex a phosphorus anion, along with hydroxyl functionality, strongly and selectively in an aqueous environment. This study reports the synthesis and characterization of two families of charged hydrogen-bonding receptors. The first family of receptors contains different binding pocket sizes to accommodate the phosphate head group of the PPG anion while the second family of receptors contains multiple binding domains for the said phosphate head group and the glycerol hydroxyl functionality from the PPG. Following the synthesis and purification, the receptors were subjected to binding studies with inorganic dihydrogenphosphate anions and phosphatidylglycerol anions monitored with both proton NMR spectroscopy and isothermal titration calorimetry to reveal the binding stoichiometry and binding thermodynamics between each receptor and the anion.

TABLE OF CONTENTS

Chapter	Page
1. INTRODUCTION.....	1
2. SYNTHESSES.....	10
2.1 Synthesis of the First Charged Receptors.....	10
2.2 Synthesis of the Control Receptors.....	34
2.3 Synthesis of the Fully Functionalized Charged Receptors.....	45
3. ANION BINDING STUDIES.....	49
3.1 ¹ H NMR Studies of Control Receptors with Phosphate Anion.....	51
3.2 ITC Titrations of Control Receptors with Phosphate Anion.....	66
3.3 ¹ H NMR and ITC Studies of Selected Control Receptors with PPG Anion	73
3.4 ¹ H NMR and ITC Studies of the Functionalized Receptors with PPG Anion.....	79
4. EXPERIMENTAL- MATERIALS AND PROCEDURES.....	84
BIBLIOGRAPHY.....	107
APPENDIX.....	112
A. Supplemental Material.....	113

LIST OF TABLES

Table	Page
1. Results of the Ether Linkage Reaction with the use of NaH as the Base.....	20
2. Results of the Ether Linkage Reaction with the use of KOH as the Base.....	22
3. Results of the Ether Linkage Reaction with the use Of K ₂ CO ₃ as the Base.....	24
4. Reductive Amination of Benzaldehyde with Diamines.....	28
5. Reductive Amination of the Compound 9 with Hexane-1,6-Diamine.....	31
6. Yields of the Second Alkyl Linkage Reaction with the Control Receptors.....	38
7. Charged Control Receptors Synthesized and their Corresponding Yields.....	42
8. Yields of the Receptors With N=5.....	44
9. Results of ¹ H NMR Studies of Control Receptors with H ₂ PO ₄ ⁻ Anion.....	64
10. ITC Results of Control Receptors with H ₂ PO ₄ ⁻ Anion at 30°C in DMSO.....	72
11. ¹ H NMR Spectroscopic Results of the Selected Control Receptors with PPG Anion at 40°C in DMF.....	77
12. ITC Titration Results of the Selected Control Receptors with PPG Anion at 40°C in DMF.....	78
13. Crystallographic data table	175

LIST OF FIGURES

Figure	Page
1. The first anion receptor reported in late 1960's, the alkyl linkers varied from 7 to 10 methylene groups while n=9 showed the highest affinity for Cl ⁻ ions.....	2
2. Receptors reported in 1970's which showed selectivity based on size.....	3
3. Receptor selective for linear azide anion.....	3
4. Cage-like receptors which bound the anions by electrostatic interactions.....	4
5. The first amide-based cyclophane receptor reported.....	4
6. Acyclic tripodal receptors selective for dihydrogen phosphate anions.....	5
7. Interaction of the Zn coordination complex with the anionic phosphate head group of the phospholipid [12].....	7
8. Examples of <i>switterionic</i> phospholipids found in eukaryotic cell membranes. A: a species of the phosphoglyceride type, B: a species of sphingolipid type. R is a long chain hydrocarbon.....	8
9. An example of an <i>anionic</i> phosphatidylglycerol molecule found in prokaryotic cell membranes.....	8
10. Structure of the proposed charged receptor(s).....	9
11. Structure of the proposed charged receptor molecule(s).....	10
12. Products obtained from the coupling reaction between compound 7 and 1,3-dibromopropane.....	14
13. Products of duff reaction with compound 3	15

LIST OF FIGURES (continued)

Figure	Page
14. TFA ester switching positions between the phenol hydroxyl and the propyl hydroxyl groups.....	17
15. Structure of the compound 24	18
16. Structure of the compound 31	27
17. Structure of the control receptor system.....	34
18. X-ray crystal structure of the complex 45 with BF_4^- anions.....	40
19. X-ray crystal structure of the complex 45 with two PF_6^- anions.....	41
20. Structures of the compounds 51-56	43
21. Proposed functionalized amide receptors.....	45
22. Synthesis of the compound 60 and 61	46
23. Control receptors with n=3.....	47
24. Structure of the fully functionalized receptor 57a	48
25. Structures of compounds 62-64	51
26. Job plot of 49 - H_2PO_4^- anion complex in DMSO-d_6 at 30°C	52
27. ^1H NMR titration curve of 49 with H_2PO_4^- anion in DMSO-d_6 at 30°C	52
28. Job plot of 50 - H_2PO_4^- complex in DMSO-d_6 at 30°C	53
29. ^1H NMR titration curve of 50 with H_2PO_4^- in DMSO-d_6 at 30°C	54
30. Control receptors with n=4.....	55
31. Job plot of 45 - H_2PO_4^- complex in DMSO-d_6 at 30°C	56
32. ^1H NMR titration curve of 45 with H_2PO_4^- in DMSO-d_6 at 30°C	56

LIST OF FIGURES (continued)

Figure	Page
33. The x-ray crystal structure of the 45 - H_2PO_4^- complex.....	57
34. Job plot of 46 - H_2PO_4^- complex in DMSO- d_6 at 30°C	58
35. ^1H NMR titration curve of 46 with H_2PO_4^- in DMSO- d_6 at 30°C	58
36. Job plot of 47 - H_2PO_4^- complex in DMSO- d_6 at 30°C showing 1:1 binding.....	59
37. ^1H NMR titration curve of 47 with H_2PO_4^- in DMSO- d_6 at 30°C	59
38. Control receptors with $n=5$	61
39. ^1H -NMR Job plot of 54 - H_2PO_4^- complex in DMSO- d_6 at 30°C	61
40. ^1H NMR titration curve of 54 with H_2PO_4^- in DMSO- d_6 at 30°C	62
41. ^1H NMR Job plot of 56 - H_2PO_4^- complex in DMSO- d_6 at 30°C	63
42. ^1H NMR titration curve of 54 with H_2PO_4^- in DMSO- d_6 at 30°C	63
43. ITC curve of receptor 49 with H_2PO_4^- at 30°C in DMSO.....	66
44. ITC curve of the receptor 50 with H_2PO_4^- at 30°C in DMSO.....	67
45. ITC curve of receptor 45 with H_2PO_4^- at 30°C in DMSO.....	68
46. ITC curve of the receptor 46 with H_2PO_4^- at 30°C in DMSO.....	69
47. ITC curve of the receptor 47 with H_2PO_4^- at 30°C in DMSO.....	70
48. ITC curve of the receptor 54 with H_2PO_4^- at 30°C in DMSO.....	71
49. Job plot of 47 – PPG anion complex in DMF- d_7 at 40°C	74
50. ^1H NMR titration curve of 47 with PPG anion in DMF- d_7 at 40°C	74
51. ^1H NMR titration curve of 54 with PPG anion in DMF- d_7 at 40°C	75
52. Job plot of 46 – PPG anion complex in DMF- d_7 at 40°C	76

LIST OF FIGURES (continued)

Figure	Page
53. ITC titration curves of the receptor 47 and 54 respectively with PPG anion at 40°C in DMF	77
54. Functionalized receptors 57a and 57b	79
55. Job plot of 57a – PPG anion complex in DMF-d ₇ at 40°C.....	80
56. Receptor 57a showing possible intra-molecular hydrogen bonding.....	80
57. ¹ H NMR titration curve of 57a with PPG anion in DMF-d ₇ at 40°C.....	81
58. ITC binding isotherm of 57a with PPG anion in DMF at 40°C.....	82
59. ¹ H NMR (top) and ¹³ C NMR (bottom) data for compound 33	114
60. GC-MS (top) and ESI-MS (bottom) data for compound 33	114
61. ¹ H NMR (top) and ¹³ C NMR (bottom) data for compound 34	115
62. GC-MS (top) and ESI-MS (bottom) data for compound 34	116
63. ¹ H NMR (top) and ¹³ C NMR (bottom) data for compound 35	117
64. HRMS (top) and ESI-MS (bottom) data for compound 35	118
65. ¹ H NMR (top) and ¹³ C NMR (bottom) data for compound 36	119
66. HRMS (top) and ESI_MS (bottom) data for compound 36	120
67. ¹ H NMR (top) and ¹³ C NMR (bottom) data for compound 37	121
68. HRMS (top) and ESI-MS (bottom) data for compound 37	122
69. ¹ H NMR (top) and ¹³ C NMR (bottom) data for compound 38	123
70. HRMS (top) and ESI_MS (bottom) data for compound 38	124
71. ¹ H NMR (top) and ¹³ C NMR (bottom) data for compound 39	125

LIST OF FIGURES (continued)

Figure	Page
72. HRMS (top) and ESI-MS (bottom) data for compound 39	126
73. ¹ H NMR (top) and ¹³ C NMR (bottom) data for compound 41	127
74. HRMS (top) and ESI-MS (bottom) data for compound 41	128
75. ¹ H NMR (top) and ¹³ C NMR (bottom) data for compound 42	129
76. HRMS (top) and ESI-MS (bottom) data for compound 42	130
77. ¹ H NMR (top) and ¹³ C NMR (bottom) data for compound 45	131
78. HRMS (top) and ESI-MS (bottom) data for compound 45	132
79. ¹ H NMR (top) and ¹³ C NMR (bottom) data for compound 46	133
80. HRMS (top) and ESI-MS (bottom) data for compound 46	134
81. ¹ H NMR (top) and ¹³ C NMR (bottom) data for compound 47	135
82. HRMS (top) and ESI-MS (bottom) data for compound 47	136
83. ¹ H NMR (top) and ¹³ C NMR (bottom) data for compound 49	137
84. HRMS (top) and ESI-MS (bottom) data for compound 49	138
85. ¹ H NMR (top) and ¹³ C NMR (bottom) data for compound 50	139
86. HRMS (top) and ESI-MS (bottom) data for compound 50	140
87. ¹ H NMR (top) and ¹³ C NMR (bottom) data for compound 51	141
88. GC-MS (top) and ESI-MS (bottom) data for compound 51	142
89. ¹ H NMR (top) and ¹³ C NMR (bottom) data for compound 52	143
90. HRMS (top) and ESI-MS (bottom) data for compound 52	144
91. ¹ H NMR (top) and ¹³ C NMR (bottom) data for compound 53	145
92. HRMS (top) and ESI-MS (bottom) data for compound 53	146

LIST OF FIGURES (continued)

Figure	Page
93. ^1H NMR (top) and ^{13}C NMR (bottom) data for compound 54	147
94. HRMS (top) and ESI-MS (bottom) data for compound 54	148
95. ^1H NMR (top) and ^{13}C NMR (bottom) data for compound 55	149
96. HRMS (top) and ESI-MS (bottom) data for compound 55	150
97. ^1H NMR (top) and ^{13}C NMR (bottom) data for compound 56	151
98. HRMS (top) and ESI-MS (bottom) data for compound 56	152
99. ^1H NMR (top) and ^{13}C NMR (bottom) data for compound 59	153
100. HRMS (top) and ESI-MS (bottom) data for compound 59	154
101. ^1H NMR (top) and ^{13}C NMR (bottom) data for compound 60	155
102. ^1H NMR (top) and ^{13}C NMR (bottom) data for compound 61	156
103. ESI-MS data for compound 61	157
104. ^1H NMR (top) and ^{13}C NMR (bottom) data for compound 62	158
105. HRMS (top) and ESI-MS (bottom) data for compound 62	159
106. ^1H NMR (top) and ^{13}C NMR (bottom) data for compound 63	160
107. ESI-MS data for compound 63	161
108. ^1H NMR (top) and ^{13}C NMR (bottom) data for compound 64	162
109. HRMS (top) and ESI-MS (bottom) data for compound 64	163
110. ^1H NMR (top) and ^{13}C NMR (bottom) data for compound 57a	164
111. ESI-MS data for compound 57a	165
112. ITC data for compound 45 with dihydrogenphosphate.....	166
113. ITC data for compound 47 with dihydrogenphosphate.....	167

LIST OF FIGURES (continued)

Figure	Page
114. ITC data for compound 49 with dihydrogenphosphate.....	168
115. ITC data for compound 54 with dihydrogenphosphate.....	169
116. ITC data for compound 56 with dihydrogenphosphate.....	170
117. ITC data for compound 47 with PPG anion.....	171
118. ITC data for compound 54 with PPG anion.....	172
119. ITC data for compound 57a with PPG anion.....	173

LIST OF SCHEMES

Scheme	Page
1. The retro-synthetic analysis of the proposed charged receptors.....	11
2. The first approach towards the synthesis of compound 8	12
3. The second approach towards the synthesis of the compound 8	15
4. The third approach towards the synthesis of compound 8	17
5. Synthesis of the compound 9 - revised protocol.....	25
6. Reductive aminations with sodiumcyanoborohydride.....	26
7. Retro-synthetic analysis of the control receptors.....	35
8. Synthesis of 35 and 36 starting from <i>p</i> -cresol.....	36

LIST OF ABBREVIATIONS

18-C-6	18-crown-6
Ac	acetyl
AcCl	acetyl chloride
Ac ₂ O	acetic anhydride
AMP	antimicrobial peptides
APCI	atmospheric pressure chemical ionization
Br	bromine
BBr ₃	boron tribromide
BH ₃	borane
BF ₄ ⁻	tetrafluoroborate anion
C	carbon
°C	degree celsius
cal.	calories
calc.	calculated
CBr ₄	carbon tetrabromide
CD ₃ OD	deuterated methanol
CDCl ₃	deuterated chloroform
CH ₂ Br ₂	dibromomethane
CH ₂ Cl ₂	dichloromethane
CHCl ₃	chloroform
CH ₂ ClCH ₂ Cl	1, 2-dichloroethane

LIST OF ABBREVIATIONS (continued)

CH_2I_2	diiodomethane
$(\text{CH}_2)_6\text{N}_4$	hexamethylenetetramine
d	doublet
D	deuterium
D_2O	deuterium oxide
DMSO	dimethylsulfoxide
DMF	N, N-dimethylformamide
ESI	electrospray ionization
Exptl.	experimental
g	grams
H	enthalpy
HCl	hydrochloric acid
HPF_6	hexafluorophosphate
H_2PO_4^-	dihydrogen phosphate anion
hrs	hours
HRMS	high resolution mass spectrometry
Hz	hertz
ITC	isothermal titration calorimetry
J	coupling constant
K	potassium
K _a	association constant

LIST OF ABBREVIATIONS (continued)

K_1, K_2	first and second association constants
K_2CO_3	potassium carbonate
KOH	potassium hydroxide
LiOH	lithium hydroxide
Log	logarithmic
m	multiplet
M	molar
MeOH	methanol
MHz	megahertz
MIC	minimum inhibitory concentration
ml	milliliters
mol.	moles
mmol.	millimoles
MS	mass spectrometry
N_2	nitrogen (gas)
Na	sodium
NaCl	sodium chloride
NaH	sodium hydride
NaOH	sodium hydroxide
Na_2CO_3	sodium carbonate
$NaBH_3CN$	sodium cyanoborohydride

LIST OF ABBREVIATIONS (continued)

NaHB(OAc) ₃	sodium triacetoxymborohydride
NaBH ₄	sodium borohydride
NMR	nuclear magnetic resonance
NH ₄ PF ₆	ammonium hexafluorophosphate
P ₂ O ₅	phosphorous pentoxide
Pd	palladium
PF ₆ ⁻	hexafluorophosphate anion
PPG	Phosphatidylglycerol
PPh ₃	triphenyl phosphine
PTSA	<i>p</i> -toluene sulfonic acid
ppm	parts per million
Py	pyridine
q	quartet, quintuplet
rt.	room temperature
S	entropy
s	singlet
SnCl ₄	stannic chloride
t	triplet
t-BuLi	tetra butyllithium
temp.	temperature
TMED	tetramethylethylenediamine

LIST OF ABBREVIATIONS (continued)

THF	tetrahydrofuran
TLC	thin layer chromatography
TFA	trifluoroacetic acid
TBA ⁺	tetrabutylammonium ion
TES	triethylsilane

LIST OF SYMBOLS

Δ	delta, or change
δ	chemical shift
μ	micro, E-6
ν	1/cm

CHAPTER 1

INTRODUCTION

Following the discovery of antimicrobial peptides, attention has been paid to developing simpler and smaller compounds that mimic the activities of those endogenous peptide antibiotics for potential clinical use and to aid in the elucidation of how small molecules disrupt bacterial membranes. Antimicrobial peptides (AMPs) are small molecular weight proteins with broad spectrum antimicrobial activity against bacteria, viruses and fungi. These evolutionarily conserved peptides are usually positively charged and have both a hydrophobic and hydrophilic side that enables the molecule to be soluble in aqueous environments yet also enter lipid-rich membranes [1]. A portion of the inner membrane's outer leaflet of bacterial phospholipids is anionic and phosphatidylglycerol (PPG) is a unique anionic phospholipid found in prokaryotic membranes and not in eukaryotic membranes. The goal of this study is to synthesize charged anion receptor(s) which mimic cationic peptide activity that exclusively recognize this bacterial membrane component in an aqueous environment.

Anions can be recognized by either neutral or positively charged receptors. Neutral receptors interact with the anions through hydrogen bonding and should contain hydrogen bond donor groups, such as N-H functionality from amides, ureas or thioureas. Positively charged receptors contain either ammonium/ tetraalkylammonium fragments or incorporated metal ions. The interaction between the charged receptor and the anion is either electrostatic or metal-ligand, depending on how the charge is incorporated in to the artificial receptor [2].

The evolution of anion recognition started in the late 1960's with the report of positively charged receptors, incorporating ammonium binding sites. Their main motif of binding depended

exclusively on coulombic or directional electrostatic attractions. The guests were halide anions which were spherical in shape and charge density [3].

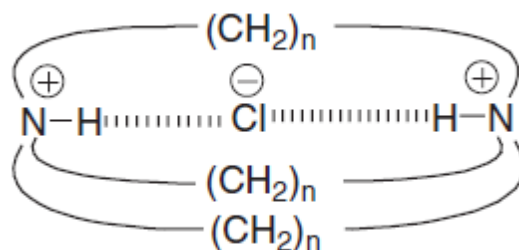


Figure 1. The first anion receptor reported in late 1960's, the alkyl linkers varied from 7 to 10 methylene groups while $n=9$ showed the highest affinity for Cl⁻ ions [3].

Following the above discovery, in mid 1970's a variety of macrobicyclic and macrotricyclic ammonium based receptors were described demonstrating how optimizing the fit of an anion for a given charged cavity could lead to strong binding. For example, the receptors shown in figure 2, upon conversion to their corresponding tetra-protonated forms, were found to bind chloride anions selectively over iodide with an association constant ($\log K_a$) of more than 4 in aqueous solution. Iodide was too large to fit into the cavity. The selectivity was based on the *size* of the anions [4, 5]. In contradiction to above receptors, the same group reported an ellipsoidal hexa-protonated cryptand which exhibited selectivity based on the *shape* of the anion [6].

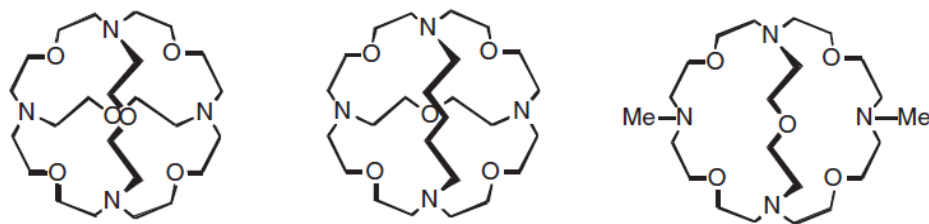


Figure 2. Receptors reported in 1970's which showed selectivity based on size

Figure 3 depicts the structure of a receptor selective for linear azide, N_3^- anion. The shape of the anion was complementary to the shape of the cavity of the receptor, and was found to show high affinity in aqueous media ($\log K_a = 4.6$) whereas the spherical chloride anion displayed a much weaker interaction ($\log K_a < 1$).

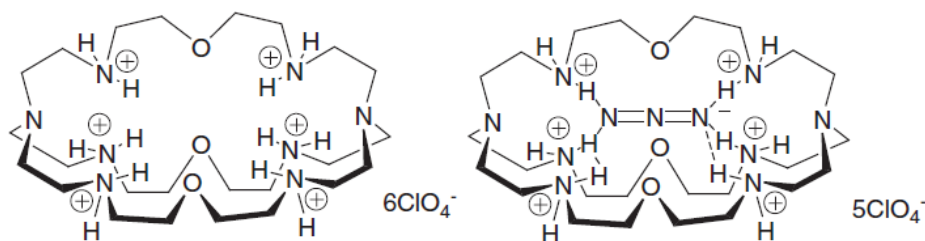


Figure 3. A receptor selective for linear azide anion.

The next series of charged anion receptors reported did not rely on hydrogen-bonding interactions to bind anions. Instead they employed quaternary ammonium groups arranged in a tetrahedral manner; hence the anion was bound to the cage-like receptor by electrostatic interactions. Altering the length of the alkyl linkers between the ammonium groups helped to 'tune' the selectivity of the receptors for particular halides.

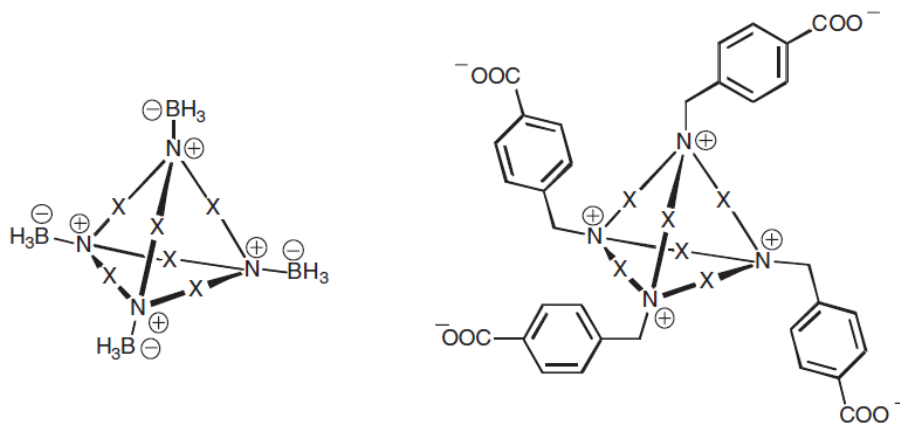


Figure 4. Cage-like receptors which bound the anions by electrostatic interactions

Complementary to the charged receptors, a wide variety of neutral anion receptors are also reported which rely on hydrogen-bonding interactions to effect anion recognition. They include amides, ureas, thioureas and pyrroles. The first neutral synthetic anion receptor which utilized ‘amide N-H···anion’ interactions was reported in 1986 which contained three amide NH groups that could be oriented to form a convergent binding site within the cyclophane host [7].

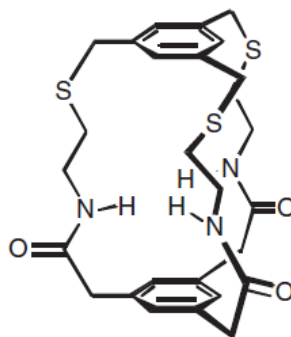


Figure 5. The first amide-based cyclophane receptor reported

In the early 1990’s a series of acyclic tripodal receptors containing amide groups were reported to bind dihydrogen phosphate anions selectively over chlorides or hydrogen sulfate when the R group was 2-naphthyl [8]. The high selectivity was assumed to be due to the

electrophilicity of the sulfonamide groups and preorganization of the binding site via π - π stacking of the naphthyl groups.

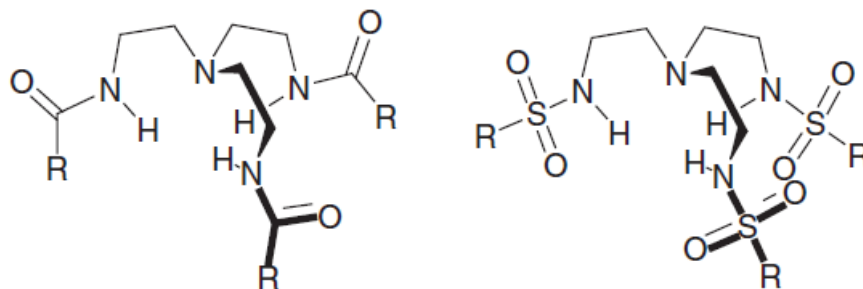


Figure 6. Acyclic tripodal receptors selective for dihydrogen phosphate anions

Urea and thio-urea groups have also been used to construct a considerable number of artificial receptors for anions probably due to the high affinities of these groups for oxo-anions. Guanidinium-based receptors also play an important role in anion recognition as they also show strong affinities for oxo-anions such as carboxylates, phosphates, sulfates and nitrates. Use of anions as templating agents for the formation of self assembled molecular architectures is another type of anion-receptor interactions which receive considerable attention in the literature [4].

However, the synthesis of artificial receptors which are specific for anions is challenging due to a number of facts. Anions are generally larger than their iso-electronic cations due to their polyatomic makeup (except halides) [3] which make them have a lower charge to radius ratio resulting in less effective electrostatic binding interactions compared to a smaller cation. Anions can have a wider range of geometries which renders it necessary to have a higher degree of design to make receptors complementary to their anionic guest. Anions can be sensitive to pH, thus the receptors should be able to bind within the pH range of the target anion [9]. This

becomes a particular problem when designing protonated /charged receptors for anions (*e.g.*, ammonium containing receptors). If the anion is present as a charge pair in solution (as is often the case in non-polar, noncompetitive solvents) the receptor must exhibit stronger, more favorable interactions to outcompete the counter ion. Solvent effects also play a major role in controlling the anion binding strength and selectivity. If the anion of interest is solvated, the potential receptor must be able to effectively compete with the solvent environment to bind with the anion. Therefore the design of selective receptors for anions requires that they are tailored to each anion's size and geometry. The nature of the solvent medium should also be taken in to account. For example, a neutral receptor that binds anions only through dipole-dipole interactions may only bind with anions in aprotic organic solvents while a charged receptor may bind with highly solvated anions in a protic solvent [9,10].

Though a large number of synthetic receptors specific for inorganic dihydrogen phosphate anions have been synthesized and reported [11], receptors specific for the anionic phosphate head groups of bacterial cell membrane phospholipids was reported only once [12]. According to the report by Bradley Smith et al, a zinc coordination complex (figure 7) was shown to be highly active (MIC of $1\mu\text{g mL}^{-1}$) against the gram positive bacteria *Staphylococcus Aureus* and moderately active against clinically important *S. aureus* strains that are resistant to various antibiotics including vancomycin and oxacillin. The mechanism of action was thought to involve the interaction of the zinc cations with the negatively charged phosphate groups of membrane phospholipids to depolarize the bacterial membrane thereby disrupting the membrane.

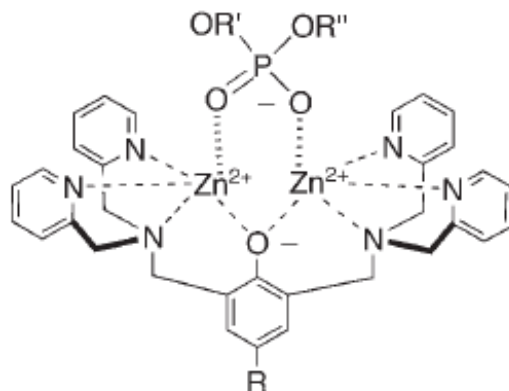


Figure 7. Interaction of the Zn coordination complex with the anionic phosphate head group of the phospholipid [12]

Almost all the antibiotics prescribed today inhibit the cellular functions of bacteria by inhibiting enzymes or other targets inside the bacterial cells and these drugs have been continuously compromised by acquired resistance of bacteria. Although research continues to develop synthetic cationic peptide mimics for clinical use, the toxicity problems associated with peptides and the effectiveness of those peptides against different bacterial species limits the clinical use of them. A small molecule which mimics the cationic peptide activity that targets and disrupts the bacterial membrane without host toxicity would be an excellent candidate as a potential antibiotic due to the fact that bacterial resistance to such agents should be very difficult for the organisms to acquire.

Even though the cell membrane is a complicated assembly of proteins and polar lipids, the eukaryotic and prokaryotic cell membranes can be differentiated by the composition and the charge of the polar lipids which are the main constituents of the cell membranes. The outer leaflet of most mammalian cell membranes is primarily composed of zwitterionic phospholipids such as sphingomyelin and phosphatidylcholine whereas that of the bacterial cell membranes contains a high fraction of anionic phospholipids and amphiphiles.

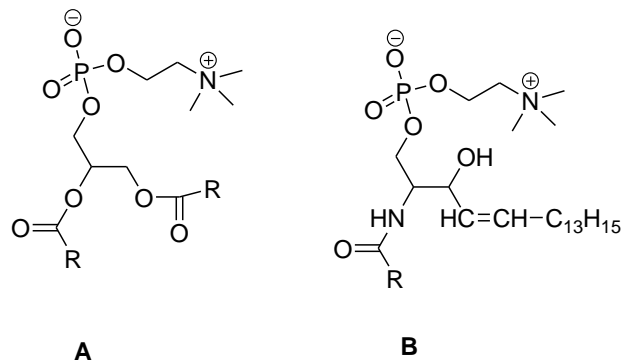


Figure 8. Examples of *zwitterionic* phospholipids found in eukaryotic cell membranes. A: a species of the phosphoglyceride type, B: a species of sphingolipid type. R is a long chain hydrocarbon [13]

Our aim in this study is to synthesize small charged receptor(s) which mimic cationic peptide activity targeting the anionic phosphate head group of the phosphatidyl glycerol (PPG), the primary anionic phospholipid found in bacterial cell membranes. The main goal is to determine if the charged receptor(s) could disrupt the bacterial cell membrane with the result of killing the bacteria without host toxicity. If no antibacterial activity was observed, then a toxic agent could be covalently attached to the receptor which would provide an antibiotic.

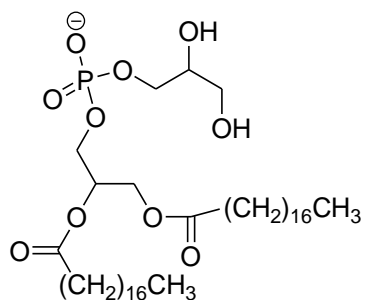
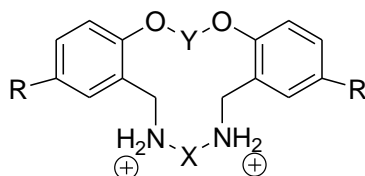


Figure 9. An example of an *anionic* phosphatidylglycerol molecule found in prokaryotic cell membranes

As the PPG anion contains a phosphate and two glycerol hydroxyl functionality in its head group, the proposed receptor(s) was intended to have multiple binding domains; a charged binding pocket that will complex with the phosphate head group of PPG anion and

hydroxyl/amide groups attached to the pocket to bind with the glycerol hydroxyl groups from the PPG. The charges were expected to help solubility of the organic receptor in an aqueous environment while making stronger charged hydrogen bonds with the oxygen(s) from the phosphate functionality.



R= -CH₃, -CH₂CH₂CH₂OH or -CH₂CH₂CONHCH₂CH₂CH₃
 Y= alkyl chain of length 1, 3, 4 or 5
 X= alkyl chain of length 3, 4, 5 or 6

Figure 10. Structure of the proposed charged receptor(s)

The following report consists of three major sections: 1) initial attempts to synthesize the first charged receptor with R= -CH₂CH₂CH₂OH which was not successful, 2) synthesis and binding studies of a series of charged control receptors (R= -CH₃) to identify the best binding pocket structure which accommodate the anionic phosphate head group of the PPG molecule by the use of binding stoichiometry and the binding strength between the receptor(s) and anions and 3) synthesis and binding studies of functionalized receptor(s) (R= -CH₂CH₂CONHCH₂CH₂CH₃) containing multiple binding domains for phosphorous anion and hydroxyl functional groups to achieve the specific recognition of the said molecule.

CHAPTER 2

SYNTHESIS

2.1 Synthesis of the First Charged Receptor(s)

The first charged anion receptors proposed (figure 11) consists of two modified phenol groups attached to each other by two linkages; an ether linkage between the two phenol oxygen atoms and an alkyl linkage *ortho* to the ether linkage which contains two ammonium groups. This was assumed to be the binding pocket for the phosphate head group of the PPG anion (figure 9). The functional groups responsible for binding with the two glycerol hydroxyl groups from the PPG anion are two primary alcohol groups attached to the two phenol rings *para* to the phenol oxygen atoms. In this molecule, X could be propane, butane, pentane or a hexane chain while Y is methane or a propane chain. Molecular model studies suggested that, it was necessary to keep the number of the CH₂ units in Y to be odd, in order to get the required shape/ rigidity of the receptor molecule to bind with the phosphate group of the PPG anion in a 1:1 stoichiometry.

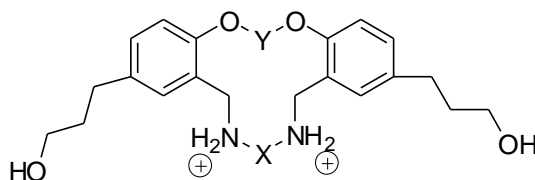
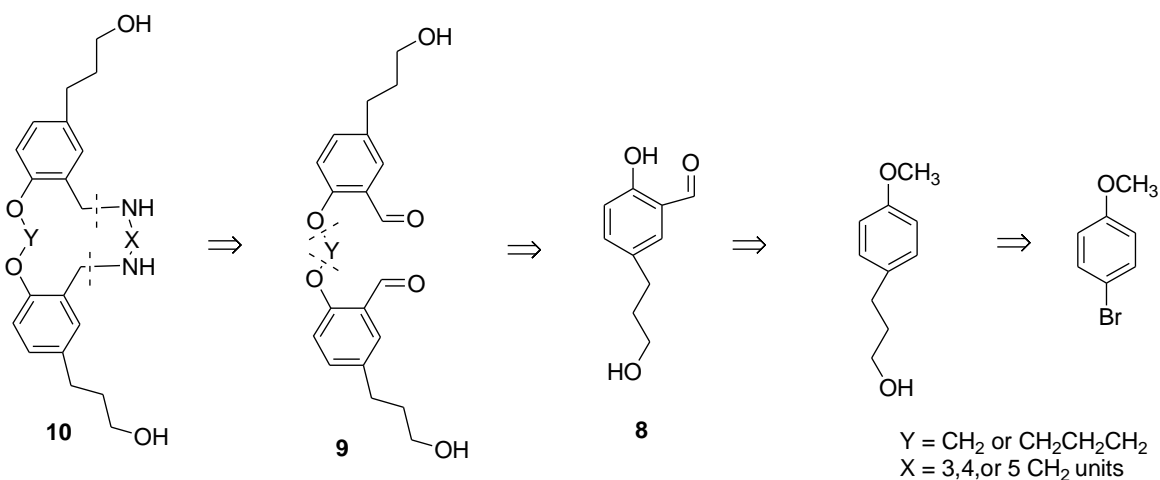


Figure 11. Structure of the proposed charged receptor molecule(s)

The planned synthesis consisted of four major steps excluding the final step, which was to convert the two amine groups into two ammonium groups with the introduction of the positive charges. Scheme 1 outlines the retro synthetic analysis of the synthesis of the first charged receptors specific for the PPG anion. It was predicted that once the compound **8** was synthesized, two of them could be linked via an ether linkage between the two phenol oxygen atoms. The

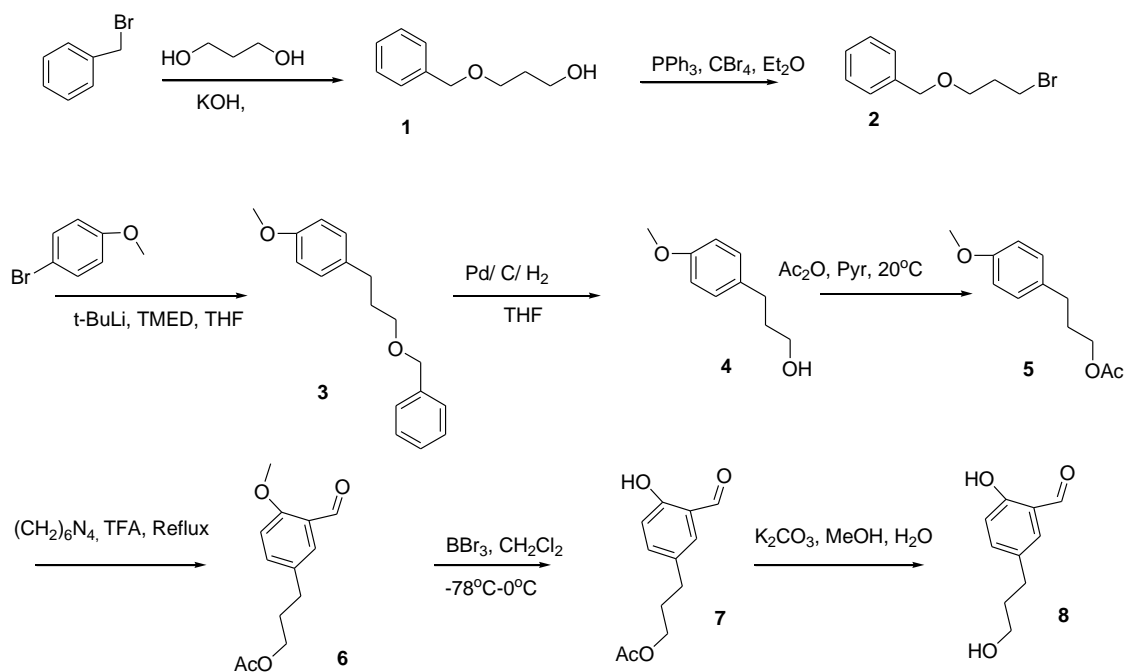
second alkyl linkage was to be constructed using a reductive amination reaction between the two formyl groups from compound **9** with the corresponding diamine.

Although the synthesis of the receptor appeared to be simple with the retro-synthetic analysis, preparation of the compound **8** which contained three functional groups - phenol, aldehyde and primary alcohol - was tedious.



Scheme 1. The retro-synthetic analysis of the proposed charged receptors

The first approach towards the synthesis of compound **8** is given in scheme 2, which started with the Williamson ether synthesis reaction of commercially available benzyl bromide with 1,3-propanediol to produce 3-benzyloxy-propan-1-ol **1** in 85% yield, which was then treated with an ethereal solution of PPh_3 and CBr_4 [14] to produce [(3-bromopropoxy) methyl]benzene **2** in 60% yield. The compound **2** was then reacted with either 4-bromophenol or 4-bromoanisole to produce the compound **3**.



Scheme 2. The first approach towards the synthesis of compound **8**

Although the literature suggests that *ortho*-formylation of *para* substituted phenols was possible, several attempts to perform an *ortho*-formylation of 4-methylphenol or methyl(4-hydroxyphenyl) acetate, using *para*-formaldehyde[15], Vilsmeier reaction[16] or modified Duff reaction[17] produced insignificant yields.

When the substrate was 4-methylanisole or 4-methylphenyl acetate the modified Duff reaction worked well. Both of the above molecules contain $-OR$ groups instead of the $-OH$ attached to the aromatic ring. Based on above results, 4-bromoanisole was used in the synthetic procedure instead of 4-bromophenol, followed by modified Duff reaction for the *ortho*-formylation. First, 4-bromoanisole was reacted with *t*-BuLi in the presence of TMED to form the 4-methoxybenzen-1-ide anion and then **2** was added into the reaction flask [18] to furnish 1-[3-(benzyloxy)propyl]-4-methoxybenzene **3** in 67% yield. Catalytic hydrogenation [19] of **3** yielded

3-(4-methoxy phenyl) propan-1-ol **4** in a quantitative yield. The primary alcohol group on **4** was then protected as the acetate ester [20] in quantitative yield before subjecting it to Duff conditions. Duff reaction of 3-(4-methoxyphenyl)propyl acetate **5** furnished a product mixture which contained the *ortho*-formylated product, with either the acetate or trifluoroacetate ester at the end of the propyl chain. Base catalyzed ester hydrolysis removed both acetate and trifluoroacetate groups. Re-acetylation [20] of the above produced 3-(3-formyl-4-methoxy phenyl)propyl acetate **6** in 65% yield. Removal of the protecting group of phenol oxygen (methyl group) with BBr_3 / CH_2Cl_2 [21] furnished 3-(3-formyl-4-hydroxyphenyl) propyl acetate **7** in quantitative yield.

Once compound **7** was in hand, two alternative methods seemed possible to construct the ether linkage; either link two molecules of **7** using the corresponding dibromoalkane followed by the removal of acetate protection or first remove the acetate protection group and then link two molecules of **7** with the use of the corresponding dibromoalkane. It was decided to follow the first method, as it made more sense to keep the acetate protection which would prevent the formation of a propoxy anion in the presence of the base used in the next coupling reaction. Coupling of two molecules of **7** with 1,3-dibromopropane in the presence of NaH in DMF [22] furnished the desired product **9b** in a trace amount and the elimination product **11** in a substantial amount.

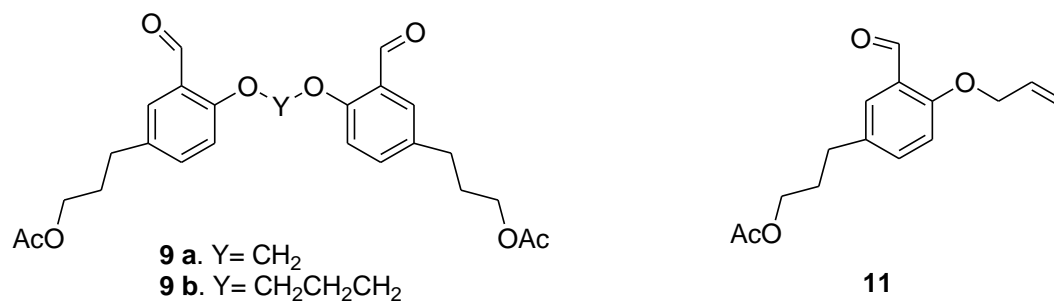


Figure 12. Products obtained from the coupling reaction between compound **7** and 1,3-dibromopropane.

When the same coupling procedure was carried out with CH₂I₂ in place of 1,3-dibromopropane to make **9a**, once again only trace amounts of the desired product was isolated and the isolation of the pure product was also problematic. With that result, it was decided to follow the second method: removal of the acetate protection first and then link two molecules with the corresponding dibromoalkane as it was suspected that the acetate group might have promoted the elimination. Removal of the acetate protection was achieved by base catalyzed ester hydrolysis to give 2-hydroxy-5-(3-hydroxypropyl)benzaldehyde **8** in 80% yield. The coupling reaction of **8** was carried out again using the same procedure as above with 1,3-dibromopropane as the linker to yield the desired product in 45% yield with impurities, again the isolation of the pure product was problematic.

Since both above methods failed to furnish the ether linkage between the two phenol oxygen groups in a substantial yield, it was decided to perform the Duff reaction with compound **3** to prepare 5-(3-(benzyloxy) propyl)-2-methoxybenzaldehyde **12**. Instead of compound **12**, the reaction furnished a mixture of the compounds **13** and **14**. The crude mixture was then subjected to base catalyzed ester hydrolysis to convert **14** to **13**. Acetylation of compound **13** furnished the compound **6** in 70% yield.

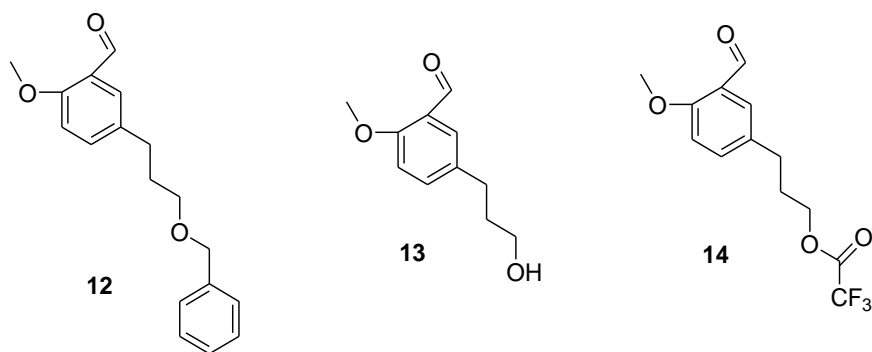
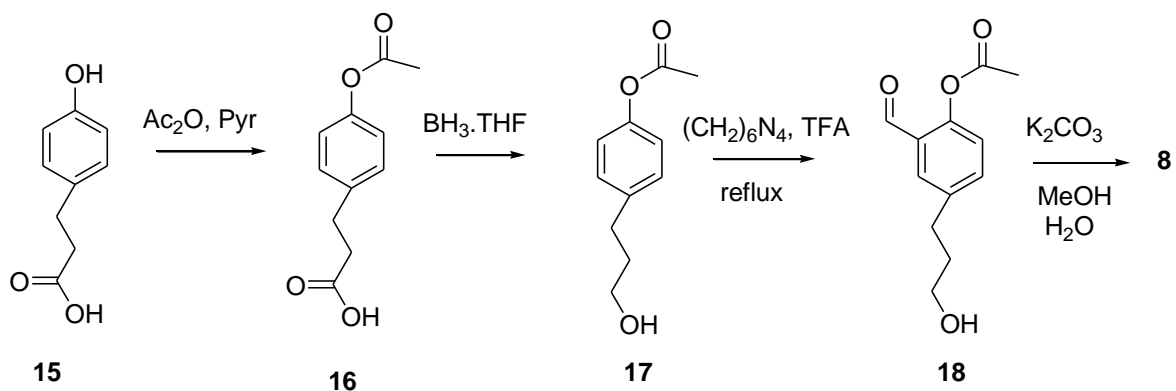


Figure 13. Products of Duff reaction with compound **3**

Although model studies suggested that having an odd number of CH₂ groups connecting the two phenol oxygen atoms, either one or three, would provide the best binding pocket structure for the phosphate head group of the PPG molecule, the synthesis proved it was problematic. The above approach involved 10 steps altogether with the protection/ de-protection steps to get the compound **8** which was ready to be coupled. After the coupling reaction, still there would be three more steps to complete the synthesis of the desired compound. Therefore, it was decided to use another approach which consists of a fewer number of steps to furnish **8** in an improved yield. Scheme 3 depicts the second approach utilized to synthesize compound **8**.



Scheme 3. The second approach towards the synthesis of the compound **8**

The first step of the new synthetic pathway was the acetylation of the phenol group of commercially available 3-(4-hydroxyphenyl)propanoic acid **15** to yield 3-(4-acetoxyphenyl)propanoic acid **16** in 73% yield with the same acetylating method previously used. The carboxylic acid **16** was then reduced to 4-(3-hydroxypropyl)phenyl acetate **17** by the use of BH_3 : THF [23]. The Duff reaction of the compound **17** furnished a mixture of products instead of just **18**. Thin layer chromatography (TLC) showed the purification of the crude reaction mixture would be problematic.

As literature results suggested that trifluoroacetate esters are easily hydrolyzed under mildly basic conditions with quantitative yields [24], the crude product mixture from the above reaction was subjected to base catalyzed hydrolysis using Na_2CO_3 , but the proton NMR spectrum of the resultant crude product mixture suggested the de-acetylation did not go to completion. Since Na_2CO_3 did not hydrolyze the TFA ester, another reaction was carried out using K_2CO_3 which was a stronger base than Na_2CO_3 , which ended up giving the same result. Based on the above observations, it was decided that much stronger conditions were necessary to perform this step. However, even with the use of LiOH /THF, it was not possible to drive the reaction to completion and the purification attempts on the crude product mixtures also were not successful. The proton NMR and mass spectra of the isolated materials showed that the TFA ester group was switching positions between the phenol hydroxyl and the propyl hydroxyl group of the molecule giving rise to structures **19**, **20** and **21** (figure 14) under basic conditions. However, acid catalyzed ester hydrolysis using PTSA in methanol/ water removed the TFA ester group without further complications.

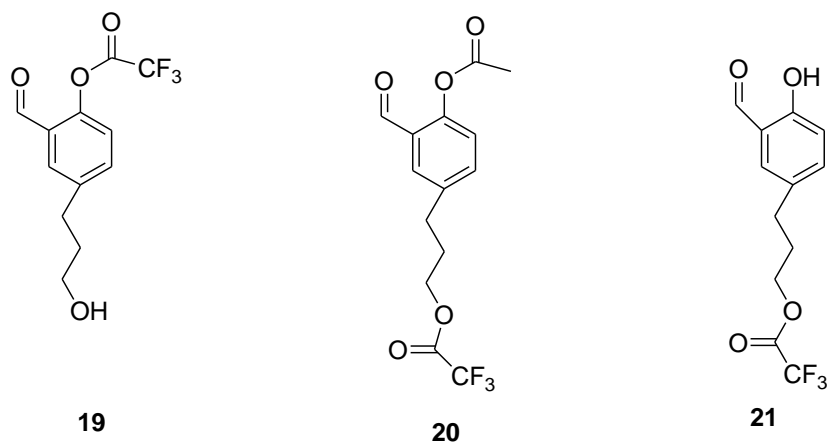
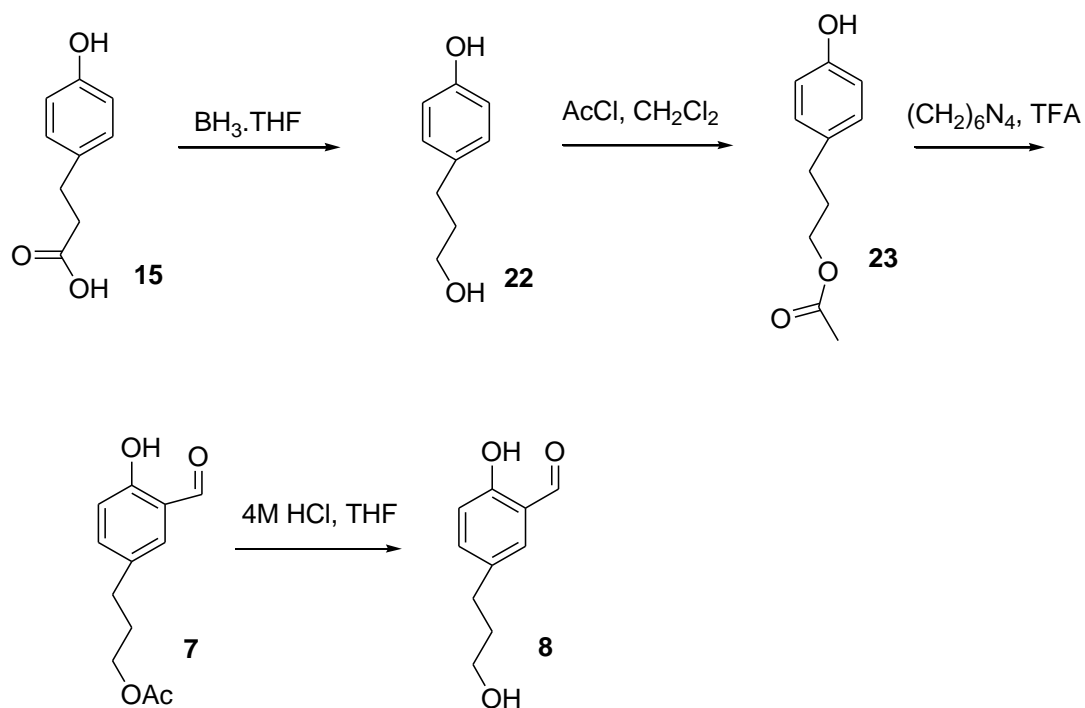


Figure 14. TFA ester switching positions between the phenol hydroxyl and the propyl hydroxyl groups

While it was possible to isolate the product **8** using this synthetic pathway, the yield was not sufficient to proceed with the remaining steps. In order to obtain viable yields, a third approach was attempted as shown in Scheme 4.



Scheme 4. The third approach towards the synthesis of compound **8**

The first step of the new approach: reduction of the commercially available 3-(4-hydroxyphenyl)propanoic acid **15** to 4-(3-hydroxypropyl)phenol **22** was achieved by stirring it with $\text{BH}_3:\text{THF}$ at 60°C overnight. Acetylation of compound **22** with the use of acetyl chloride resulted in a mixture of the compounds **23** and **24**. Acetylation of the above using excess acetyl chloride exclusively furnished the compound **24**. Duff reaction followed by acid catalyzed ester hydrolysis of **24** furnished the product **8** but in less than 20% overall yield.

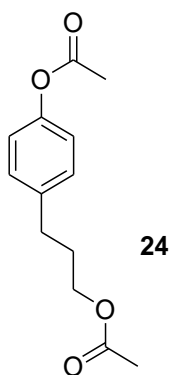


Figure 15. Structure of the compound **24**

Literature documents a method [25] to prepare compound **8** in three steps starting from compound **22**, in 33 % yield. There were two differences between the literature method and ours: 1) an extra step to synthesize **22** and 2) the method of formylation. While we utilized the Duff conditions, the literature method used SnCl_4 , triethylamine/toluene and *para*-formaldehyde.

Carrying out the same experimental procedure with commercially available 4-(3-hydroxypropyl) phenol **22** increased the product yield up to 40% from 20%. After comparing the yields obtained with our Duff conditions (40%) to the literature SnCl_4 / *para*-formaldehyde method (33%), it was decided to utilize the Duff reaction in the syntheses.

While attempts were made to prepare compound **8** in an acceptable yield, a different set of reactions were carried out to study/optimize the reaction which coupled two modified phenols

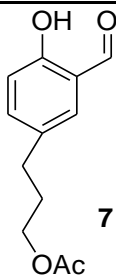
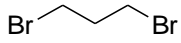
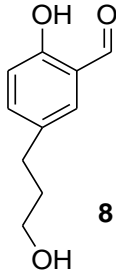
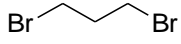
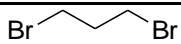

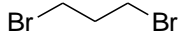
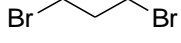
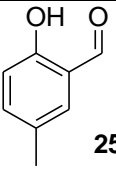
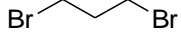
through an ether linkage to produce compound **9**. Table 1 summarizes the reactions that were carried out using sodium hydride as the base in the coupling/ linkage reaction.

When this reaction was carried out with compound **7**, using 1,3-dibromopropane as the linker (Table 1, entry 1) the proton NMR spectrum of the crude product mixture showed the presence of both the linked product and the elimination product (**9b** and **11**). Isolation of the desired product was problematic with column chromatography either with silica gel or alumina gel, but silica gel column chromatography followed by radial chromatography (Chromatotron) with the use of a solvent gradient furnished the desired product in a low yield with some minor impurities. Isolation of pure product was not achieved.

Based on the assumption that the acetate group was capable of promoting the elimination, the next reaction was conducted under the same experimental conditions using compound **8** as the substrate, which contained a hydroxyl group in place of the acetate functionality (entry 2, table 1). Furthermore, it was expected that a compound with a hydroxyl functionality would make the purification less problematic compared to a compound with an acetate group due to the polarity differences between the two molecules. However, the reaction produced low yields and the purification was problematic again, due to the presence of some irremovable impurities.

TABLE 1

ETHER LINKAGE REACTION WITH THE USE OF NaH AS THE BASE

	Starting Molecule	Linker	Exptl. Conditions	Result
1	 7		NaH (1:1) DMF 60°C	< 25% with some minor impurities
2	 8		NaH (1:1) DMF 60°C	< 40% with impurities
3	8	CH ₂ I ₂	NaH (1:1) DMF, 60°C	Mixture of products, Isolation not achieved
4	8	CH ₂ Br ₂	NaH(1:1) TEA, DMF, 60°C	Mixture of products, Isolation not achieved
5	8	CH ₂ I ₂	NaH(1:1) THF, 60°C	No reaction
6	8	CH ₂ Br ₂	NaH (1:1) DMF, 60°C	25 % yield with some impurities
7	8	CH ₂ Br ₂	NaH,(1:1.1) DMF, 60°C	Same as above
8	p-cresol		NaH, DMF 60°C	24% isolated in pure form
9	4-bromophenol		NaH, DMF 60°C	35 % isolated in pure form
10	4-bromophenol		NaH, DMF rt, 24hr	36% isolated in pure form
11	4-bromophenol		NaH, DMF rt, 48hr	38 % isolated in pure form
12	 25		NaH, DMF 60°C	42 % yield, isolated
13	25	CH ₂ I ₂	NaH, DMF 60°C	86% yield, isolated

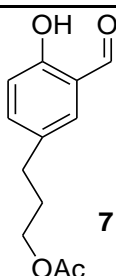
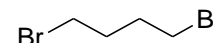
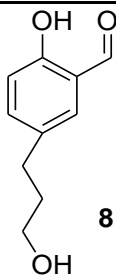
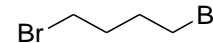
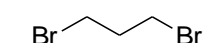
Since the linker with three carbons produced the elimination product in substantial yields (Table 1, entry 1 and 2), the next set of reactions (Table 1, entry 3-7) were performed using either CH₂I₂ or CH₂Br₂ as the linker. With each reaction either the solvents used or the equivalency of NaH used were changed one at a time to see the effects of those changes as well. Changing the length of the linker from three to one increased the yields but the problem of purification remained the same. Changing the solvent to THF from DMF prevented the reaction from taking place. Increasing the equivalents of NaH, or the addition of TEA neither improved the product yield nor simplified the purification significantly.

To study the effect of the substituent at the *p*-position (to the phenolic OH) on yields and purification, another set of reactions were performed using *p*-cresol (Table 1, entry 8), 4-bromoanisole (table 1, entry 9-11) and 2-hydroxy-5-methylbenzaldehyde **25** (table 1, entry 12) as substrates, respectively. 1,3-dibromopropane was used as the linker with all above reactions (table 1, entry 8-12). Even though the yields of those reactions were low, isolation of the products in pure form was attainable with all three substrates which confirmed that the presence of a hydroxyl or acetate functionality caused problems associated with purification. Furthermore, the next two reactions performed with compound **25** (table 1, entry 12-13) showed that the attached formyl group had little or no effect on the experimental yield or the purification. Additionally, the last entry of the table 1 showed, when the length of the linker was one carbon, the yield of the desired product did increase significantly.

To study the effect of reaction temperature on the formation of elimination product, three reactions were performed using the same substrate and the linker at 60°C, at room temperature with a reaction time of 24 hrs and at room temperature with a reaction time of 48 hrs respectively (table 1, entry 9-11). All three reactions gave comparable results, confirming that the temperature

was not the reason which promoted the elimination. Based on above experimental results it was concluded that the method which utilized NaH as the base was not a viable option with our synthesis. The next set of reactions summarized in table 2 was carried out to see whether it was possible to increase the yields by changing the base used and/ or the length of the linker used.

TABLE 2
RESULTS OF THE ETHER LINKAGE REACTION
WITH THE USE OF KOH AS THE BASE

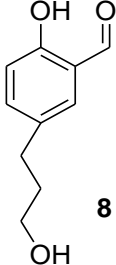
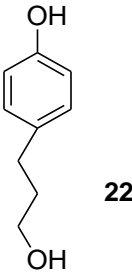
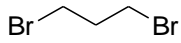
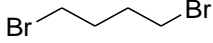
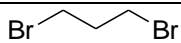
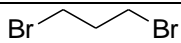
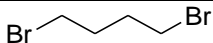
Starting Molecule	Linker	Exptl. Conditions	Result
 <p>7</p>		KOH, EtOH reflux	¹ H NMR of the crude showed peaks of the linked product, but isolation was impossible
 <p>8</p>		KOH, EtOH reflux	¹ H NMR of the crude showed peaks of the linked product, but isolation was impossible
8		KOH, EtOH reflux	¹ H NMR of the crude showed the presence of the linked product and the elimination product. Isolation in pure form was impossible

Following a literature method with a similar system [26], the linkage reaction was carried out utilizing NaOH as the base. The compound **8** did not give any pure product; therefore NaOH was substituted with KOH. Care was taken to control the equivalents of the base used, as one to one with respect to the moles of the substrate was used. However all the reactions conducted with compound **7** or **8** furnished crude product mixtures which proved the isolation of the desired

products were problematic. At this point, it was thought that the use of strong bases may be deprotonating the propyl hydroxyl groups leading to the formation of polymers as the proton NMR signals of the crude product mixtures were broad. Based on this assumption, it was decided to change the base utilized in the reaction. The next set of experiments was carried out using potassium carbonate as the base. The equivalents of the base used were carefully controlled to be one to one with respect to the moles of the substrate used.

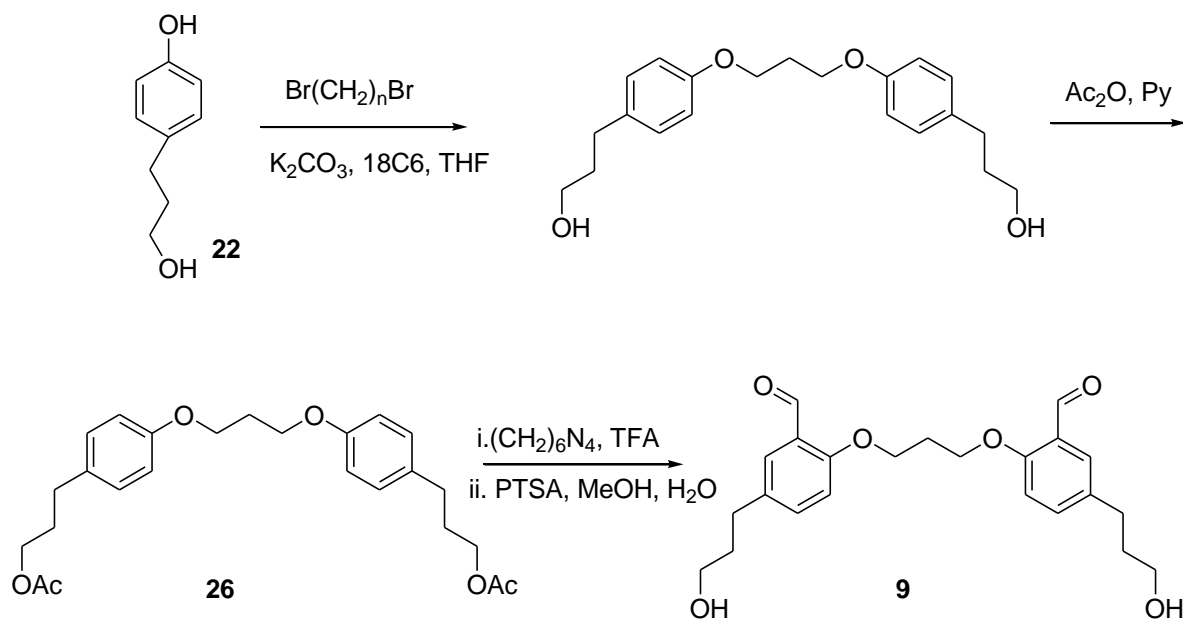
The table 3 summarizes the results of the coupling reaction carried out utilizing K_2CO_3 and 18-C-6 with different modified phenols and linkers with different chain lengths which produced improved results compared to what was observed with previous methods. The compound **8** when reacted with the CH_2I_2 linker under the new reaction conditions (K_2CO_3 / 18-C-6 method) furnished the desired product as evidenced by the proton NMR spectroscopy, but was never isolated (table 3, entry 1) due to the problems associated with purification. When the length of the linker was four carbons (entry 3 and 6), the yields were much better compared to the corresponding yields with linker length of three carbons (entry 2 and 4). With the new method, the isolation of the desired products also was possible with column chromatography and/ or radial chromatography. The entry 4 and 5 compares the effect of temperature on the above coupling reaction with 1, 3-dibromopropane which showed that a lower temperature was not effective for the formation of the desired product.

TABLE 3
RESULTS OF THE ETHER LINKAGE REACTION
WITH THE USE OF K₂CO₃ AS THE BASE

	Starting Molecule	Linker	Exptl. Conditions	Result
1	 8	CH ₂ I ₂	K ₂ CO ₃ , 18-C-6 THF, reflux	Never isolated the product in pure form
2	 22		K ₂ CO ₃ , 18-C-6 THF, reflux	Pure product isolated in 60% yield
3	22		K ₂ CO ₃ , 18-C-6 THF, reflux	Pure product isolated in 84% yield
4	p-cresol		K ₂ CO ₃ , 18-C-6 THF, reflux	Pure product isolated in 58% yield
5	p-cresol		K ₂ CO ₃ , 18-C-6 THF, room temp	Pure product isolated in 28% yield
6	p-cresol		K ₂ CO ₃ , 18-C-6 THF, reflux	Pure product isolated in 88% yield

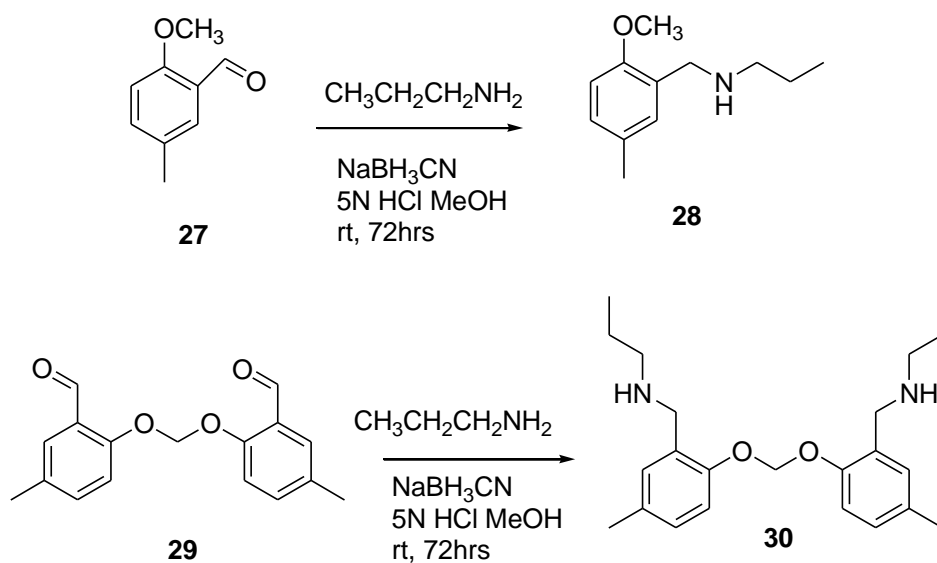
The above results also suggest that if the synthesis began with compound **22** and performed the coupling reaction as the first step, it would help increase the yields by reducing the number of protection/ de-protection steps involved, provided that the coupled product could be efficiently formylated. Based on this postulation, a new synthetic scheme was proposed which is shown in scheme 5. If successful this method would provide compound **9** in only four steps, leaving two more steps to complete the synthesis of the target receptor. The new synthesis started

with the coupling of two molecules of **22** using 1,3-dibromopropane as the linker. It was decided to use the commercially available **22** as the starting material because the synthesis and isolation of compound **22** from commercially available 3-(4-hydroxyphenyl)propanoic acid **15** was problematic. Once the linked product was isolated in pure form, the primary hydroxyl groups were protected as acetates (**26**) before proceeding to the next step. Duff reaction followed by acid catalyzed hydrolysis of the acetate/trifluoroacetate esters produced compound **9** in 60% yield, making the overall yield 29% after 4 steps.



Scheme 5. Synthesis of the compound **9**- revised protocol

Having compound **9** in hand, the next step to perform was the second alkyl linkage between the two formyl functions of compound **9** with the use of a reductive amination reaction. As the amount of compound **9** in hand was limited, it was decided to use a model system first, to perform the trial experiments. 2-methoxy-5-methylbenzaldehyde **27** was chosen as a good candidate for this purpose as it was easily synthesized by the Duff reaction of 1-methoxy-4-methylbenzene which is commercially available (scheme 6). Reaction of **27** with propylamine in the presence of sodium cyanoborohydride produced N-(2-methoxy-5-methylbenzyl)propan-1-amine **28** in 47% yield. When the same reaction was carried out using 6,6'-methylenebis(oxy)bis(3-methylbenzaldehyde) **29** as the substrate, the reaction did work but produced the compound **30** in only 27% yield. Results suggested that performing two reductive aminations with the same molecule would produce lower yields compared to that with one functional group.



Scheme 6. Reductive aminations with sodium cyanoborohydride

Based on the above result, the prediction was that, the use of cyanoborohydride would not furnish the desired product in a substantial yield in the actual synthesis as it needed two formyl groups to undergo reductive amination forming a cyclic structure. Therefore it was decided to find another reducing agent which would reduce the two formyl groups more efficiently. The reaction of compound **9** with propyl amine using sodium triacetoxyborohydride [27] as the reducing agent (stirred at room temperature for 2 hours) produced the compound **31** (figure 16) in 28% yield. Isolation of the pure product was achieved by column chromatography followed by radial chromatography.

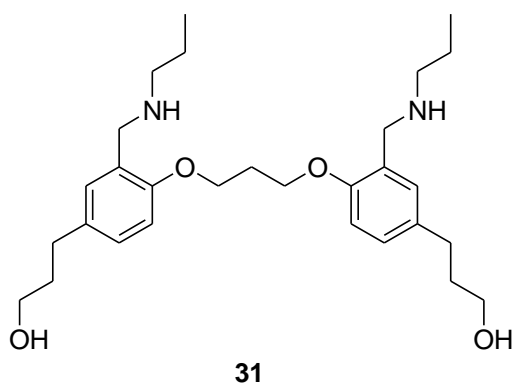
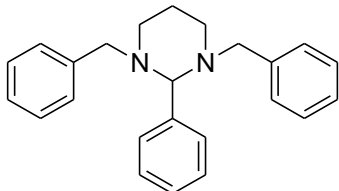


Figure 16. Structure of the compound **31**

The target receptor(s) require the connection of two formyl groups with a di-amine linker which closes the ring. All of the above reactions were carried out with monoamines. Therefore, to better model the required reaction benzaldehyde was reacted with either propane-1,3-diamine or hexane-1,6-diamine in the presence of sodium triacetoxyborohydride as the reducing agent. Once the reaction conditions were optimized, the same experimental conditions would be applied with the real system converting the compound **9** to make compound **10**. Table 4 summarizes the results of the control reactions performed with benzaldehyde as the substrate and sodium triacetoxyborohydride as the reducing agent.

TABLE 4

REDUCTIVE AMINATION OF BENZALDEHYDE WITH DIAMINES

	Experimental conditions	Results
1	THF, [0.25], room temp, 2 hrs NaHB(OAc) ₂ added to the stirred solution of the diamine and the carbonyl. Linker: propane-1,3-diamine	 Structure confirmed by x-ray analysis
2	THF, [0.1], room temp, 2 hrs Linker: propane-1,3-diamine	Reaction didn't go to completion NMR, MS show the presence of the product, but was not isolated
3	THF,[0.1], room temp, 2 hrs Linker: hexane-1,6-diamine	Mixture of linked (product) + mono amine
4	THF,[0.1], room temp, 8 hrs Linker: hexane-1,6-diamine	Pure product in 39% yield
5	THF,[0.05], room temp, 30 hrs Linker: hexane-1,6-diamine	Pure product in 82% yield

The first reductive amination reaction between benzaldehyde and propane-1,3-diamine using sodium triacetoxyborohydride yielded pure crystals, but the proton NMR signals were not indicative of the desired product. X-ray analysis of the crystals of this provided the structure shown in the table 4, entry 1 which agreed with the proton NMR signals. It was believed that the high concentration of the reaction mixture was causing the formation of the undesired product. Therefore, a second reaction (table 4, entry 2) was conducted by diluting the reaction mixture from 0.25M to 0.10M; all other experimental parameters were kept the same. The proton NMR spectrum of the crude product mixture of this showed that the reaction did not go to completion. Therefore further purifications were not attempted. Furthermore, literature reports that aldehydes also could undergo reduction with sodium triacetoxyborohydride to produce the corresponding

alcohols under the reaction conditions used[28]. Thus the possibility existed that the reduction of the aldehyde would compete with the reductive amination under the standard conditions. In addition, the formation of dialkylated amines was a common side reaction in reductive aminations of aldehydes with primary amines, which could be suppressed by the addition of up to 5% molar excess of the primary amine [28]. In our synthesis, it was not viable due to the possibility of formation of polymers.

In order to avoid the reduction of the formyl group into the hydroxyl in the presence of sodium triacetoxyborohydride, it was necessary to change the sequence of addition of reactants into the reaction flask. With previous experiments, the carbonyl compound and the reducing agent were sequentially added into a stirred solution of the diamine in a round bottom flask. A new reaction was conducted by stirring the carbonyl and the diamine for half an hour in a round bottom flask prior to the introduction of the reducing agent. The linker was changed from propane-1,3-diamine to hexane-1,6-diamine. After stirring for 2 hours at room temperature, the resulting crude product was a mixture of the desired product and the monoamine as shown in table 4, entry 3. It was not attempted to isolate the desired product, as a substantial amount of the crude mixture contained the monoamine. However stirring the reaction mixture for 8 hours at room temperature furnished the pure product in 39% yield. Above observations made it apparent that diluting the reaction mixture and stirring it for extended time periods improved the yield of the desired product. Therefore the next reaction was carried out by reducing the concentration of the reaction mixture to 0.05M, and increasing the reaction time to 30 hours which furnished the desired product in 82% yield as shown in the entry 5, table 4. However, when the same experiment was performed with the real system, (molecule **9**) the result was not similar to that obtained with benzaldehyde. Instead it yielded what was thought to be a polymeric material

(very broad ^1H NMR signals) of which the isolation proved problematic. Therefore it was necessary to optimize the reaction conditions again so that it would tolerate the functional groups present in the molecule of interest. The attempts to optimize the product yields by changing the reaction conditions and the results obtained with the real system (**9**) with hexane-1,6-diamine as the linker are summarized in table 5.

The first reaction between the compound **9** and hexane-1,6-diamine was carried out using the same experimental conditions as with benzaldehyde (entry 1, table 5). But the substrate did not dissolve completely and the crude product was a yellow/ orange sticky mass which did not dissolve in water, ethyl acetate, methylene chloride or methanol. Mixing the carbonyl with the di-amine before adding the solvent was the suspected cause of the problem. Further purification of the crude was not attempted as the proton NMR spectrum of the crude material did not indicate the presence of the desired product. The second reaction was carried out using the same experimental conditions, except that the concentration of the reaction mixture was reduced from 0.05M to 0.01M as in entry 2, Table5. In addition, the carbonyl and the diamine were dissolved in the solvent separately before mixing them. The proton NMR spectrum of the crude product mixture showed the starting material in a substantial amount indicating that the reaction did not work.

TABLE 5

REDUCTIVE AMINATION OF THE COMPOUND 9 WITH HEXANE-1,6-DIAMINE

	Experimental conditions	Results
1	CH ₂ ClCH ₂ Cl,[0.05], room temp, 30 hrs Reducing agent: NaHB(OAc) ₃	Product not isolated
2	CH ₂ ClCH ₂ Cl,[0.01], room temp, 30 hrs Reducing agent: NaHB(OAc) ₃	No presence of the product in the crude NMR
3	MeOH, [0.05], room temp, 3 hrs Reducing agent: NaBH ₄	No presence of the product in the crude NMR
4	MeOH, [0.05], 0°C, 3 hrs Reducing agent: NaBH ₄	Mass spec showed the presence of the product, did not isolate as it was present in trace amounts
5	MeOH, [0.0225], 0°C, 10 hrs Reducing agent: NaBH ₄	15% of the desired product was isolated
6	MeOH, [0.0225], 0°C, 10 hrs Reducing agent: NaBH ₄ Syringe addition of the carbonyl and the amine to a stirred solution of NaBH ₄	NMR showed the reduction of the formyl group
7	CH ₂ Cl ₂ , [0.0225], 0°C, 10 hrs Reducing agent: NaHB(OAc) ₃ Syringe addition of the carbonyl and the amine to a stirred solution of NaHB(OAc) ₃	No products, possible polymer formation
8	Formation of the bisimine followed by reduction with NaBH ₄	No product isolated
9	Formation of the bisimine followed by reduction with Silica gel/ NaBH ₄ system	Presence of the product confirmed by Mass spec., but was not isolated

Since sodium triacetoxyborohydride did not furnish the desired product, it was decided to use NaBH₄ in the reductive amination reaction. With previous results it was obvious that benzaldehyde was not a good model compound for our molecule of interest. Therefore, it was decided to use compound **9** for the study with NaBH₄ rather than benzaldehyde. Table 5, entry 3,

shows the results from the first attempt of the reductive amination with sodium borohydride as the reducing agent. It was thought; at room temperature the NaBH_4 had reacted too fast, therefore the same reaction was carried out again at 0°C . The mass spectrum of the crude mixture indicated the presence of the desired product (table 5, entry 4) which was not isolated in pure form. The same reaction, with a higher dilution (from 0.05M to 0.0225M) and an increased reaction time from 2 hours to 10 hours furnished the product in 15% yield (table 5, entry 5).

Entry 6 shows the results of the same experiment conducted as a high dilution experiment. Syringe addition of the carbonyl compound and the diamine to a stirred dilute solution of NaBH_4 in methanol caused the reduction of the formyl group instead of reductive amination. Based on the hypothesis that NaBH_4 was a much stronger reducing agent, it was decided to perform the same reaction, utilizing the same addition method with the use of sodium triacetoxyborohydride in place of sodium borohydride (table 5, entry 7), which was futile in giving the desired product.

The last two entries in the table 5 used another approach; formation of the bisimine followed by the reduction. The bisimine was first formed by refluxing the dialdehyde and the diamine in MeOH for three hours [29]. Reduction of the bisimine was tried out using two different methods. In the first method, the crude bisimine was re-dissolved in methanol and treated with sodium borohydride followed by stirring at room temperature overnight (entry 8). The proton NMR spectrum of the crude material was complicated and the purification attempts were unsuccessful. In the second method, the crude bisimine was ground with NaBH_4 and mixed with silica gel. The reaction was initiated by adding a few drops of chloroform followed by the quenching of the reaction with water [29]. The proton NMR spectrum of the crude material

showed the presence of the desired product which was confirmed by mass spectrometry, but the purification attempts were again unsuccessful.

Regardless of the reducing agents or the methodology used in above experiments, it was not possible to isolate the desired products in pure form after the reductive amination step. While different attempts were proceeding towards finding a suitable method to make the second alkyl link with diamines with different chain lengths, it was suggested to make a control receptor system for comparison purposes with the real receptor(s). The control receptors were to be prepared without functional groups that bind to glycerol hydroxyl groups of the PPG for two reasons. 1.) These receptors would be needed anyway as controls for the fully functionalized receptors for later comparison purposes (The fully functionalized receptors were considered to contain binding units for both the phosphate portion of the PPG molecule and the glycerol hydroxyl groups). 2.) The control receptors were supposed to be utilized for the determination of binding stoichiometry between the inorganic dihydrogen phosphate anion and the receptor molecule in order to determine the best binding pocket structure for the phosphate head group of the PPG. Having more than one binding unit would make this determination problematic as it is possible for two or more anions to bind to the receptor via both binding domains. Furthermore, it was predicted that the preparation of the control receptors would be easier with less functionality. After considering all above factors, it was decided that *p*-cresol would be a good candidate as the starting material in the synthesis of the control receptor system.

2.2 Synthesis of the Control Receptors

With the use of p-cresol as the starting material, the hypothesis was that the family of control receptors synthesized (figure 17) would provide the best structure of the binding pocket necessary for effective binding between the receptor and dihydrogenphosphate in a 1:1 stoichiometry, which would translate to a functionalized receptor pocket that would also bind to the anionic phosphate head group of the PPG in a 1:1 ratio. Furthermore the model system would act as the control for the fully functionalized receptor system(s) for future comparisons.

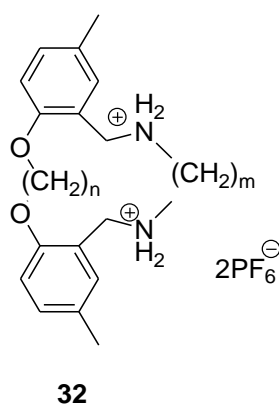
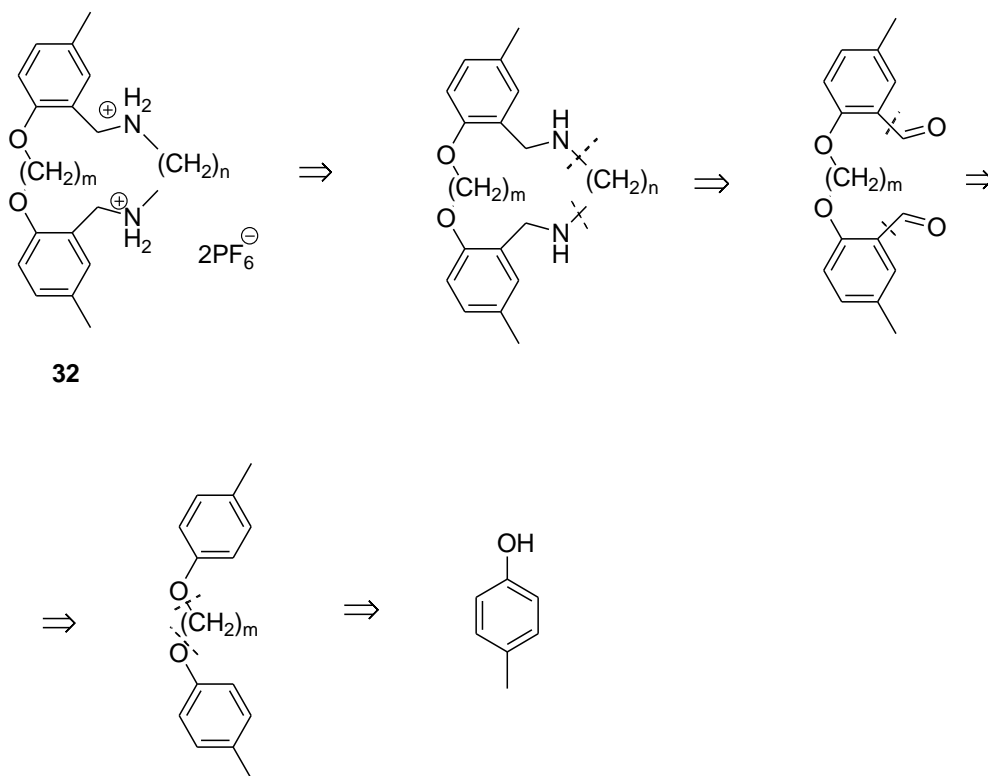


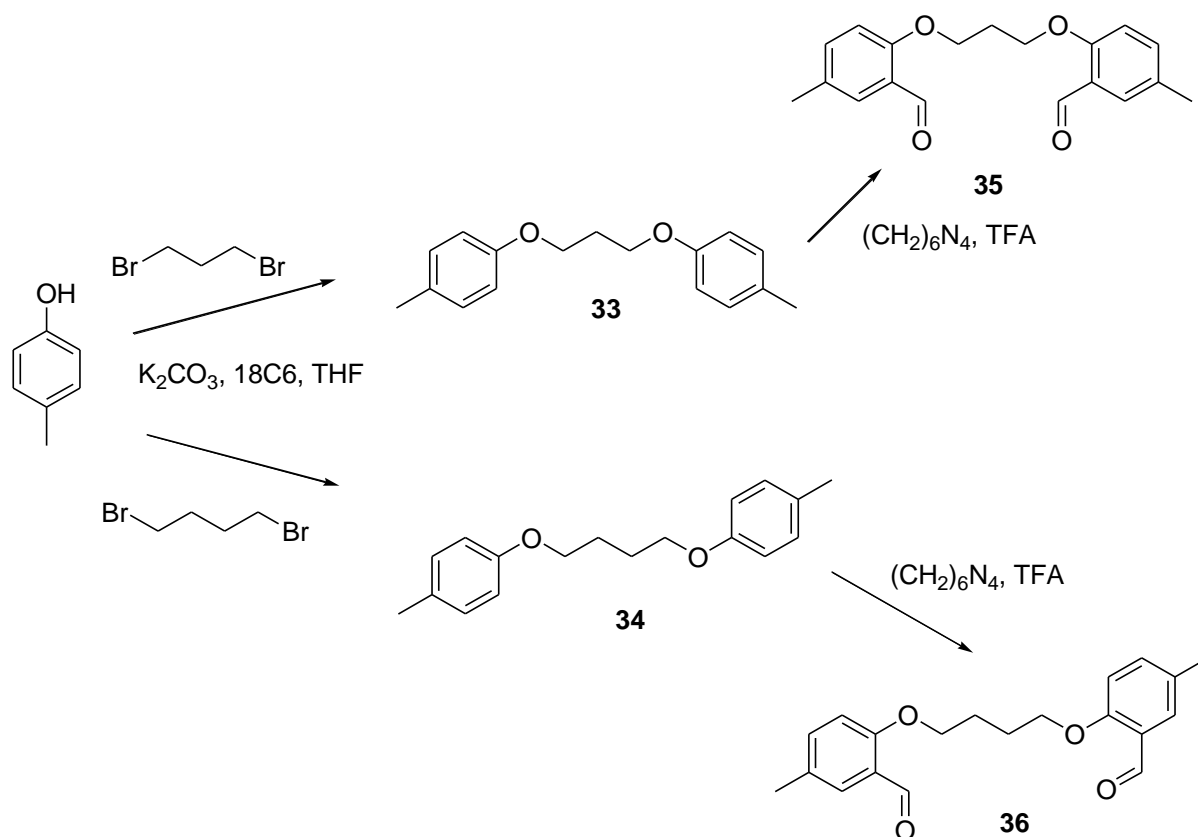
Figure 17. Structure of the control receptor system

Retro-synthetic analysis of the proposed model system is presented in scheme 7. The proposal was to keep the length of the ether linkage between the two phenol oxygen atoms as three or four methylene units and vary the second alkyl linkage containing two ammonium groups from 3 to 6 methylene units. If all the reactions work well, we would have 8 model compounds with different spacer lengths.



Scheme 7. Retro-synthetic analysis of the control receptors

The first step of the synthesis shown in scheme 8 was the formation of the ether linkage between two molecules of *p*-cresol with 1,3-dibromopropane or 1,4-dibromobutane using the $K_2CO_3/18-C-6$ method described earlier which furnished compounds **33** and **34** in 76% and 73% yields respectively. The next step was the Duff formylation reaction with linked compounds **33** and **34** which furnished the expected products **35** and **36** in 37.5% and 53% yields respectively. Once again, having the compounds **35** and **36** in hand the challenge was to find the best reaction conditions to perform the reductive amination reaction closing the ring.



Scheme 8. Synthesis of **35** and **36** starting from *p*-cresol

Previous results showed that during the reductive amination reaction the reduction of the aldehyde functional group was competitive with the bisimine formation. Therefore, formation of the bisimine followed by the reduction appeared to be more feasible. But again, while synthesizing the control receptors, it was necessary to develop a reliable methodology that could be utilized for the synthesis and purification of the fully functionalized system. Thus careful consideration was given to methods in the literature that had been used to synthesize and then reduce bisimines involved in formation of ring compounds.

Miguel A. Sierra et al. [30] synthesized bisimines on systems which were very similar to our molecules, except that, those molecules did not have any substituent groups on the *p*-position to the ether linkage. Their method of synthesis for the bisimines was similar to ours: refluxing in

MeOH. However, two differences were noticed: very long refluxing times ranging from 3 to 24 hours depending on the substrate molecule (dialdehyde) and the use of much more dilute reaction mixtures as low as 0.01M or less. It was predicted this would be the best method for our systems as well.

The next goal was to find the most efficient method to reduce bisimines without affecting the other functional groups present in the receptor molecules. A method developed by Pijus K. Mandal and John S. McMurray [31] appeared to be perfect for our system. The method involved the in situ generation of molecular hydrogen by the addition of triethylsilane (TES) to palladium-charcoal catalyst which resulted in rapid and efficient reduction of imines under mild, neutral conditions. Use of neutral conditions was assumed to be advantageous with the molecules we were interested in, as they could be acid/ base sensitive.

After the careful selection of the above two methods, it was decided to try them out with compound **36** first. Reaction of **36** with hexane-1,6-diamine in refluxing ethanol produced the corresponding bisimine which was confirmed by mass spectrometry. Removal of the ethanol under vacuum followed by the reduction using TES and Pd-C in anhydrous methanol gave the corresponding bisamine **37** in 72% yield. Isolation of the pure product was not problematic as with the previous reductive amination product of compound **9** to form **10**. Following the isolation of the compound **37** in pure form, a series of reactions were carried out to prepare the family of control receptors with $n=3$ or $n=4$ and $m=3, 4, 5$ or 6 . The results are summarized in table 6.

TABLE 6
YIELDS OF THE SECOND ALKYL LINKAGE REACTION WITH THE CONTROL
RECEPTORS

n	m	Structure	% yield
4	6	37	72
4	5	38	49
4	4	39	67
4	3	40	12
3	6	41	74
3	5	42	67
3	4	43	No product was formed
3	3	44	No product was formed

All the reactions furnished the expected products in reasonable quantities except the compounds **43** (n=3, m=4) and **44** (n=3, m=3). It was notable that compound **40** (n=4, m=4) gave a lower yield compared to the other systems. Several attempts to synthesize the above three compounds (**40**, **43** and **44**) were not successful. It was believed when the length of the ether linker “n” is 3 or 4, that linkage was too short to direct the second aldehyde on the ring towards the second amine to form the bisimine. Therefore it was decided to proceed with the molecules in hand.

Having compound **37** through **42** in hand, the next step was to find a method to introduce the positive charges on to each molecule. At this point our concern was that the formation of two positive charges might be difficult due to electrostatic repulsion. It was decided to use PF_6^- as the

counter ion of the charged receptors as it made charged receptors more soluble in organic solvents. Furthermore, the PF_6^- counter ion was known to facilitate crystallization of charged organic complexes. The first attempt to convert the amine groups into ammonium was carried out by stirring the neutral compound **37** with HPF_6 (1:2 eq.) in CH_2Cl_2 . It was thought if the exact equivalents were used; no further purifications of the charged complex would be needed. After the mixture was stirred for half an hour, the resultant solid was filtered under vacuum. The proton NMR spectrum of the resultant material did not differ from that of the starting neutral compound. Therefore it was decided to use excess HPF_6 in the synthesis.

In the second attempt, the compound **37** was stirred with excess HPF_6 for half an hour at room temperature in CH_2Cl_2 . Then the reaction mixture was equilibrated with water over night assuming excess HPF_6 would go into the aqueous phase leaving the charged complex in the organic layer. Furthermore, it was thought that the charged complex would solidify upon the removal of the organic solvent. However, the removal of the organic solvent produced an oil instead of a solid material, the proton NMR spectrum of which appeared to be slightly different from the neutral compound. The appearance of new peaks corresponding to ammonium protons and the movement of the signals corresponding to the protons adjacent to the ammonium groups in the proton NMR spectrum, together with their integral values confirmed the presence of the doubly charged molecule. Mass spectrometry (ESI, positive) revealed the presence of the M^+ ion and ($\text{M}^{2+}/2$) ion with the corresponding mass to charge ratio.

However, the presence of an additional peak in the above mass spectrum made us examine the counter ion present in the charged complex. The mass spectrum (ESI) in the negative ion mode presented a signal corresponding to the m/z of BF_4^- anion instead of PF_6^- anion. Furthermore, the additional peak presented in the positive spectrum was in accordance

with the m/z of the ($M^{2+}BF_4^-$). While struggling to explain the presence of the unknown peak in the mass spectrum, attempts were taken to crystallize the above charged complex. After several unsuccessful attempts, crystallization of the complex was achieved by the use of boiling chloroform. The X-ray crystallography revealed the structure shown in figure 18, which contained doubly charged organic molecule, with 2 BF_4^- anions as the counter ions confirming what had been predicted with mass spectrometry was correct.

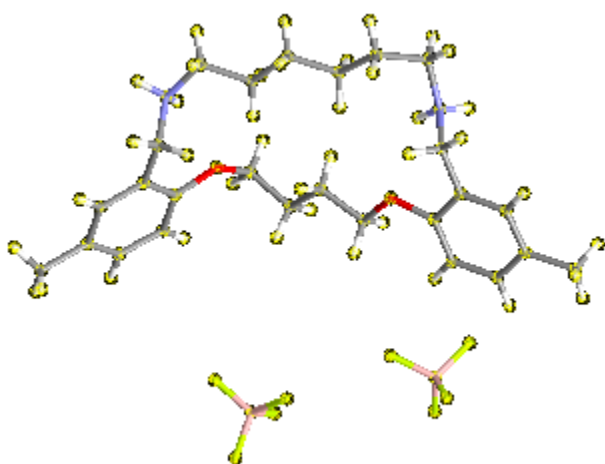


Figure 18. X-ray crystal structure of the complex **45** with BF_4^- anions

The next challenge was to find an explanation for the presence of BF_4^- in the charged receptor complex without the addition of it in to the system. Following several experiments conducted in Pyrex glassware and in polytetrafluoroethylene (PTFE) beakers, it was decided that boron, a component in Pyrex glass was bleeding in to the reaction mixture in the presence of HPF_6 which was a very strong acid. One journal article [32] which reported the exchange of SiF_5^- with BF_4^- when a reaction was conducted in Pyrex glass also supported our observation.

The above finding proved that the use of HPF_6 would cause problems. Therefore, it was necessary to use another approach to charge the organic molecules.

The next attempt towards the charge introduction involved stirring the neutral molecule with 6N HCl in methanol followed by anion exchange using NH_4PF_6 [33]. To accomplish this, first, the compound **37** in methanol was stirred with 6N HCl at room temperature for 6 hours. Then the solvent was removed under vacuum and the resultant substance was redissolved in water. A large excess of NH_4PF_6 (>20 eq.) dissolved in CH_2Cl_2 was added to the aqueous solution and was stirred vigorously at room temperature for 4 hours. An off white solid was formed in between the layers which was neither soluble in water nor in dichloromethane which was easily isolated by filtration. The proton NMR spectroscopy and mass spectrometry were used to prove that the charged control receptor complex **45** was formed with the PF_6^- as the counter ion. X-ray crystallography was used to further confirm the presence of two positive charges and the presence of PF_6^- counter ions.

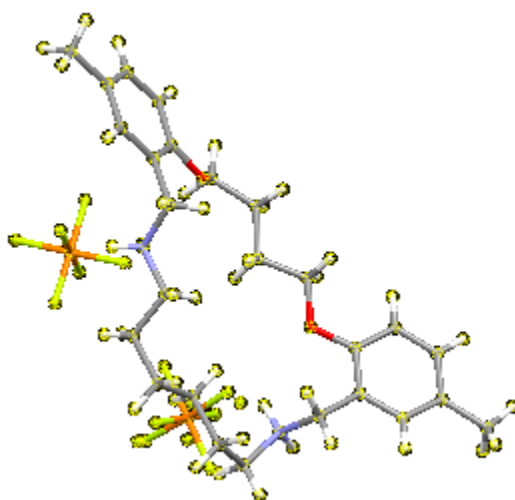
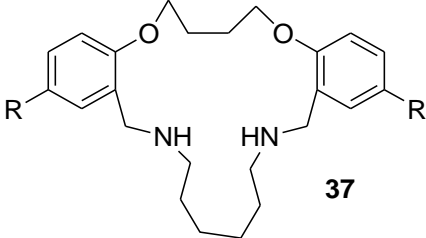
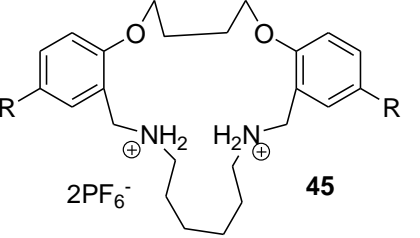
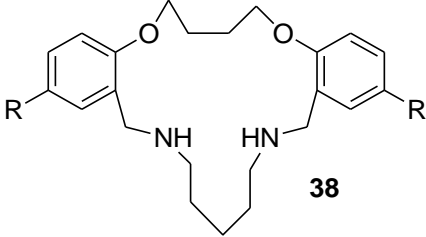
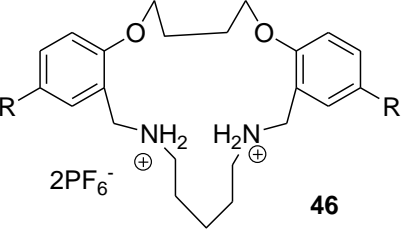
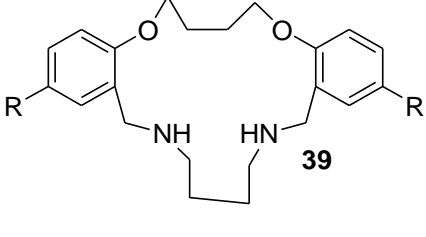
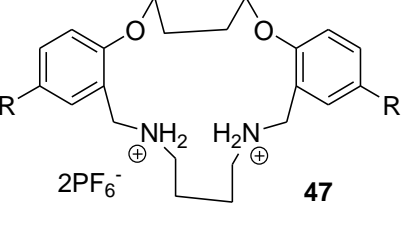
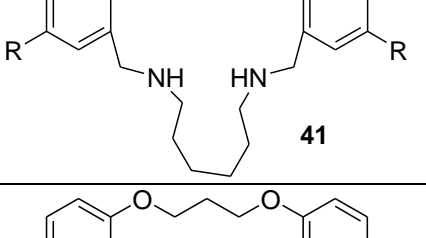
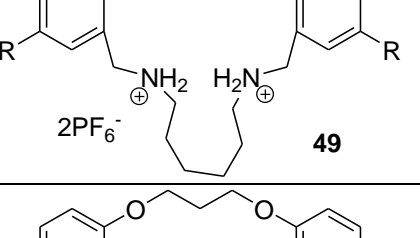
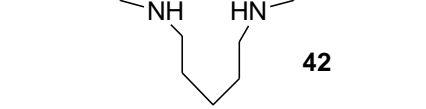
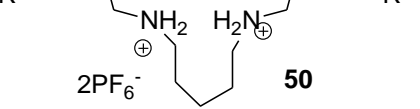


Figure 19. X-ray crystal structure of the complex **45** with two PF_6^- anions

TABLE 7
CHARGED CONTROL RECEPTORS SYNTHESIZED AND THEIR
CORRESPONDING YIELDS

Bisamine	Charged complex	Yield charge	% Yield Overall
 <p style="text-align: right;">37</p>	 <p style="text-align: right;">45</p>	72%	20%
 <p style="text-align: right;">38</p>	 <p style="text-align: right;">46</p>	41%	8%
 <p style="text-align: right;">39</p>	 <p style="text-align: right;">47</p>	55%	15%
 <p style="text-align: right;">41</p>	 <p style="text-align: right;">49</p>	45%	10%
 <p style="text-align: right;">42</p>	 <p style="text-align: right;">50</p>	40%	8%

Following the above result, same experimental procedure was performed with the rest of the bisamines synthesized in the previous step. Table 7 summarizes the charged control receptor systems synthesized with their corresponding percentage yields.

When the length of the ether linkage between the two phenol oxygen atoms “n” was 3 or 4, it was not possible to synthesize control systems with m=3. Even though it was possible to synthesize compound **40** (n=4, m=3) in a 12% yield, several attempts to charge that system was unsuccessful.

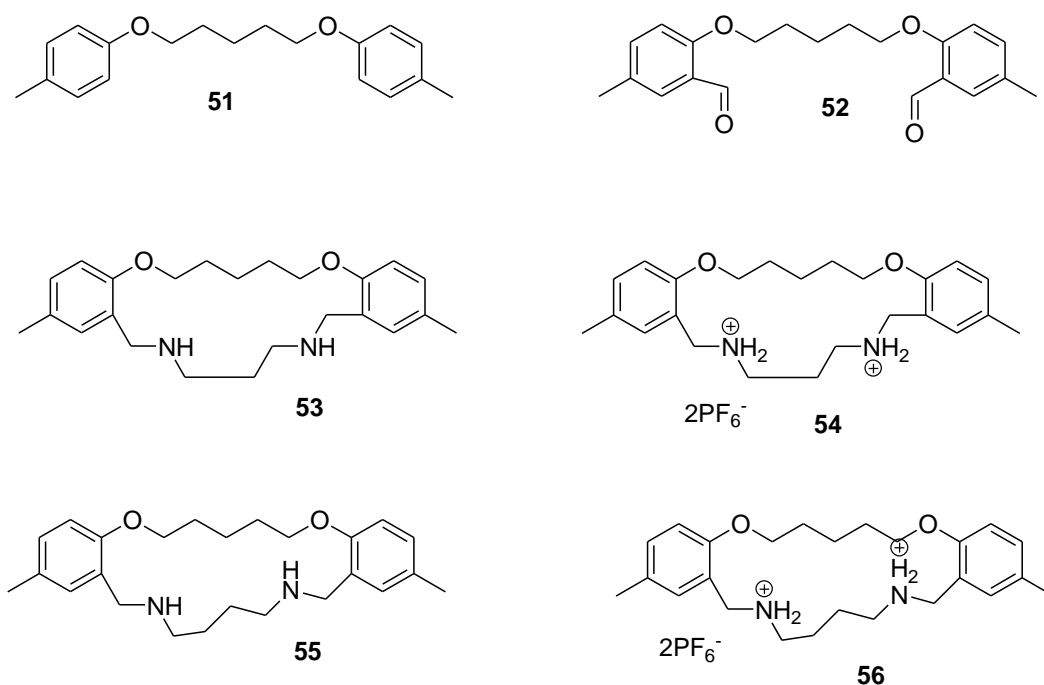


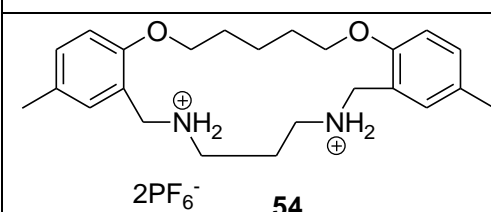
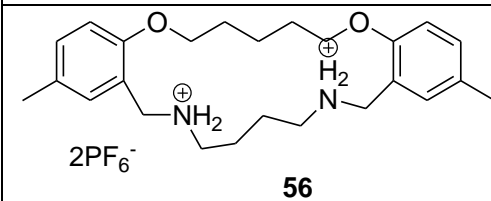
Figure 20. Structures of the compounds **51-56**

It was assumed that, if the length of the ether linkage was increased (n=3 or 4 to n=5), it would be possible to make an m=3 system. Following the same experimental procedures utilized

in the synthesis of the other complexes, two new charged control receptors **54** ($n=5$, $m=3$) and **56** ($n=5$, $m=4$) were synthesized starting from p-cresol Figure 20 shows the intermediate compounds synthesized in the production of compound **54** and **56**.

The table 8 summarizes the charged control receptors synthesized with the ether linkage $n=5$ with their corresponding percentage yields.

TABLE 8
YIELDS OF THE RECEPTORS WITH $n=5$

Receptor Complex	% Yield Charge	% yield Overall
 <p>54</p>	35%	9%
 <p>56</p>	92%	32%

After the synthesis of seven charged control receptors and characterizing them with different methods, the next challenge was the synthesis of the fully functionalized receptors. Because of the purification problems associated with the previously proposed real system which contained propyl hydroxyl groups, it was decided to change the functional groups responsible for the binding of the glycerol hydroxyl groups of the PPG anion. Changing the propyl hydroxyl functionality to an amide group provided the structure of the revised charged receptor(s) which will be discussed in the next section.

2.3 Synthesis of the (Revised) Fully Functionalized Charged Receptors

Based on the results of the binding studies conducted with the control receptors (discussed in the next chapter), two binding pocket sizes ($n=4$, $m=4$ and $n=5$, $m=3$) were chosen to have the most likely structures to bind with the anionic phosphate portion of the PPG molecule in a 1:1 stoichiometry. Therefore, it was decided to synthesize two functionalized receptor systems **57a** and **57b** with those pocket sizes. The functional group responsible for the binding with the glycerol hydroxyl groups were changed from hydroxyl propyl (the first proposed receptors) to amides as discussed earlier. Structures of the revised, fully functionalized receptors are given in figure 21.

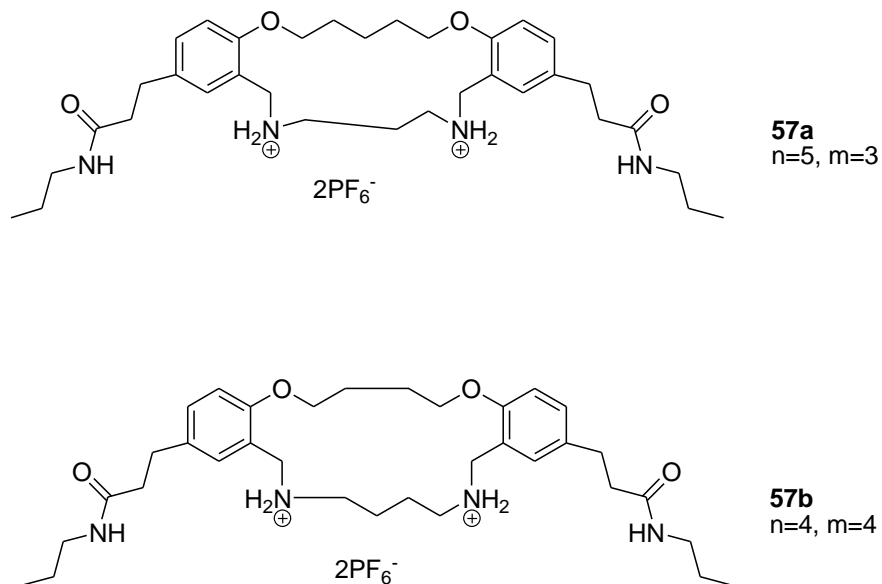


Figure 21. Proposed functionalized amide receptors

As a reliable methodology had already been developed for the synthesis of the charged receptor systems, it was decided to follow the same reaction sequence utilized with the synthesis of the control receptor system.

The synthesis started with the conversion of commercially available 3-(4-hydroxyphenyl) propanoic acid **15** into 3-(4-hydroxyphenyl)-N-propylpropanamide **59** in two steps. The first step converted the starting acid **15** into the corresponding acid chloride **58** with the use of thionyl chloride. The second step converted the acid chloride to the corresponding amide **59** with the use of excess propyl amine in a 75% yield. As described with the previous syntheses, the ether linkage between the two phenol oxygen atoms was made next with the corresponding dibromoalkanes: giving the compound **60** (n=4) and **61** (n=5) in 20% and 21 % yields respectively. The yields were low, but at this point the focus was to synthesize the amide receptors rather than to optimize the yields.

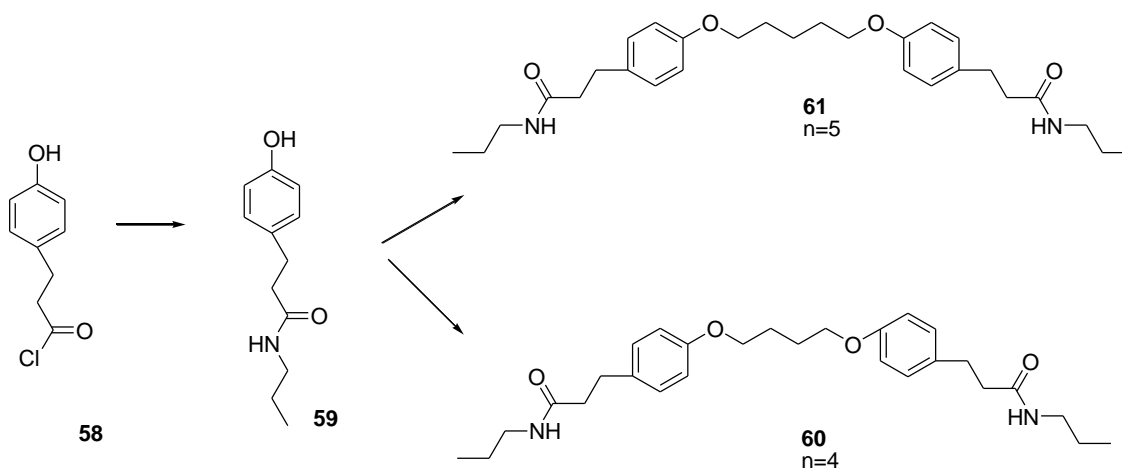


Figure 22. Synthesis of the compound **60** and **61**

The Duff formylation of compound **60** furnished the bisaldehyde **62** in 67% yield and the same with the compound **61** furnished the bisaldehyde **63** in 46% yield. With the amide substituent, the purification was problematic, but silica gel column chromatography followed by preparative thin layer chromatography yielded the pure products in both above cases.

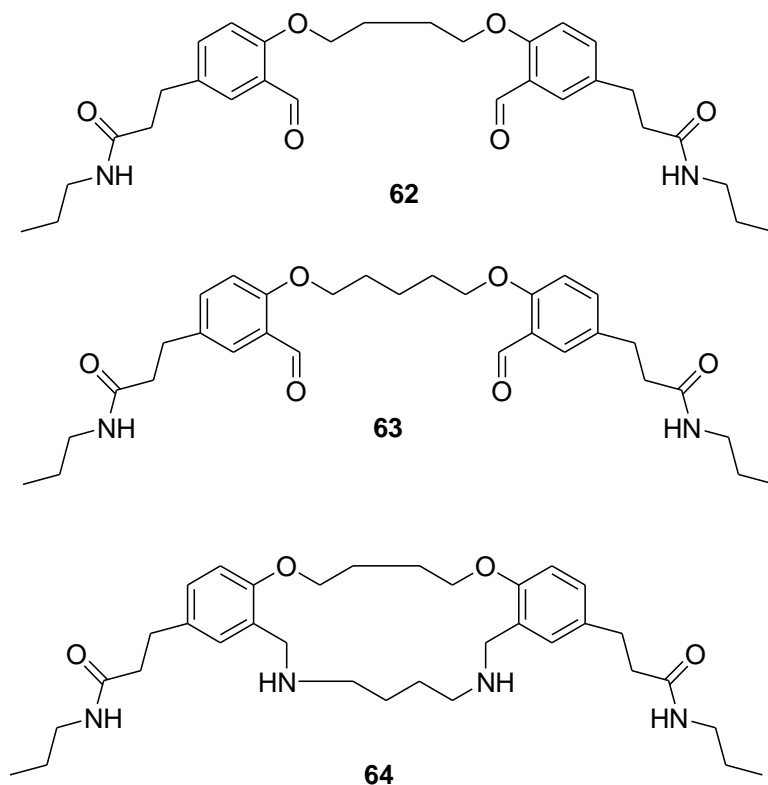


Figure 23. Structures of compounds 62-64

The next step was to make the second alkyl linkage which contains the amine groups using a reductive amination reaction. Compound **62**, when refluxed with butane-1,4-diamine in ethanol produced the corresponding bisimine which was then reduced to the corresponding bisamine with the use of TES and Pd-C in anhydrous methanol to furnish compound **64** ($n=4$, $m=4$) in 42% yield. When the same reaction sequence was carried out with compound **63** and

propane-1,3-diamine, it furnished the corresponding bisimine which was confirmed by mass spectrometry. However, the reduction of the bisimine in the presence of TES/ Pd-C did not produce the corresponding bisamine. The reason was assumed that, when the linker length 'm' was 3, the conformation of the molecule might be not facilitating the hydrogenation reaction which takes place on C surface.

The last step of the synthesis of the functionalized amide receptors also was the introduction of the charges, which was achieved by following the same protocol utilized with the control receptors. Charging of the compounds **64** furnished the final product **57a** in 73% yield. Overall yield of this product was 3%. Even though it was decided to synthesize two fully functionalized receptors, we ended up synthesizing only one. It was decided to carry out the proton NMR titrations and the ITC studies with the compound in hand before moving on to synthesizing more similar compounds.

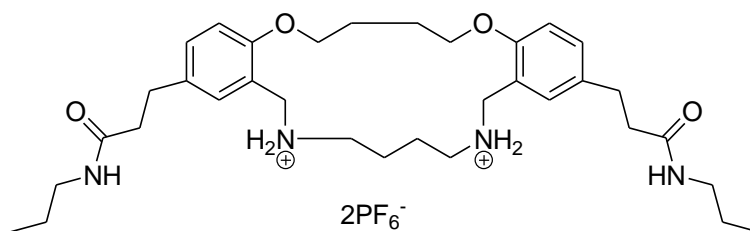


Figure 24. Structure of the fully functionalized receptor **57a**

CHAPTER 3

ANION BINDING STUDIES

Anion binding studies of all the charged receptors began with proton NMR Job plots to reveal the binding stoichiometry between the charged receptors and the anions being studied. Anions studied were inorganic dihydrogen phosphate H_2PO_4^- from $\text{TBA}^+\text{H}_2\text{PO}_4^-$ and the tetrabutylammonium phosphatidylglycerol anion (PPG anion) which was synthesized in our lab [34]. Once the binding stoichiometry was determined, the next step was the determination of anion binding constants for the receptors. This was accomplished by the use of proton NMR titration data of the receptor-anion complexes together with the use of the computer program EQNMR non-linear regression analysis [35].

The proton NMR titrations were conducted by the addition of tetrabutylammonium salts TBA^+X^- ($\text{X} = \text{H}_2\text{PO}_4^-$ or PPG^-) to a DMSO-d_6 or DMF-d_7 solutions of the charged receptor and monitoring the shifts in the receptor (host) protons. The starting concentration of the receptor was kept at 0.05M; the initial proton NMR spectrum of the charged receptor was recorded. This was followed by the addition of stoichiometric amounts of the anion. After each addition, the proton NMR profile was recorded and changes in the chemical shifts of the host protons were observed. Although it was presumed that the ammonium protons were the best to monitor, their disappearance after a few additions of the anion made it impossible to follow those protons. However, they did move before complete disappearance showing that they were binding to the anion. Therefore, the methylene protons on the carbon in between the ammonium group and the aromatic ring were monitored. The shifts in the host proton signals together with the

concentrations of the receptor and the anion after each addition was used to estimate the stability or binding constants of the complexes using EQNMR.

Following the proton NMR studies, the charged receptors were subjected to isothermal titration calorimetric studies (ITC) for comparative purposes with the NMR results. Depending on the exothermic/ endothermic nature of the binding event of a particular system, the ITC measures the ΔH specific for the system directly and from that derives the other thermodynamic data as well as the binding constants. Though the binding constants obtained with NMR data are specific to each receptor-anion complex, ITC examines the thermodynamic properties of an entire system including the solvent effects, counter ion effects and other non specific binding events which are very important in determining the binding constant of a receptor-anion complex. Therefore, the binding constant obtained with ITC perhaps is more predictive towards a binding event between a receptor and an anion in in-vivo studies.

3.1 ^1H NMR Studies of Control Receptors with Phosphate anion

It was decided to study the control receptors first to determine the binding stoichiometries between the control receptors and inorganic H_2PO_4^- , as the hypothesis was that the systems which show 1 to 1 binding with inorganic H_2PO_4^- anion would show the same binding stoichiometry with the phosphate anion portion of PPG.

All the proton NMR titration studies were conducted in DMSO-d_6 at 30°C . The first control receptor studied was **49** which had the proper spacer lengths ($n=3$, $m=6$) predicted for 1:1 binding between the receptor and the anion by the CPK models and molecular modeling.

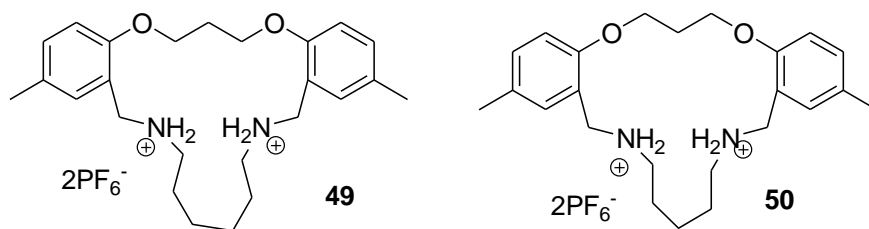


Figure 25. Control receptors with $n=3$

However, with the proton NMR Job plot, the binding stoichiometry of **49** was found to be 1 to 2; one molecule of the receptor bound to two H_2PO_4^- anions as contradictory to what was suggested by molecular modeling. It brought up the question whether $n=3$ was not the optimal spacer length of the ether linkage for 1:1 binding stoichiometry.

The proton NMR titration of the above receptor was conducted and the binding isotherm was obtained.

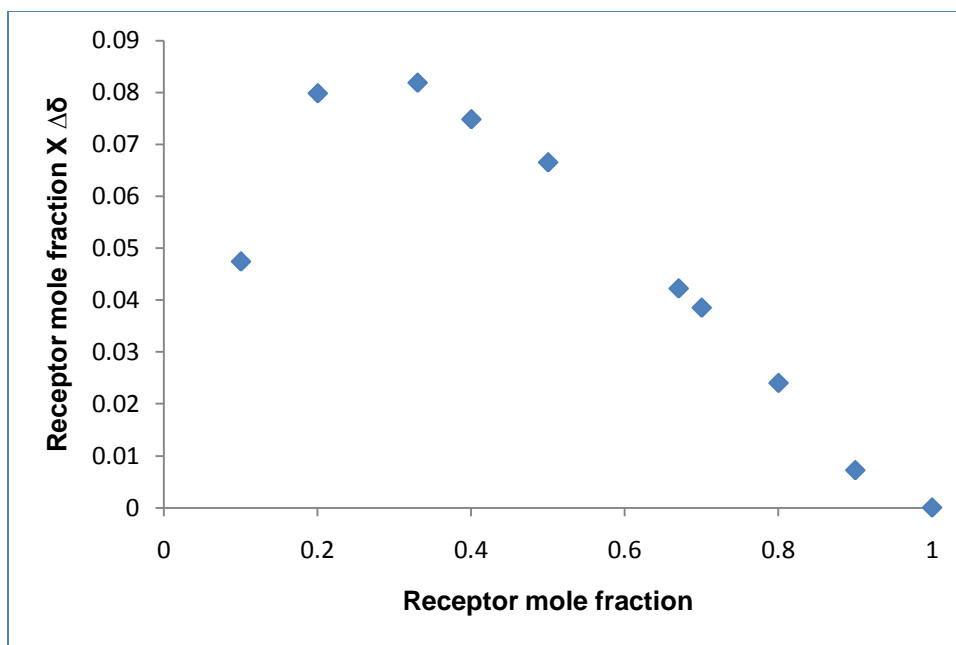


Figure 26. Job plot of **49** - H_2PO_4^- anion complex in DMSO-d_6 at 30°C

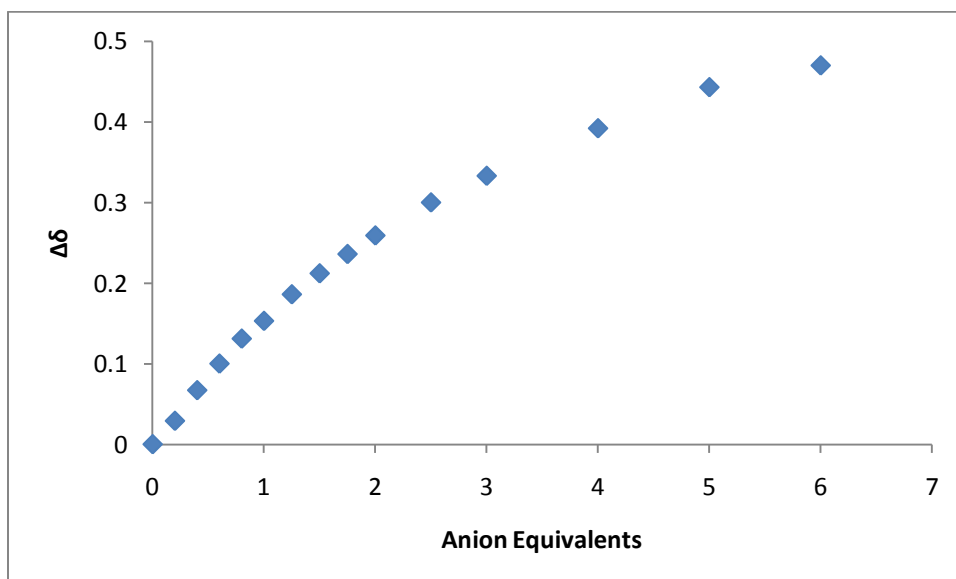


Figure 27. ^1H NMR binding isotherm of **49** with H_2PO_4^- anion in DMSO-d_6 at 30°C

When determining the binding constants, using EQNMR, the inflection point at $x=1$ is generally used as the end point for the proton resonance change in a 1:1 anion- receptor complex.

Since the above curve does not show any inflection points, the EQNMR calculation was carried out with the 1 to 2 binding model [35] using the $\Delta\delta$ value at $x=1$ as the end point for the first saturation. The K_1 and K_2 obtained were 183.43 M^{-1} and 28.06 M^{-1} respectively, with an error of more than 100% in both cases. It was attempted to get logarithmic estimates for K_1 and K_2 by using the method discussed in the doctoral dissertation of Alex Meece [34] which again was unsuccessful. However, as the main focus of this study was to select the receptor system which complexes with the anion in a 1:1 stoichiometry, the studies were continued with the remaining receptor complexes.

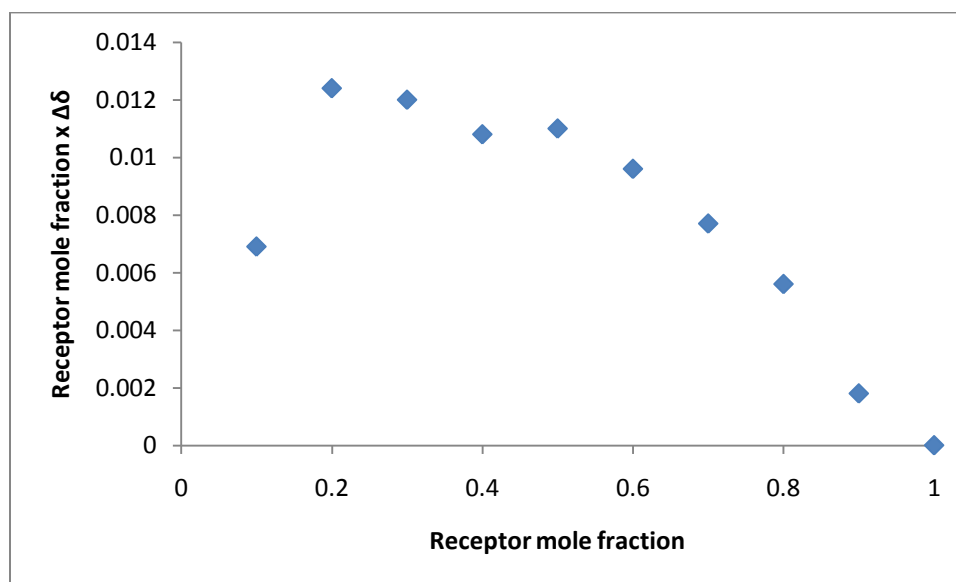


Figure 28. Job plot of **50** - H_2PO_4^- complex in DMSO-d_6 at 30°C

The proton NMR Job plot of the control receptor **50** ($n=3$ and $m=5$), showed several binding stoichiometries and the system was not well behaved. Figure 28 shows the job plot of the complex **50** and figure 29 shows the binding curve. The EQNMR calculations were not done with this particular system as it was not possible to fit the data to any of the available binding models.

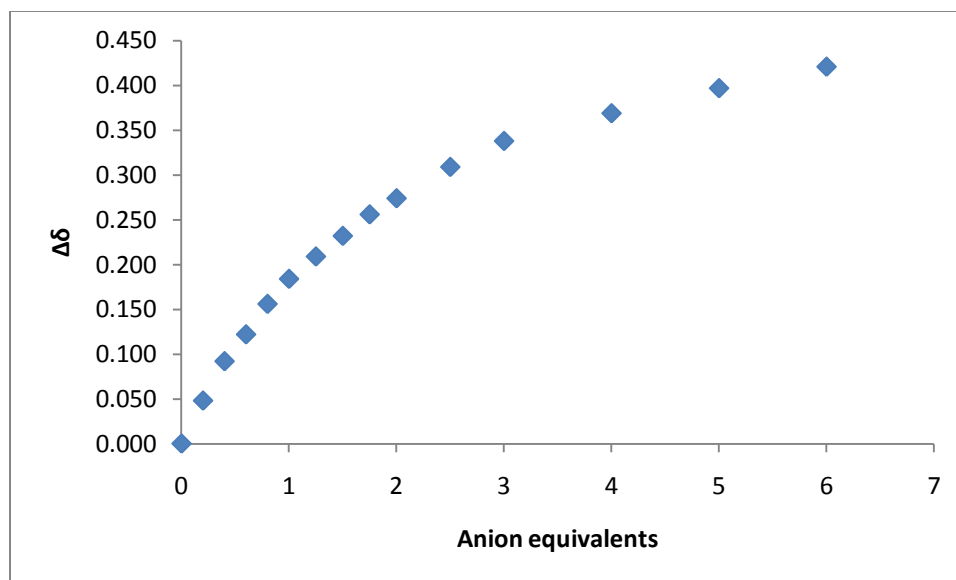


Figure 29. ^1H NMR titration curve of **50** with H_2PO_4^- in DMSO-d_6 at 30°C

Both control receptors studied so far, which had $n=3$ did not give 1:1 binding stoichiometry with dihydrogen phosphate anions. That suggested either our modeling was incorrect or it was not the length of the ether linkage which determines the binding stoichiometry between the receptor and the anion at least when the anion is inorganic H_2PO_4^- . Since it was not possible to synthesize the $m=3$ or $m=4$ receptors with $n=3$ (discussed in the previous chapter), studies proceeded with the $n=4$ receptors shown in figure 30.

The Job plot of receptor **45** ($n=4$ and $m=6$), resulted in the same binding stoichiometry as with the receptor **49** ($n=3$ and $m=6$) which implied the length of the second alkyl linkage was important in the binding stoichiometry due to the fact that both above receptors had the same spacer lengths “ m ” and they both showed the same binding stoichiometries with dihydrogen phosphate anions.

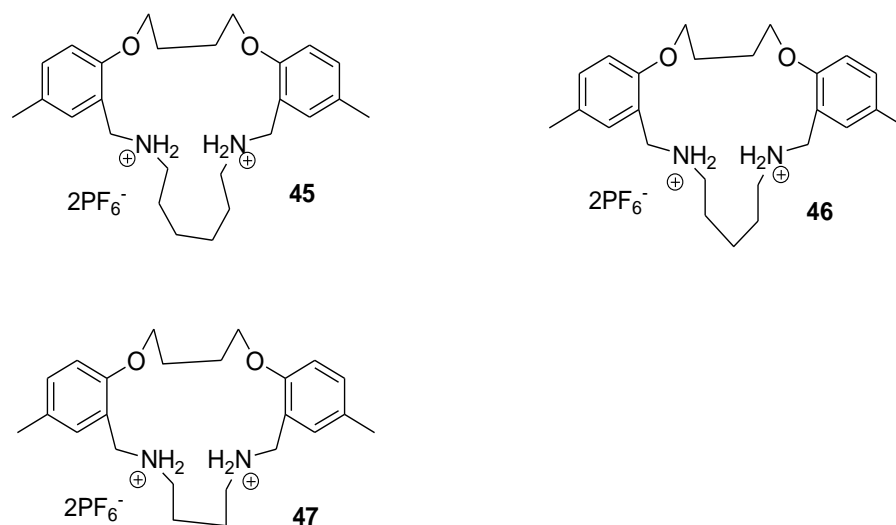


Figure 30. Control receptors with $n=4$

The proton NMR titration curve of the receptor **45** also showed a similar shape to that of the receptor **49**. EQNMR calculation of **45** was done with the 1 to 2 model as described above, the values obtained for K_1 and K_2 were 183.43 M^{-1} and 28.06 M^{-1} respectively, with associated errors exceeding 100 percent as with the receptor **49**. Attempts to fit the data to get logarithmic estimates as described earlier again were unsuccessful.

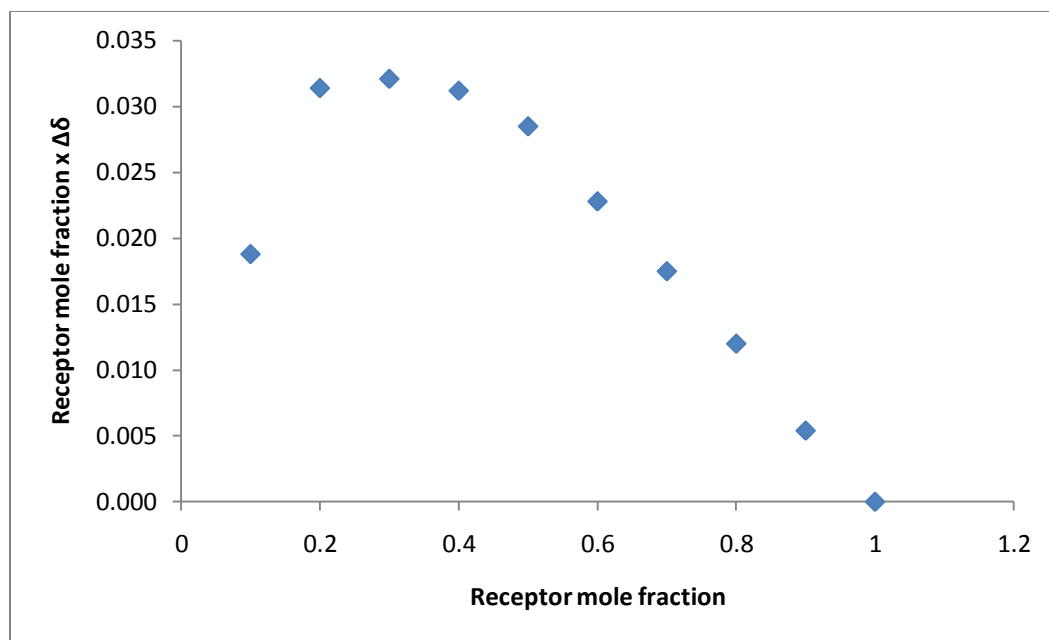


Figure 31. Job plot of **45** - H_2PO_4^- complex in DMSO-d_6 at 30°C

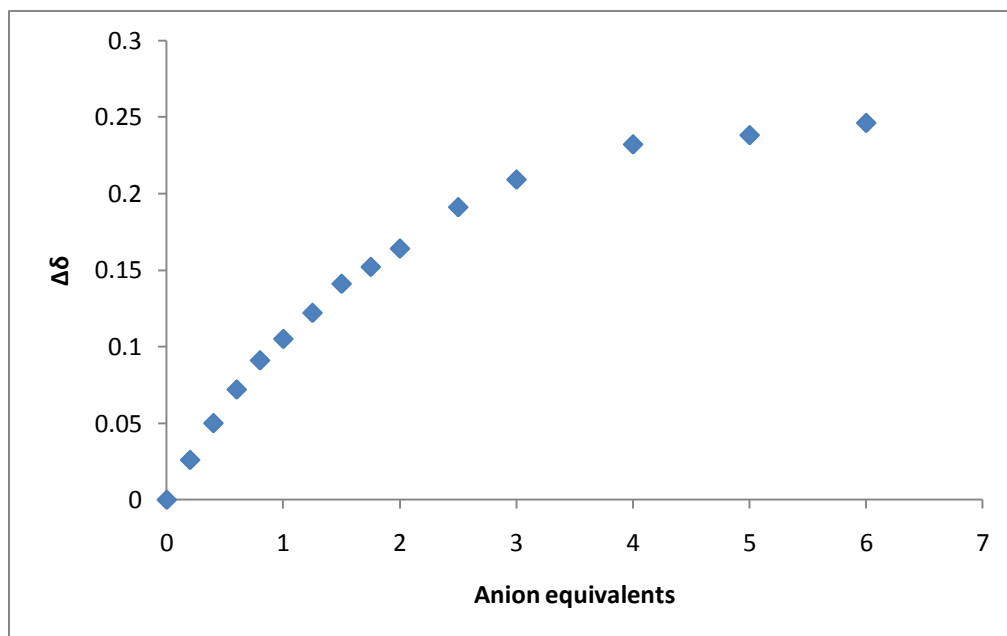


Figure 32. ^1H NMR titration curve of **45** with H_2PO_4^- in DMSO-d_6 at 30°C

Growing a single crystal of the receptor **45**- H_2PO_4^- complex, followed by x-ray crystallography revealed the structure presented in figure 33 which shows that one charged receptor molecule does binds with two H_2PO_4^- anions which corroborated Job plot data. A chloroform molecule too was present in the system; CHCl_3 was used as one of the solvents used in the crystallization by slow diffusion.

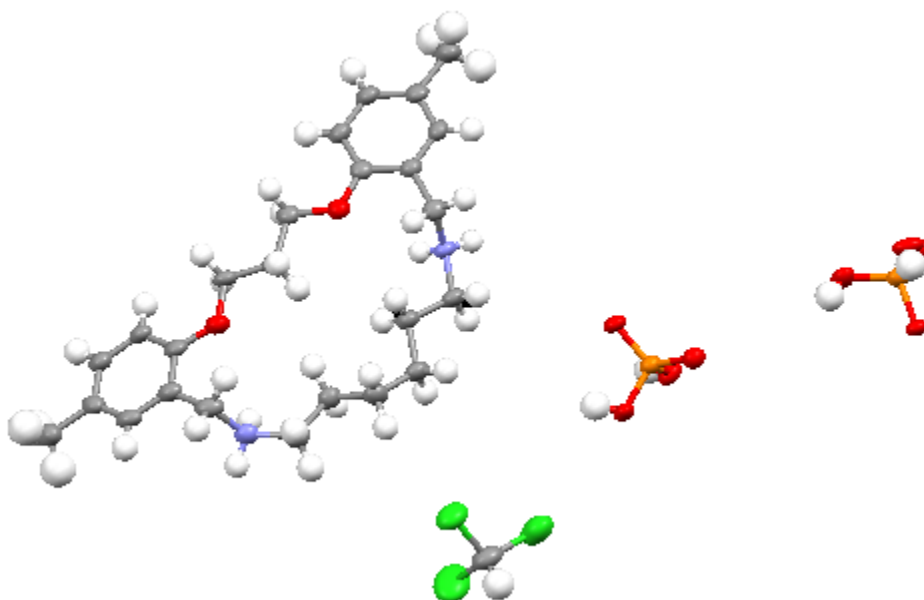


Figure 33. The x-ray crystal structure of the **45**- H_2PO_4^- complex

At this point of time, with the proof of the Job plot data and x-ray crystallography, it was decided that when $m=6$, the distance between the two ammonium groups present in the receptor was too far apart to bind with just one H_2PO_4^- anion, but was optimal to bind with two H_2PO_4^- anions. So it was suggested that the length of the second alkyl linker with the ammonium “ m ”, not the length of the ether linker “ n ”, was important in determining the binding stoichiometry of the receptor-anion complex.

The proton NMR studies of the receptor **46** ($n=4$ and $m=5$) showed comparable results to those obtained with the receptor **50** ($n=3$ and $m=4$): the Job plot showed mixed binding and the titration curve had a similar shape. The EQNMR calculations were not done with this system due to the same reasons mentioned with receptor **50**.

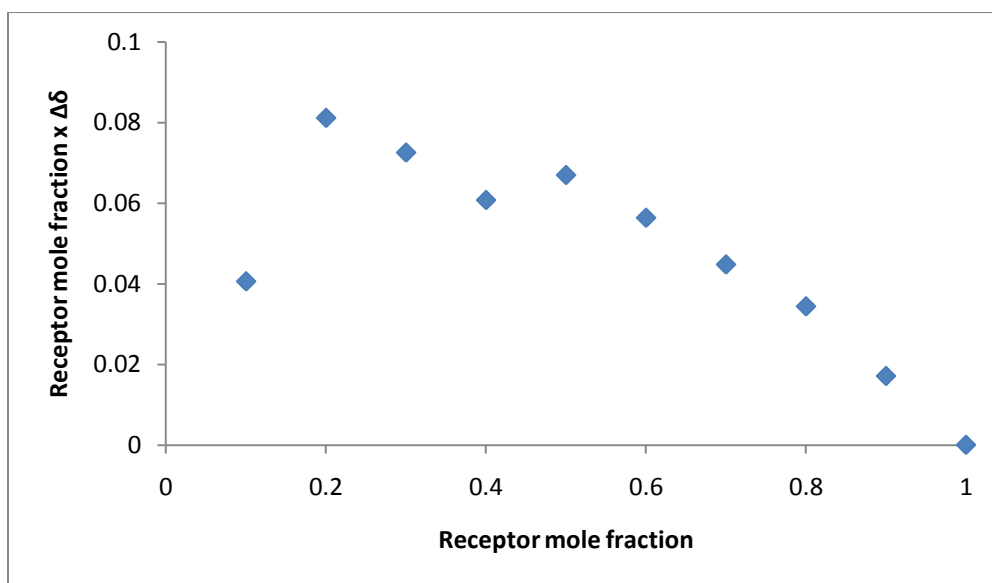


Figure 34. Job plot of **46** - H_2PO_4^- complex in DMSO-d_6 at 30°C

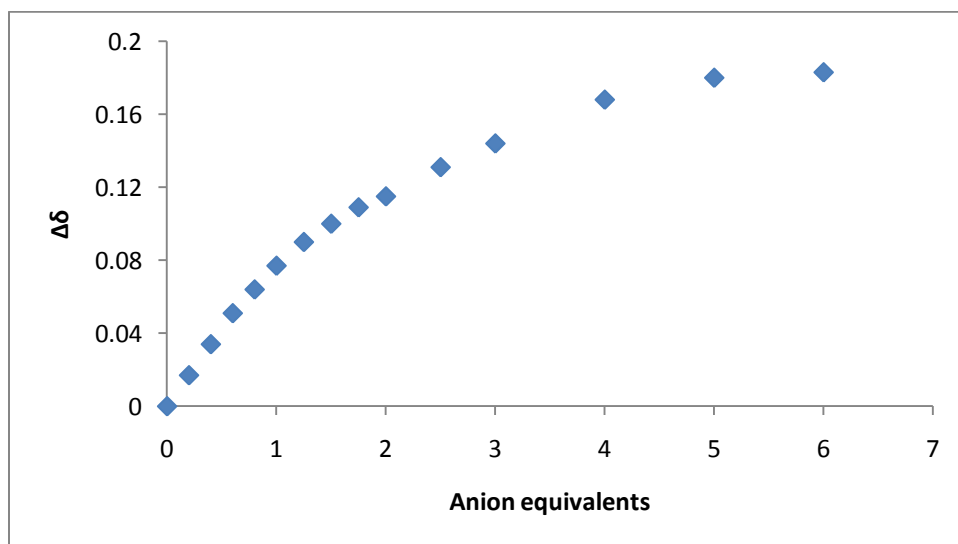


Figure 35. ^1H NMR titration curve of **46** with H_2PO_4^- in DMSO-d_6 at 30°C

Unlike with any of the previous receptors **45**, **46**, **49** or **50**, the Job plot of the receptor **47** showed a strong 1: 1 binding stoichiometry with H_2PO_4^- anion in DMSO-d_6 at 30°C .

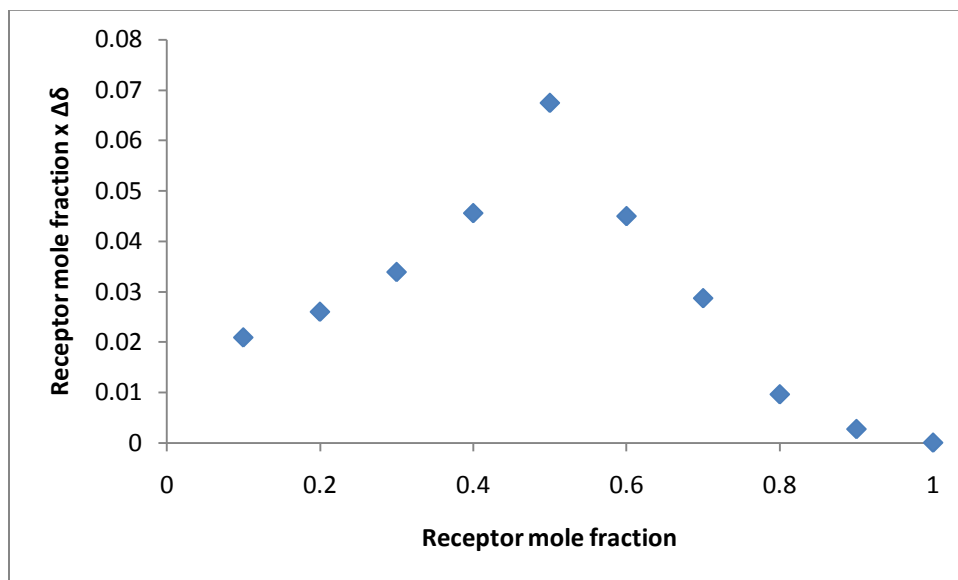


Figure 36. Job plot of **47** - H_2PO_4^- complex in DMSO-d_6 at 30°C showing 1 to 1 binding

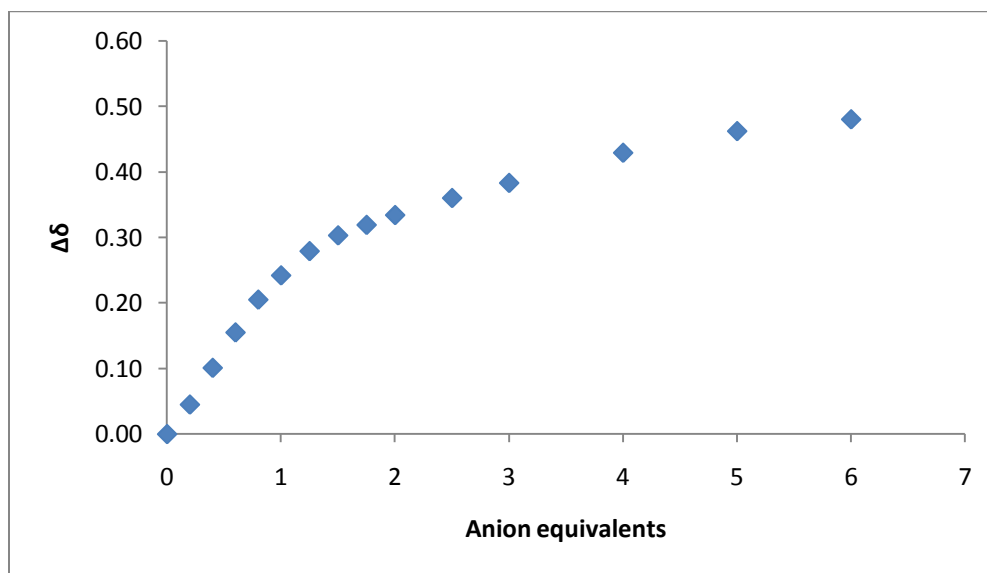


Figure 37. ^1H NMR titration curve of **47** with H_2PO_4^- in DMSO-d_6 at 30°C

Following the Job plot, this complex too was subjected to proton NMR titration studies. The binding constant estimated with the use of EQNMR with the 1 to 1 binding model was 694.15M^{-1} with only a 9% error. The binding constant obtained was realistic and binding strength was moderate.

With the results obtained for the receptor **47** ($n=4$ and $m=4$), we were able to draw some important conclusions about the factors which determine the binding stoichiometry between the control/ functionalized receptors and the phosphate anions. As discussed earlier, when $m=6$, the distance between the two ammonium groups of the receptor was large, it could bind with two H_2PO_4^- anions. When $m=4$, the said distance was short making it possible for the system to show 1:1 binding stoichiometry, thus making $m=5$ in between, resulting in a mixed binding stoichiometry.

It was obvious that the length of the ether linker “n” was not the determining factor when it comes to binding with inorganic H_2PO_4^- . However, “n” was important in the synthesis of the receptor molecules. When “n” was 3 or 4, it was not possible to synthesize receptors with $m=3$ or 4. Hence during the synthesis, the length “n” controls the flexibility of the two ring system and there by dictates second imine formation. Complexes **54** ($n=5$ and $m=3$) and **56** ($n=5$ and $m=4$) were synthesized in order to prove the above point. In addition, it gave a receptor system with $m=3$ for the study. The figure 38 gives the structures of the receptors **54** and **56**.

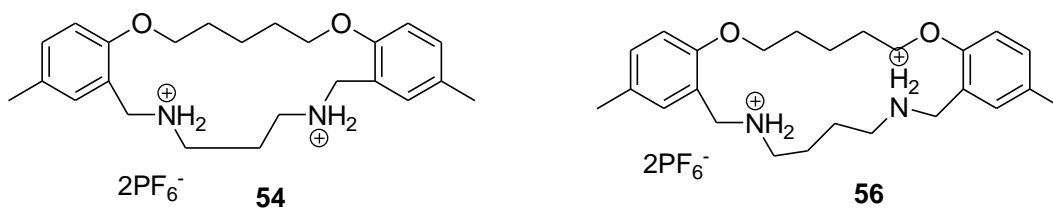


Figure 38. Control receptors with $n=5$

As expected, the Job plots with both **54** and **56** showed 1 to 1 binding stoichiometry with the dihydrogen phosphate anion proving the point that it was the distance between the two ammonium groups in the second alkyl linker “m” which determined the binding stoichiometry with inorganic H_2PO_4^- anion not the length of the ether linker “n”. The ability to synthesize receptors **54** and **56** with $m=3$ and $m=4$ utilizing the corresponding compounds with $n=5$ proved the fact that “n” was the factor which determined the flexibility of the molecule in the synthesis.

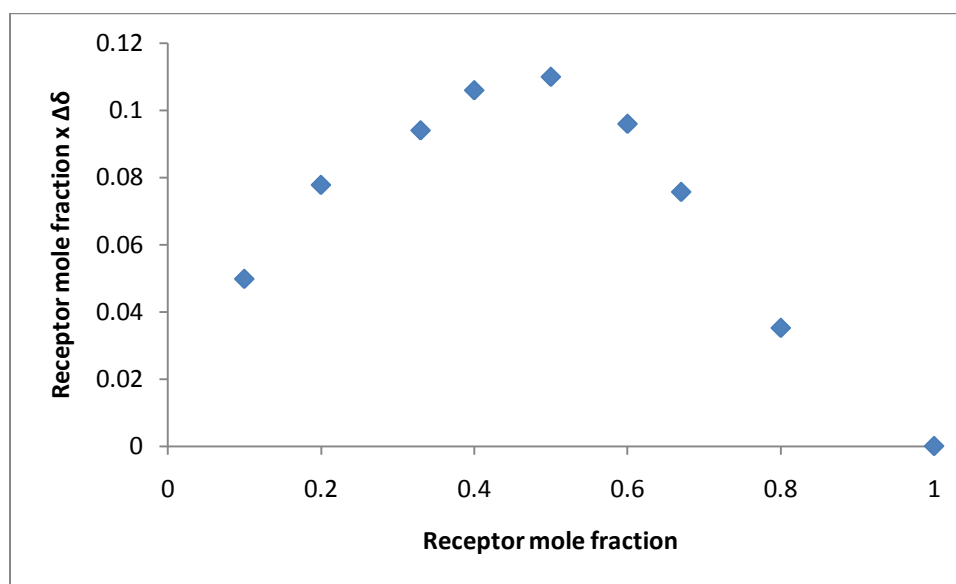


Figure 39. ^1H -NMR Job plot of **54** - H_2PO_4^- complex in DMSO-d_6 at 30°C

The EQNMR estimated a binding constant value of 641.79 M^{-1} with a 21% error for the receptor **54** with the use of the 1 to 1 binding model. Again the binding was moderately strong, but the trend was in good agreement with what was predicted.

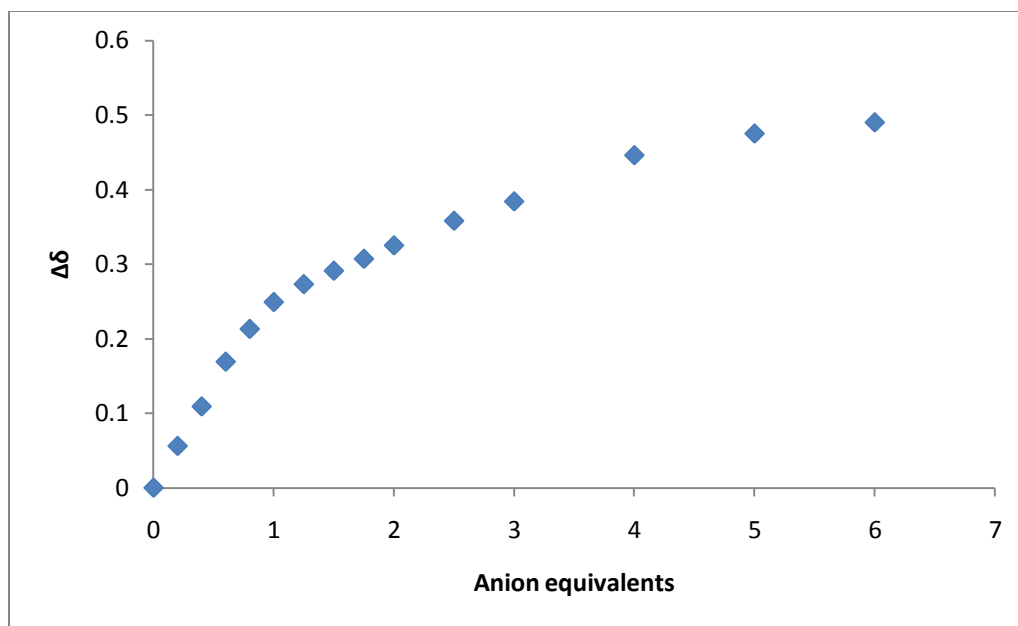


Figure 40. ^1H NMR titration curve of **54** with H_2PO_4^- in DMSO-d_6 at 30°C

Similar to the receptors **47** and **54**, the Job plot of receptor **56** resulted in 1:1 binding stoichiometry between the receptor and the dihydrogen phosphate anion and the EQNMR estimated a binding constant of 422.14 M^{-1} with a 13% error, which showed a moderately strong binding.

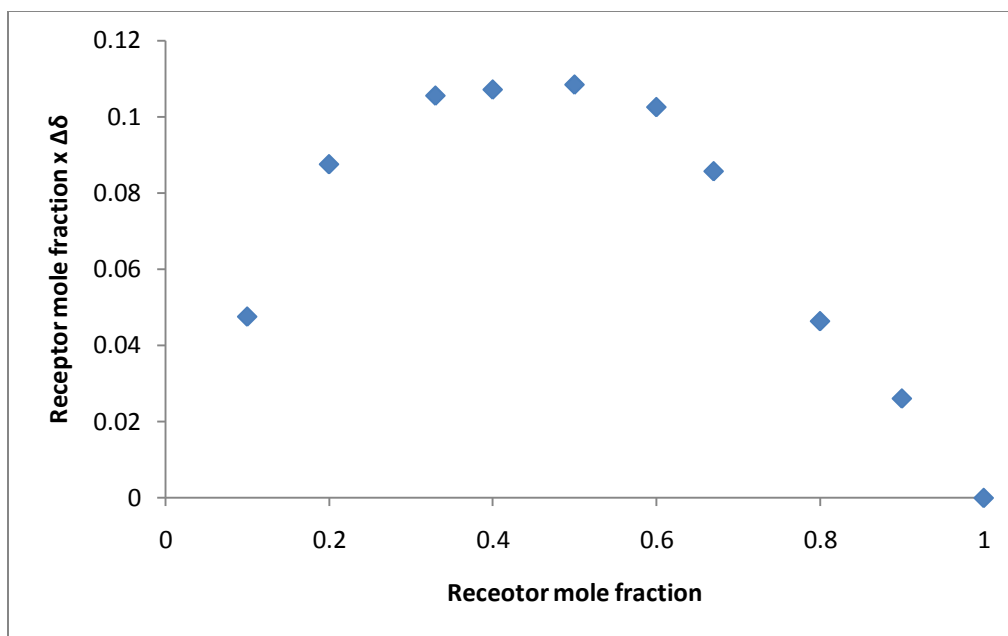


Figure 41. ^1H NMR Job plot of **56** - H_2PO_4^- complex in DMSO-d_6 at 30°C

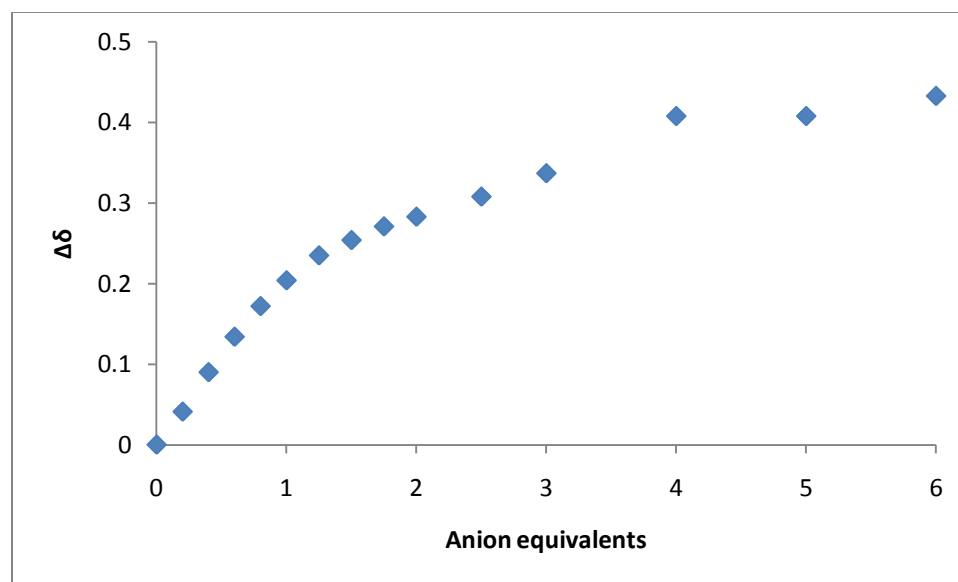


Figure 42. ^1H NMR titration curve of **54** with H_2PO_4^- in DMSO-d_6 at 30°C

Table 9 summarizes the binding stoichiometry obtained with Job plots and the binding constants estimated with EQNMR calculations for the charged control receptors studied.

TABLE 9
RESULTS OF ¹H NMR STUDIES OF CONTROL RECEPTORS with H₂PO₄⁻ anion

Receptor	Binding pocket size	Binding stoichiometry	Binding constant M ⁻¹	Error
49	n=3, m=6	1:2	K ₁ = 183.43 K ₂ = 28.06	>100 %
50	n=3, m=5	mixed	-	-
45	n=4, m=6	1:2	K ₁ = 183.43 K ₂ = 28.06	>100 %
46	n=4, m=5	mixed	-	-
47	n=4, m=4	1:1	694	9 %
54	n=5, m=3	1:1	642	21 %
56	n=5, m=4	1:1	422	13 %

- Overall the ¹H NMR titration studies of the model complexes with inorganic H₂PO₄⁻ anion helped to recognize the importance of the length of the ether linker “n” and the length between the two ammonium groups in the second alkyl linker “m” in the synthesis and in determining the binding stoichiometries respectively. Contradictory to the initial prediction, it was concluded that the length “m”: was the factor which determined the binding stoichiometry, not “n”. But in the synthesis the formation of length m=3 or m=4 receptors were dependant on the length “n”.
- Based on the results from the Job plots, the three receptors which had shown 1 to 1 binding stoichiometry with inorganic H₂PO₄⁻ anion (**47**, **54** and **56**) were chosen as

having the best binding pocket structures for the anionic phosphate head group of the PPG. The hypothesis was that the structure of the binding pocket found effective for binding one inorganic dihydrogenphosphate anion would bind effectively with one anionic phosphate head group of the PPG.

3.2 ITC Titrations of Control Receptors with Dihydrogenphosphate Anion

As noted earlier, all the control receptors synthesized were subjected to isothermal calorimetric studies with the inorganic dihydrogenphosphate anion (H_2PO_4^-) in order to compare with the results from ^1H NMR spectroscopic studies. All the ITC studies were done at 30°C using DMSO as the solvent.

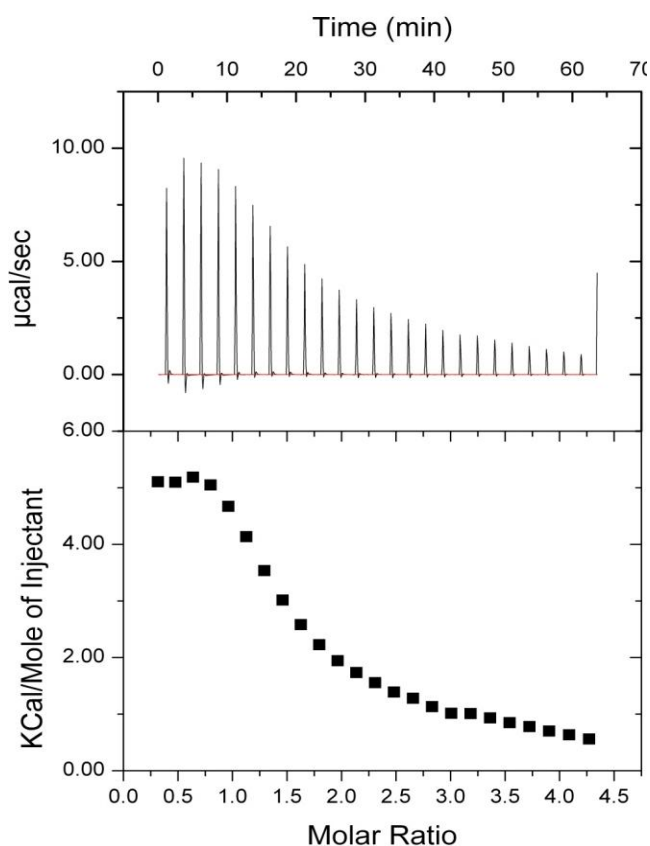


Figure 43. ITC curve of receptor **49** with H_2PO_4^- at 30°C in DMSO

Figure 43 shows the ITC titration curve for the receptor **49** which was an endotherm. When analyzed with two binding sites model, it generated the thermodynamic data without problems. The K_1 and K_2 obtained were $1.38 \times 10^5 \text{ M}^{-1}$ with a 23% error and $5.77 \times 10^3 \text{ M}^{-1}$ with a 21% error. The ΔH values obtained were 5521 cal/mole with a 3% error and 1501 cal/mole

with a 34% error for the first and second binding respectively. The ΔS for the first binding was 41.8 cal/ mol/°C and that for the second binding was 22.2 cal/ mol/°C.

Isothermal calorimetric titration of the receptor **50** with the dihydrogen phosphate anion generated the curve shown in figure 44. When analyzing the titration data, there was a confusion of whether to use the model with one binding site or the one with two binding sites, because the ^1H NMR Job plot resulted in mixed binding for this receptor. Therefore, attempts were taken to analyze the data using both above models. However the data obtained did not make it clear whether it was binding in a 1:1 or a 1:2 stoichiometry. The ΔS for the binding suggested that the binding was entropy driven.

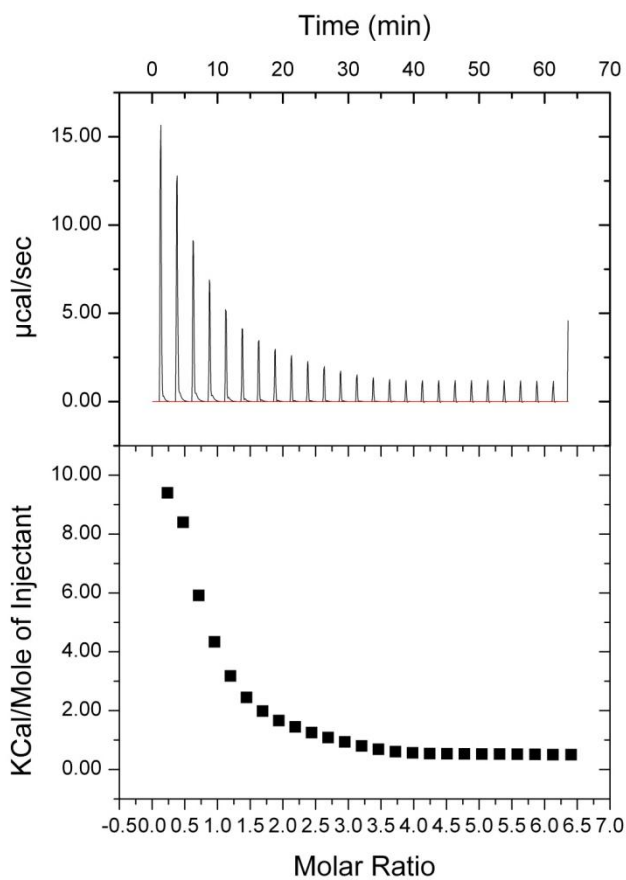


Figure 44. ITC curve of the receptor **50** with H_2PO_4^- at 30°C in DMSO

ITC curves of receptor **45** and **46** looked similar to those of **49** and **50**. With **45**, The K_1 and K_2 obtained were $6.60 \times 10^5 \text{ M}^{-1}$ with a 26% error and $1.84 \times 10^4 \text{ M}^{-1}$ with a 27% error. The ΔH values obtained were 4024 cal/mole with a 1% error and 439 cal/mole with an 8% error for the first and second binding respectively. The ΔS for the first binding was 39.9 cal/ mol/ $^\circ\text{C}$ and that for the second binding was 21 cal/ mol/ $^\circ\text{C}$.

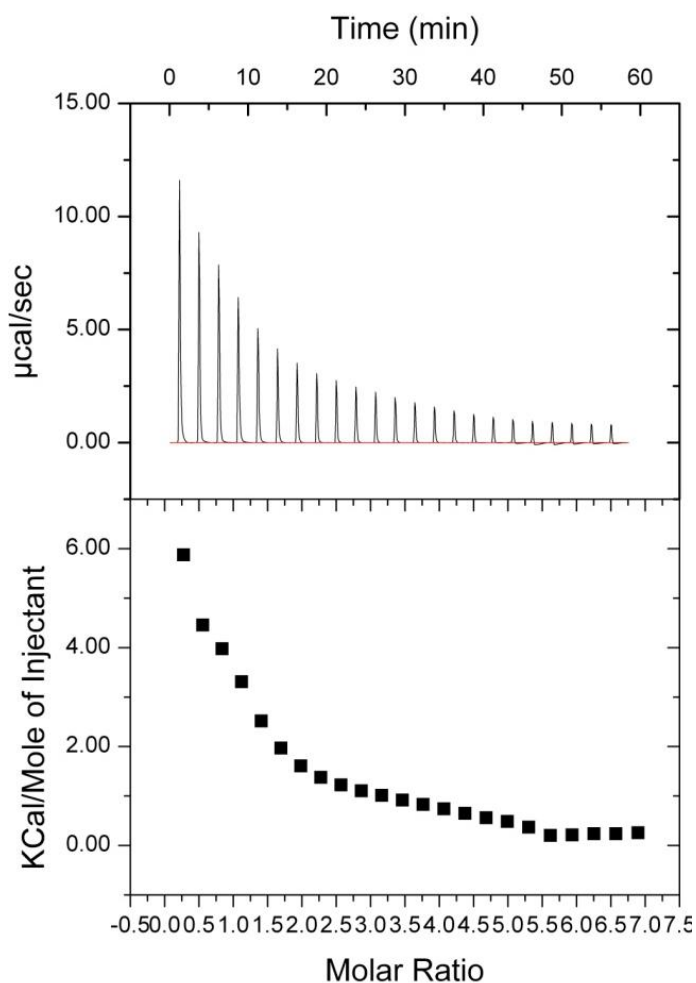


Figure 45. ITC curve of receptor **45** with H_2PO_4^- at 30°C in DMSO

Similar to receptor **50**, receptor **46** also showed mixed binding with the ^1H NMR Job plot study. Therefore it was difficult to fit the ITC data in to a suitable binding site model. In

accordance with the previous receptors studied, the ΔS obtained suggested the binding was entropy driven.

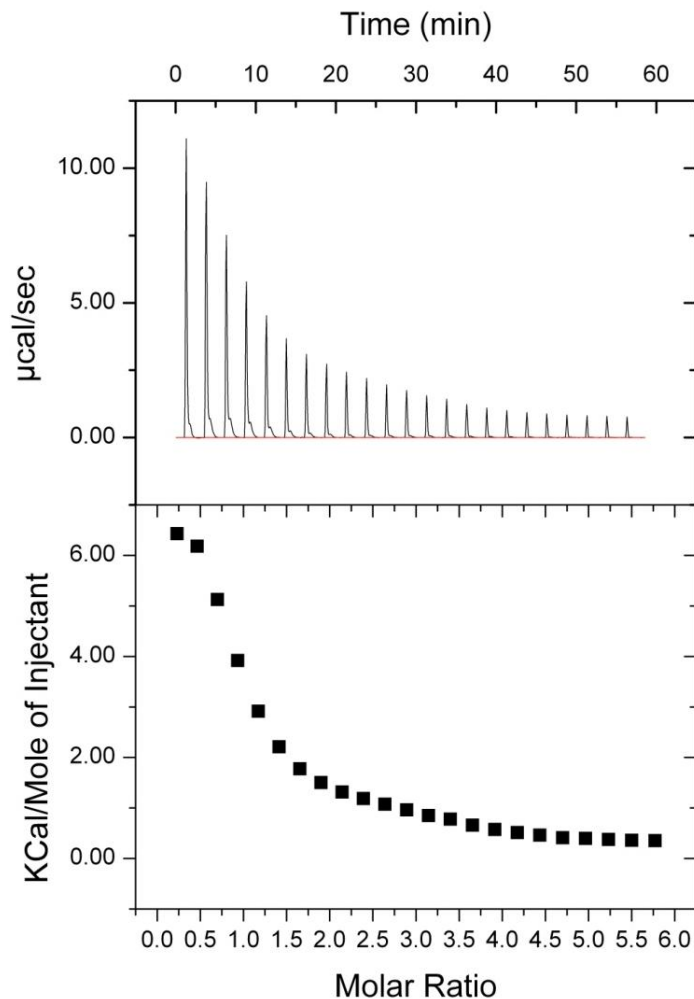


Figure 46. ITC curve of the receptor **46** with H_2PO_4^- at 30°C in DMSO

The ITC curve of the receptor **47** ($n=4$, $m=4$), which showed a 1:1 binding stoichiometry with NMR spectroscopic data showed a steeper endotherm compared to the other ITC curves. When fitted to the model with one binding site, it produced a K value of $4.67 \times 10^4 \text{ M}^{-1}$ with 10% error, a ΔH value of 11960 cal/ mole with 2% error and a ΔS value of $60.8 \text{ cal/ mol/}^\circ\text{C}$.

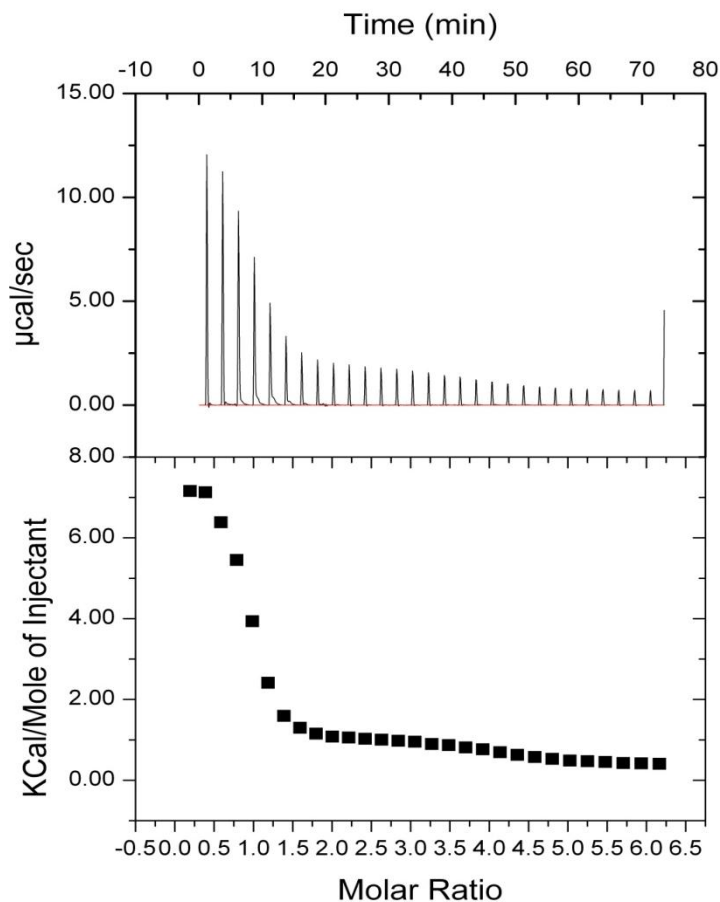


Figure 47. ITC curve of the receptor **47** with H_2PO_4^- at 30°C in DMSO

The ITC curves of the receptor **54** and **56** exhibited the same trend as with **47**. The model with one binding site was fitted well with the experimental data generated with both above compounds resulting a K value of $1.01 \times 10^5 \text{ M}^{-1}$ with 6% error, a ΔH value of 7318 cal/ mole with 1% error and a ΔS value of 47 cal/ mol/ $^\circ\text{C}$ for **54** and a K value of $1.06 \times 10^5 \text{ M}^{-1}$ with 9% error, a ΔH value of 4972 cal/ mole with 1% error and a ΔS value of 39.4 cal/ mol/ $^\circ\text{C}$ for **56**.

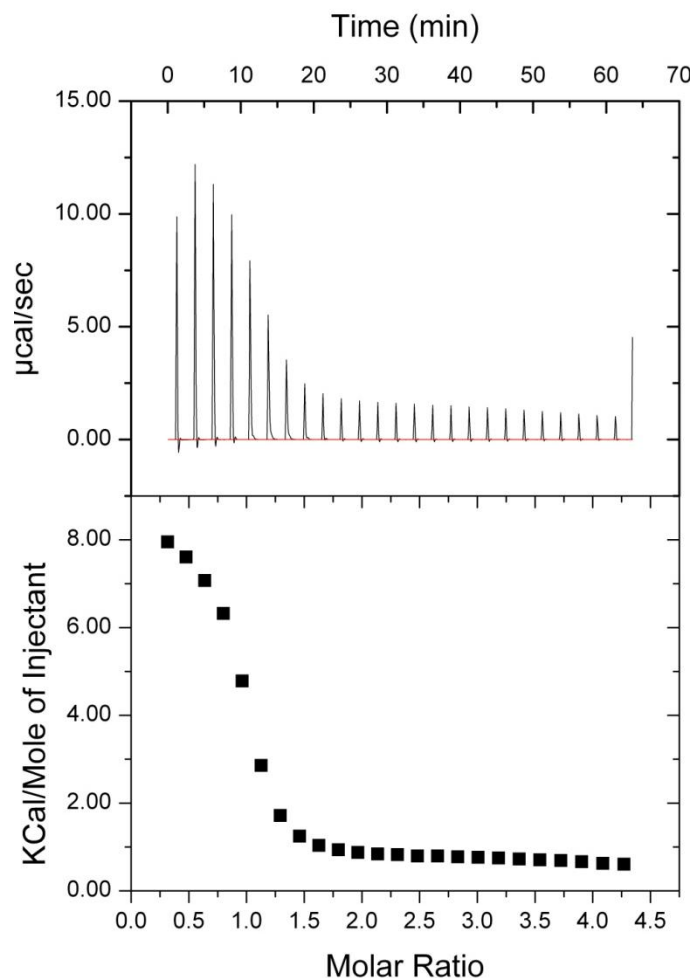


Figure 48. ITC curve of the receptor **54** with H_2PO_4^- at 30°C in DMSO

For convenience, ITC titrations data of the control receptors with inorganic H_2PO_4^- at 30°C in DMSO are summarized in table 10. The systems which showed 1:1 binding are given in bold numbers.

- The binding constants obtained with ITC studies were 2-3 orders of magnitude greater than those obtained with comparable ^1H NMR spectroscopic titrations with all the receptors studied. This was expected as the two methods look at the system in two different manners: The NMR gives information specific to a receptor-anion complex while ITC examines the thermodynamic properties of an entire system including the

solvent effects, counter ion effects and other non specific binding events which are very important in determining the binding constant of a receptor-anion complex.

TABLE 10

ITC RESULTS OF CONTROL RECEPTORS WITH H_2PO_4^- ANION AT 30°C IN DMSO

Receptor	K M^{-1}	Error %	ΔH Cal/mol	Error %	ΔS cal/ mol/°C
45	6.60×10^5	26	4024	1	39.9
	1.84×10^4	27	439.3	8	21
46	mixed	-	-	-	-
47	4.67×10^4	10	11960	2	60.8
49	$K_1=1.38 \times 10^5$	23	5521	3	41.8
	$K_2= 5.77 \times 10^3$	21	1501	34	22.2
50	mixed	-	-	-	-
54	1.01×10^5	6	7318	1	47
56	1.06×10^5	9	4972	1	39.4

- The thermodynamic data suggests that the binding process for all above receptors with H_2PO_4^- anion was entropy driven (ΔS positive), which is the usual case for charged systems in polar solvents.
- The receptors which exhibited 1:1 binding stoichiometry with dihydrogen phosphate anion resulted higher ΔS and ΔH values compared to other receptors while receptor **47** showed the highest values proving it had the best binding pocket structure.

3.3 NMR and ITC Studies of Selected Control Receptors with PPG anion

Following the ^1H NMR and ITC titrations of the control receptors with inorganic H_2PO_4^- anion, the three receptors which showed 1:1 binding stoichiometry with the said anion were chosen for further studies with TBA salt of the PPG anion.

According to the initial hypothesis, the control receptors which bound to the inorganic dihydrogen phosphate anion in a 1:1 stoichiometry contained the best binding pocket structure for the anionic phosphate head portion of the PPG molecule. In this particular study, the chosen receptors were titrated with TBA salt of the PPG anion at 40°C in DMF. Though the solvent of choice was DMSO, it was necessary to use DMF due to solubility problems associated with PPG anion, and the temperature had to be increased up to 40°C due to the same reason. Since the dielectric constants of the two solvents used were not very different, it was assumed that both DMSO and DMF would have the same solvent effects towards the receptors studied.

The Job plot obtained by the titration of the receptor **47** with the PPG anion at 40°C in DMF is shown in figure 49. As expected, it showed one to one binding with the PPG anion proving our hypothesis about the binding pocket structure was correct. Following the Job plot studies, the ^1H NMR spectroscopic titration of the receptor with the PPG anion was carried out. The EQNMR calculations with one binding site model estimated K of 260.78 M^{-1} with a 7% error which was moderate binding. The binding constant estimated above was less than half of what was estimated with the inorganic dihydrogen phosphate anion, for the same receptor. But considering the facts that the absence of functional groups bind with glycerol hydroxyl groups in the control receptor and the bulkiness of the PPG anion, the K value obtained was accepted. Figure 50 shows the titration curve of the receptor **47** with PPG anion.

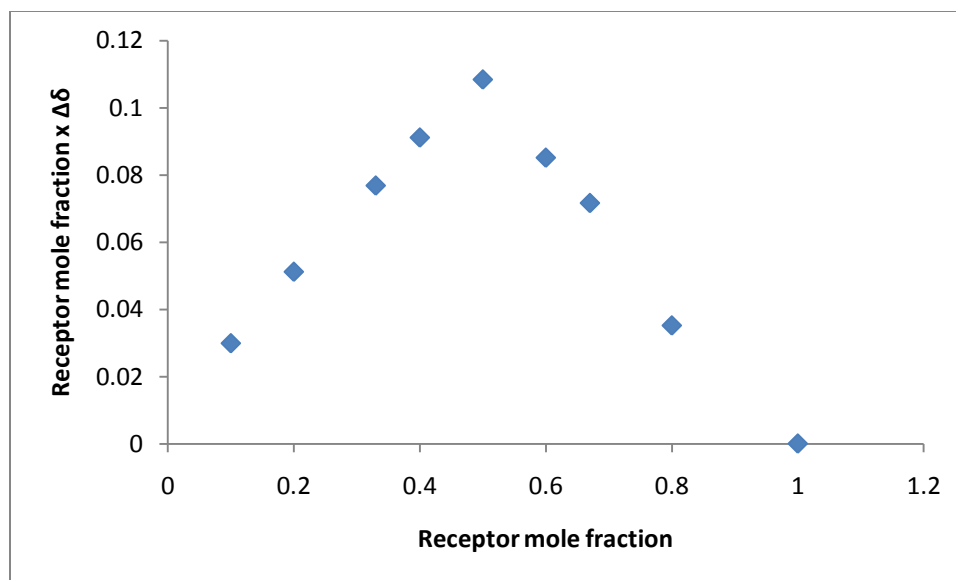


Figure 49. Job plot of **47** – PPG anion complex in DMF-d₇ at 40°C

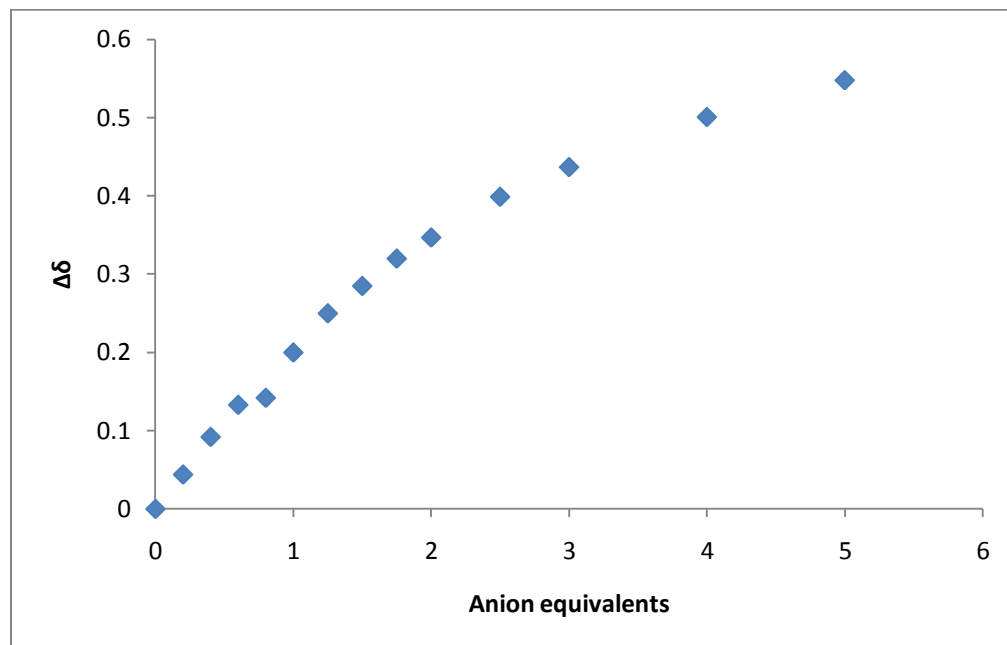


Figure 50. ¹H NMR titration curve of **47** with PPG anion in DMF-d₇ at 40°C

Following the above result, the receptor **54** (n=5, m=3), was subjected to ¹H-NMR spectroscopic and ITC titrations with the PPG anion. This again showed one to one binding

stoichiometry with the PPG anion confirming our hypothesis about the binding pocket structure was correct. Figure 51 shows the ^1H NMR titration curve of the complex **54** with the PPG anion. The EQNMR calculation estimated a K value of 202.45 M^{-1} with a 0.1% error for this system which was again moderately strong binding. The K value estimated for the receptor **54** with dihydrogen phosphate anion was 642 M^{-1} which was three times greater than that with the PPG. However, due to the same reasons described above, the estimated K value was considered consistent.

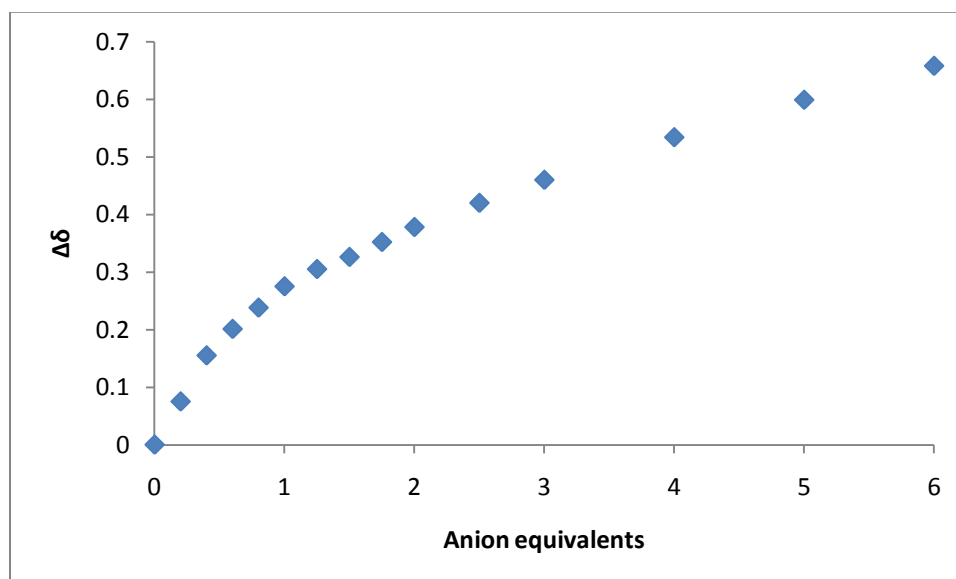


Figure 51. ^1H NMR titration curve of **54** with PPG anion in DMF-d_7 at 40°C

So far, the control receptor systems which showed one to one binding stoichiometry with inorganic H_2PO_4^- anion exhibited the same binding stoichiometry with the PPG anions as well. However, it was decided to study either the receptor **46** or **50** which showed mixed binding stoichiometries with dihydrogen phosphate anion, with anionic PPG considering the fact that there was a possibility for those two receptors to bind with the PPG anion in a 1 to 1 stoichiometry due to the bulkiness of it. But the job plot of the receptor **46** ($n=4$, $m=5$) with PPG

anion, figure 52 showed it was not well behaved. Therefore further studies were not carried out with those receptors which resulted mixed binding stoichiometries with the inorganic H_2PO_4^- anion.

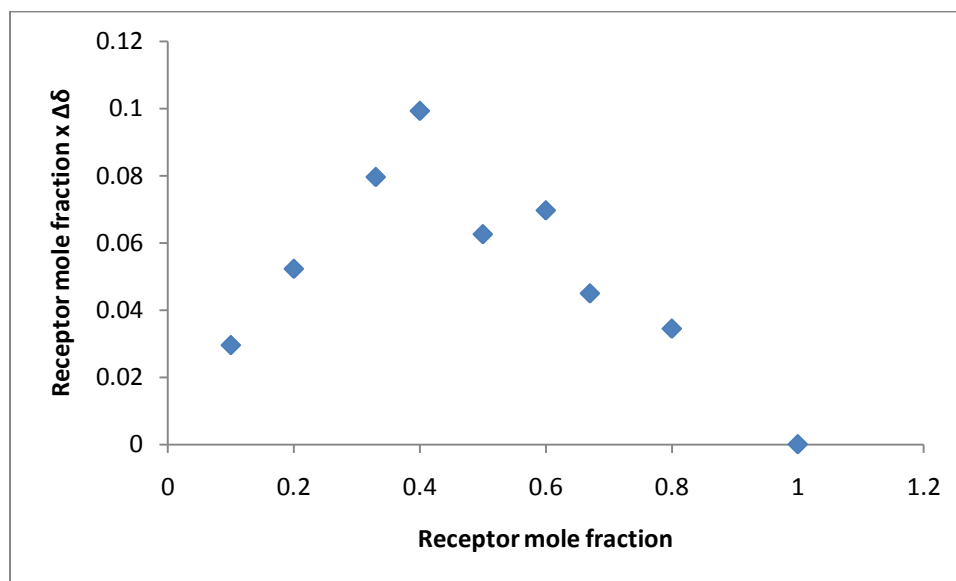


Figure 52. Job plot of **46** – PPG anion complex in DMF- d_7 at 40°C

Following the ^1H NMR titrations of the selected control receptors with the PPG anion, they were subjected to ITC studies. All the ITC experiments were done in DMF at 40°C. Figure 53 shows the ITC titration curves obtained for the receptor **47** ($n=4$, $m=4$) and **54** ($n=5$, $m=3$) respectively. Table 11 and 12 summarize the results from the proton NMR and ITC studies of the selected control receptors with PPG anion at 40°C in DMF.

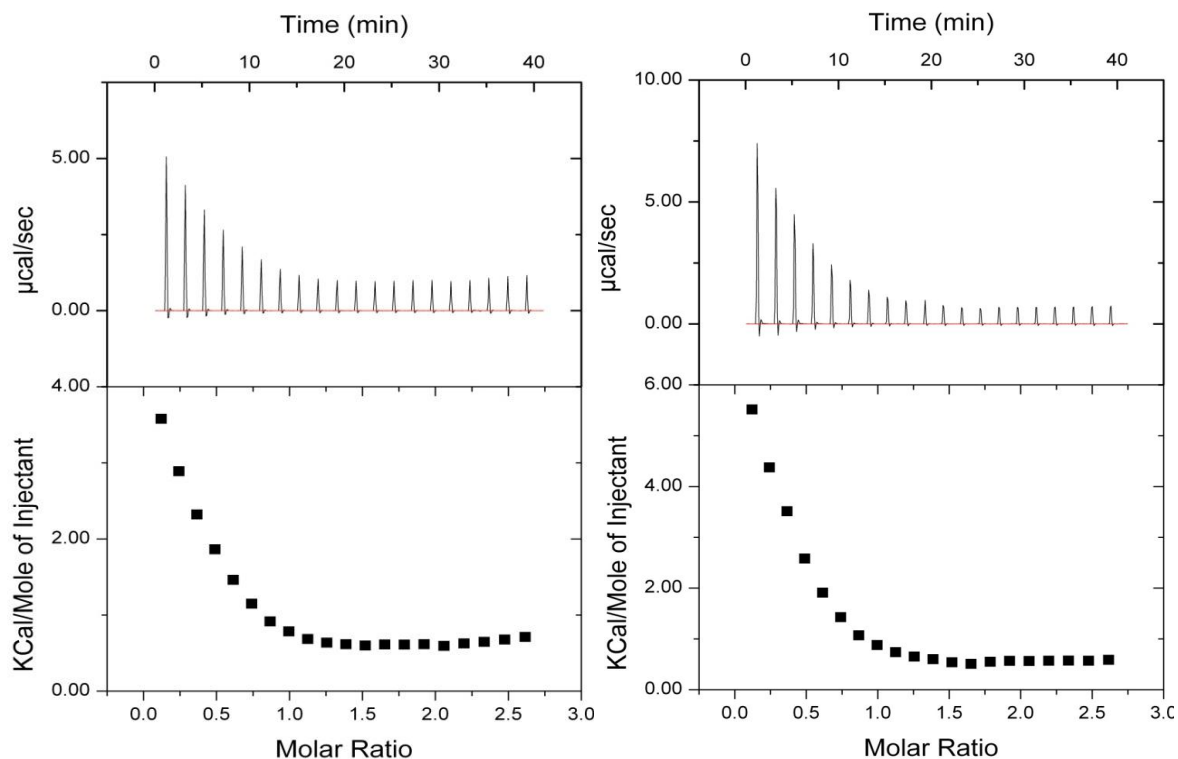


Figure 53. ITC titration curves of the receptor **47** and **54** respectively with PPG anion at 40°C in DMF

TABLE 11

¹H NMR TITRATION RESULTS OF THE SELECTED CONTROL RECEPTORS WITH PPG ANION AT 40°C IN DMF

Receptor	Binding pocket size	Binding stoichiometry	Binding constant M ⁻¹	Error
46	n=4, m=5	mixed	-	-
47	n=4, m=4	1:1	261	7 %
54	n=5, m=3	1:1	202	0.1 %

TABLE 12

ITC TITRATION RESULTS OF THE SELECTED CONTROL RECEPTORS WITH PPG ANION AT 40°C IN DMF

Model complex	K M ⁻¹	Error %	ΔH Cal/mol	Error %	ΔS cal/ mol/°C
47	2.26 X 10 ⁴	27	2746	12	28.7
54	4.06 X 10 ⁴	16	4214	5	34.5

- Based on the ¹H NMR titration studies between the selected control receptors and the PPG anion, it was confirmed that the hypothesis about binding pocket size: the systems which give 1 to 1 binding stoichiometry with inorganic H₂PO₄⁻ would show the same binding stoichiometry with the phosphate head group of the PPG anion, was correct.
- With both anions studied, the binding constants obtained for the receptor **47** and **54** by EQNMR calculations were comparable, even though the values obtained with dihydrogen phosphate anion were 2-3 times greater than those obtained with the PPG anion.
- ITC titrations estimated comparable binding constants for both the receptors **47** and **54** with each anion, and they were 2 to 3 orders of magnitude greater than those obtained with the EQNMR calculations giving an insight in to the entire system including the solvent effects, counter ion effects and other non specific binding events.

3.4 NMR and ITC Studies of the Functionalized Receptors with PPG Anion

Following the above experimental evidence, the next step was to study the functionalized receptor system **57a** with PPG anion. Both proton NMR and ITC studies of the functionalized receptor **57a** with PPG anion were carried out in DMF at 40°C.

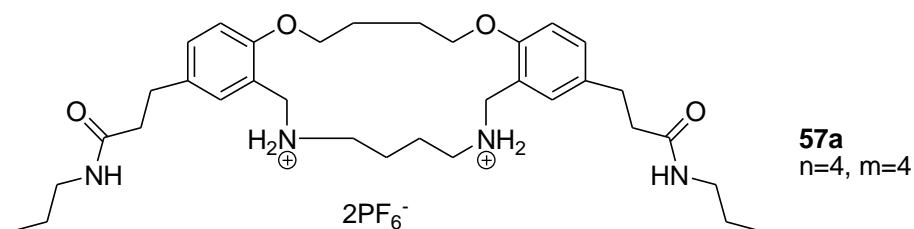


Figure 54. Fully functionalized receptor **57a**

The proton NMR Job plot of the functionalized receptor **57a** revealed a 1:2 binding stoichiometry with the PPG anion, whereas the control receptor with the same binding pocket structure (n=4 and m=4) showed 1:1 binding stoichiometry both with the dihydrogen phosphate anion and the PPG anion. The only difference between the control receptor and the functionalized receptor was the R group *para* to the phenolic oxygen atom. The control receptor contained a CH₃ group at the *p*-position while the functionalized receptor contains an amide group.

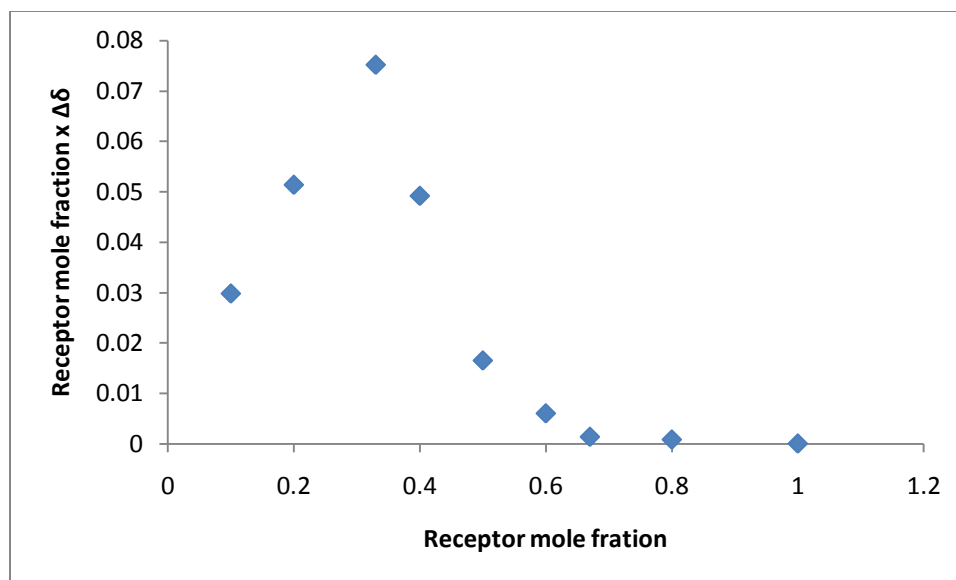


Figure 55. Job plot of **57a** – PPG anion complex in DMF-d₇ at 40°C

Amide groups have been widely utilized in building many supra-molecular assemblies involving hydrogen bonding interactions. In our study, the prediction was, the two amide functional groups would hydrogen bond with the two hydroxyl groups from the glycerol head group of the PPG anion. But after the results from the ¹H NMR Job plot, careful analysis of the real molecule showed that it was possible for the amide groups to make charged intra-molecular hydrogen bonding with the ammonium hydrogen atoms present in the molecule resulting 10 member rings as shown in the figure 56 which creates two binding pockets.

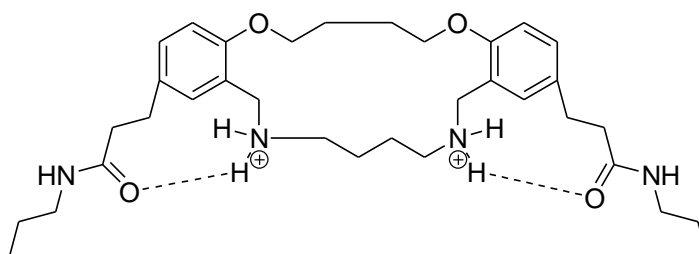


Figure 56. Receptor **57a** showing possible intra-molecular hydrogen bonding

Even though the experimental binding stoichiometry between the functionalized receptor and the PPG anion was different from what was predicted, it was assumed that a 1:2 binding stoichiometry between the receptor and the PPG anions was not affecting our purpose provided additional functionality could be introduced into this receptor in order to bind with the glycerol hydroxyl groups. Otherwise the specificity of the receptor towards the PPG anion would not present any more. However, it was decided to perform the proton NMR and ITC studies with this receptor to complete the study.

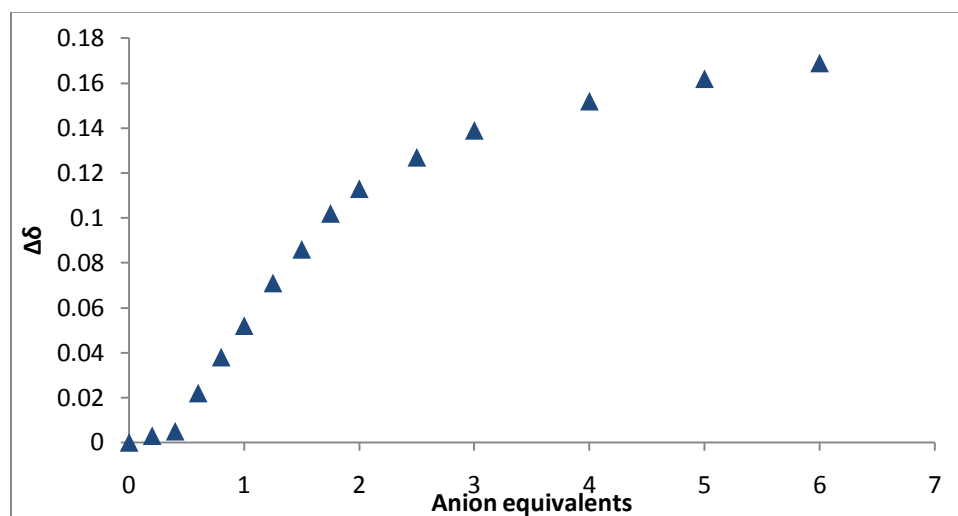


Figure 57. ^1H NMR titration curve of **57a** with PPG anion in DMF-d_7 at 40°C

The EQNMR calculation of the data obtained with the proton NMR titration did not produced a binding constant when fitted to the 1:2 binding model. Several attempts to fit the data with this model using logarithmic values were again unsuccessful.

ITC studies of the fully functionalized receptor **57a** produced the binding isotherm shown in figure 58 which was an exotherm at the beginning and changed to an endotherm after the addition of 1.25 molar equivalents of the anion. The association constant value was not estimated because the software did not let the data to be fitted in to any of the available binding models.

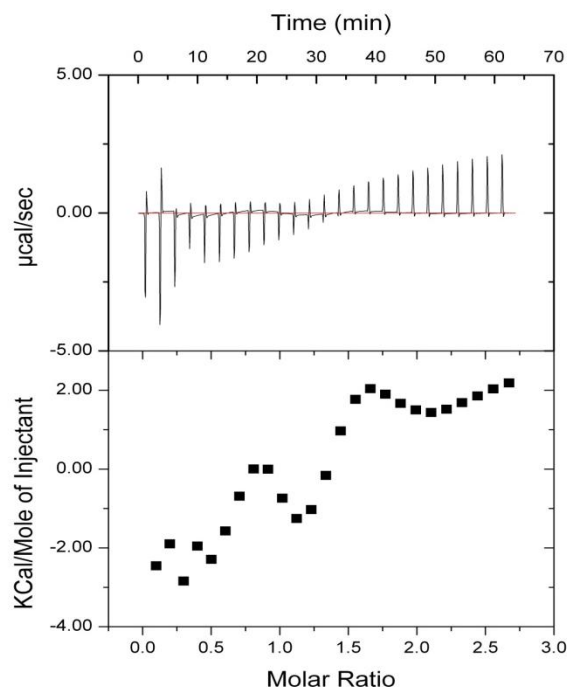


Figure 58. ITC binding isotherm of **57a** with PPG anion in DMF at 40°C

According to the above experimental evidence, one fully functionalized receptor molecule is binding with 2 PPG anions. If this happens the way it is shown in figure 56, then there is no selectivity of this receptor for the PPG anion as the amide groups are now binding with the phosphate head groups rather than with the glycerol hydroxyl groups. This must be true at least in DMF. Therefore, similar studies will be carried out in the future with different solvent(s) to see the effect of the solvent on the binding stoichiometry. Depending on the results, it will be decided whether it is necessary to introduce some additional functional groups into the receptor to achieve the expected selectivity.

CONCLUSION

A reliable methodology was developed for the synthesis of the said family of control receptors and the functionalized receptors. The importance of the ether linker length 'n' and the bisammonium linker length 'm' were identified. The ether linker length 'n' is important in the synthesis and the bisammonium linker length 'm' is the factor which determines the binding stoichiometry between the control receptors and the two anions used in the study.

Proton NMR Job plots revealed the binding stoichiometries between the charged receptors and the anions studied. Based on the results of the binding studies conducted with the control receptors, two binding pocket sizes (n=4, m=4 and n=5, m=3) were chosen to have the most likely structures to bind with the anionic phosphate portion of the PPG molecule in a 1:1 stoichiometry.

Proton NMR titrations and ITC studies produced the binding constants and the thermodynamic parameters for all the receptor anion complexes studied. All the binding events were identified as entropy driven which is the usual case for charged receptors.

Comparison of the binding constants obtained with the interaction between the receptor and the two anions studied, revealed that the binding motif of the two structurally different anions were similar

However, the Job plot of the fully functionalized receptor-anion complex showed 1:2 binding stoichiometry in DMF which was suspected to be an artifact of the solvent of choice. Future studies will clear this suspicion and reveal the correct binding stoichiometry.

CHAPTER 4

EXPERIMENTAL-MATERIALS AND PROCEDURES

All melting points (Mel-Temp) are uncorrected. ^1H NMR spectra were recorded at 400MHz in CDCl_3 using the chloroform peak as the reference or in DMSO-d_6 using DMSO as the reference. ESI-MS/ APCI-MS were obtained with a Varian 1200L Quadrupole MS. X-ray crystal structures were obtained by Bruker Kappa Apex II single crystal diffractometer. Purity affirmation was accomplished by HRMS of analytical samples by the Mass Spectrometry Lab at the University of Kansas. Column chromatography was carried out on silica gel (Davisil 633). Prep thin-layer chromatography was performed on pre-coated 1500 mm plates from Analtech (silica gel F). Radial chromatography when performed was accomplished using a Chromatotron (Harrison Research, Palo Alto, California).

During the syntheses, THF was freshly distilled from Na/K in the presence of benzophenone for each reaction. Ethanol and methanol used were anhydrous in all cases. Drying and purification procedures of other solvents and reagents used in the syntheses are described as part of each experiment when appropriate. All the reactions described were performed under a nitrogen atmosphere.

1,3-bis(4-methylphenoxy)propane (33): p-Cresol (5.00g, 0.046mol) was dissolved in 330 ml of dry THF in a round bottom flask under N₂. K₂CO₃ (4.54g, 0.033mol) and 18-Crown-6 (2.61g, 0.0099mol) were added and was set up for reflux under N₂. 1, 3-dibromopropane (2.34ml, 0.023mol) was added through the condenser drop wise via syringe and refluxed for 20 hrs. The reaction was allowed to cool to room temperature and quenched with 10 % HCl. The layers were separated and the aqueous was extracted with CH₂Cl₂ (3x40ml). The combined organic layer was washed with sat. sodium bicarbonate (2x40ml) and brine (40ml) sequentially and dried with anhydrous Na₂SO₄. Removal of the solvent under reduced pressure yielded the crude product as a white solid. Column chromatography (silica gel) with 35% ethyl acetate and 65% hexanes yielded the pure product as a white crystalline solid (4.50g, 0.017mol, 76% yield): mp 87-88°C; ¹H NMR (400 MHz, CDCl₃) δ 2.19-2.23 (m, 2H); 2.26 (s, 6H); 4.10 (t, 4H, J=5.8 Hz); 6.78 (d, 4H, J=8.5 Hz); 7.04 (d, 4H, J= 8.5 Hz); ¹³C NMR (100 MHz, CDCl₃) δ 20.67, 29.61, 64.78, 114.57, 130.09, 156.96; MS (ESI) m/z 279.1(M+Na)⁺; HRMS(EI) calcd for C₁₇H₂₀O₂ (M+H) 256.1724, found 256.1724.

1,4-bis(4-methylphenoxy)butane (34): p-Cresol (0.9978g, 0.009mol) was dissolved in 55 ml of dry THF in a round bottom flask under N₂. K₂CO₃ (1.275g, 0.009mol) and 18-Crown-6 (0.365g, 0.0013mol) were added and set up for reflux under N₂. 1, 4-dibromobutane (0.55ml, 0.0046mol) was added through the condenser drop wise and refluxed 20 hrs. The reaction mixture was allowed to cool to room temperature and quenched with 10 % HCl. Layers were separated and the aqueous was extracted with CH₂Cl₂ (3 x 10ml). The combined organic layers were washed with sat. sodium bicarbonate (2 x 10ml) and brine (10ml) sequentially and dried with anhydrous Na₂SO₄. Removal of the solvent under reduced pressure gave (1.3g) crude material. Column

chromatography (silica gel) with 35% ethyl acetate and 65% hexanes gave the pure product as an off white solid (0.9g,0.0033mol, 73% yield): mp 94-95°C; ^1H NMR (400 MHz, CDCl_3) δ 1.92-1.95 (m, 4H); 2.26 (s, 6H); 3.98 (t, 4H, $J=5.5$ Hz); 6.78 (d, 4H, $J=9.1$ Hz); 7.05(d, 4H, $J=8.6\text{Hz}$); ^{13}C NMR (100 MHz, CDCl_3) δ 20.69, 26.28, 67.73, 77.44, 114.56, 130.01, 130.09, 157.08; MS (ESI) m/z 271.1 ($\text{M}+\text{H}$) $^+$, 293.0 ($\text{M}+\text{Na}$) $^+$; HRMS(EI) calcd for $\text{C}_{18}\text{H}_{22}\text{O}_2$ ($\text{M}+\text{H}$) 270.1586, found 270.1586.

1,3-bis(2-formyl-4-methylphenoxy)propane (35): Compound **33** which had been previously dried under vacuum over P_2O_5 (1.66g, 0.0064 mol) and Duff reagent (1.82g, 0.0129 mol) were mixed in a round bottom flask and set up for reflux under N_2 . 20ml of TFA was added through the condenser under N_2 and the reaction mixture was refluxed for 24 hrs at 85°C. The mixture was concentrated under vacuum and extracted into CH_2Cl_2 from water. The aqueous phase was acidified with concentrated HCl and extracted in to CH_2Cl_2 (2 x 50ml). Combined organic extract was washed sequentially with of 4N HCl (2 x 50 ml), 50ml of saturated aq. Na_2CO_3 and 50 ml of brine. Removal of the solvent under vacuum gave 7.3 g of the crude product as a brown gluey mass. Column chromatography (silica gel) with hexanes yielded the pure product as a white crystalline solid (0.759g, 0.0024mol, 37.5 %): mp 77-79°C, ^1H NMR (100 MHz, CDCl_3) δ 2.29 (S, 6H); 2.34-2.40 (m,2H); 4.26 (t, 4H, $J=5.9$ Hz); 6.89 (d, 2H, $J=8.4$ Hz); 7.34 (d, 2H, $J=8.2$ Hz); 7.61 (s, 2H); 10.44 (s, 2H); ^{13}C NMR (100 MHz, CDCl_3) δ 20.46, 29.37, 64.59, 112.66, 124.75, 128.83, 130.60, 136.89, 159.32, 189.84; MS(ESI) m/z 335.0 ($\text{M}+\text{Na}$) $^+$; HRMS(ESI) calcd for $\text{C}_{19}\text{H}_{20}\text{O}_4$ ($\text{M}+\text{Na}$) 335.1259, found 335.1248.

1,4-bis(2-formyl-4-methylphenoxy)butane (36): 1,4-bis (p-tolyloxy) butane **34** which had been dried over P₂O₅ (5.15g, 0.019 mol) and Duff reagent (6.75g, 0.048mol) were mixed in a round bottom flask and set up for reflux. 75ml of TFA was added through the condenser under N₂ and the reaction mixture was refluxed 24 hrs at 85°C. The resultant mixture was concentrated under vacuum and extracted in to CH₂Cl₂ from water. The aqueous phase was acidified with concentrated HCl and extracted in to CH₂Cl₂ (2x50 ml). The combined organic extract was washed sequentially with 4N HCl (2x50 ml), 50ml saturated aq. Na₂CO₃ and 50 ml brine and then dried over anhydrous sodium sulfate. Removal of the solvent under vacuum gave 7.3 g of the crude product as a brown gluey mass. Column chromatography (silica gel) with hexanes gave the pure product as a white crystalline solid (3.3g, 0.010mol, 53%): mp 117-118°C, ¹H NMR (400 MHz, CDCl₃) δ 2.04-2.06 (m, 4H); 2.29 (s, 6H); 4.13 (t, broad, 4H, J=5.6 Hz); 6.89 (d, 2H, J=9.1 Hz); 7.33 (d, 2H, J= 8.6 Hz); 7.60 (s, 2H); 10.44 (s, 2H); ¹³C NMR (100 MHz, CDCl₃) δ 20.48, 26.15, 68.14, 112.61, 124.73, 128.68, 130.38, 136.86, 159.50, 189.99; MS(ESI) m/z 349.0 (M+Na)⁺; HRMS(ESI) calcd for C₂₀H₂₂O₄ (M+Na) 349.1416, found 349.1415.

9, 22-dimethyldibenzo-[f, s]-1, 6-dioxa-10, 17-diaza-2, 3, 4, 5, 6, 9, 10, 11, 12, 13, 14, 15, 16, 17, 18-pentadecahydro-1H-cycloicosene (37): Compound **(36)** (0.410g, 0.0012 mol), which has been previously dried over P₂O₅ under vacuum, was suspended in 126 ml of dry ethanol, purged with dry N₂ for 30 minutes and set up for reflux under N₂. Hexane-1,6-diamine (0.146g, 0.0012mol) was dissolved in 50 ml of dry ethanol under N₂ and cannulated in to an addition funnel. The diamine was added drop wise through the addition funnel and refluxed for 20 hrs under N₂. Removal of the solvent under reduced pressure yielded the bis-imine as a yellow thick oil which was then subjected to reduction without further purification.

Crude bis-imine was re-dissolved in 5 ml of anhydrous methanol under N₂. 10% Pd-C (0.2 g) was added and the reaction mixture was started stirring. Triethylsilane (3.0 ml, 0.0185mol) was added drop wise into the methanolic bis-imine solution with an addition funnel the top of which was attached to a rubber balloon. After the addition was complete, the mixture was stirred for additional 6 hrs at room temperature, and then filtered through celite. Removal of the solvent under vacuum yielded the crude product as a yellow oil. Silica gel column chromatography with 5% CHCl₃, 4% isopropyl amine and 91% diethyl ether furnished the compound (**37**) as a yellow oil. (0.352g, 0.857mmols, 71% after both steps); ¹H NMR (400 MHz, CDCl₃) 1.30-1.34 (m, 4H); 1.48-1.55 (m, 4H); 1.97-1.98 (m, 4H); 2.25 (s,6H); 2.61 (t, 4H, J=6.6 Hz); 3.73 (s,4H); 4.00 (t, 4H, J=5.4 Hz); 6.74 (d, 2H, J=4.1 Hz); 6.98 (d, 2H, J=8.1 Hz); 7.04 (s, 2H); ¹³C NMR (100 MHz, CDCl₃) δ 20.63, 26.47, 26.86, 29.29, 48.75, 49.54, 68.18, 111.27, 128.59, 128.65, 130.02, 131.54, 155.27; MS(ESI) m/z 411.1 (M+H)⁺; HRMS(ESI) calcd for C₂₆H₃₈O₂N₂ (M+H) 411.3012, found 411.3016.

9, 21-dimethyldibenzo-[g, r]-1, 6-dioxa-10, 16-diaza-2, 3, 4, 5, 6, 9, 10, 11, 12, 13, 14, 15, 16, 17-tetradecahydro-1H-cyclononadecene (38): Compound **36**, which has been previously dried over P₂O₅ under vacuum (0.400g, 0.0012 mol), was suspended in 125 ml of dry ethanol, purged with dry N₂ for 30 minutes and set up for reflux. Butane-1, 5-diamine (0.14 ml, 0.0012mol) was dissolved in 50 ml of dry ethanol under N₂ and cannulated in to an addition funnel. The diamine was added drop wise through the addition funnel and the reaction mixture was refluxed for 20 hrs under N₂. Removal of the solvent under reduced pressure yielded the bis-imine as a yellow solid which was then subjected to reduction without further purification.

Crude bis-imine was re-dissolved in 5 ml of anhydrous methanol under N₂. 10% Pd-C (0.3 g) was added and the reaction mixture started stirring. Triethylsilane (3.0 ml, 0.0185 mol) was added drop wise into the methanolic bis-imine solution with an addition funnel, the top of which was attached to a rubber balloon. After the addition was complete, the mixture was stirred for additional 6 hrs at room temperature. The reaction mixture was filtered through Celite, and removal of the solvent under vacuum yielded the crude product as a yellow oil. Silica gel column chromatography with 5% CHCl₃, 4% isopropyl amine and 91% diethyl ether furnished the compound (**38**) as a yellowish solid. (0.2307g, 0.582mmol, 48.5% after both steps): mp 116-117°C, ¹H NMR (400 MHz, DMSO) δ 1.22-1.29 (m, 2H); 1.41-1.48 (m, 4H); 1.89 (s, broad, 4H); 2.15 (s, 6H); 2.54 (t, 4H, J= 6.3 Hz); 3.61 (s, 4H); 3.92 (t, 4H, J=5.4 Hz); 6.64 (d, 2H, J=8.7 Hz); 6.91 (d, 2H, J=7.1 Hz); 6.92 (s, 2H); ¹³C NMR (100 MHz, DMSO) δ 20.73, 24.79, 26.40, 29.44, 48.93, 49.92, 64.39, 67.73, 111.58, 129.04, 129.18, 131.67, 155.45; MS(ESI) m/z 397.1(M+H)⁺; HRMS(ESI) calcd for C₂₅H₃₆O₂N₂ (M+H) 397.2855, found 397.2864.

9, 20-dimethyldibenzo-[g, q]-1,6-dioxa-10, 15- diaza-2, 3, 4, 5, 6, 9, 10, 11, 12, 13, 14, 15, 16-tridecahydro-1H-cyclooctadecene (39): Compound (**36**) (0.4992g, 0.0015 mol) was suspended in 155 ml of dry ethanol, purged with dry N₂ for 30 minutes and set up for reflux. Butane-1, 4-diamine (0.1539 ml, 0.0015mol) was dissolved in 61.25 ml of dry ethanol under N₂ and cannulated in to an addition funnel. The diamine was added drop wise through the addition funnel and the reaction mixture was refluxed for 20 hrs under N₂. Removal of the solvent under reduced pressure yielded the bis-imine as a yellow solid, which was then subjected to reduction without further purification.

Crude bis-imine was re-dissolved in 5 ml of anhydrous methanol under N₂. 10% Pd-C (0.3 g) was added and the reaction mixture started stirring. Triethylsilane (3.0 ml, 0.0185 mol) was added drop wise into the methanolic bis-imine solution with an addition funnel, the top of which was attached to a rubber balloon. After the addition was complete, the mixture was stirred for additional 6 hrs at room temperature. The reaction mixture was filtered through Celite, and removal of the solvent under vacuum gave the crude product as a yellow oil. Silica gel column chromatography with 5% CHCl₃, 4% isopropyl amine and 91% diethyl ether furnished the compound **39** as a yellowish solid. (0.3826g, 0.001mol, 67% after both steps): mp 140-142°C, ¹H NMR (400 MHz, DMSO) δ 1.62 (s, broad, 4H); 1.95 (s, broad, 4H); 2.23 (s, 6H); 2.72 (m, broad, 4H); 3.78 (s, broad, 4H); 4.06 (s, broad, 4H); 6.94 (d, 2H, J=9.4); 7.1 (m, 4H); ¹³C NMR (100 MHz, DMSO) δ 20.70, 26.42, 47.49, 49.26, 68.17, 112.34, 129.56, 130.63, 132.37, 155.48; MS(ESI) m/z 383.3(M+H)⁺ ; HRMS(ESI) calcd for C₂₄H₃₄O₂N₂ (M+H) 383.2699, found 383.2714.

8, 21-dimethyldibenzo-[f, r]-1,5-dioxa-9,16-diaza-2, 3, 4, 5, 8, 9, 10, 11, 12, 13, 14, 15, 16,17-tetradecahydro-1H-cyclononadecene (41): Compound **35** (0.4170g, 0.0013 mol) which has been previously dried over P₂O₅ under vacuum was suspended in 133 ml of dry ethanol, purged with dry N₂ for 30 minutes and set up for reflux under N₂. Hexane-1, 6-diamine (0.155g, 0.0013mol) was dissolved in 50 ml of dry ethanol under N₂ and cannulated in to an addition funnel. The diamine was added drop wise through the addition funnel and refluxed for 20 hrs under N₂. Removal of the solvent under reduced pressure yielded the bis-imine as a yellow solid which was then subjected to reduction without further purification.

Crude bis-imine was re-dissolved in 5 ml of anhydrous methanol under N₂. 10% Pd-C (10 %) (0.3 g) was added and the reaction mixture was started stirring. Triethylsilane (3.0 ml, 0.0185 mol) was added drop wise into the methanolic bis-imine solution with an addition funnel, the top of which was attached to a rubber balloon. After the addition was complete, the mixture was stirred for additional 6 hrs at room temperature and filtered through celite. Removal of the solvent under vacuum yielded the crude product as a yellow oil. Silica gel column chromatography with 5% CHCl₃, 4% isopropyl amine and 91% diethyl ether furnished the compound **41** as a yellow oil.(0.3826g, 0.00096mols, 74% after both steps); ¹H NMR (400 MHz, CDCl₃) δ 1.26 (s, broad, 4H); 1.18-1.54 (m, 4H); 2.25 (s, 6H); 2.32 (t, 4H, J= 6.8 Hz); 2.58 (t, 4H, J=7.1 Hz); 3.74 (s, 4H); 4.14 (t, 4H, J=6.5 Hz); 6.75 (d, 2H, J=8.3 Hz); 7.00 (d, 2H, J=8.3 Hz); 7.02 (s, 2H); ¹³C NMR (100 MHz, CDCl₃) δ 20.63, 26.14, 28.88, 30.23, 48.27, 49.91, 64.86, 111.10, 129.00, 130.25, 131.89, 155.05; MS(ESI) m/z 397.1 (M+1)⁺; HRMS(ESI) calcd for C₂₅H₃₆O₂N₂ (M+H) 397.2855, found 397.2870.

8, 20-dimethyldibenzo-[f, q]-1, 5-dioxa-9, 15-diaza-2, 3, 4, 5, 8, 9, 10, 11, 12, 13, 14, 15, 16-tridecahydro cyclooctadecene (42): Compound **35** (0.509g, 0.0016 mol) which has been previously dried over P₂O₅ under vacuum was suspended in 165 ml of dry ethanol, purged with dry N₂ for 30 minutes and set up for reflux under N₂. Pentane-1, 5-diamine (0.167g, 0.0016mol) was dissolved in 65 ml of dry ethanol under N₂ and cannulated in to an addition funnel. The diamine was added drop wise through the addition funnel and the mixture was refluxed for 20 hrs under N₂. Removal of the solvent under reduced pressure yielded the bis-imine as yellow thick oil which was then subjected to reduction without further purification.

Crude bis-imine was re-dissolved in 7 ml of anhydrous methanol under N₂. Pd-C (10 %) (0.3 g) was added and started stirring. Triethylsilane (3.0 ml, 0.0185mol) was added drop wise into the methanolic bis-imine solution with an addition funnel attached to a rubber balloon. After the addition was complete, the mixture was stirred for additional 6 hrs at room temperature, filtered through celite. Removal of the solvent under vacuum yielded the crude product as a yellow oil. Silica gel column chromatography with 5% CHCl₃, 4% isopropyl amine and 91% diethyl ether furnished the compound **42** as a yellow oil. (0.410g, 0.0011mols, 67% after both steps); ¹H NMR (400 MHz, CDCl₃) δ 1.31-1.36 (m, 2H); 1.55-1.61 (m, 4H); 2.25 (s,6H); 2.31-2.36 (m,2H); 2.71 (t, 4H, J=6.8 Hz); 3.85 (s,4H); 4.20 (t, 4H, J=6.1 Hz); 6.78 (d, 2H, J=8.5 Hz); 7.06 (d, 2H, J=8.1 Hz); 7.14 (s, 2H); ¹³C NMR (100 MHz, CDCl₃) δ 20.61, 24.13, 26.26, 29.86, 46.75, 47.46, 65.64, 111.64, 130.42, 130.66, 132.77, 155.12; MS(ESI) m/z 383.1 (M+1)⁺; HRMS(ESI) calcd for C₂₄H₃₄O₂N₂ (M+H) 383.2699, found 383.2702.

9, 22-dimethyldibenzo-[f, s]-1, 6-dioxa-10, 17-diaza-2, 3, 4, 5, 6, 9, 10, 11, 12, 13, 14, 15, 16, 17, 18-pentadecahydro-1H-cycloicosenediium bis(hexafluorophosphate) (45): Bis-amine (**37**) (162 mg, 0.394 mmols) was dissolved in 3 ml of methanol. 6N HCl (5ml) was added and stirred for 3 hours at room temperature. The solvent was removed under vacuum and the crude reaction mixture was re-dissolved in 3 ml of H₂O. Ammonium hexafluorophosphate (>30 equivalents) in CH₂Cl₂ was added and stirred over night. The compound (**45**) precipitated from the solvents as an off white solid (199mg, 0.283 mmol, 72%): decomposes > 200°C, ¹H NMR (400 MHz, DMSO) δ 1.32-1.38 (m, broad, 4H); 1.36 (m, broad, 4H); 1.65-1.68 (m, 4H); 1.94 (s, broad, 4H); 2.27 (s, 6H); 2.88 (s, broad, 4H); 4.08 (m, 8H); 7.03 (d, 2H, J=8.9 Hz); 7.22 (m, 4H); 8.50 (s, broad, 4H); ¹³C NMR (100 MHz, DMSO) δ 20.61, 24.76, 25.66, 26.36, 44.46, 46.24,

68.80, 112.64, 119.90, 129.98, 131.92, 132.86, 155.73; MS(ESI) m/z 411.2(M)⁺, 206.2(M²⁺/2)⁺, 557.1(M²⁺·PF₆⁻)⁺; HRMS(ESI) calcd for C₂₆H₃₉O₂N₂ (M⁺) 411.3012, found 411.3015.

9, 21-dimethyldibenzo-[g, r]-1, 6-dioxa-10, 16-diaza-2, 3, 4, 5, 6, 9, 10, 11, 12, 13, 14, 15, 16, 17-tetradecahydro-1H-cyclononadecenediium bis(hexafluorophosphate) (46): Bis-amine (38) (51 mg, 0.128 mmols) was dissolved in 3 ml of methanol. 6N HCl (3ml) was added and stirred for 3 hours at room temperature. The solvent was removed under vacuum and the crude reaction mixture was re-dissolved in 3 ml of H₂O. Ammonium hexafluorophosphate (>30 equivalents) in CH₂Cl₂ was added and stirred over night. The compound (46) was precipitated from the solvents as an off white solid (36mg, 0.052 mmol, 41%): decomposes > 161°C, ¹H NMR (400 MHz, DMSO) δ 1.38-1.44 (m, 2H); 1.62-1.68 (m, 4H); 1.94 (s, broad, 4H); 2.26 (s, 6H); 2.90 (s, broad, 4H); 4.06(s, 4H); 4.07 (t, 4H, J=6.4 Hz) 7.02 (d, 2H, J=8.1 Hz); 7.22 (s, 2H); 7.24 (d, 2H, J=7.9 Hz); 8.49 (s, broad, 4H); ¹³C NMR (100 MHz, DMSO) δ 20.62, 22.60, 24.54, 26.42, 45.14, 46.15, 68.66, 112.43, 119.82, 129.89, 131.97, 132.95, 155.71; MS(ESI) m/z 397.1(M)⁺, 199.2(M²⁺/2)⁺, 543.1(M²⁺·PF₆⁻)⁺; HRMS(ESI) calcd for C₂₅H₃₇O₂N₂ (M⁺) 397.2855, found 397.2870.

9, 20-dimethyldibenzo-[g, q]-1,6-dioxa-10, 15- diaza-2, 3, 4, 5, 6, 9, 10, 11, 12, 13, 14, 15, 16-tridecahydro-1H-cyclooctadecenediium bis(hexafluorophosphate) (47): Bis-amine (39) (100mg, 0.261mmols) was dissolved in 3 ml of methanol. 6N HCl (7ml) was added and stirred for 3 hours at room temperature. The solvent was removed under vacuum and the crude reaction mixture was re-dissolved in 3 ml of H₂O. Ammonium hexafluorophosphate (>30 equivalents) in

CH₂Cl₂ was added and stirred over night. The compound (**47**) was precipitated from the solvents as an off white solid. (96mg, 0.142mmol, 55%): decomposes >210°C, ¹H NMR (400 MHz, DMSO) δ 1.72 (s, broad, 4H); 1.96 (s, broad, 4H); 2.26 (s, 6H); 2.97 (s, broad, 4H); 4.08 (s, 8H); 7.03 (d, 2H, J=8.9 Hz); 7.22 (s, 2H); 7.23 (d, 2H, J=8.3 Hz); 8.50 (s, broad, 4H); ¹³C NMR (100 MHz, DMSO) δ 20.61, 22.79, 26.43, 46.35, 68.48, 112.56, 120.03, 129.93, 131.96, 132.90, 155.69; MS(ESI) m/z 383.1(M)⁺, 192.1(M²⁺/2)⁺, 529.1 (M²⁺·PF₆⁻)⁺; HRMS(ESI) calcd for C₂₄H₃₅O₂N₂ (M+H) 383.2699, found 383.2702.

8, 21-dimethyldibenzo-[f, r]-1,5-dioxa-9,16-diaza-2, 3, 4, 5, 8, 9, 10, 11, 12, 13, 14, 15, 16,17-tetradecahydro-1H-cyclononadecenediium bis(hexafluorophosphate) (49): Bis-amine (**41**) (65mg, 0.164 mmols) was dissolved in 3 ml of methanol. 6N HCl (5ml) was added and stirred for 3 hours at room temperature. The solvent was removed under vacuum and the crude reaction mixture was re-dissolved in 3 ml of H₂O. Ammonium hexafluorophosphate (>30 equivalents) in CH₂Cl₂ was added and stirred over night. The compound (**49**) was precipitated from the solvents as an off white solid. (50mg, 0.073mmol, 45%): decomposes >226°C, ¹H NMR (400 MHz, DMSO) δ 1.34-1.36 (m, 4H); 1.63-1.70 (m, broad, 4H); 2.27 (s, 6H); 2.30 (s, 4H); 2.89 (t, broad, 4H, J=5.5 Hz); 4.08 (s, broad, 4H); 4.18 (t, 4H, J=6.9); 7.03 (d, 2H, J=8.5 Hz); 7.22 (s, 2H); 7.24 (d, 4H, J=8.1 Hz); 8.44 (s, broad, 4H); ¹³C NMR (100 MHz, DMSO) δ 20.61, 24.95, 25.85, 29.85, 44.83, 46.27, 65.44, 112.43, 112.00, 130.08, 131.99, 132.96, 155.52; MS(ESI) m/z 397.1(M)⁺, 199.2(M²⁺/2)⁺, 543.0(M²⁺·PF₆⁻)⁺; HRMS(ESI) calcd for C₂₅H₃₇O₂N₂ (M+H) 397.2855, found 397.2865.

8, 20-dimethyldibenzo-[f, q]-1, 5-dioxa-9, 15-diaza-2, 3, 4, 5, 8, 9, 10, 11, 12, 13, 14, 15, 16-tridecahydro cyclooctadecenediium bis(hexafluorophosphate) (50): Bis-amine (42) (50mg, 0.13 mmols) was dissolved in 3 ml of methanol. 6N HCl (5ml) was added and stirred for 3 hours at room temperature. The solvent was removed under vacuum and the crude reaction mixture was re-dissolved in 3 ml of H₂O. Ammonium hexafluorophosphate (>30 equivalents) in CH₂Cl₂ was added and stirred over night. The compound (1) was precipitated from the solvents as an off white solid. (35mg, 0.052mmol, 40%): decomposes >201°C, ¹H NMR (400 MHz, DMSO) δ 1.32-1.38 (m, broad, 4H); 1.56-1.64 (m, broad, 4H); 2.26-2.29 (m, 10H); 2.81 (t, broad, 4H, J=8.1 Hz); 4.07 (s, 4H); 4.19 (t, 4H, J=6.5 Hz) 7.03 (d, 2H, J=8.1 Hz); 7.22-7.24 (m, 4H); 8.44 (s, broad, 4H); ¹³C NMR (100 MHz, DMSO) δ 20.62, 23.56, 24.78, 29.67, 44.50, 45.83, 65.28, 112.61, 120.00, 130.10, 132.04, 133.32, 155.65; MS(ESI) m/z 383.1(M)⁺ , 192.2(M²⁺/2)⁺, 529.1(M²⁺·PF₆⁻)⁺; HRMS(ESI) calcd for C₂₄H₃₅O₂N₂ (M+H) 383.2699, found 383.2708.

1,5-bis(4-methylphenoxy)pentane (51): p-Cresol (5.17g, 0.048mol) was dissolved in 475 ml of dry THF in a round bottom flask under N₂. K₂CO₃ (6.54g, 0.047mol) and 18-Crown-6 (2.59g, 0.007mol) were added and was set up for reflux under N₂. 1, 5-dibromopentane (3.32ml, 0.024mol) was added through the condenser drop wise and the reaction mixture was refluxed for 20 hrs. The reaction was allowed to cool to room temperature and quenched with 10 % HCl. The layers were separated and the aqueous was extracted with CH₂Cl₂ (3x40ml). The combined organic layer was washed with sat. sodium bicarbonate (2x40ml) and brine (40ml) sequentially and dried with anhydrous Na₂SO₄. Removal of the solvent under reduced pressure yielded the crude product as a white solid. Column chromatography (silica gel) with 35% ethyl acetate and 65% hexanes yielded the pure product as a white crystalline solid (6.73g, 0.023mol, 98.6%

yield): mp 58-60°C; ¹H NMR (400 MHz, CDCl₃) δ 1.61-1.66 (m, 2H); 1.80-1.87 (m, 4H); 2.27 (s, 6H); 3.94 (t, 4H, J=6.7 Hz); 6.78 (d, 4H, J=7.9 Hz); 7.06 (d,4H, J=8.5 Hz); ¹³C NMR (100 MHz, CDCl₃) δ 20.67, 22.96, 29.32, 68.04, 114.60, 129.94, 130.07, 157.15; MS (ESI) m/z 307.1(M+Na)⁺; HRMS(ESI) calcd for C₁₉H₂₄O₂ (M+Na) 307.1674, found 307.1740.

1,5-bis(2-formyl-4-methylphenoxy)pentane (52): Compound **51** which had been previously dried under vacuum over P₂O₅ (1.58g, 0.0055 mol) and Duff reagent (1.82g, 0.0129 mol) were mixed in a round bottom flask and set up for reflux under N₂. 20ml of TFA was added through the condenser under N₂ and the reaction mixture was refluxed for 24 hrs at 85°C. The mixture was concentrated under vacuum and extracted into CH₂Cl₂ from water. The aqueous phase was acidified with concentrated HCl and extracted into CH₂Cl₂ (2 x 50ml). The combined organic extract was washed sequentially with 2x50 ml of 4N HCl, 50ml of saturated aq. Na₂CO₃ and 50 ml of brine. Removal of the solvent under vacuum gave the crude product as a brown gluey mass. Column chromatography (silica gel) with hexanes yielded the pure product as a white crystalline solid (0.75g, .0022mol, 40 %): mp 76-77°C, ¹H NMR (400 MHz, CDCl₃) δ 1.66-1.72 (m, 2H); 1-88-1.95 (m, 4H); 2.29 (s, 6H); 4.07 (t, 4H, J=6.2 Hz); 6.96 (d, 2H, J=8.7 Hz); 7.32 (d, 2H, J=8.6 Hz); 7.61 (s, 2H); 10.46 (s, 2H); ¹³C NMR (100 MHz, CDCl₃) δ 20.47, 23.02, 29.10, 68.51, 112.71, 124.76, 130.26, 136.84, 159.69, 190.14; MS(ESI) m/z 409.0 (M+Na)⁺; HRMS(ESI) calcd for C₂₁H₂₄O₄ (M+Na) 363.1572, found 363.1584.

10, 20-dimethyldibenzo-[h, q]-1,7-dioxa-13, 17-diaza-2, 3, 4, 5, 6, 7, 10, 11, 12, 13, 14, 15, 16-tridecahydro-1H-cyclooctadecene (53): Compound (**52**) (0.200g, 0.587 mmol) was suspended in 60 ml of dry ethanol, purged with dry N₂ for 30 minutes and set up for reflux. Propane-1, 3-

diamine (0.050 ml, 0.587mmol) was dissolved in 24 ml of dry ethanol under N₂ and cannulated in to an addition funnel. The diamine was added drop wise through the addition funnel and the reaction mixture was refluxed for 20 hrs under N₂. Removal of the solvent under reduced pressure yielded the bis-imine as a yellow solid which was then subjected to reduction without further purification.

Crude bis-imine was re-dissolved in 3 ml of anhydrous methanol under N₂. 10% Pd-C (0.2 g) was added and the reaction mixture was started stirring. Triethylsilane (2.0 ml, 0.012 mol) was added drop wise into the methanolic bis-imine solution with an addition funnel, the top of which was attached to a rubber balloon. After the addition was complete, the mixture was stirred for additional 6 hrs at room temperature, and then filtered through Celite, removal of the solvent under vacuum gave the crude product as a yellow oil. Silica gel column chromatography with 10% CHCl₃, 4% isopropyl amine and 86% diethyl ether furnished the compound **53** as an off white solid. (0.142g, 0.371 mmol, 63% after both steps): mp 108-109°C, ¹H NMR (400 MHz, DMSO) δ 1.49-1.56 (m, 2H); 1.66-1.82 (m, 2H); 1.76-1.80 (m, 4H); 2.21 (s,6H); 2.53 (t, 4H, J=7.0 Hz); 3.62 (s, 4H); 3.97 (t, 4H, J=5.2 Hz); 6.83 (d, 2H, J=8.2 Hz); 6.98 (d, 2H, J=8.2 Hz); 7.05 (s, 2H); ¹³C NMR (100 MHz, DMSO) δ 20.82, 24.77, 29.90, 46.95, 47.76, 68.52, 112.06, 128.74, 129.28, 130.99, 155.34; MS(ESI) m/z 383.1(M+H)⁺; HRMS(ESI) calcd for C₂₄H₃₄O₂N₂ (M+H) 383.2699, found 383.2703.

10, 20-dimethyldibenzo-[h, q]-1,7-dioxa-13, 17-diaza-2, 3, 4, 5, 6, 7, 10, 11, 12, 13, 14, 15, 16-tridecahydro-1H-cyclooctadecenediium bis(hexafluorophosphate) (54): Bis-amine (**53**) (28mg, 0.073mmols) was dissolved in 2 ml of methanol. 6N HCl (2ml) was added and stirred for 3 hours at room temperature. The solvent was removed under vacuum and the crude reaction

mixture was re-dissolved in 3 ml of H₂O. Ammonium hexafluorophosphate (>30 equivalents) in CH₂Cl₂ was added and stirred over night. The compound (**54**) precipitated from the solvents as an off white solid. (18mg, 0.026 mmol, 35%): decompose >160°C, ¹H NMR (400 MHz, DMSO) δ 1.65-1.74 (m, 2H); 1.84-1.91 (m, 4H); 2.04-2.12 (m, 2H); 2.26 (s, 6H); 3.02-3.08 (m, broad, 4H); 4.06 (t, 4H, J=5.1 Hz); 4.11 (s, 4H); 7.02 (d, 2H, J=9.1 Hz); 7.22-7.23 (m, 4H); 8.60 (s, 4H); ¹³C NMR (100 MHz, DMSO) δ 20.60, 21.68, 25.10, 44.04, 45.11, 69.20, 112.51, 119.89, 129.86, 131.96, 132.65, 155.70; MS(ESI) m/z 383.1(M)⁺, 192.1(M²⁺/2)⁺; HRMS(ESI) calcd for C₂₄H₃₅O₂N₂ (M+H) 383.2699, found 383.2710.

10, 21-dimethyldibenzo-[h, r]-1,7-dioxa-13, 18-diaza-2, 3, 4, 5, 6, 7, 10, 11, 12, 13, 14, 15, 16, 17-tetradecahydro-1H-cyclononadecene (55): Compound (**52**) (0.06g, 0.176 mmol) was suspended in 22 ml of dry ethanol, purged with dry N₂ for 30 minutes and set up for reflux. Butane-1, 4-diamine (0.0224 ml, 0.222mol) was dissolved in 9 ml of dry ethanol under N₂ and cannulated in to an addition funnel. The diamine was added drop wise through the addition funnel and the reaction mixture was refluxed for 20 hrs under N₂. Removal of the solvent under reduced pressure yielded the bis-imine as a yellow solid which was then subjected to reduction without further purification.

Crude bis-imine was re-dissolved in 2 ml of anhydrous methanol under N₂. 10% Pd-C (0.1 g) was added and the reaction mixture was started stirring. Triethylsilane (1.0 ml, 0.006 mol) was added drop wise into the methanolic bis-imine solution with an addition funnel, the top of which was attached to a rubber balloon. After the addition was complete, the mixture was stirred for additional 6 hrs at room temperature. The reaction mixture was filtered through Celite and removal of the solvent under vacuum gave the crude product as a yellow oil. Silica gel

column chromatography with 10% CHCl₃, 4% isopropyl amine and 86% diethyl ether furnished the compound **55** as an off white solid. (0.060g, 0.151 mmol, 86% after both steps): mp 95-96°C, ¹H NMR (400 MHz, DMSO) δ 1.39-1.42 (m, 4H); 1.62-1.67 (m, 4H); 1.77-1.84 (m, 4H, J=6.87 Hz); 2.21 (s, 6H); 2.47 (t, 4H, J=5.6 Hz); 3.61 (s, 4H); 3.96 (t, 4H, J=5.9 Hz); 6.85 (d, 2H, J=8.2 Hz); 6.99 (d, 2H, J=8.8 Hz); 7.04 (s, 2H); ¹³C NMR (100 MHz, DMSO) δ 20.80, 24.69, 27.24, 29.85, 48.31, 48.46, 68.91, 112.50, 128.71, 128.93, 129.41, 131.41, 155.52; MS(ESI) m/z 397.1(M+H)⁺; HRMS(ESI) calcd for C₂₅H₃₆O₂N₂ (M+H) 397.2855, found 397.2852.

10, 21-dimethyldibenzo-[h, r]-1,7-dioxa-13, 18-diaza-2, 3, 4, 5, 6, 7, 10, 11, 12, 13, 14, 15, 16, 17-tetradecahydro-1H-cyclononadecenediium bis(hexafluorophosphate (56): Bis-amine (55) (15mg, 0.038mmols) was dissolved in 3 ml of methanol. 6N HCl (2ml) was added and stirred for 3 hours at room temperature. The solvent was removed under vacuum and the crude reaction mixture was re-dissolved in 3 ml of H₂O. Ammonium hexafluorophosphate (>30 equivalents) in CH₂Cl₂ was added and stirred over night. The compound (**56**) precipitated from the solvents as an off white solid. (24mg, 0.034 mmol, 92%): decompose >165°C, ¹H NMR (400 MHz, DMSO) δ 1.71 (s, broad, 4H); 1.82-1.87 (m, 4H, J=5.9 Hz); 2.26 (s, 6H); 2.92 (s, broad, 4H); 4.04 (t, 4H, J=5.4 Hz); 7.01 (d, 2H, J=8.7 Hz); 7.21-7.23 (m, 4H); 8.49 (s, 4H); ¹³C NMR (100 MHz, DMSO) δ 20.61, 22.63, 25.06, 29.88, 45.22, 46.08, 69.21, 112.71, 119.94, 129.91, 131.98, 132.92, 155.89; MS(ESI) m/z 397.1(M)⁺, 199.2(M²⁺/2)⁺, 543.1(M²⁺·PF₆⁻)⁺; HRMS(ESI) calcd for C₂₅H₃₇O₂N₂ (M+) 397.2855, found 397.2864.

3-(4-hydroxyphenyl)propanoyl chloride (58): 3-(4-Hydroxyphenyl)propionic acid (5.0 g, 0.03 mol) was dissolved in 20 ml of dry CH₂Cl₂ and equipped for reflux under N₂. Two drops of

DMF was added through the condenser as the accelerator for the reaction, followed by 2.60 ml (0.036 mol) of thionyl chloride. The reaction mixture was refluxed for 1 ½ hours. Removal of the solvent and excess thionyl chloride under vacuum yielded the crude acid chloride which was used in the next step without further purification or characterization.

3-(4-methylphenyl)-N-propylpropanamide (59): Acid chloride **58** was re-dissolved in 20 ml of dry methylene chloride. Excess propylamine (25 ml, 0.305 mol) was added in excess followed by 2 drops of pyridine. The mixture was stirred at room temperature under N₂ for 5 hours and the excess amine was removed under vacuum. Silica gel column chromatography (40:60 EtOAc: CH₂Cl₂) furnished the compound as a yellow oil. (4.62 g, 0.022 mol, 74%) ¹H NMR (400 MHz, CDCl₃) δ 0.82 (t, 3H, J=7.5 Hz); 1.37-1.46 (m, 2H); 2.42 (t, 2H, J=7.3 Hz); 2.86 (t, 2H, J=7.2 Hz); 3.14 (q, 2H, J=7.5 Hz); 5.43 (s, broad, 1H); 6.74 (d, 2H, J=8.58 Hz); 7.00 (d, 2H, J=8.83 Hz); ¹³C NMR (100 MHz, CDCl₃) δ 11.49, 22.96, 31.17, 39.11, 41.50, 115.64, 129.60, 132.52, 154.76, 172.77; HRMS(ESI) calcd for C₁₂H₁₇O₂N (M+H) 208.1338, found 208.1315.

3,3'-[butane-1,4-diylbis(oxy-4,1-phenylene)]bis(N-propylpropanamide) (60): 3-(4-methylphenyl)-N-propylpropanamide **59** (1.234g, 5.95mmol) was dissolved in 60 ml of dry THF in a round bottom flask under N₂. K₂CO₃ (0.824g, 5.95mmol) and 18-Crown-6 (0.326g, 1.233mmol) were added and set up for reflux under N₂. 1, 4-dibromobutane (0.356ml, 2.975mmol) was added through the condenser drop wise and the reaction mixture was refluxed 20 hrs. The reaction mixture was allowed to cool to room temperature and quenched with 10 % HCl. Layers were separated and the aqueous was extracted with CH₂Cl₂ (3x10ml). Combined organic layers

were washed with sat. sodium bicarbonate (2x10ml) and brine (10ml) sequentially and dried with anhydrous Na₂SO₄. Removal of the solvent under reduced pressure gave the crude product as a solid. Recrystallization with hot methanol furnished the pure product as a white solid(1.045g, 2.23mmol, 75% yield): mp 199-200°C, ¹H NMR (400 MHz, DMSO) δ 0.79 (t, 6H, J=7.7 Hz); 1.32-1.38 (m, 4H); 1.83 (s, broad, 4H); 2.30 (t, 4H, J=8.0 Hz); 2.72 (t, 4H, J=7.4 Hz); 2.96 (q, 4H, J=7.4 Hz); 3.97 (s, broad, 4H); 6.83 (d, 4H, J=8.87 Hz); 7.08 (d, 4H, J=8.3 Hz); 7.77 (t, 2H, J=5.96 Hz); ¹³C NMR (100 MHz, DMSO) δ 11.52, 23.04, 26.24, 31.17, 39.14, 41.41, 67.71, 114.75, 129.52, 133.17, 157.67, 172.29; MS(ESI) m/z Calc M+H C₂₈H₄₀O₄N₂ = 469.63 found 466.1

3,3'-[pentane-1,5-diylbis(oxy-4,1-phenylene)]bis(N-propylpropanamide) (61): 3-(4-methylphenyl)-N-propylpropanamide **59** (1.12g, 5.4mmol) was dissolved in 54 ml of dry THF in a round bottom flask under N₂. K₂CO₃ (0.744g, 5.4mmol) and 18-Crown-6 (0.294g, 0.806mmol) were added and was set up for reflux under N₂. 1, 5-dibromopentane (0.378ml, 2.7mmol) was added through the condenser drop wise and refluxed for 20 hrs. The reaction was allowed to cool to room temperature and quenched with 10 % HCl. The layers were separated and the aqueous was extracted with CH₂Cl₂ (3x20ml). The combined organic layers were washed with sat. sodium bicarbonate (2x20ml) and brine (20ml) sequentially and dried with anhydrous Na₂SO₄. Removal of the solvent under reduced pressure yielded the crude as a white solid. Recrystallization with hot methanol yielded the pure product as a white crystalline solid (0.97g, 2.01mmol, 74.5% yield): mp 161-162°C, ¹H NMR (400 MHz, CDCl₃) δ 0.83 (t, 6H, J=7.5 Hz); 1.38-1.47 (m, 4H); 1.58-1.64 (m, 2H); 1.78-1.85 (m, 4H); 2.40 (t, 4H, J=7.3 Hz); 2.88 (t, 4H,

J=7.81 Hz); 3.15 (q, 4H, J=6.7 Hz); 3.93 (t, 4H, J=6.9 Hz); 5.29 (s, broad, 2H); 6.79 (d, 4H, J=8.9 Hz); 7.08 (d, 4H, J=8.8 Hz); ¹³C NMR (100 MHz, CDCl₃) 11.51, 22.90, 23.03, 29.22, 31.16, 39.14, 41.39, 67.97, 114.76, 129.48, 133.09, 172.28, 189.75; MS(ESI) m/z Calc M+H C₂₉H₄₂O₄N₂ = 483.65 found 483.2

3,3'-{butane-1,4-diylbis[oxy(3-formyl-4,1-phenylene)]}bis(N-propylpropanamide)(62):

Compound **60** which had been dried over P₂O₅ (0.782g, 1.67mmol) and Duff reagent (0.607g, 4.33mmol) were mixed in a round bottom flask and set up for reflux. 7ml of TFA was added through the condenser under N₂ and the reaction mixture was refluxed 24 hrs at 85°C. The mixture was concentrated under vacuum and extracted into CH₂Cl₂ from water. Aqueous phase was acidified with concentrated HCl and extracted into 2x10 ml CH₂Cl₂. The combined organic extract was washed sequentially with 2x10 ml 4N HCl, 10 ml saturated aq. Na₂CO₃ and 10 ml brine. Removal of the solvent under vacuum gave the crude as a brown gluey mass. Column chromatography (silica gel with 10:90 ethanol: diethyl ether) gave the pure product as a white solid (0.59g, 0.12mmol, 67%): mp 128-129°C, ¹H NMR (400 MHz, CDCl₃) δ 0.84 (t, 6H, J=7.2 Hz); 1.38-1.50 (m, 4H); 2.05 (s, 4H); 2.42 (t, 4H, J=7.8 Hz); 2.91 (t, 4H, J=7.6 Hz); 3.15 (q, 4H, J=6.7 Hz); 4.15 (s, 4H); 5.57 (s, broad, 4H); 6.86 (d, 2H, J=8.9 Hz); 7.36 (dd, 2H, J₁=8.5 Hz, J₂=2.38 Hz); 7.56 (d, 2H, J=2.4 Hz); 10.30 (s, 2H); ¹³C NMR (100 MHz, CDCl₃) δ 11.53, 23.03, 26.06, 30.79, 38.54, 41.44, 68.09, 112.68, 124.77, 127.87, 133.66, 136.64, 159.84, 171.91, 189.58; HRMS(ESI) calcd for C₃₀H₄₂O₆N₂ (M+H) 525.2965, found 525.2952.

3,3'-{pentane-1,5-diylbis[oxy(3-formyl-4,1-phenylene)]}bis(N-propylpropanamide)(63):

Compound **61** which had been dried over P₂O₅ (0.155g, 0.321mmol) and Duff reagent (0.125g,

0.89mmol) were mixed in a round bottom flask and set up for reflux. 5ml of TFA was added through the condenser under N₂ and the reaction mixture was refluxed 24 hrs at 85°C. The mixture was concentrated under vacuum and extracted into CH₂Cl₂ from water. Aqueous phase was acidified with concentrated HCl and extracted into 2x5 ml CH₂Cl₂. The combined organic extract was washed sequentially with 2x5 ml 4N HCl, 5ml saturated aq. Na₂CO₃ and 5 ml brine. Removal of the solvent under vacuum gave the crude as a brown gluey mass. Column chromatography (silica gel with 10:90 ethanol: diethyl ether) gave the pure product as a white solid (0.081g, 0.150mmol, 46.5%): mp 77-78°C, ¹H NMR (400 MHz, CDCl₃) δ 0.83 (t, 6H, J=7.4 Hz); 1.38 -1.46 (m, 4H); 1.66-1.70 (m, 2H); 1.88-1.93 (m,4H); 2.42 (t, 4H, J=8.4 Hz); 2.91 (t, 4H, J=7.2 Hz); 3.15 (q, 4H, J=7.8 Hz); 4.07 (t, 4H, J=6.4 Hz); 5.40 (s, broad, 4H); 6.86 (d, 2H, J=8.7 Hz); 7.37 (dd, 2H, J1=8.6 Hz, J2=2.39 Hz); 7.62 (d, 2H, J=2.5 Hz); 10.42 (s, 2H); ¹³C NMR (100 MHz, CDCl₃) δ 11.49, 22.98, 23.03, 29.00, 30.74, 38.46, 41.42, 68.50, 112.90, 124.91, 127.71, 133.46, 136.58, 160.14, 189.92; MS(ESI) m/z Calc M+H C₃₁H₄₂O₆N₂ = 539.67 found 539.1

9, 20- di(N-propylpropanamide)dibenzo-[g, q]-1,6-dioxa-10, 15- diaza-2, 3, 4, 5, 6, 9, 10, 11, 12, 13, 14, 15, 16-tridecahydro-1H-cyclooctadecene (64): Compound (62) (0.140g, 0.266 mmol) was suspended in 27 ml of dry ethanol, purged with dry N₂ for 30 minutes and set up for reflux. Butane-1, 4-diamine (0.027 ml, 0.266 mmol) was dissolved in 9 ml of dry ethanol under N₂ and cannulated in to an addition funnel. The diamine was added drop wise through the addition funnel and the reaction mixture was refluxed for 20 hrs under N₂. Removal of the solvent under reduced pressure yielded the bis-imine as a yellow solid.

Crude bis-imine was re-dissolved in 5 ml of anhydrous methanol under N₂. 10% Pd-C (0.3 g) was added and the reaction mixture started stirring. Triethylsilane (1.5 ml, 9.25mmol) was added drop wise into the methanolic bis-imine solution with an addition funnel attached to a rubber balloon. After the addition was complete, the mixture was stirred for additional 6 hrs at room temperature. The reaction mixture was filtered through Celite and removal of the solvent under vacuum gave the crude product as a yellow oil. Column chromatography followed by preparative thin layer chromatography with 50% Ethanol, 5% Isopropyl amine and 45% Diethyl ether furnished the compound **65** as a white solid. (0.065g, 0.112mmol, 42% after both steps): mp 138-139°C, ¹H NMR (400 MHz, CDCl₃) δ 0.84 (t, 6H, J=7.77 Hz); 1.41-1.46 (m, 4H, J=6.9 Hz); 2.01 (s, broad, 4H); 2.42 (t, 4H, J=8.6 Hz); 2.68 (s, broad, 4H); 2.86 (t, 4H, J=7.8 Hz); 3.14 (q, 4H, J=8.3 Hz); 3.67 (s, 4H); 4.04 (s, 4H); 5.35 (s, broad, 2H); 6.75 (d, 4H, J=8.4 Hz); 7.05 (d, 4H, J=8.9 Hz); 7.13 (s, 2H); ¹³C NMR (100 MHz, DMSO) δ 11.86, 22.98, 26.67, 27.15, 31.10, 38.18, 48.88, 67.95, 111.72, 128.58, 130.99, 133.62, 155.68, 172.16; HRMS(ESI) calcd for C₃₄H₅₂O₄N₄ (M+H) 581.4067, found 581.4047.

9, 20- di(N-propylpropanamide)dibenzo-[g, q]-1,6-dioxa-10, 15- diaza-2, 3, 4, 5, 6, 9, 10, 11, 12, 13, 14, 15, 16-tridecahydro-1H-cyclooctadecenediium bis(hexafluorophosphate) (57a):

Bis-amine (**64**) (50 mg, 0.086mmols) was dissolved in 3 ml of methanol. 6N HCl (7ml) was added and stirred for 3 hours at room temperature. The solvent was removed under vacuum and the crude reaction mixture was re-dissolved in 3 ml of H₂O. Ammonium hexafluorophosphate (>30 equivalents) in CH₂Cl₂ was added and stirred over night. The compound (**57a**) precipitated from the solvents as an off white solid. (55 mg, 0.063 mmol, 73%) mp 178-180°C, ¹H NMR (400 MHz, DMSO) δ 0.80 (t, 6H, J=7.6 Hz); 1.32-1.41 (m, 4H, J=8.1 Hz); 1.73 (s, broad, 4H); 1.96

(s, broad, 4H); 2.34 (t, 4H, J=7.6 Hz); 2.77 (t, 4H, J=7.6 Hz); 2.98 (q, 4H, J=6.0 Hz); 4.08(s, broad, 8H); 5.02 (s, broad, 2H); 7.04 (d, 2H, J=8.41 Hz); 7.22 (s, 2H); 7.24 (d, 2H, J=8.4 Hz); 7.79 (t, 2H, J=5.7 Hz); 8.48 (s, 4H); ^{13}C NMR (100 MHz, DMSO) δ 12.05, 22.80, 23.06, 26.42, 30.77, 37.76, 39.56, 45.54, 46.42, 68.53, 112.54, 120.00, 131.20, 132.33, 134.13, 156.03, 171.62; MS(ESI) m/z Calc M^+ $\text{C}_{34}\text{H}_{53}\text{O}_4\text{N}_4 = 581.80$ found 581.2.

1,2-Distearoyl-sn-glycero-3-phospho-sn-1-glycerol, tetrabutylammonium salt: This compound was first synthesized and characterized by a previous graduate student from our lab. The following method gives the same procedure except one modification during the first half of the synthesis: to remove the NaCl formed as a byproduct.

1,2-Distearoyl-sn-glycero-3-phospho-sn-1-glycerol, tetrabutylammonium salt: 0.52 g (0.65 mmol) of 1,2-Distearoyl-sn-glycero-3-phospho-sn-1-glycerol sodium (Genzyme Pharmaceuticals, Liestal, Switzerland) was placed in a ternary mixture of 2 ml of 1.5 M HCl, 12 ml of isopropanol, and 11 ml of chloroform. The mixture was stirred at room temperature until complete salvation occurred (about 5 minutes), then the solvents were removed under reduced pressure (using a rotovap attached to a Welch pump) at room temperature to furnished a white slurry which contained the neutral phospholipid and NaCl byproduct. Washing the white slurry with plenty of water removed the NaCl byproduct. The neutral phospholipid was precipitated using cold acetone, and collected by filtration as a white, waxy solid (0.47 g, 0.6 mmol, 93% yield). This material was characterized by ^{31}P NMR, ^{13}C NMR, and ^1H NMR. The ^{31}P NMR

spectrum showed a single, well-resolved peak at 0.8 ppm (in ternary mixture of 3:3:0.5 CD₃OD: CDCl₃: D₂O) while the peak from that of the sodium salt was at 1.6 ppm in the same solvent mixture. The melting point of the neutral acid was 134-136 °C, while that of the sodium salt was over 200 °C. The above material (0.47 g, 0.6 mmol) was re-suspended in 30 ml of chloroform, and 0.125 g (0.48 mmol) of tetrabutylammonium hydroxide was added to the mixture. The mixture was allowed to stir at room temperature for 5 minutes to dissolve the base, and allowed to stir an additional five minutes before removal of the solvent under high vacuum at room temperature. The resultant semi-solid was re-suspended in 50:50 acetone: hexanes and filtered to remove neutral phospholipid. The solvents were removed from the filtrate under high vacuum, and the resultant material was taken up into warm hexanes and transferred to the freezer, where it was left overnight. The next day, a precipitate had set up and was collected by filtration, giving 0.36 g (0.35 mmol, 60% yield) of product as a white, semicrystalline solid: mp 52.5-55 °C; ¹H NMR (400 MHz, CDCl₃) δ 0.87 (t, 6H, J=6.8 Hz); 1.00 (t, 12H, J=7.2 Hz); 1.24 (broad singlet, 62H); 1.44 (q, 8H, J=7.2 Hz); 1.65 (broad singlet, 10H); 2.28 (q, 4H, J=6.4 Hz); 3.29 (t, 8H, J=8.0 Hz); 3.61-3.76 (m, 4H); 3.89-4.05 (m, 3H); 4.15-4.20 (m, 1H); 4.40-4.42 (m, 1H); 5.21 (broad singlet, 1H); ¹³C NMR (100 MHz, CDCl₃) δ 13.9, 14.3, 20.0, 22.9, 24.2, 25.1, 29.4, 29.6, 29.7, 29.9, 32.1, 34.4, 34.5, 59.0, 63.1, 63.5, 65.2, 66.3, 70.8, 71.8, 173.3, 173.7; ³¹P NMR (162 MHz, CDCl₃) δ 3.06; FTIR (KBr) ν 1472, 1734, 3421 cm⁻¹; MS (ESI) 160 m/z 777.6 (M)⁻, 242.2 (M)⁺; HRMS (ESI) calc. (M)⁻ C₄₂H₈₂O₁₀P 777.5646, (M)⁺ C₁₆H₃₆N 242.2848, found (M)⁻ 777.5641, (M)⁺ 242.2821

BIBLIOGRAPHY

BIBLIOGRAPHY

- [1] A. Izadpanah and R. Gallo, 'Antimicrobial Peptides' *Journal of the American Academy of Dermatology*, volume 52, issue 3, 381-390.
- [2] Valeria Amendola, Marco Bonizzoni, David Esteban-Gomez, Luigi Fabbrizzi, Maurizio Licchelli, Felix Sancenon and Angelo Taglietti, 'Some guidelines for the design of anion receptors' *Coordination Chemistry Reviews*, 250(2006) 1451-1470.
- [3] *Supramolecular Chemistry of Anions*; Edited by Antonio Bianchi, Kristan Bowman-James, Enrique Garcia-Espana, 1997, Wiley & Sons, Inc. Chapter 2, Historical View on the Development of Anion Coordination Chemistry, written by Bernard Dietrich and Mir Wais Hosseini.
- [4] *Anion Receptor Chemistry*; Jonathan L Sessler (Author), Philip Gale (Author), Won-Seob Cho (Author), 2006, RSC Publishing.
(<http://www.rsc.org/ebooks/archive/free/BK9780854049745/BK9780854049745-00001.pdf>) Date cited:02/22/2010.
- [5] Ernest Graf and Jean-Marie Lehn, 'Synthesis and Cryptate Complexes of a Spheroidal Macrotricyclic Ligand with Octahedrotetrahedral Coordination' *Journal of the American Chemical Society*, 97:17, August 20, 1975.; Ernest Graf and Jean-Marie Lehn, 'Anion Cryptates: Highly Stable and Selective Macrotricyclic Anion Inclusion Complexes' *Journal of the American Chemical Society*, 98:20, September 29, 1976.
- [6] Jean-Marie Lehn, Etienne Sonveaux and Alvin K. Willard, 'Molecular Recognition. Anion Cryptates of a Macrobicyclic Receptor Molecule for Linear Triatomic Species' *Journal of the American Chemical Society*, 100:15, July 19, 1978.
- [7] R. A. Pascal, J. Spergel, and D. Van Engen, 'Synthesis and X-ray Crystallographic Characterization of a (1,3,5) Cyclophane with Three Amide N-H Groups Surrounding a Central Cavity. A Neutral Host for Anion Complexation' *Tetrahedron Letters*, 1986, 27, 4099.
- [8] S. Valiyaveetil, J. Spergel and D. V. Engbersen, 'Synthesis and Complexation Studies of Neutral Anion Receptors' *Angew. Chem. Int. Ed.*, 1993, 32, 900.
- [9] P. D. Beer and P. A. Gale, 'Anion Recognition and Sensing: The State of The Art and Future Perspectives' *Angew. Chem. Int. Ed.*, 2001, 40, 486 – 516.

- [10] Supramolecular Chemistry of Anions; Edited by Antonio Bianchi, Kristan Bowman-James, Enrique Garcia-Espana, 1997, Wiley & Sons Inc., Chapter 4, 'Artificial Anion Hosts. Concepts for Structure and Guest Binding' written by Franz P. Schmidtchen.
- [11] i. Pawe Dydio, Tomasz Zielin' ski and Janusz Jurczak, 'Anion Receptors Based on 7,7'-diamido-2,2'-diindolylmethane' *Chem. Commun.*, 2009, 4560–4562.; ii. C. Caltagirone, Andrea Mulas, Francesco Isaia, Vito Lippolis, Philip A. Gale and Mark E. Light, 'Metal-induced pre-organisation for Anion Recognition in a Neutral Platinum-containing Receptor' *Chem. Commun.*, 2009, 6279–6281.; iii. Pedro Mateus, Rita Delgado, Paula Brandao and Vitor Felix, ' Polyaza Cryptand Receptor Selective for Dihydrogen Phosphate' *J. Org. Chem.*, 2009, 74, 8638–8646.; iv. Andrea Bencini, Silvia Biagini, Claudia Giorgi, Henri Handel, Michel Le Baccon, Palma Mariani, Piero Paoletti, Paola Paoli, Patrizia Rossi, Raphaël Tripier, and Barbara Valtancoli, 'A Tris-Macrocyclic with Proton Sponge Characteristics as Efficient Receptor for Inorganic Phosphate and Nucleotide Anions, *Eur. J. Org. Chem.* 2009, 5610–5621.; v. Pawel Dydio, Tomasz Zielin Ski, and Janusz Jurczak, '7,7'-Diureido-2,2'-diindolylmethanes: Anion Receptors Effective in a Highly Competitive Solvent, Methanol' *Org. Lett.*, Vol. 12, No. 5, 2010.
- [12] Kristy M. DiVittorio, W. Matthew Leevy, Edward J. O'Neil, James R. Johnson, Sergei Vakulenko, Joshua D. Morris, Kristine D. Rosek, Nathan Serazin , Sarah Hilker, Scott Hurley, Manuel Marquez, and Bradley D. Smith, 'Zinc (II) Coordination Complexes as Membrane Active Fluorescent Probes and Antibiotics' *ChemBioChem.*, 2008, 9, 286-293.
- [13] Donald J. Hanahan, ' A Guide to Phospholipid Chemistry', 1997, Oxford University Press.
- [14] Alexander J. Y. Lan, Robert O. Heuckeroth and Patrick S. Mariano, 'Electron-Transfer-Induced Photocyclization Reactions of Arene-Iminium Salt Systems. Effects of Cation Diradical Deprotonation and Desilylation on the Nature and Efficiencies of Reaction Pathways Followed' *J. Am. Chem. Soc.* 1987, 109, 2738-2745.
- [15] Giovanni Casiraghi, Giuseppe Casnati, Giuseppe Puglia, Giovanni Sartori and Giuliana Terenghi, 'Selective Reactions between phenols and formaldehyde. A novel route to salicylaldehydes' *JCS Perkins I*, (1980) 1862-1865.
- [16] Syoji Morimura, Hideo Horiuchi and Keisuke Murayama, 'Vilsmeier Reaction of Phenols. I. Synthesis of Aryl Formates' *Bulletin of the Chemical Society of Japan*, vol.50, No.8 (1977) 2189-2190.

- [17] L. F. Lindoy, G. V. Meehan and N. Svenstrup, 'Mono- and Diformylation of 4-Substituted Phenols: A New Application of the Duff reaction' *Synthesis*, 1998, 7, 1029-1032.
- [18] Dennis H. Burns, Jeffrey D. Miller and Jacqueline Santana, 'Synthesis and Characterization of [3.3.3] Metacyclophane' *J. Org. Chem.*, 1993, 58, 6526-6528.
- [19] David T. Fox and C. Dale Poulter, 'Synthesis and Evaluation of 1-deoxy-D-xylulose 5-phosphoric Acid Analogues to Alternate Substrates for Methylerythritol Phosphate Synthase' *J. Org. Chem.*, 2005, 70, 1978-1985.
- [20] H. Weber and H.G. Khorana; *J. Mol. Biol.*, 72, 219, 1972.
- [21] Theodora Greene, 'Greene's Protective Groups In Organic Synthesis', New York, Wiley, 4th edition, 2007, Chapter 2, pg 27.
- [22] Wenming Liu, Joanna Szewczyk, Liladhar Waykole, Oljan Repic and Thomas J. Blacklock, 'Practical Synthesis of Diaryloxymethanes', *Synthetic Communications*, vol.33, No.10, pp 1751-1754, 2003.
- [23] Kende A.S. & Fludzinski P., *Organic Syntheses Collective Volumes*).
- [24] Theodora Greene, 'Greene's Protective Groups In Organic Synthesis', New York, Wiley, 4th edition, 2007, Chapter 2, pg 244.
- [25] Kazuhiro Maruyama, Fumikazu Kobayashi and Atsuhiro Osuka, 'Salen- Capped Porphyrins as an Active Site Model of Metalloenzymes: Synthesis and Their Intramolecular Interactions Between the Metal complexes' *Bulletin of the Chemical Society of Japan*, 63, 2672-2681(1990).
- [26] Cristian Simion, Alina Simion, Yoshiharu Mitoma, Satoko Magashima, Takatoshi Kawaji, Iwao Hashimoto and Masashi Tashiro, 'Synthesis of New Dihydroxy-Dioxygenated *ortho*-[2,x] Cyclophanes' *Heterocycles*, vol 53, No 11, pp 2459-2470, 2000.
- [27] Ahmed F. Abdel-Magid, Cynthia a. Maryanoff and Kenneth G. Carson, 'Reductive Amination of Aldehydes and Ketones by Using Sodium Triacetoxyborohydride' *Tetrahedron Letters*, vol 31, No.39, pp 5595-5598,1990.

- [28] Ahmed F. Abdel-Magid, Kenneth G. Carson, Bruce D. Harris, Cynthia a. Maryanoff and Rekha D. Shah, 'Reductive Amination of Aldehydes and Ketones with Sodium Triacetoxyborohydride. Studies on Direct and Indirect Reductive Amination Procedures' *J. Org. Chem.*, 1996, 61, 3849-3862.
- [29] V. Sridharan, S. Muthusubramanian, S. Sivasubramanian, 'A facile Reduction Procedure for N,N'-bis[5-substituted salicylidene]-m/p-phenylenediamines with Sodiumborohydride-Silica Gel System' *Synthetic Communications*, vol.34, no. 6, pp.1087-1096, 2004.
- [30] Miguel A. Sierra, Daniel Pellico, Mar Go'mez-Gallego, Mari'a Jose, Manchen~O and Rosario Torres, 'Synthesis of Highly Functionalized Macrocycles by the Peripheral Functionalization of Macrocyclic Diimines' *J. Org. Chem.* 2006, 71, 8787-8793.
- [31] J. S. McMurray and P. K. Mandal, 'Pd-C-Induced Catalytic Transfer Hydrogenation with Triethylsilane' *J. Org. Chem.* 2007, 72, 6599-6601.
- [32] H.C.Clark, P.W.R. Corfield, K.R.Dixon and James A. Ibers, 'An Unexpected Product in the Reaction of $\text{PtHCl}(\text{P}(\text{C}_2\text{H}_5)_3)_2$ with C_2F_4 . The Structure of the $\text{PtCl}(\text{CO})(\text{P}(\text{C}_2\text{H}_5)_3)_2^+$ Cation and Evidence for the Existence of the SiF_5^- Ion' *Journal of the American Chemical society*, 89:13, June 21, 1967, pp3360-3361.
- [33] Lagili O. Abouderbala, Warwick J. Belcher, Martyn G. Boutelle, Peter J. Cragg, Jonathan W. Steed, David R. Turner and Karl J. Wallace, 'Cooperative Anion Binding and Electrochemical Sensing by Modular Podands' *PNAS*, April 16, 2002, vol. 99, no. 8, 5001-5006.
- [34] 'Studies Towards Small-Molecule-Receptors Selective for Phospholipid Anionic Head Groups in Bacterial Membranes', A Doctoral Dissertation by Frederick A. Meece, May 2009.
- [35] Michael J. Hynes, 'WinEQNMR. A Program for the Calculation of Equilibrium Constants from NMR Chemical Shift Data' *Journal of the Chemical Society, Dalton Transactions*, 1993, 311-312.

APPENDIX

SUPPLEMENTAL MATERIAL

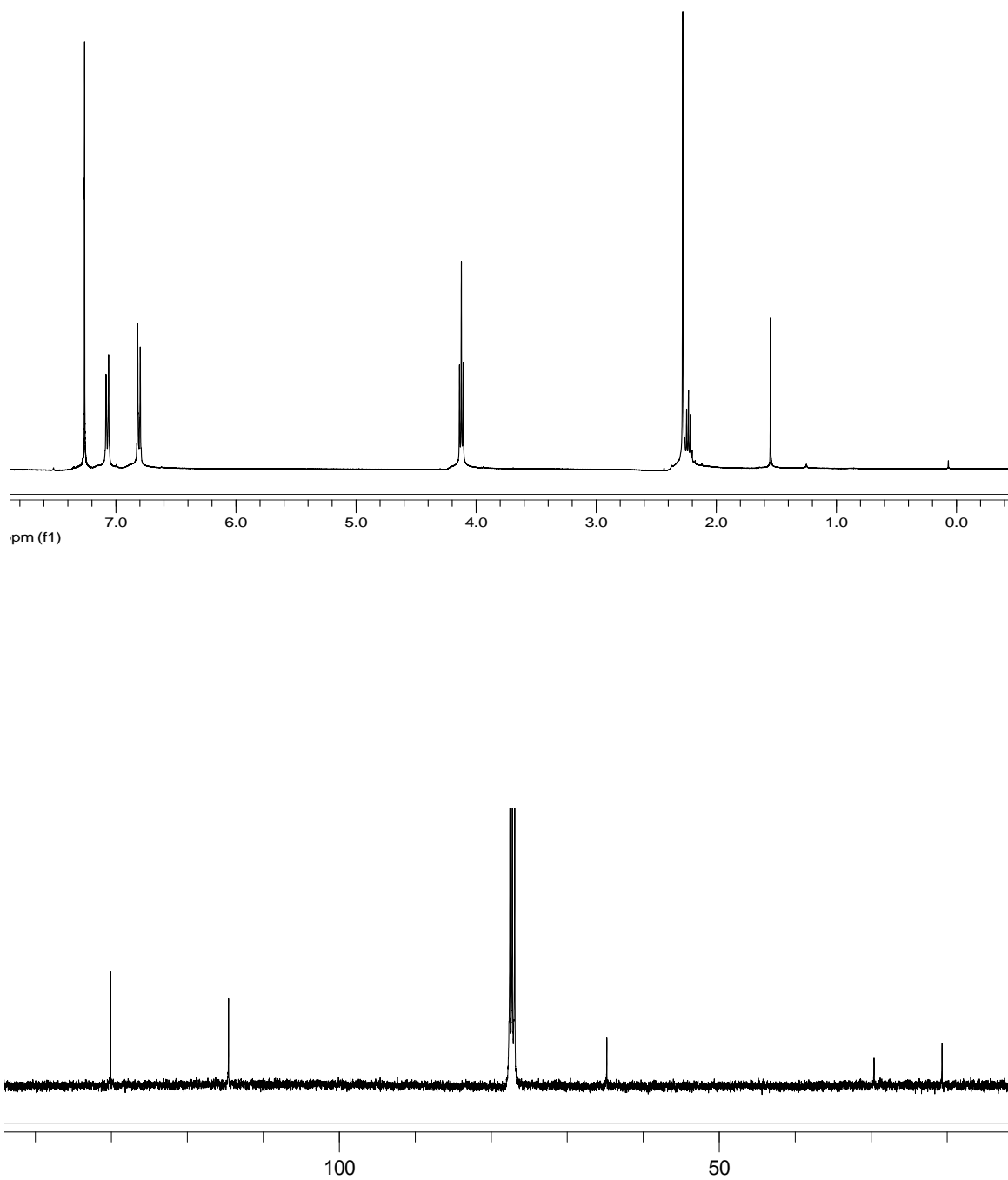


Figure 59. ^1H NMR (top) and ^{13}C NMR (bottom) data for compound **33**

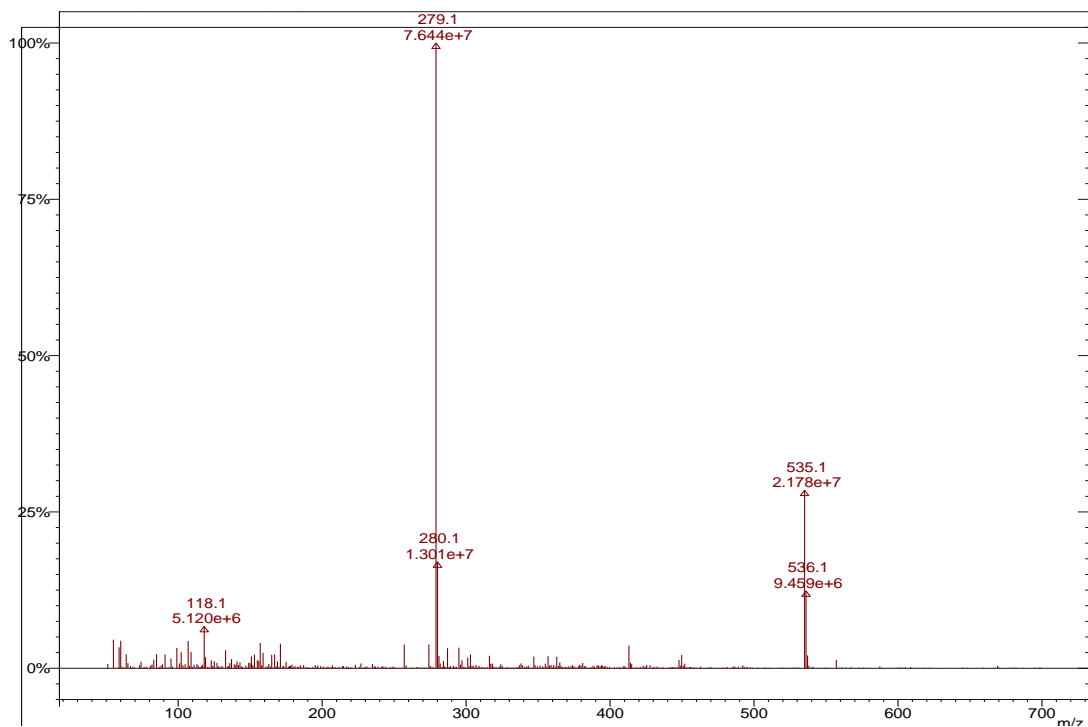
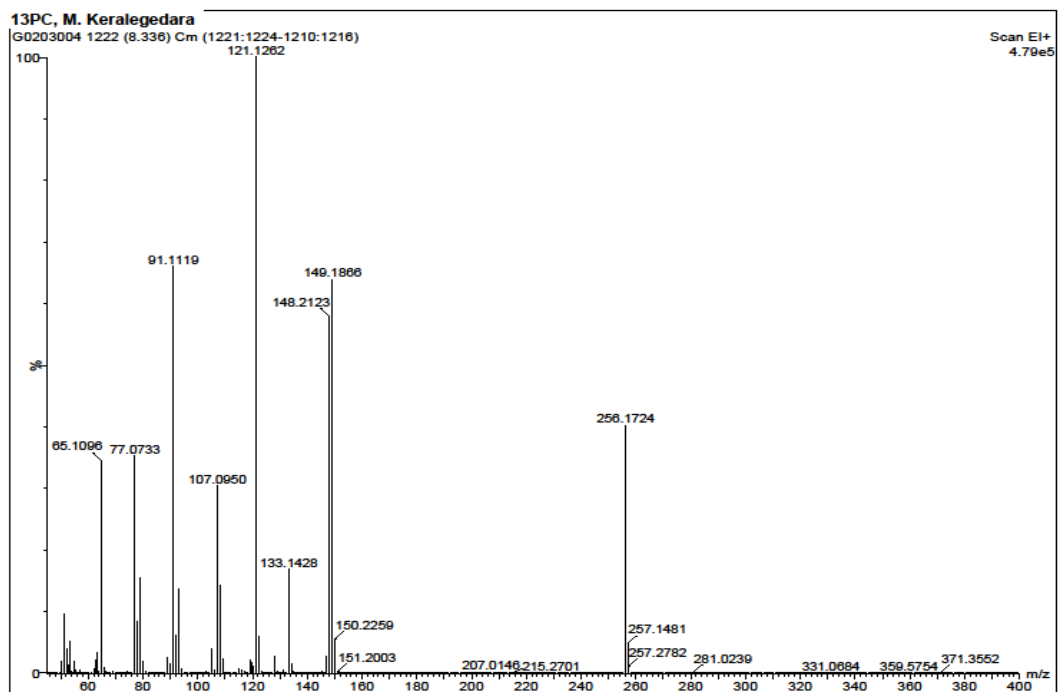


Figure 60. GC-MS (top) and ESI-MS (bottom) data for compound **33**

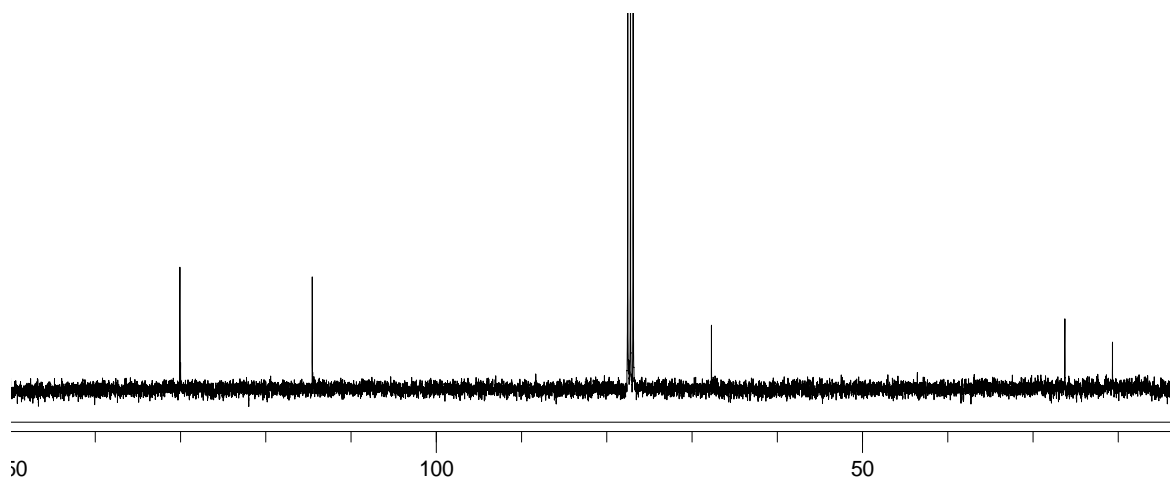
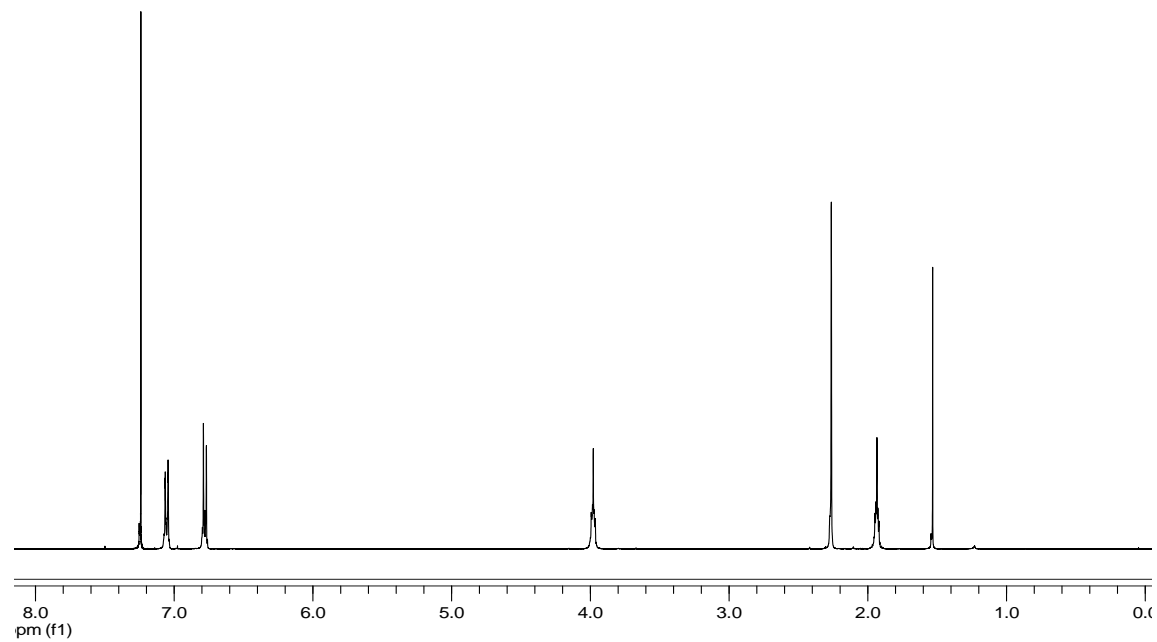


Figure 61. ^1H NMR (top) and ^{13}C NMR (bottom) data for compound **34**

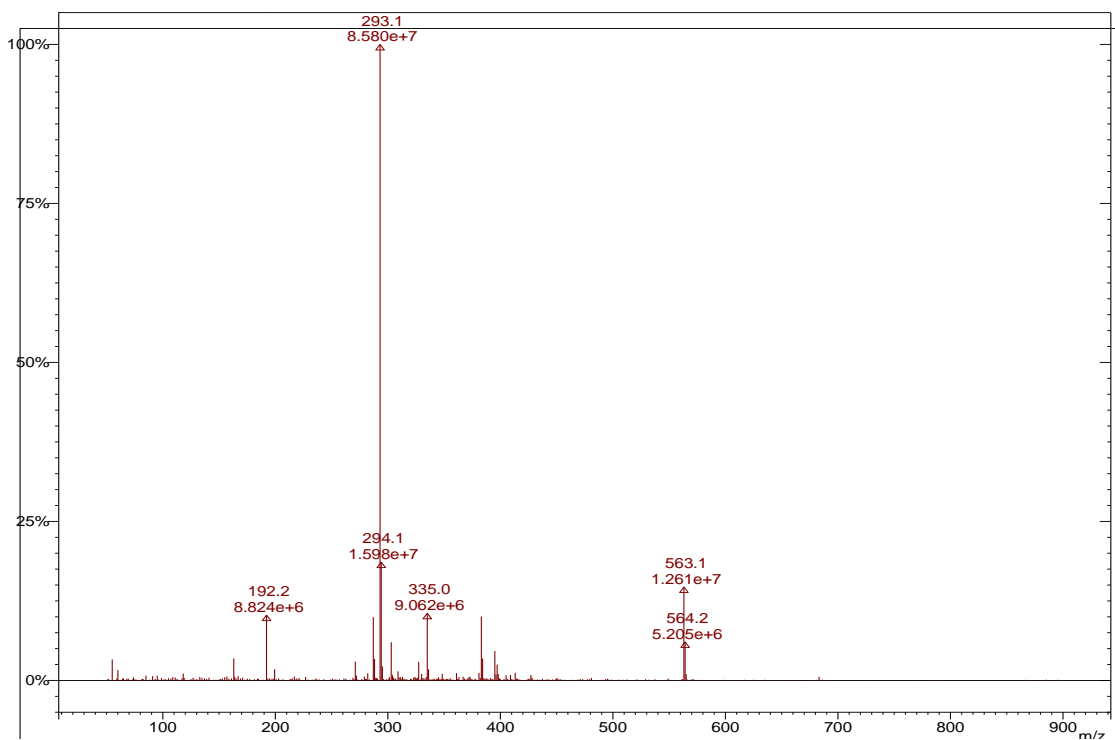
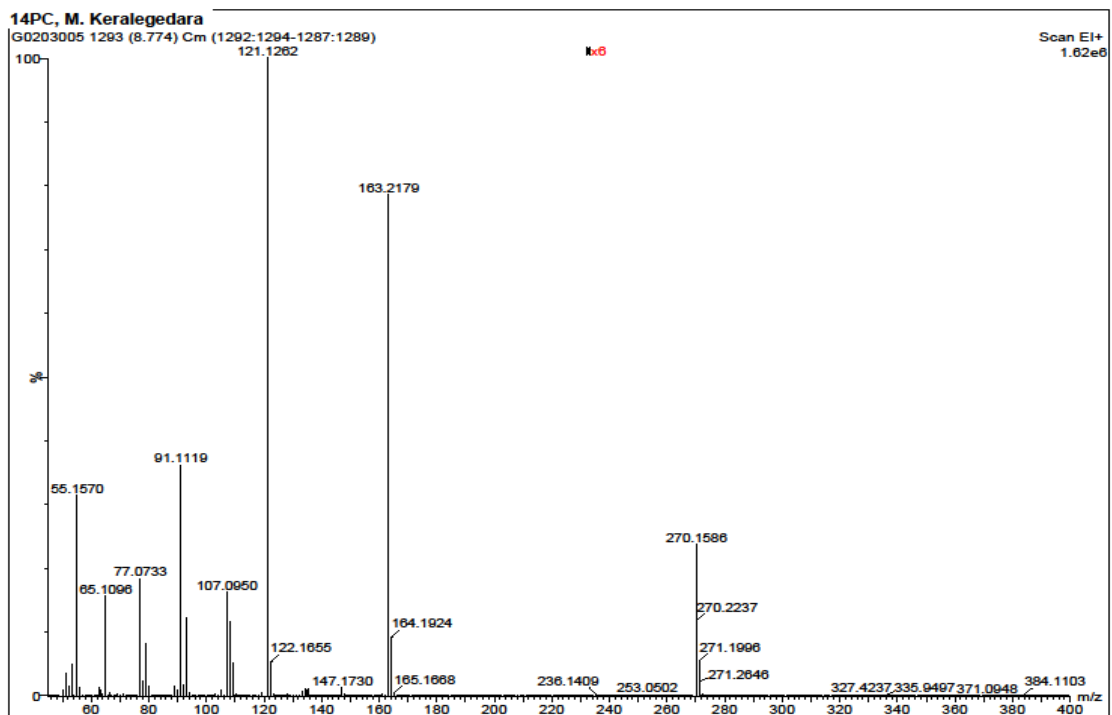


Figure 62. GC-MS (top) and ESI-MS (bottom) data for compound **34**

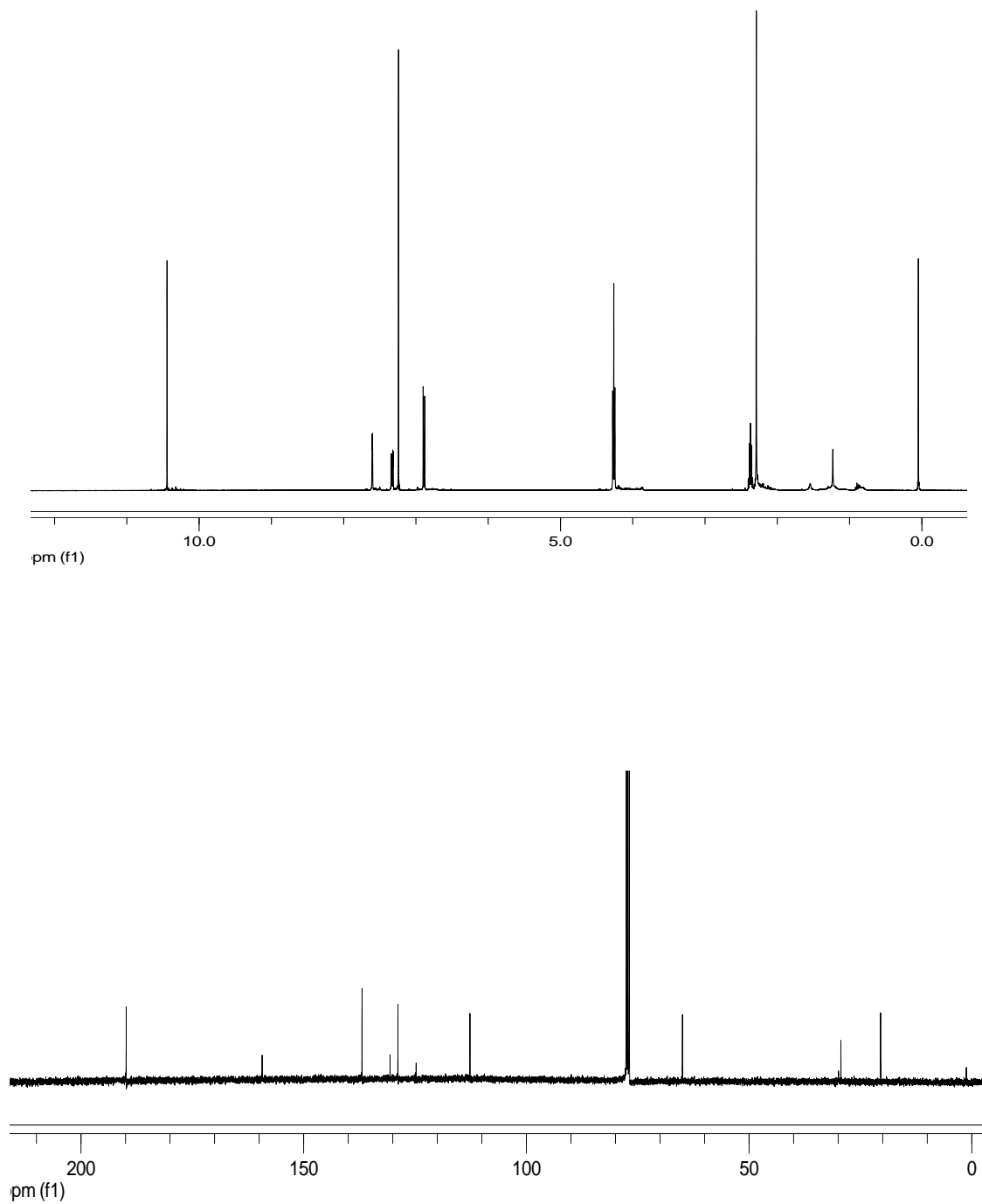


Figure 63. ^1H NMR (top) and ^{13}C NMR (bottom) data for compound **35**

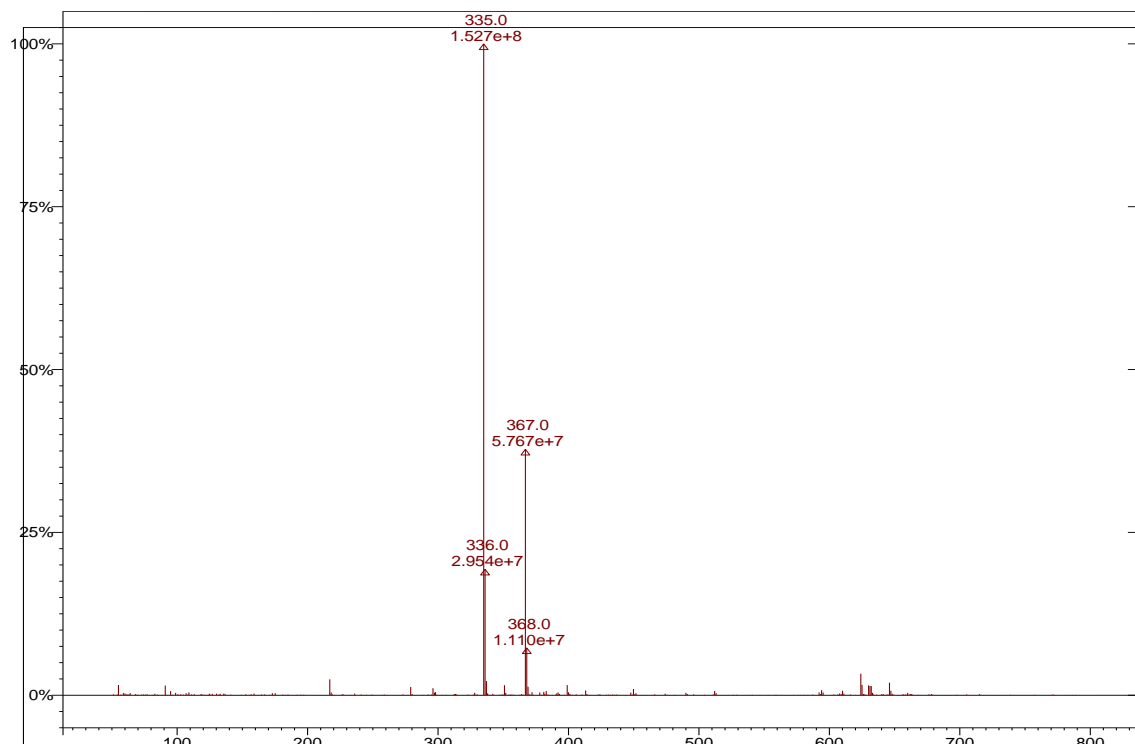
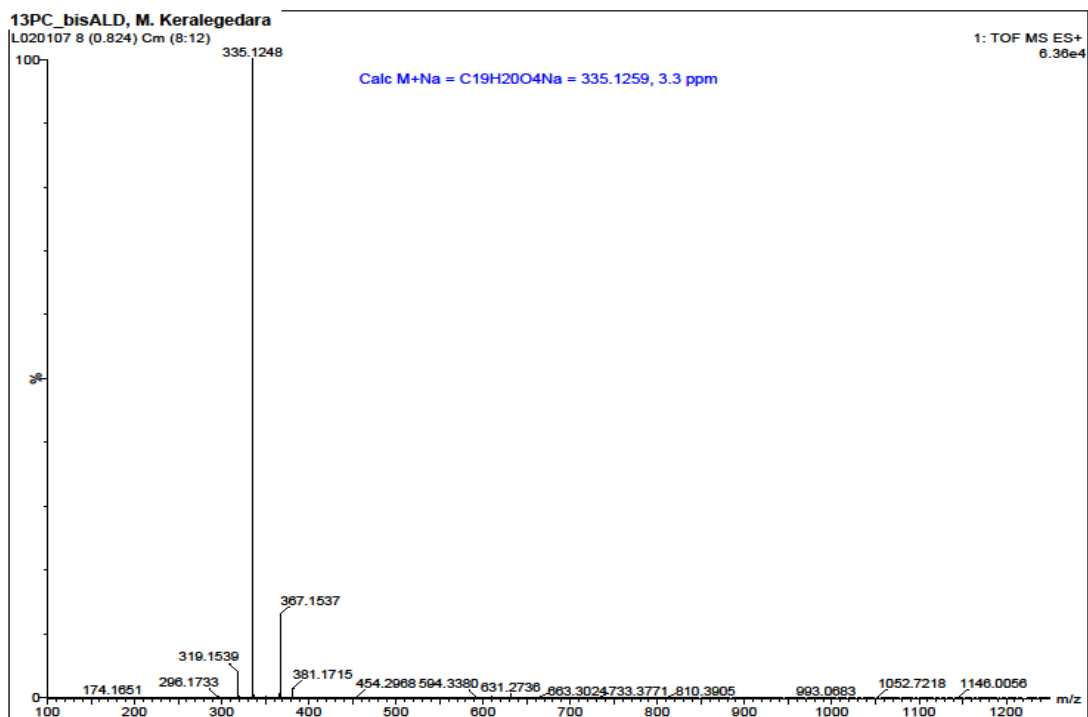


Figure 64. HRMS (top) and ESI-MS (bottom) data for compound **35**.

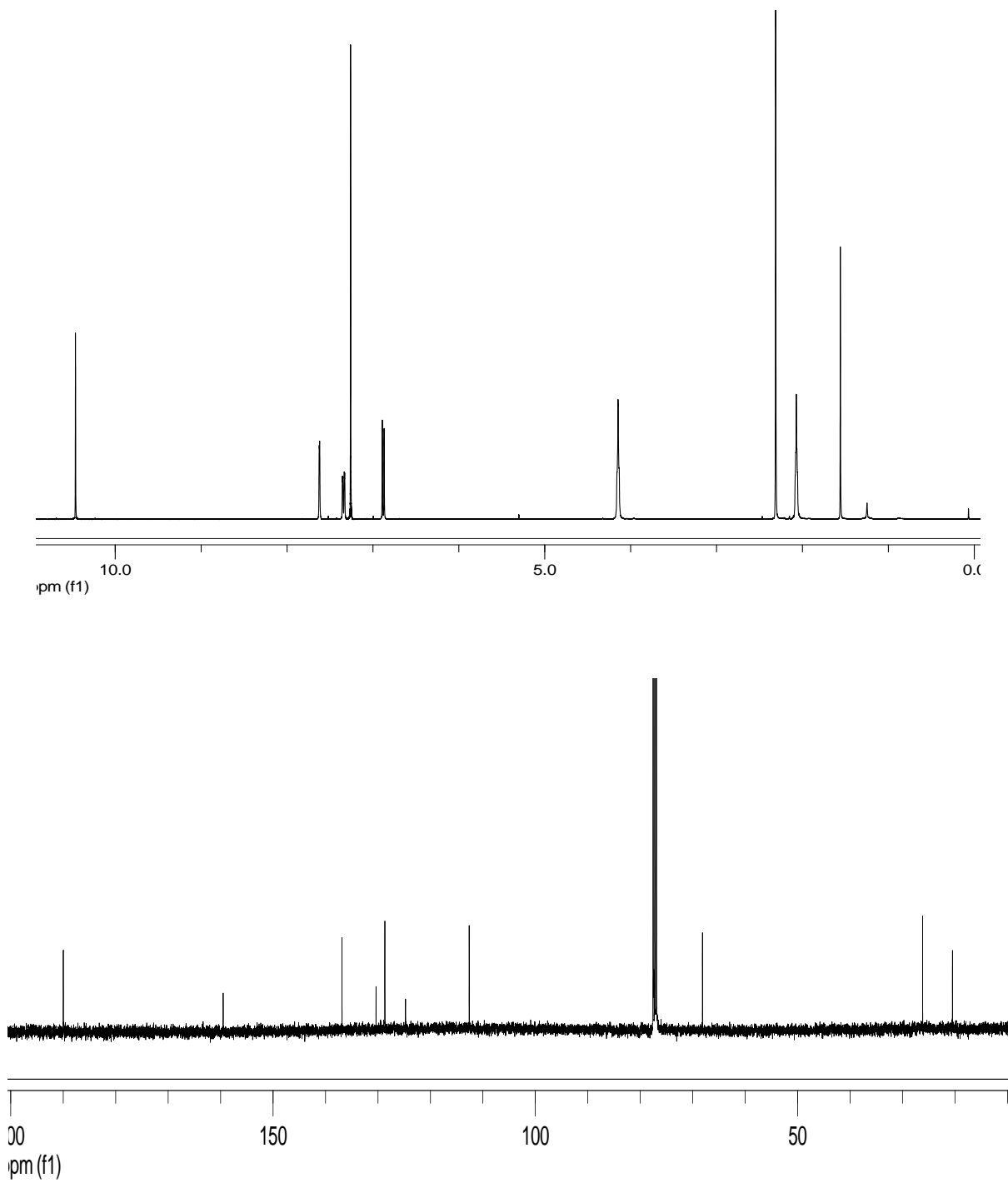


Figure 65. ^1H NMR (top) and ^{13}C NMR (bottom) data for compound **36**

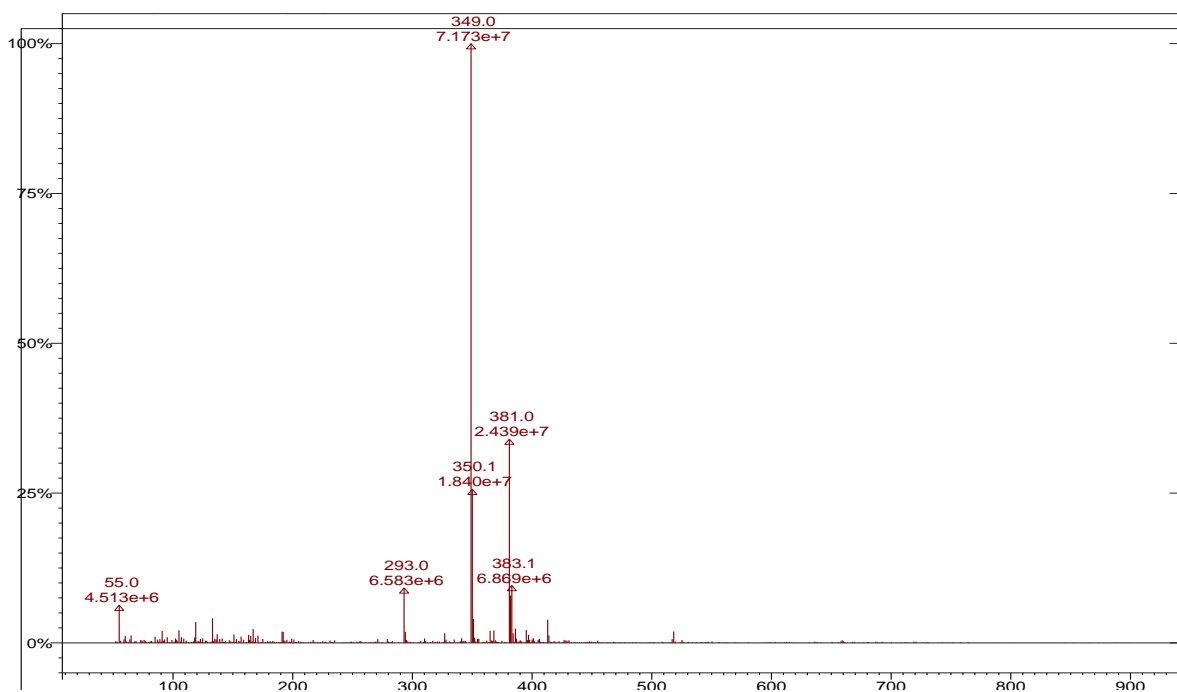
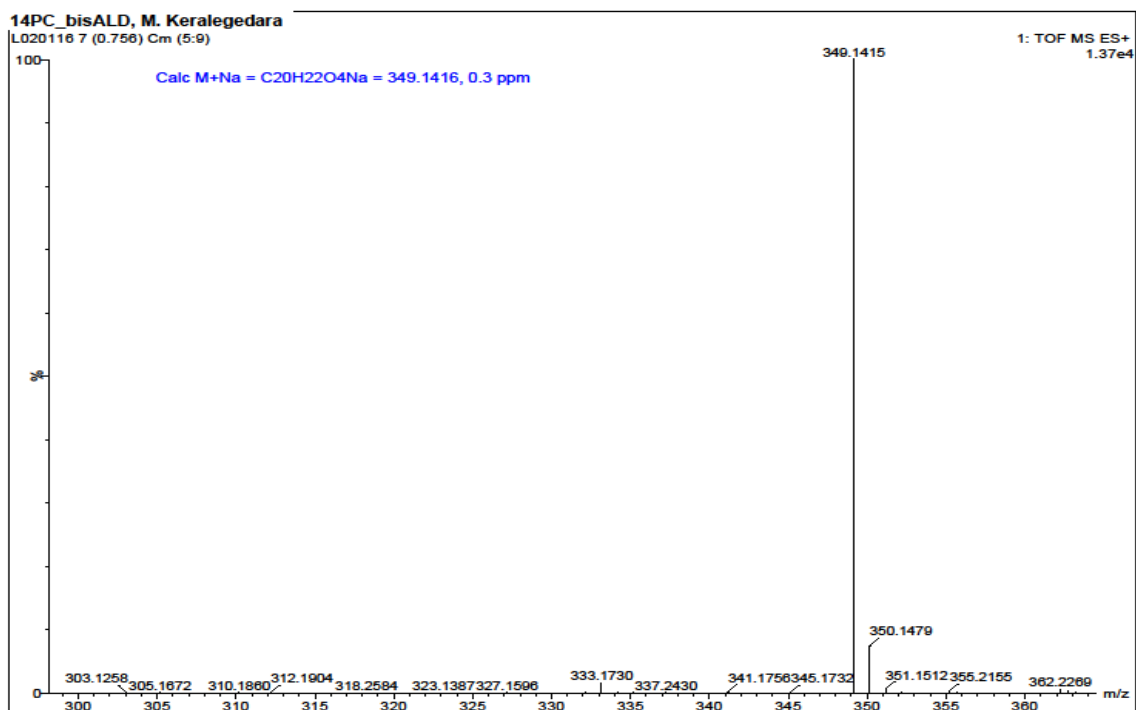


Figure 66. HRMS (top) and ESI_MS (bottom) data for compound **36**.

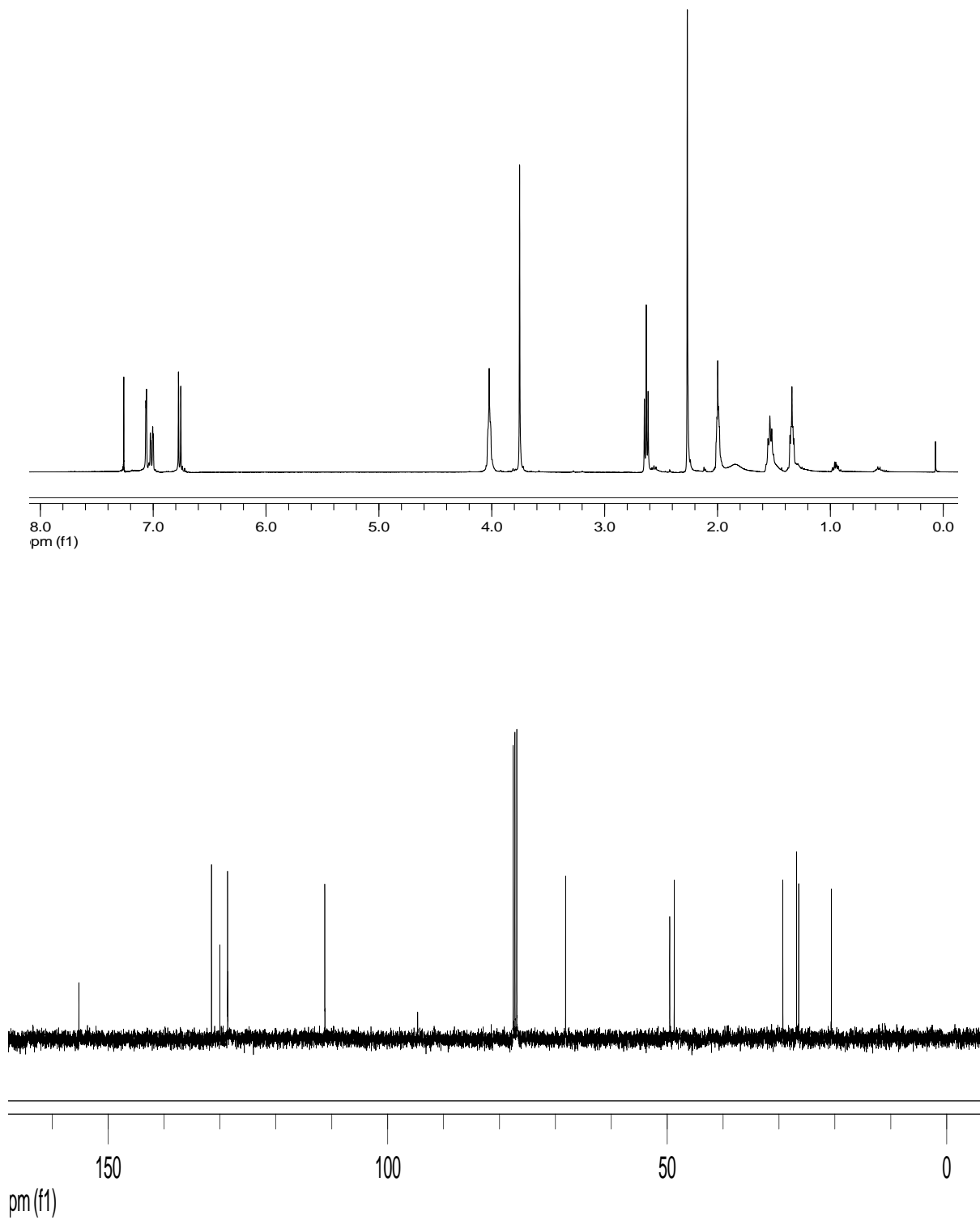


Figure 67. ^1H NMR (top) and ^{13}C NMR (bottom) data for compound **37**

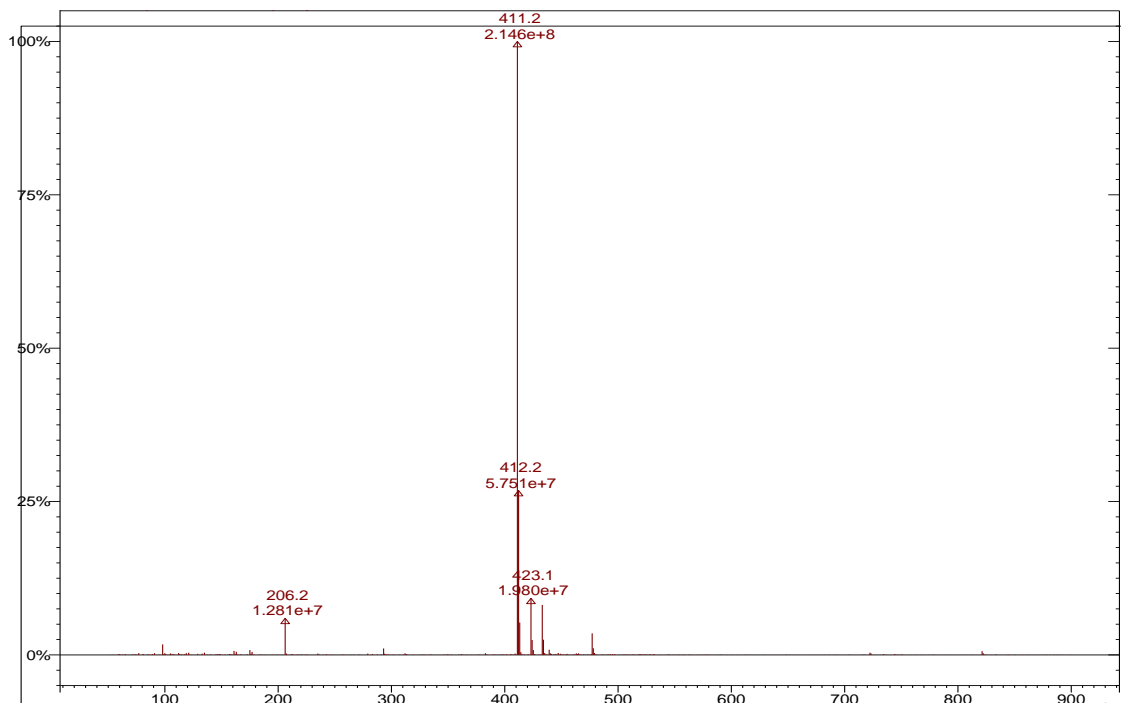
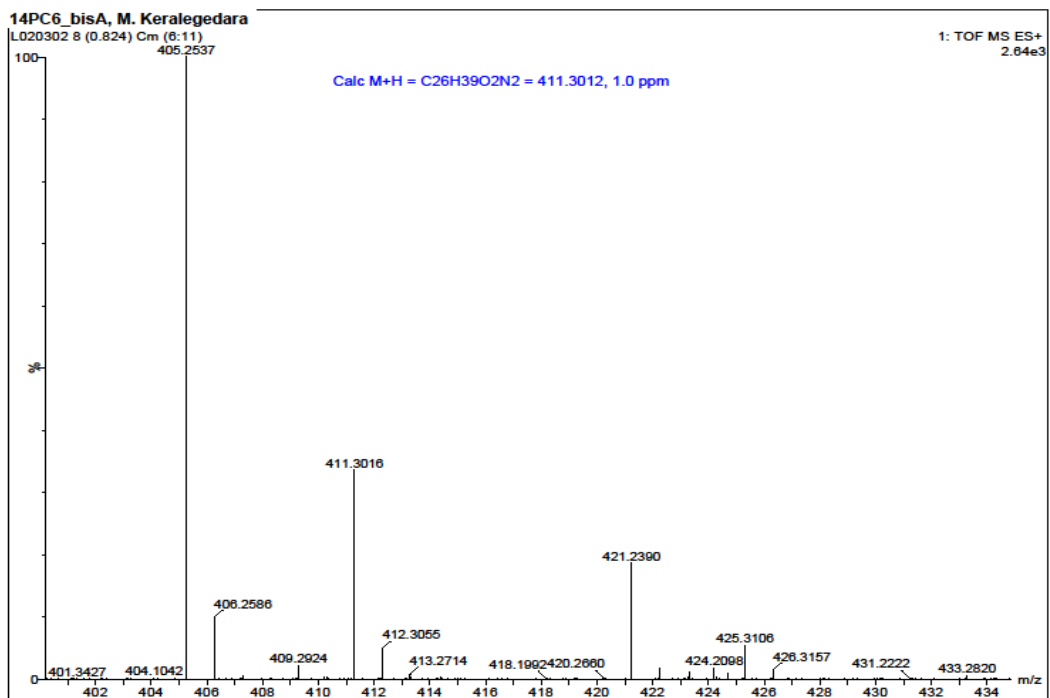


Figure 68. HRMS (top) and ESI-MS (bottom) data for compound **37**

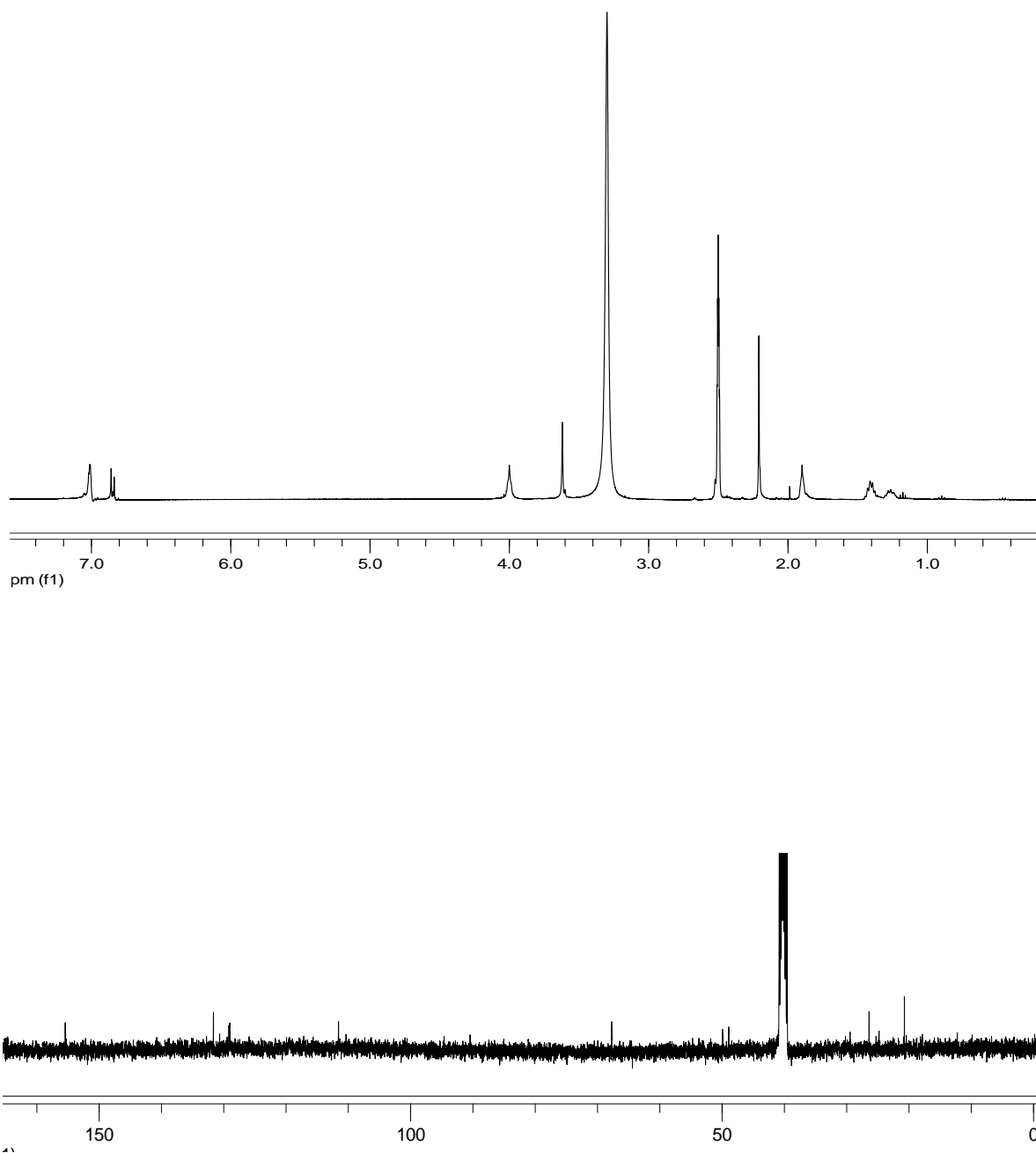


Figure 69. ^1H NMR (top) and ^{13}C NMR (bottom) data for compound **38**

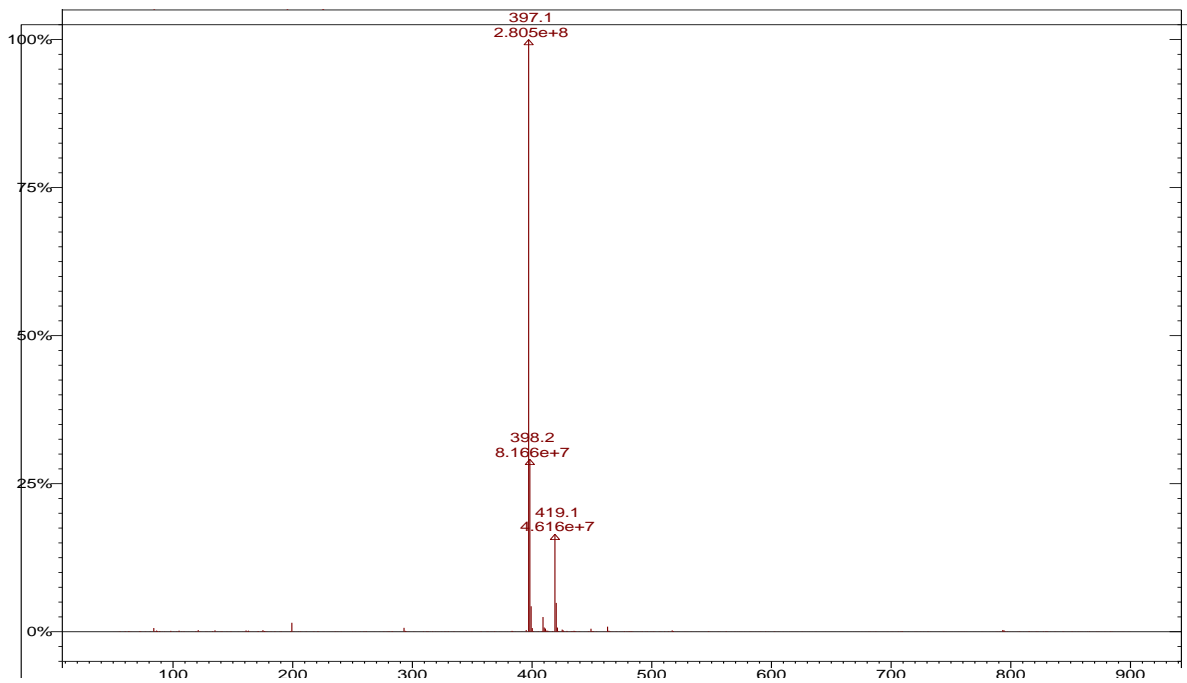
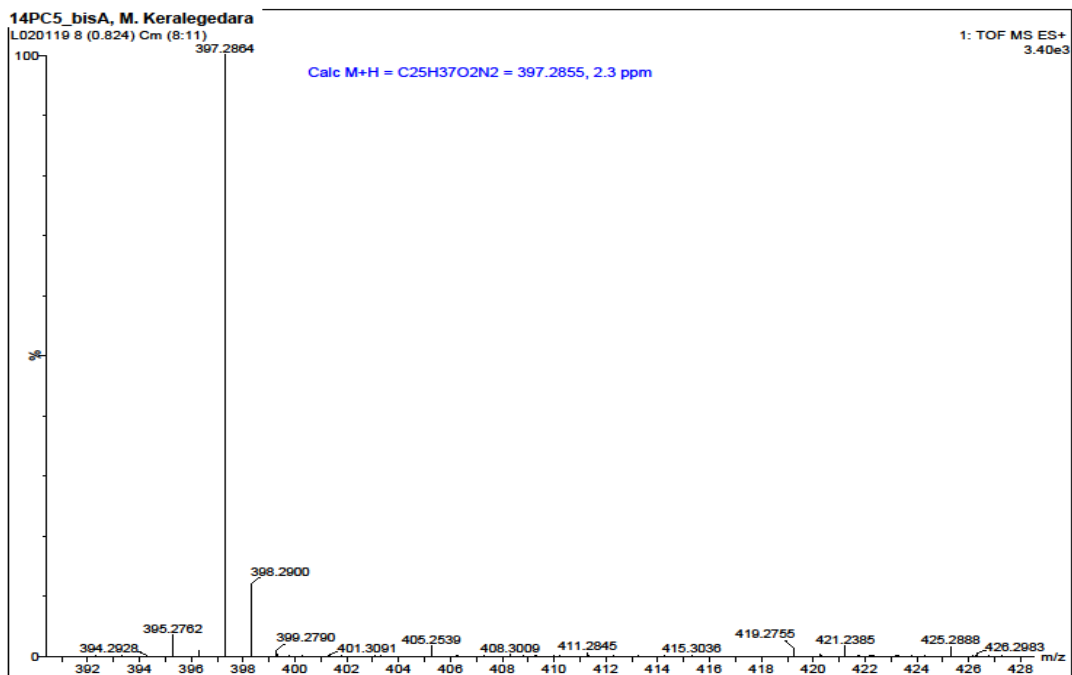


Figure 70. HRMS (top) and ESI_MS (bottom) data for compound **38**.

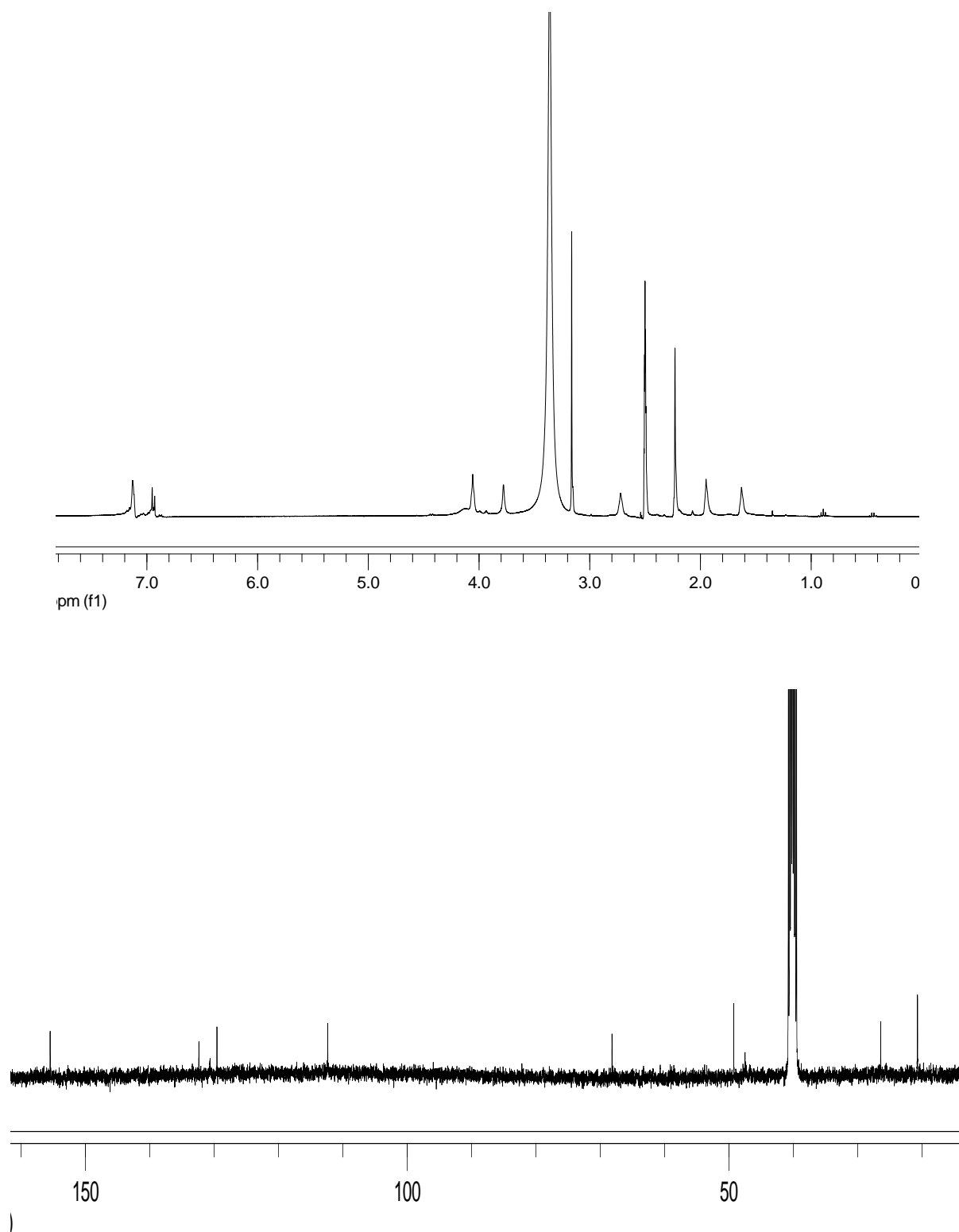


Figure 71. ^1H NMR (top) and ^{13}C NMR (bottom) data for compound **39**

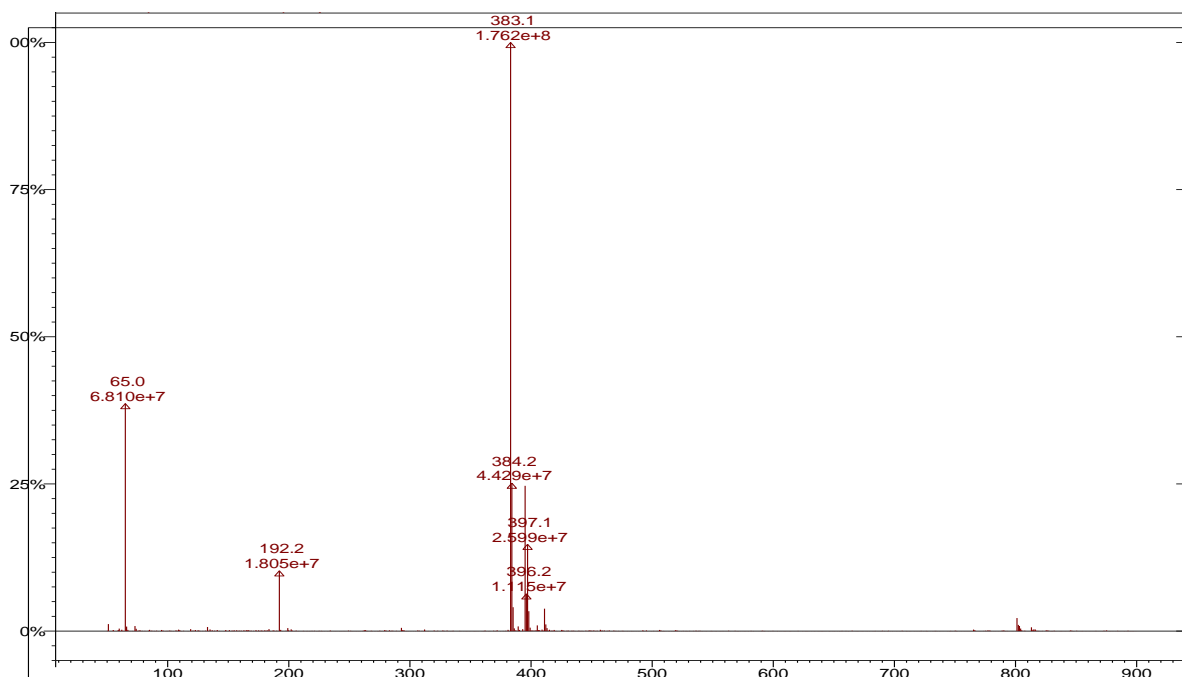
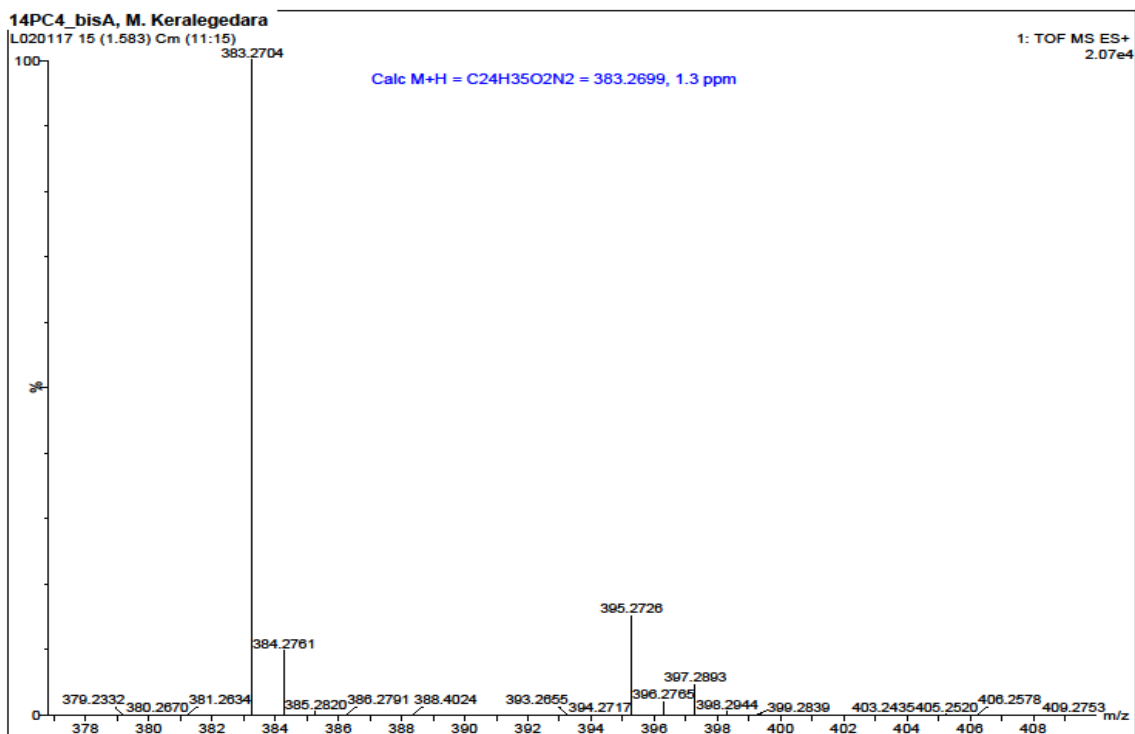


Figure 72. HRMS (top) and ESI-MS (bottom) data for compound **39**.

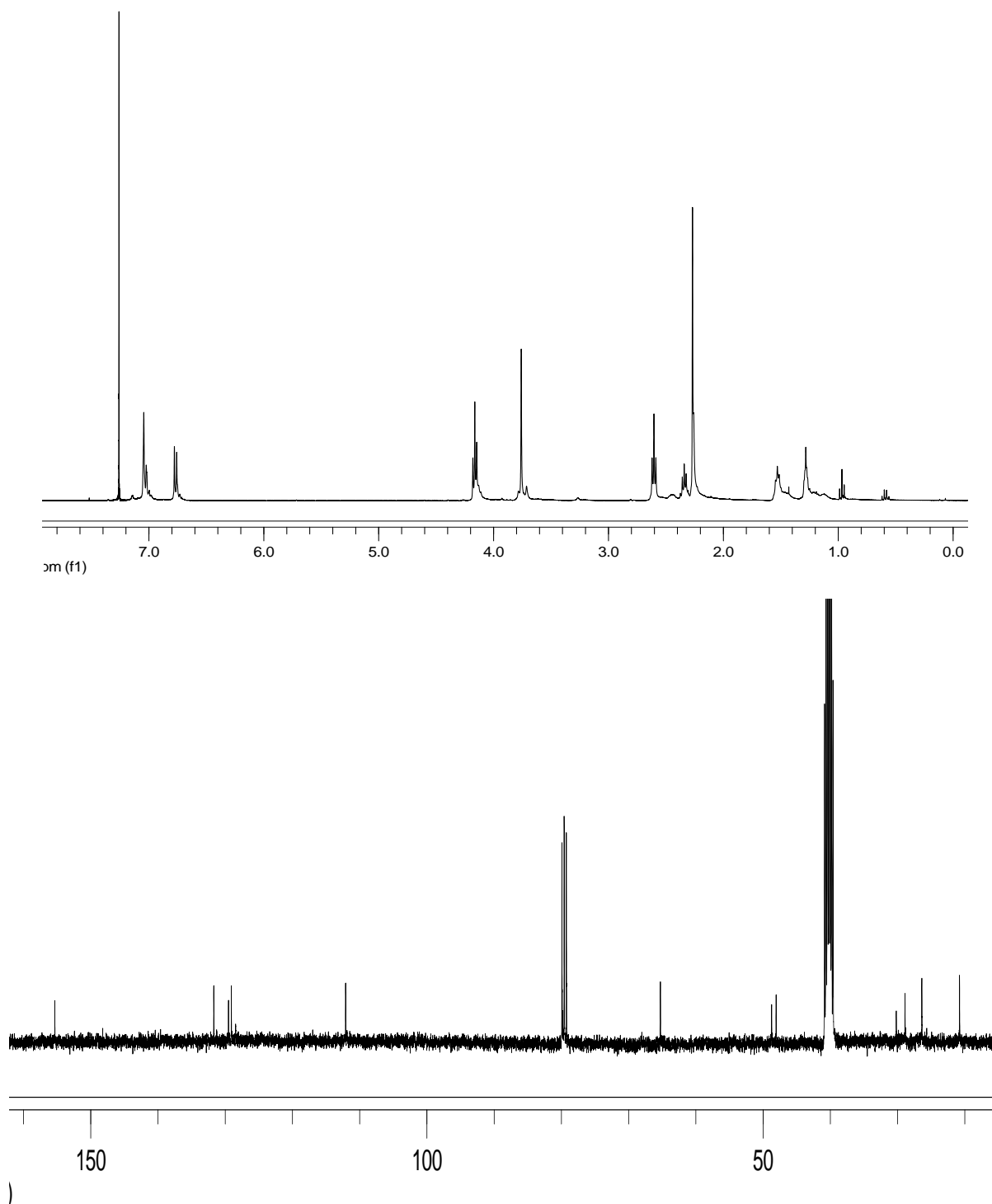


Figure 73. ^1H NMR (top) and ^{13}C NMR (bottom) data for compound **41**

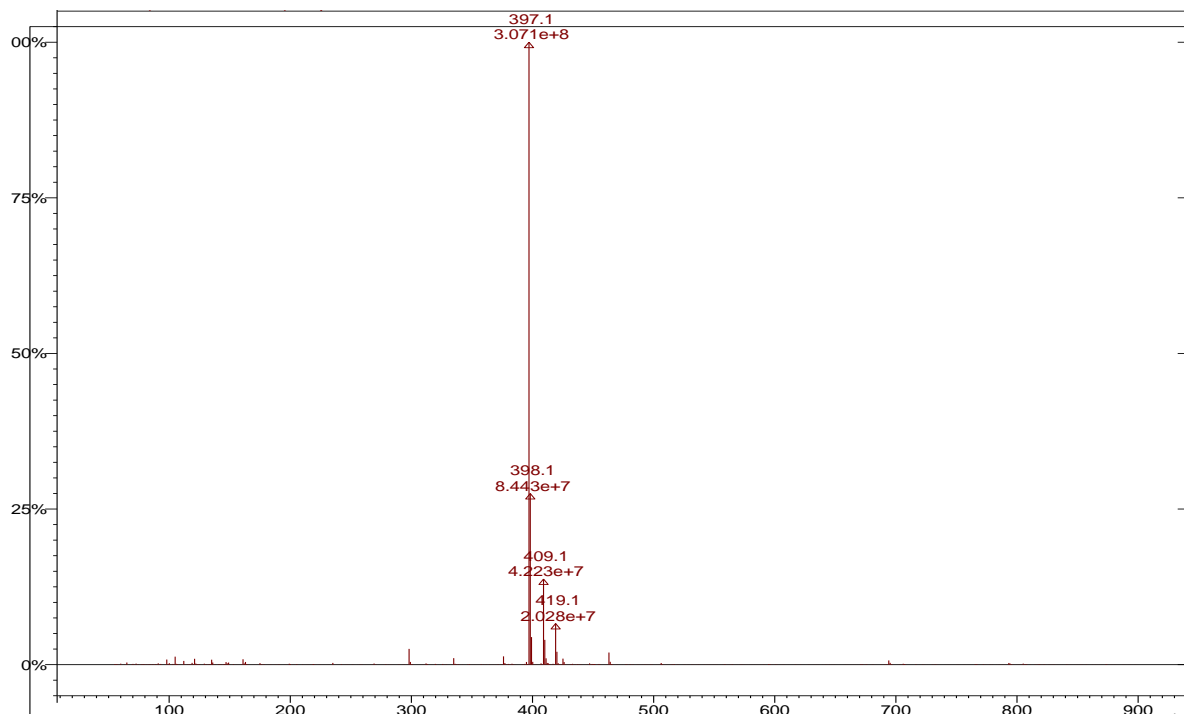
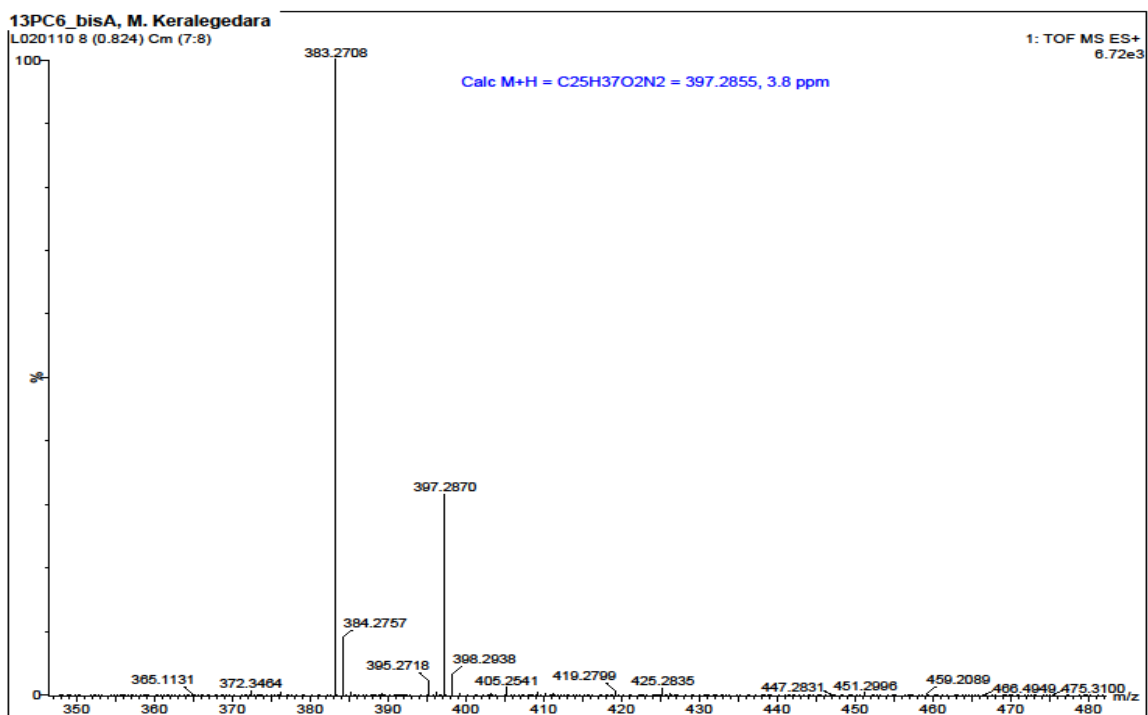


Figure 74. HRMS (top) and ESI-MS (bottom) data for compound **41**.

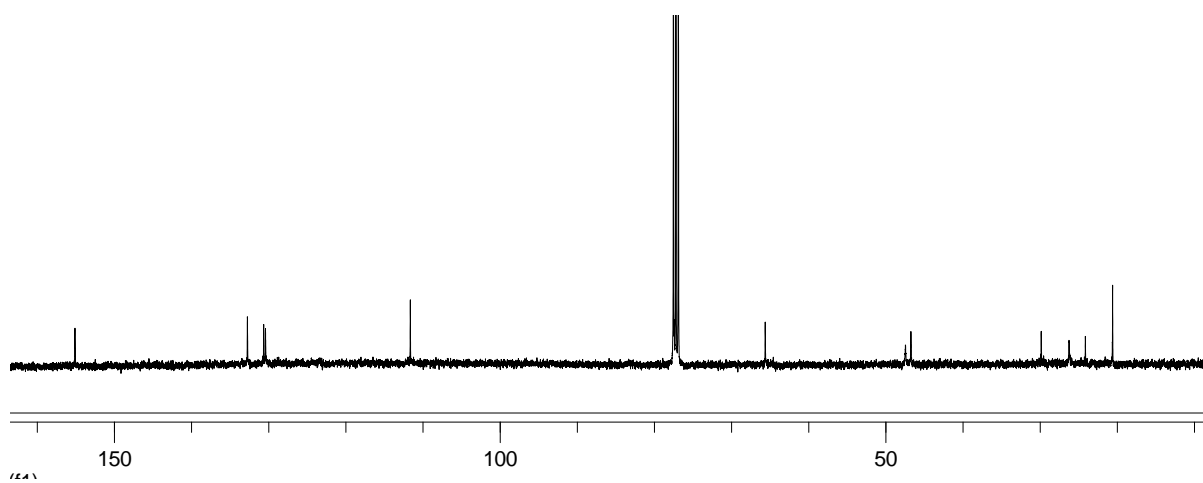
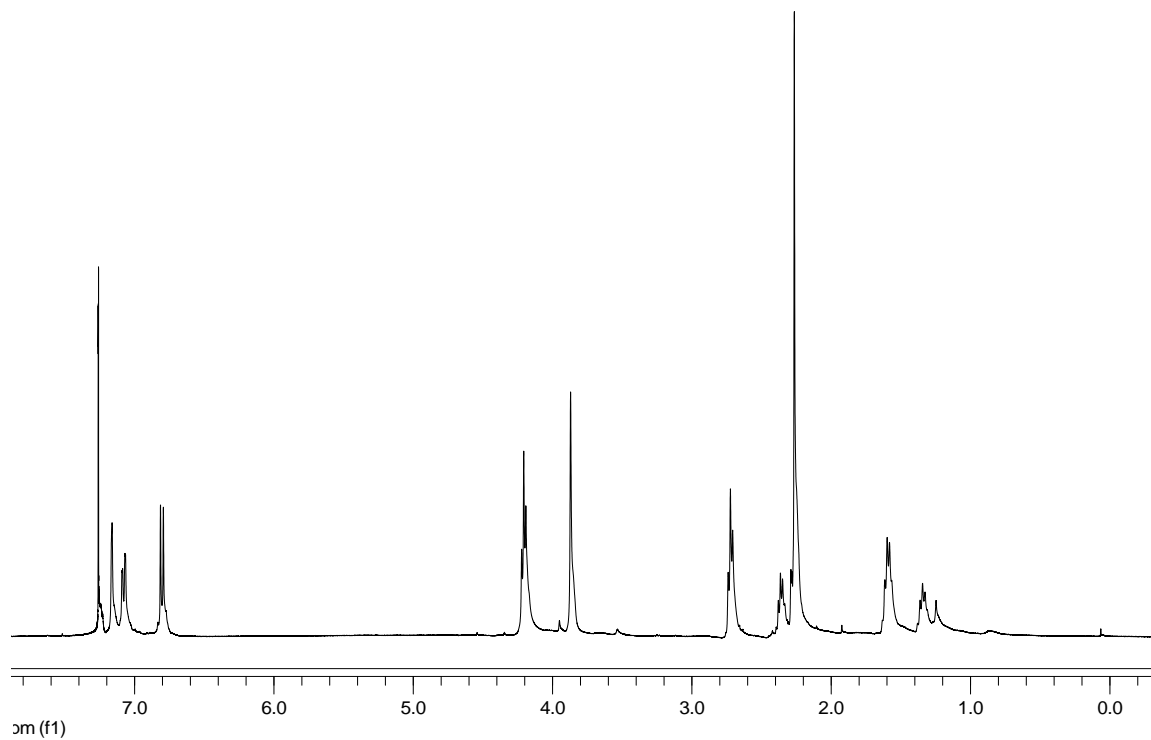


Figure 75. ^1H NMR (top) and ^{13}C NMR (bottom) data for compound **42**

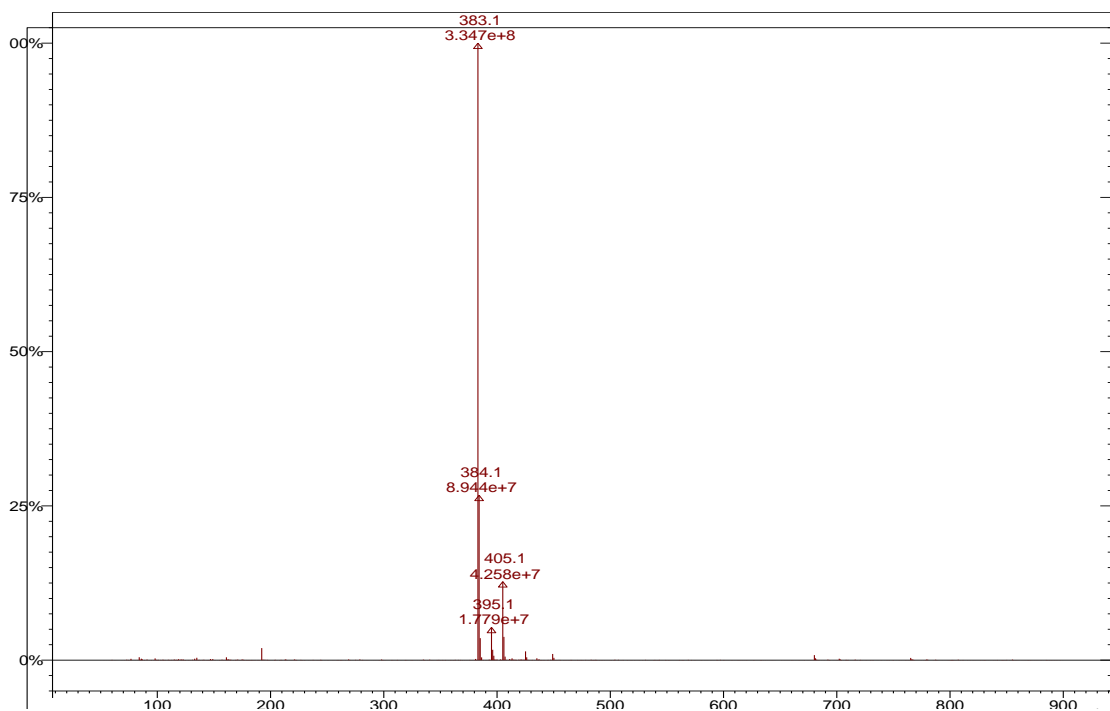
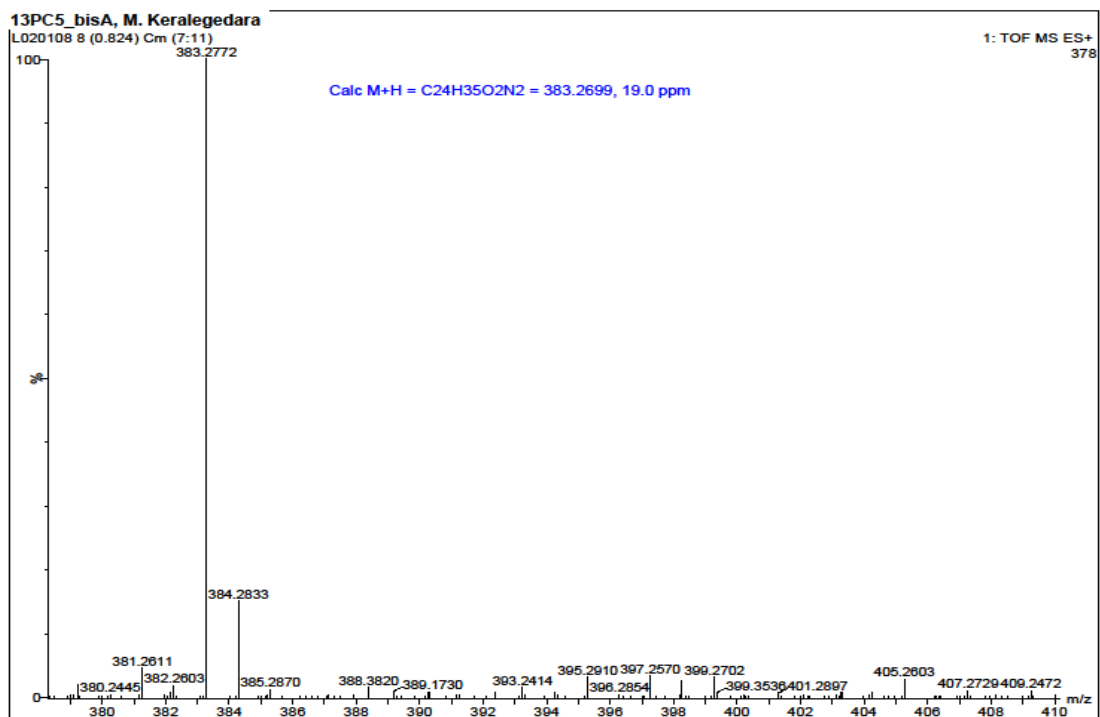


Figure 76. HRMS (top) and ESI-MS (bottom) data for compound **42**.

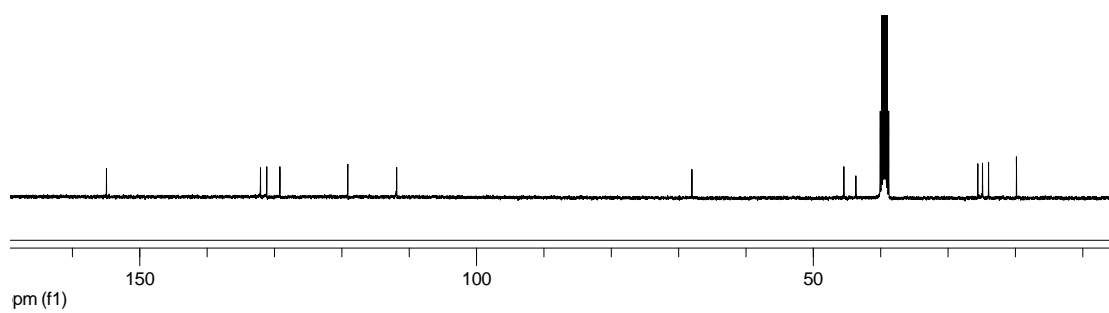
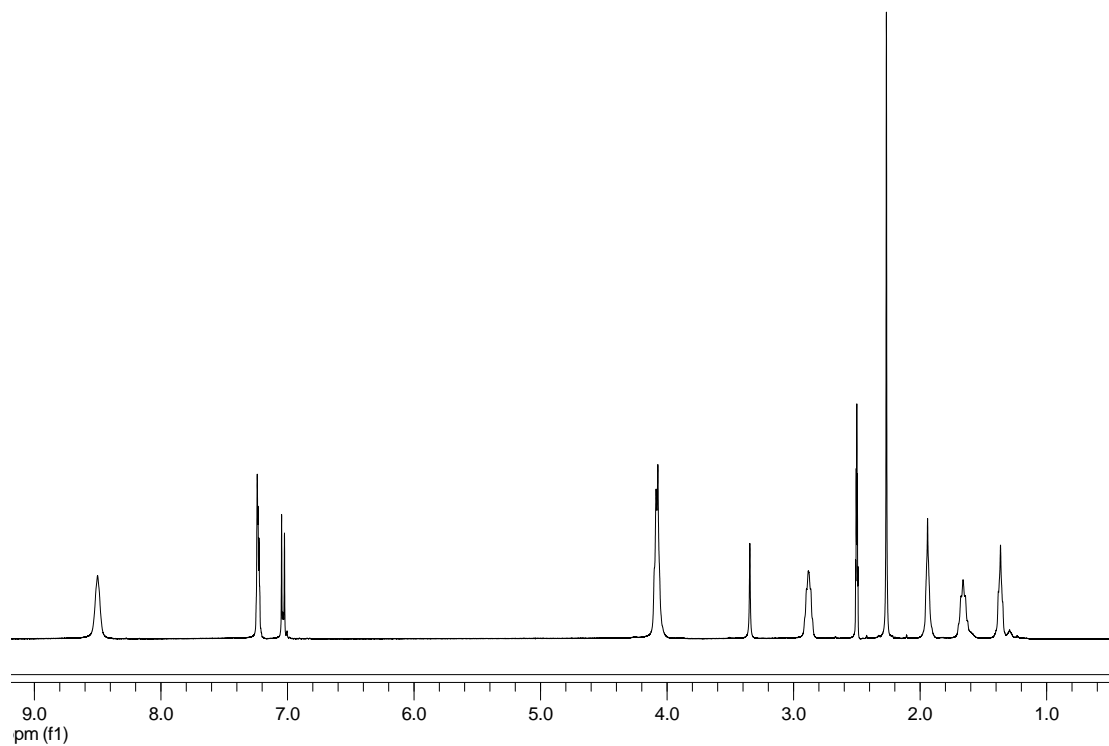


Figure 77. ^1H NMR (top) and ^{13}C NMR (bottom) data for compound **45**

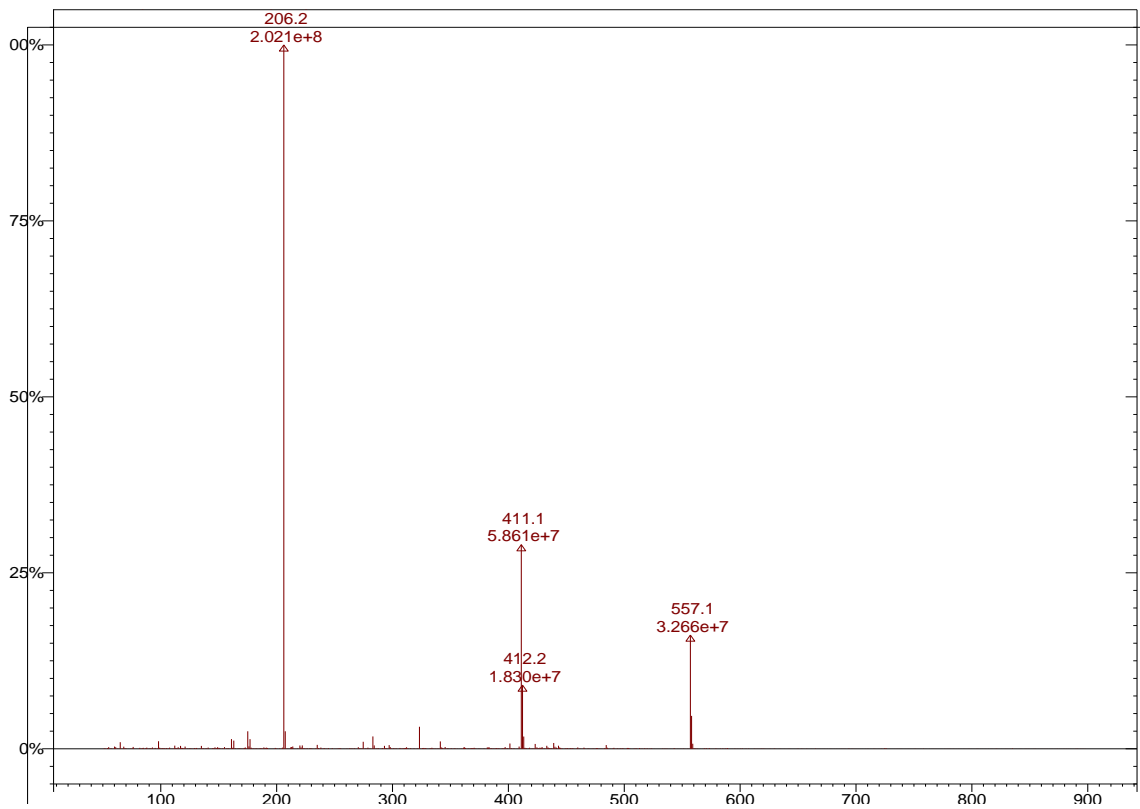
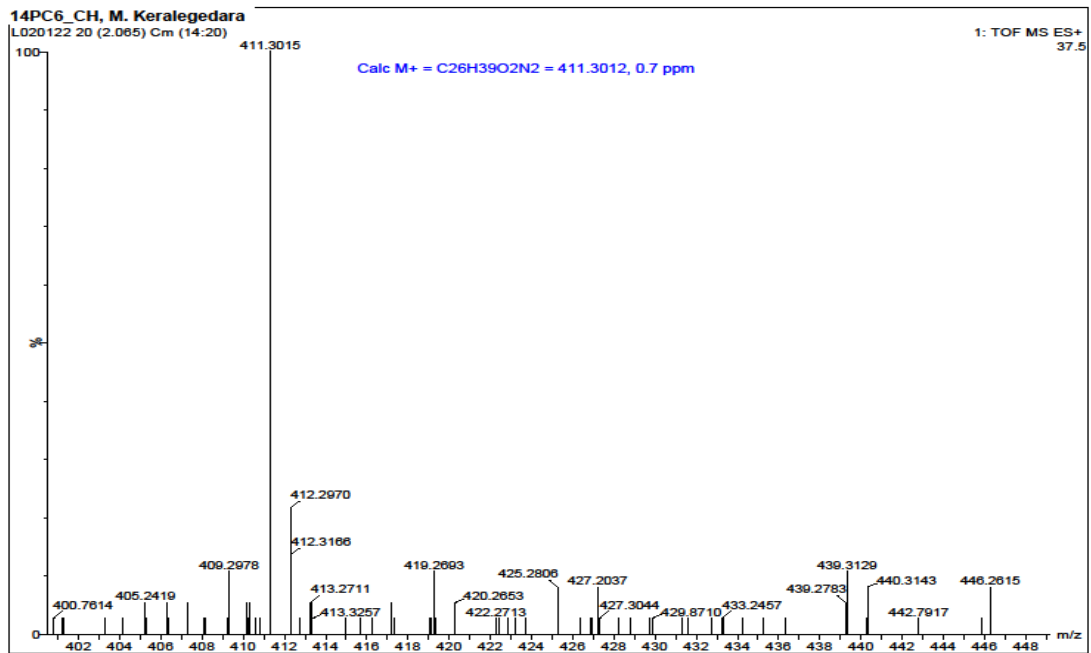


Figure 78. HRMS (top) and ESI-MS (bottom) data for compound **45**.

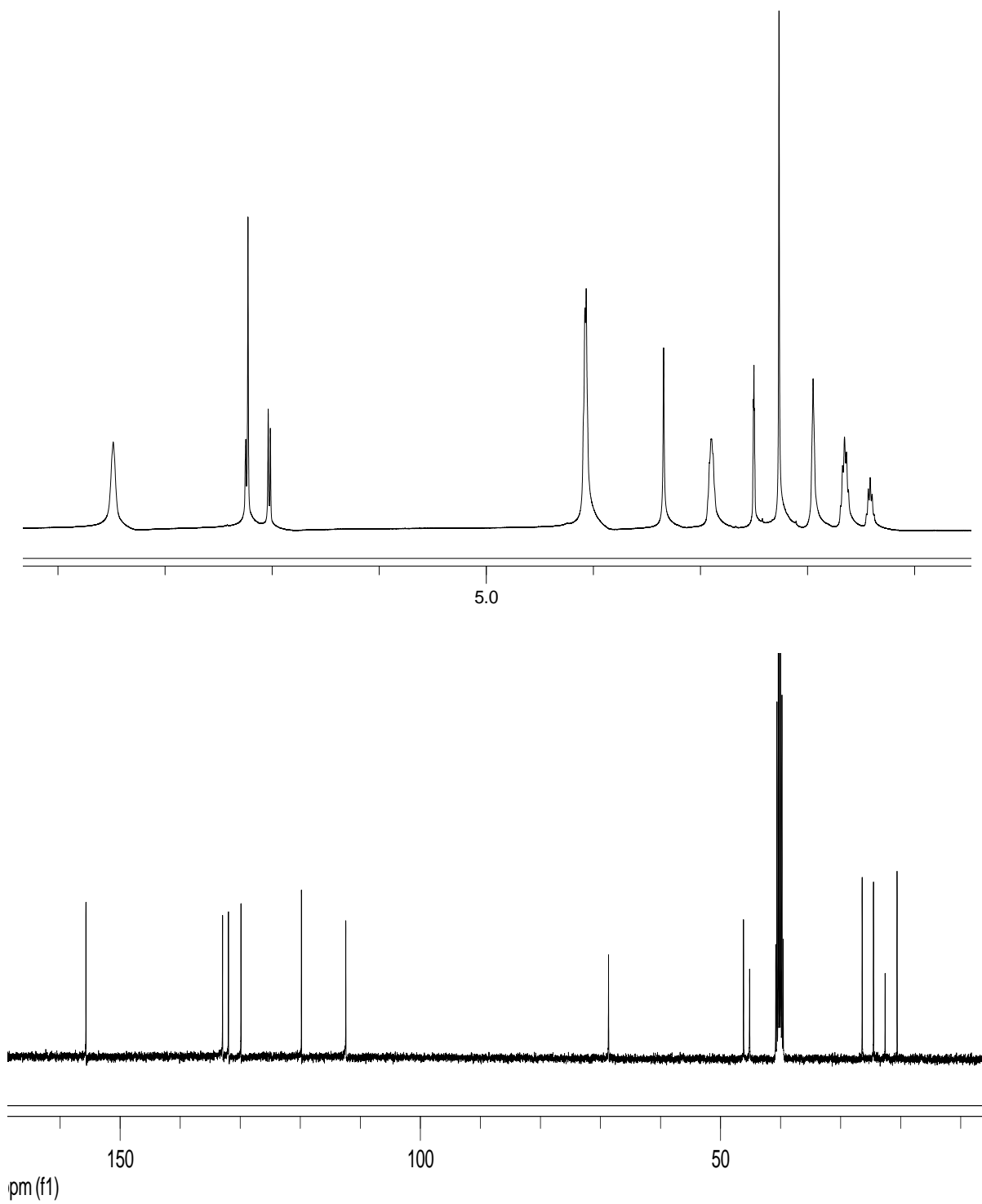


Figure 79. ^1H NMR (top) and ^{13}C NMR (bottom) data for compound **46**

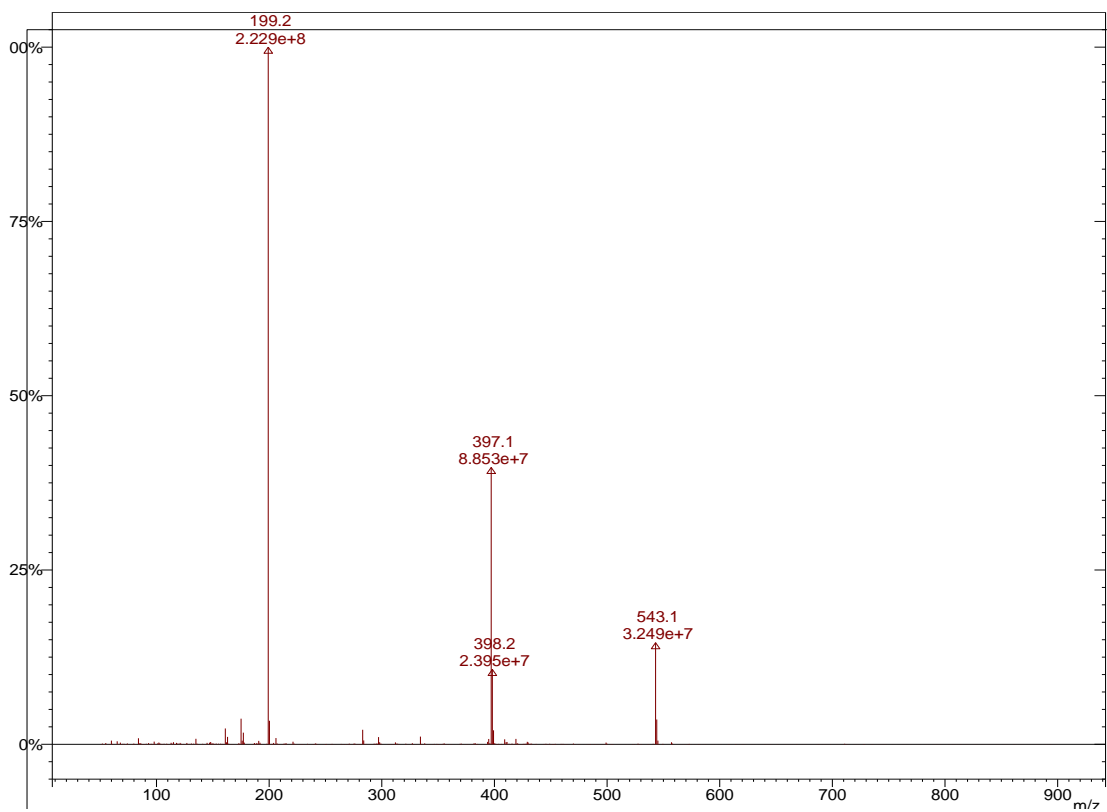
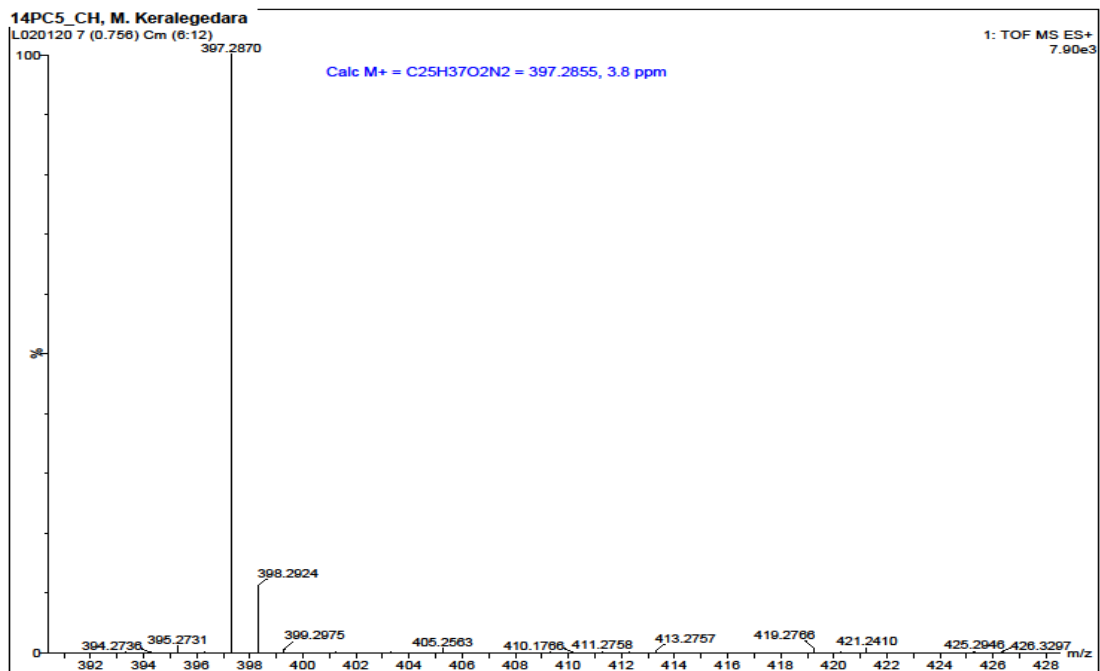


Figure 80. HRMS (top) and ESI-MS (bottom) data for compound **46**.

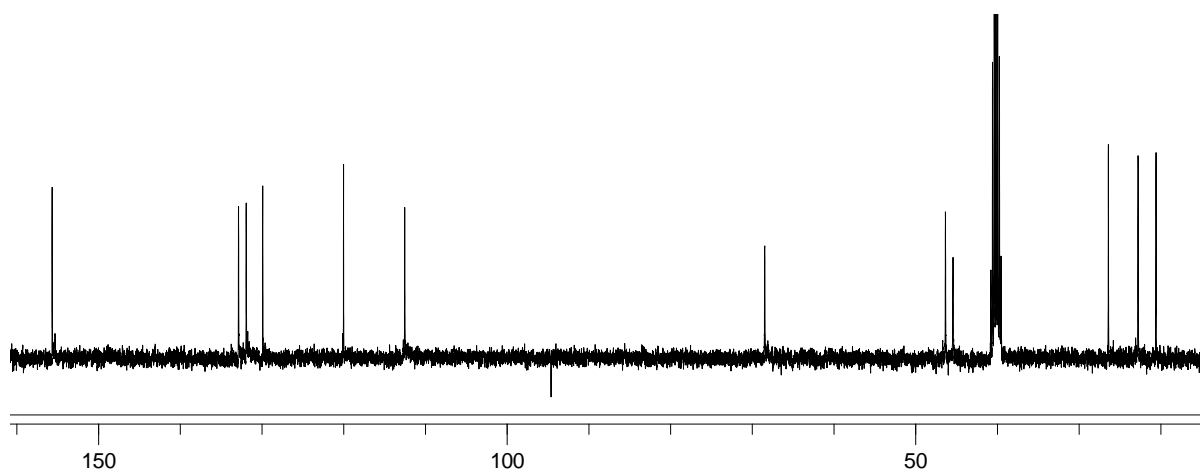
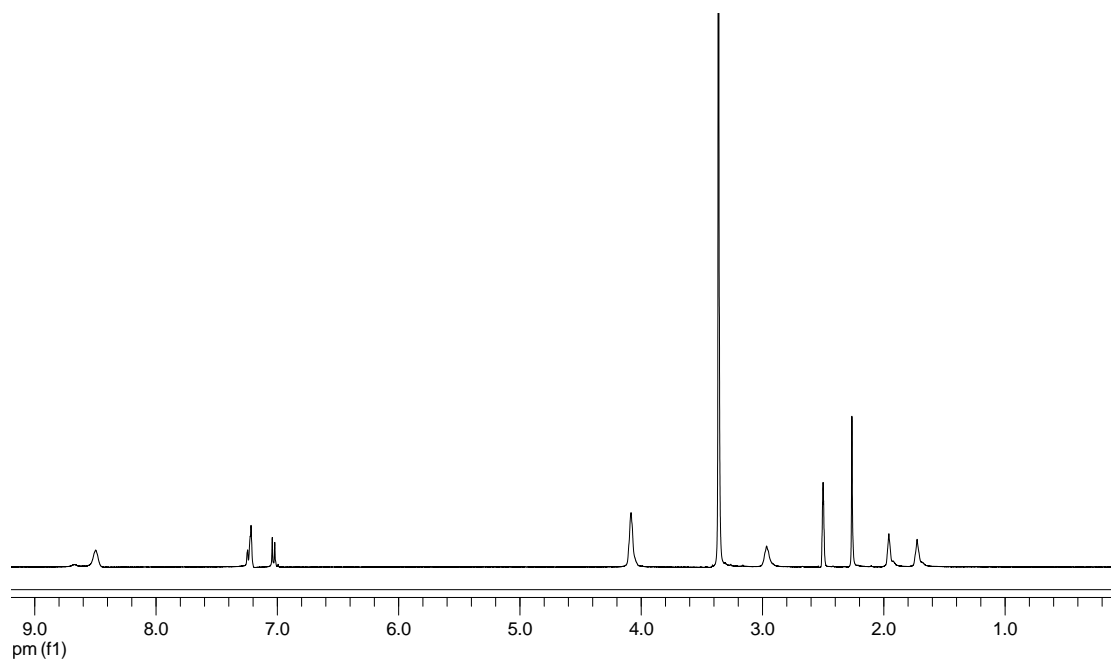


Figure 81. ^1H NMR (top) and ^{13}C NMR (bottom) data for compound **47**

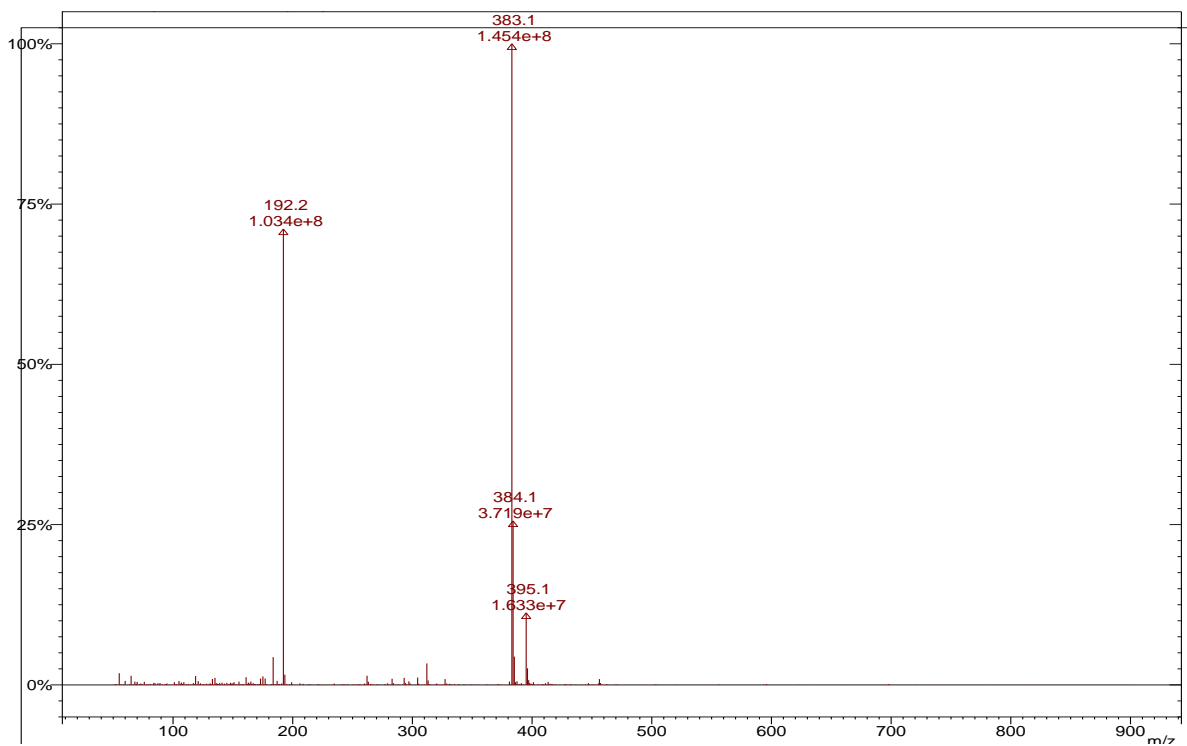
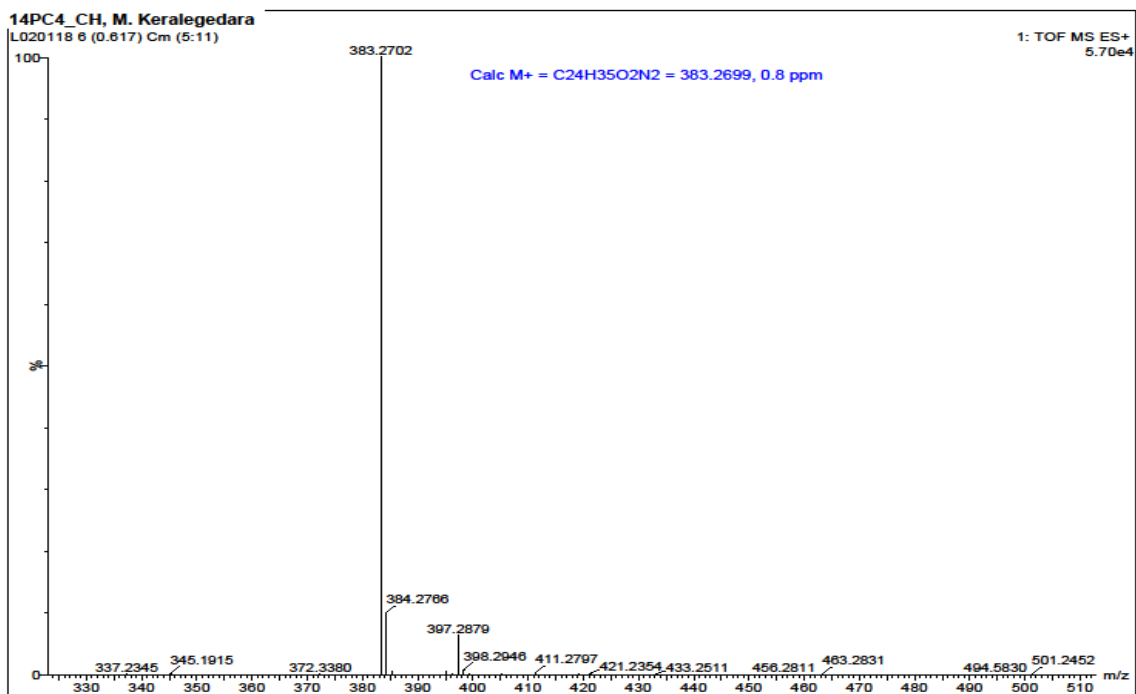


Figure 82. HRMS (top) and ESI-MS (bottom) data for compound **47**

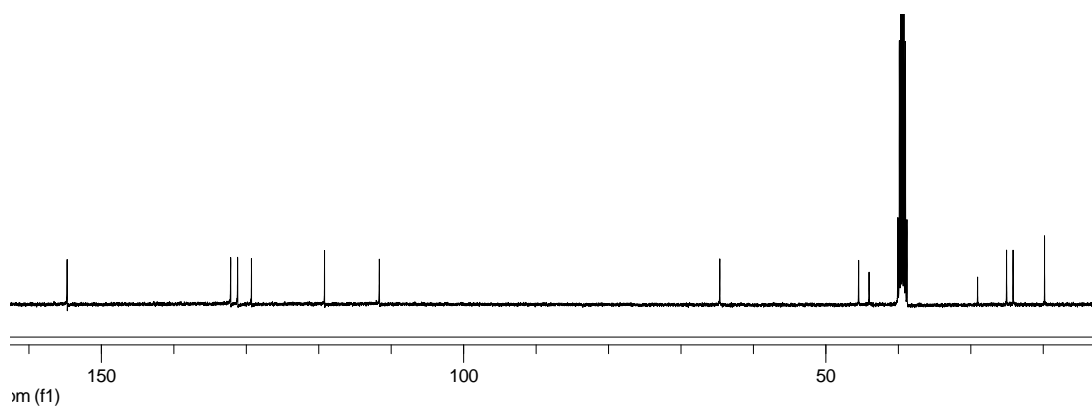
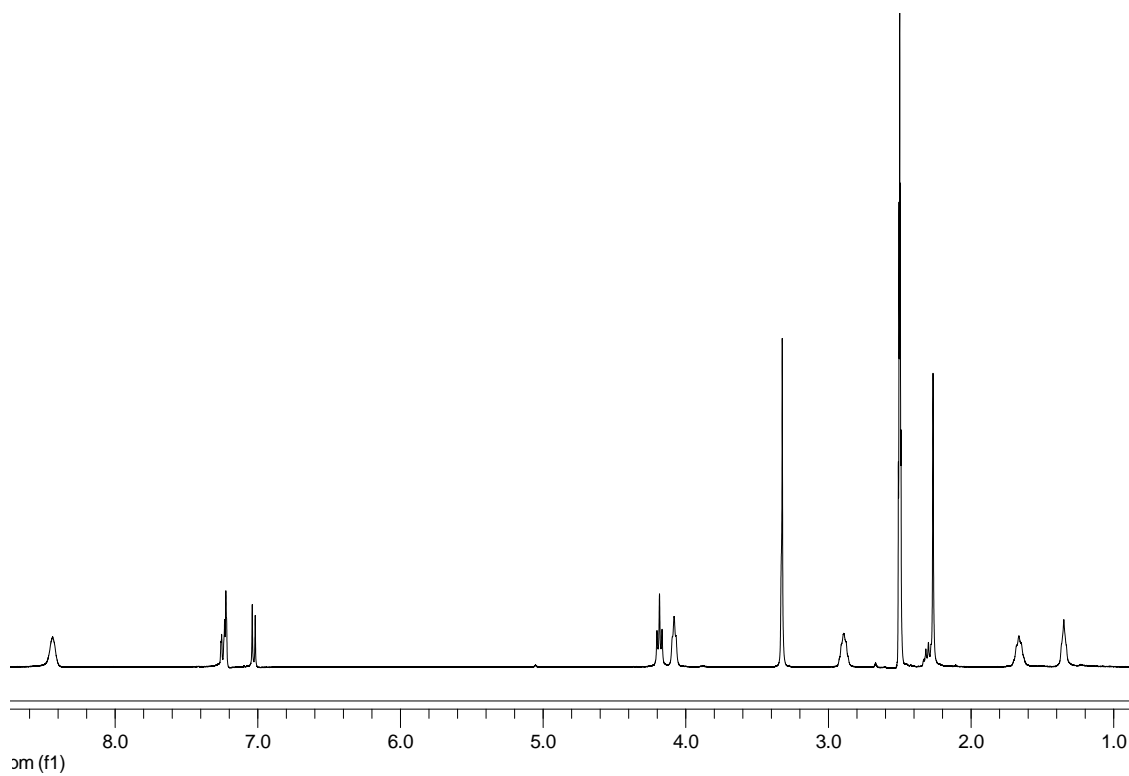


Figure 83. ^1H NMR (top) and ^{13}C NMR (bottom) data for compound **49**

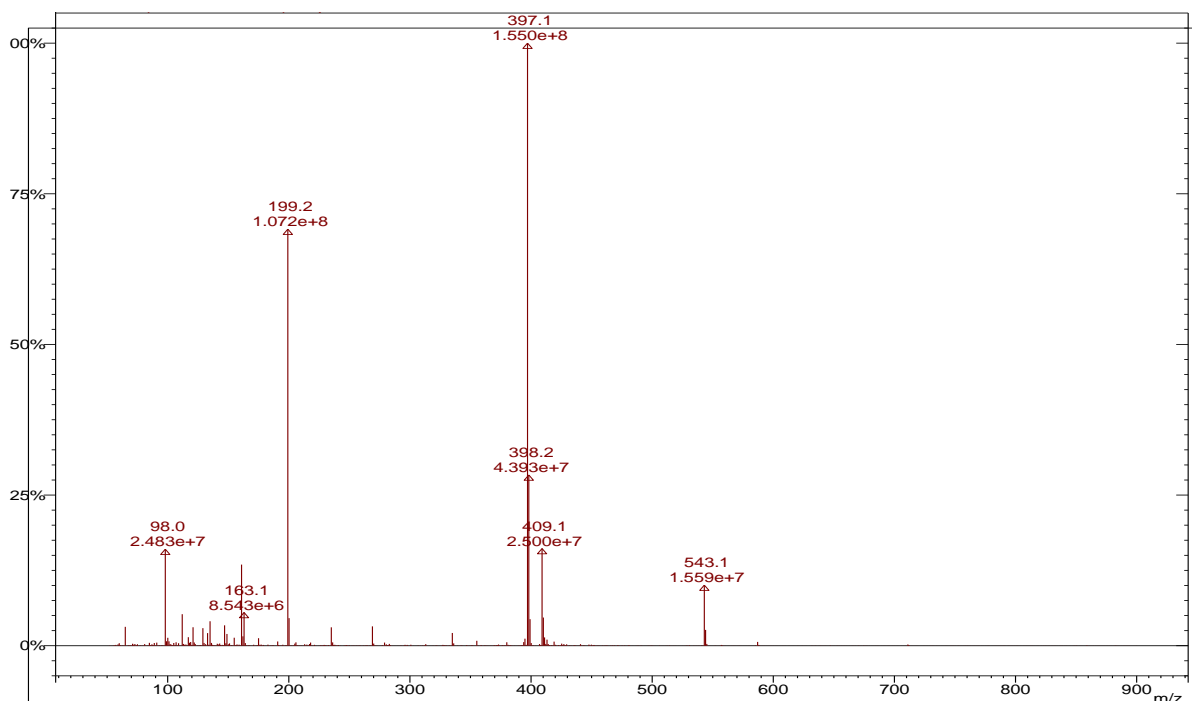
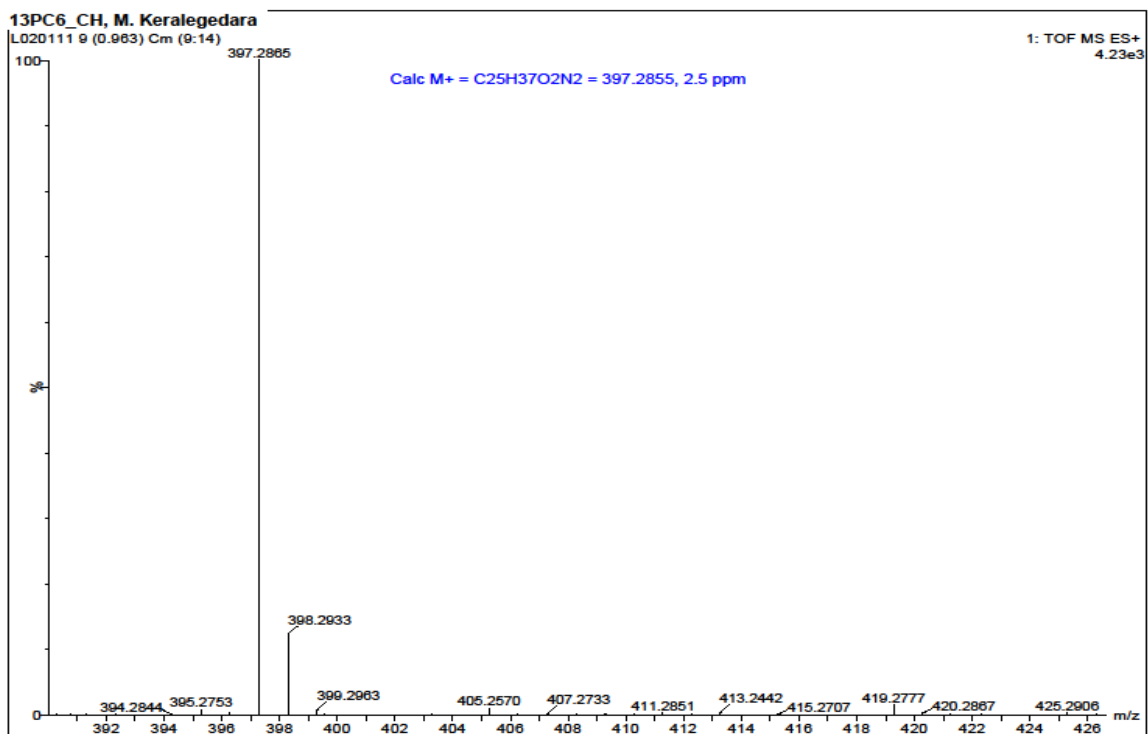


Figure 84. HRMS (top) and ESI-MS (bottom) data for compound **49**.

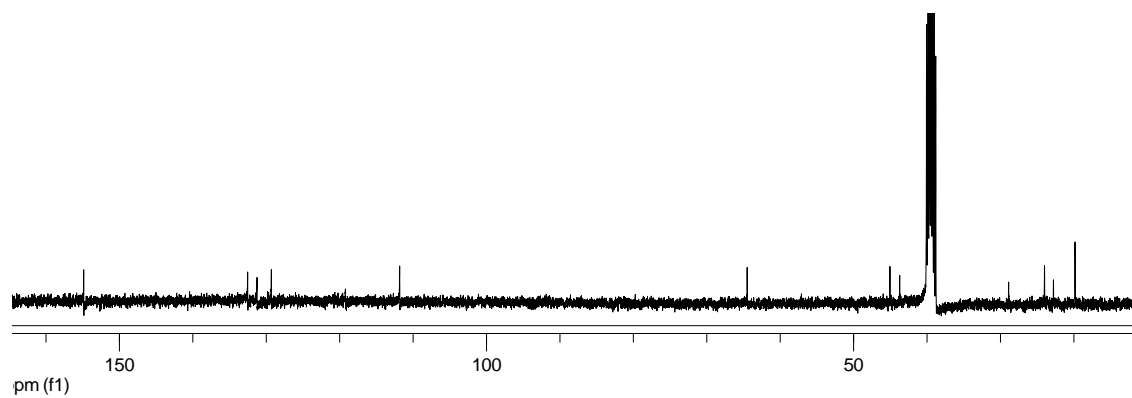
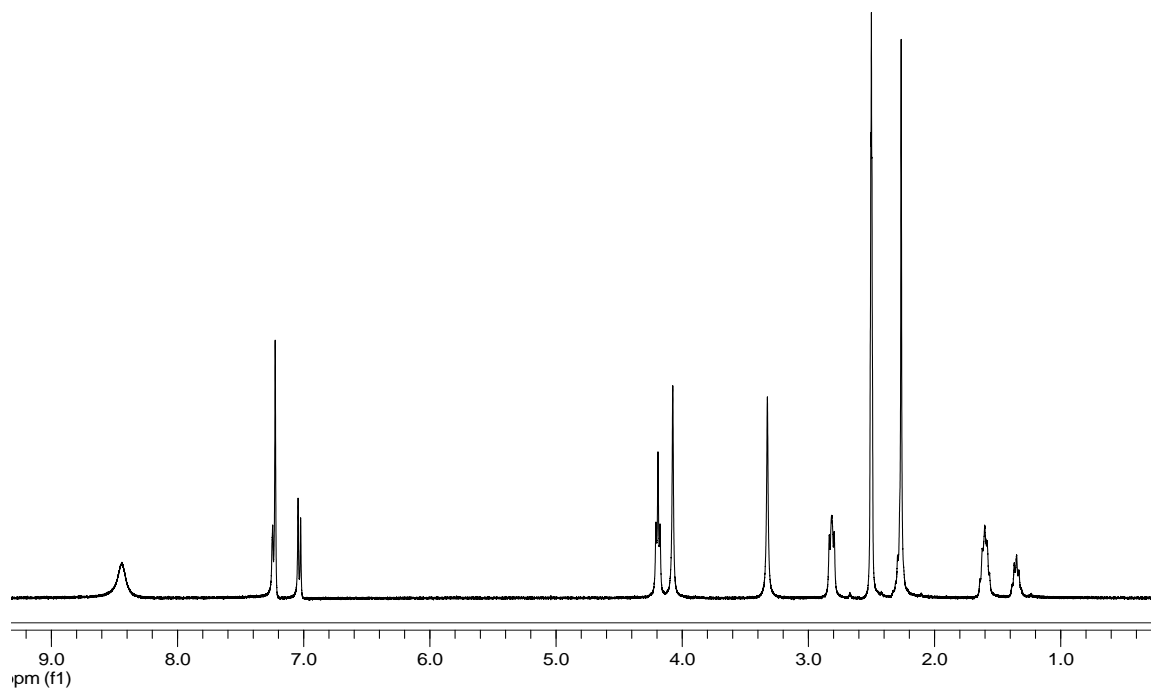


Figure 85. ^1H NMR (top) and ^{13}C NMR (bottom) data for compound **50**

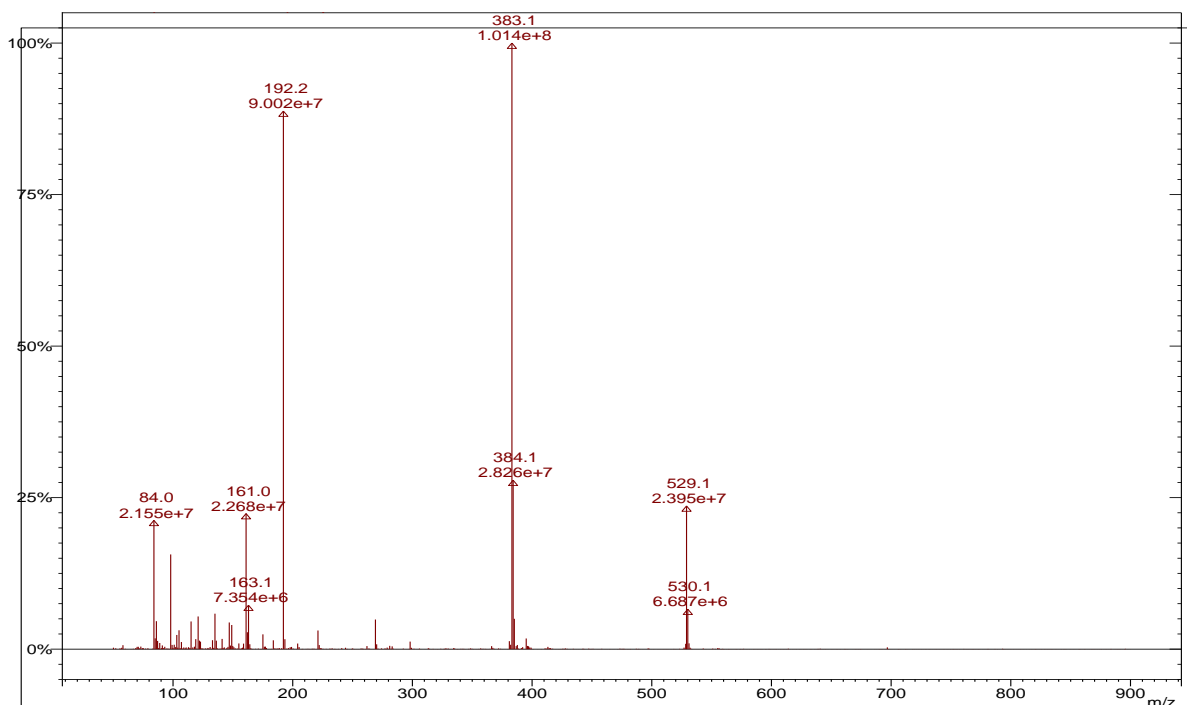
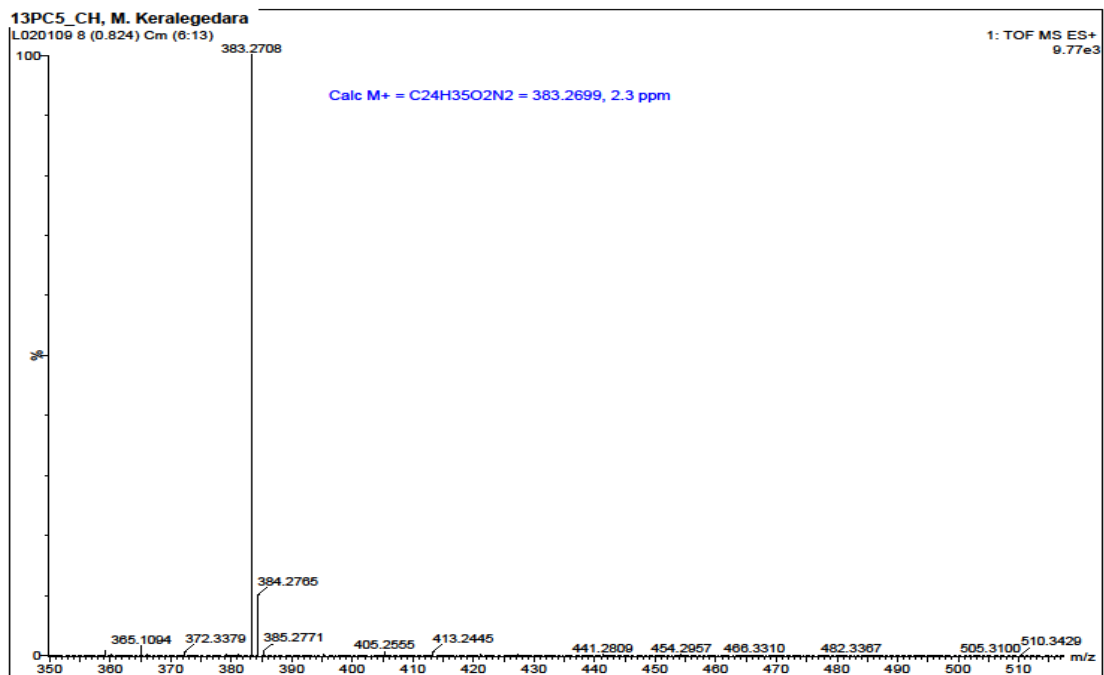


Figure 86. HRMS (top) and ESI-MS (bottom) data for compound 50.

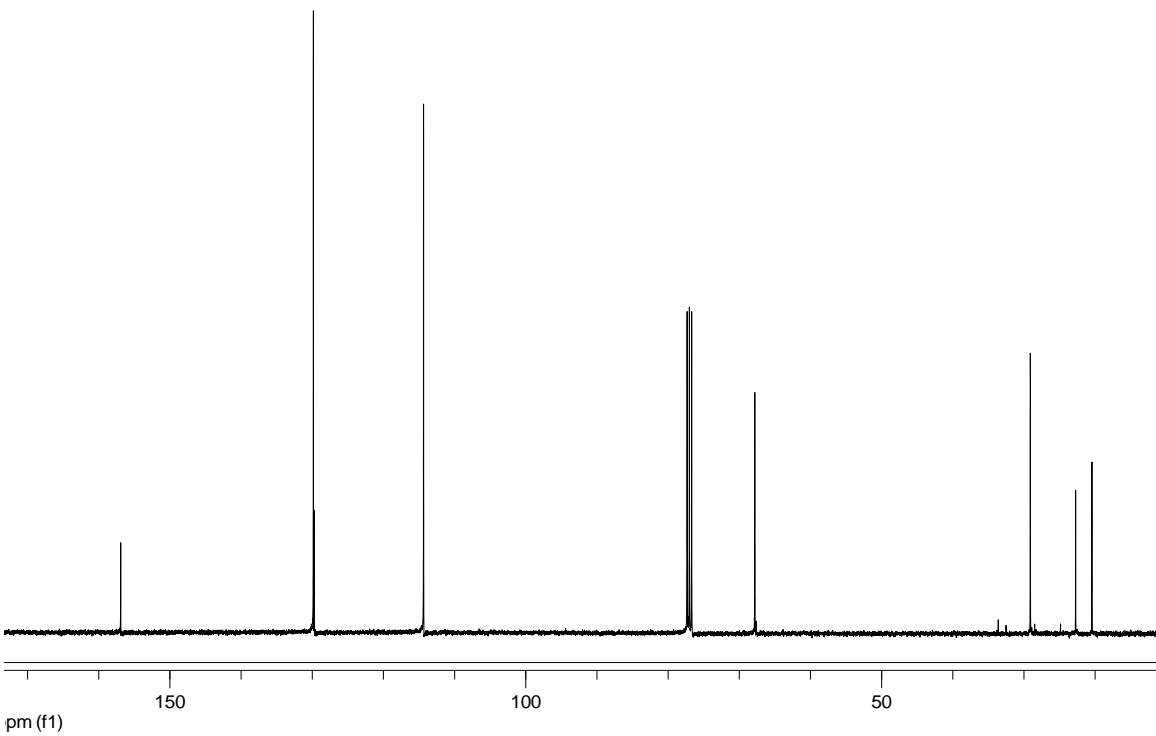
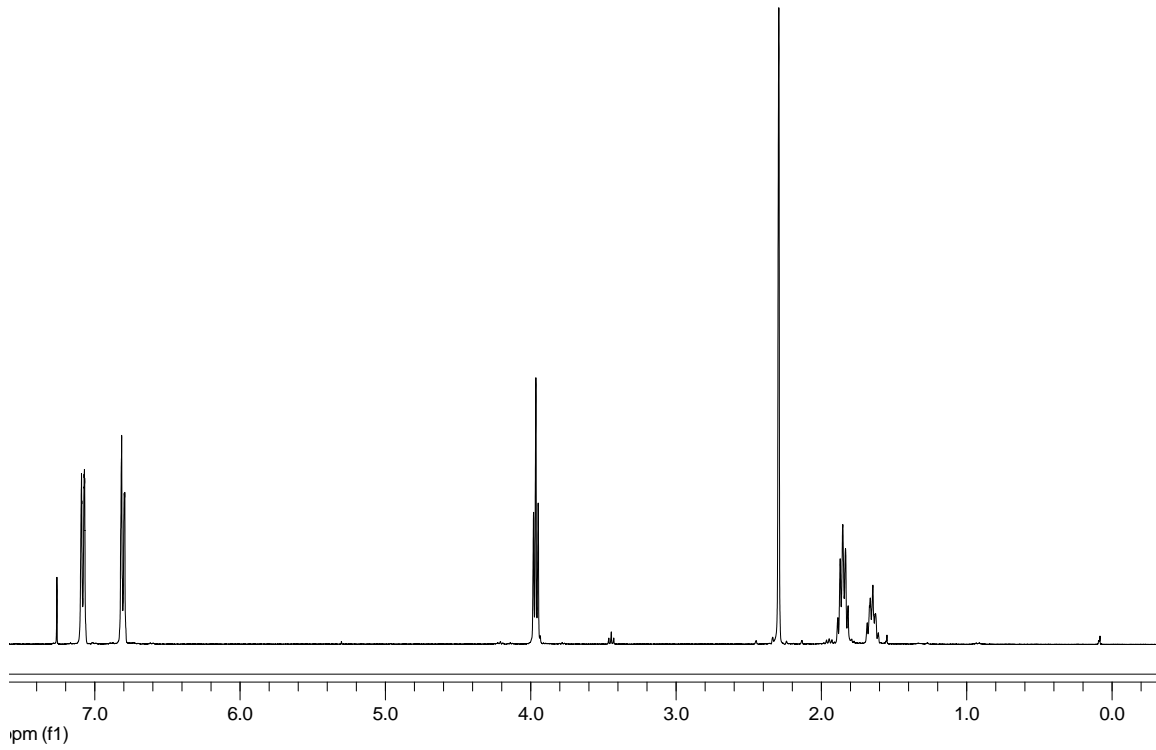


Figure 87. ^1H NMR (top) and ^{13}C NMR (bottom) data for compound **51**

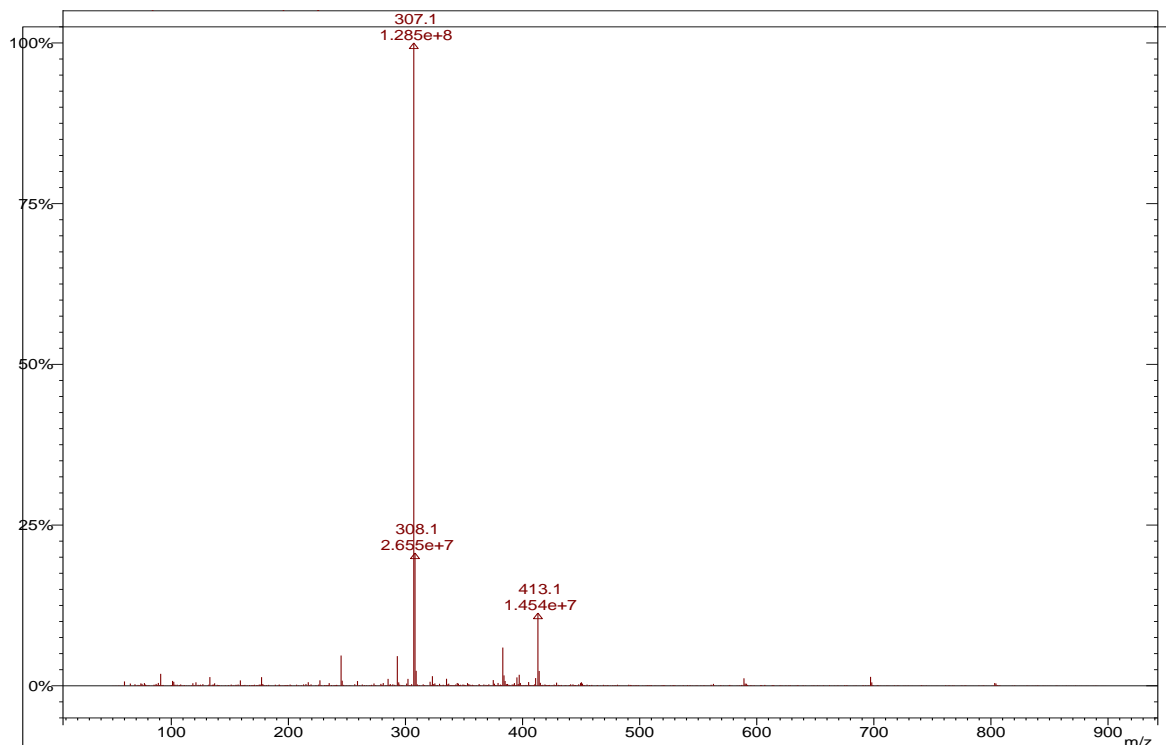
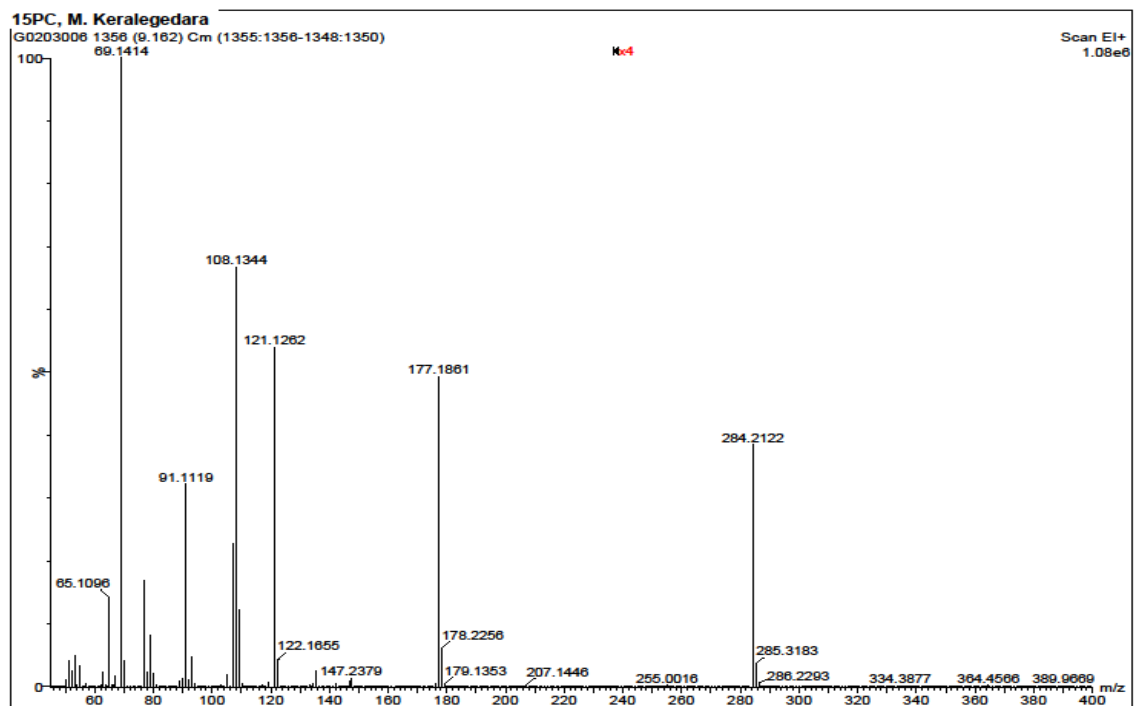


Figure 88. GC-MS (top) and ESI-MS (bottom) data for compound **51**.

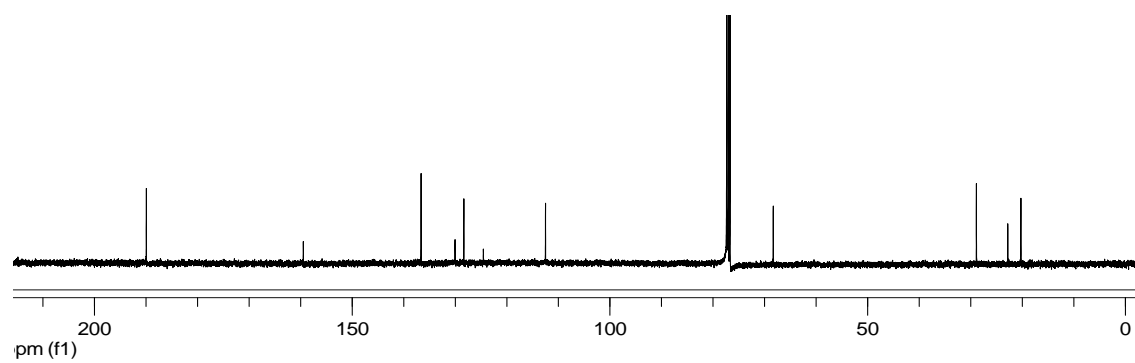
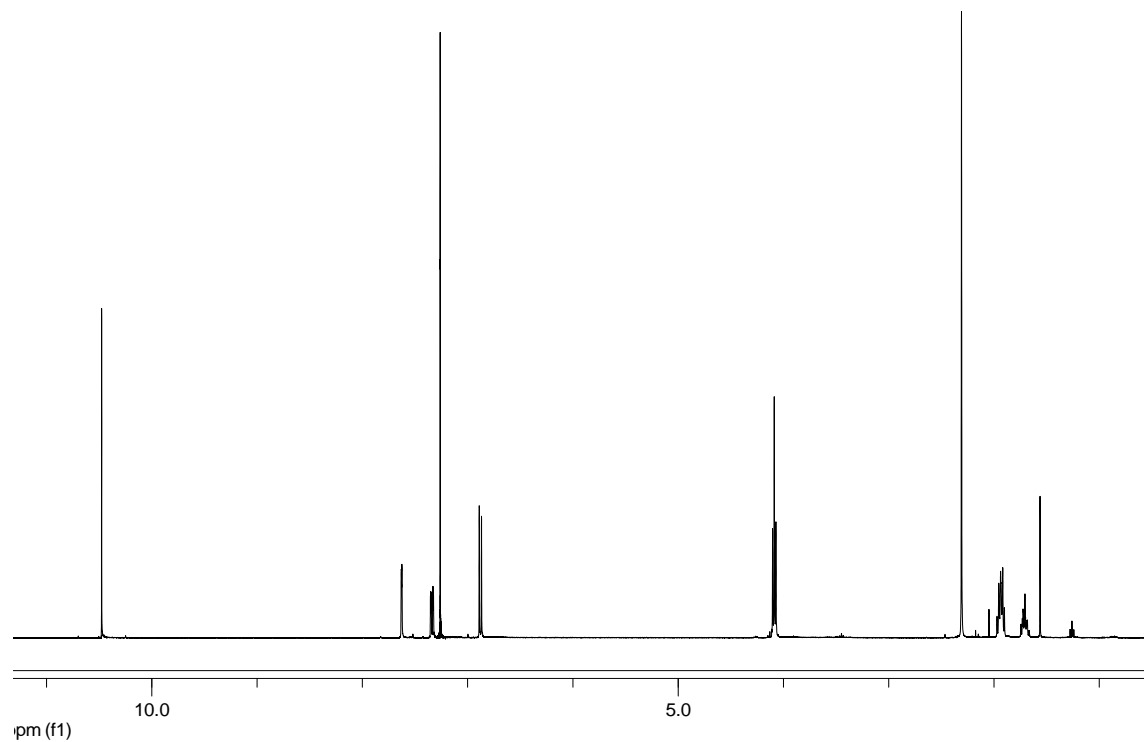


Figure 89. ^1H NMR (top) and ^{13}C NMR (bottom) data for compound **52**

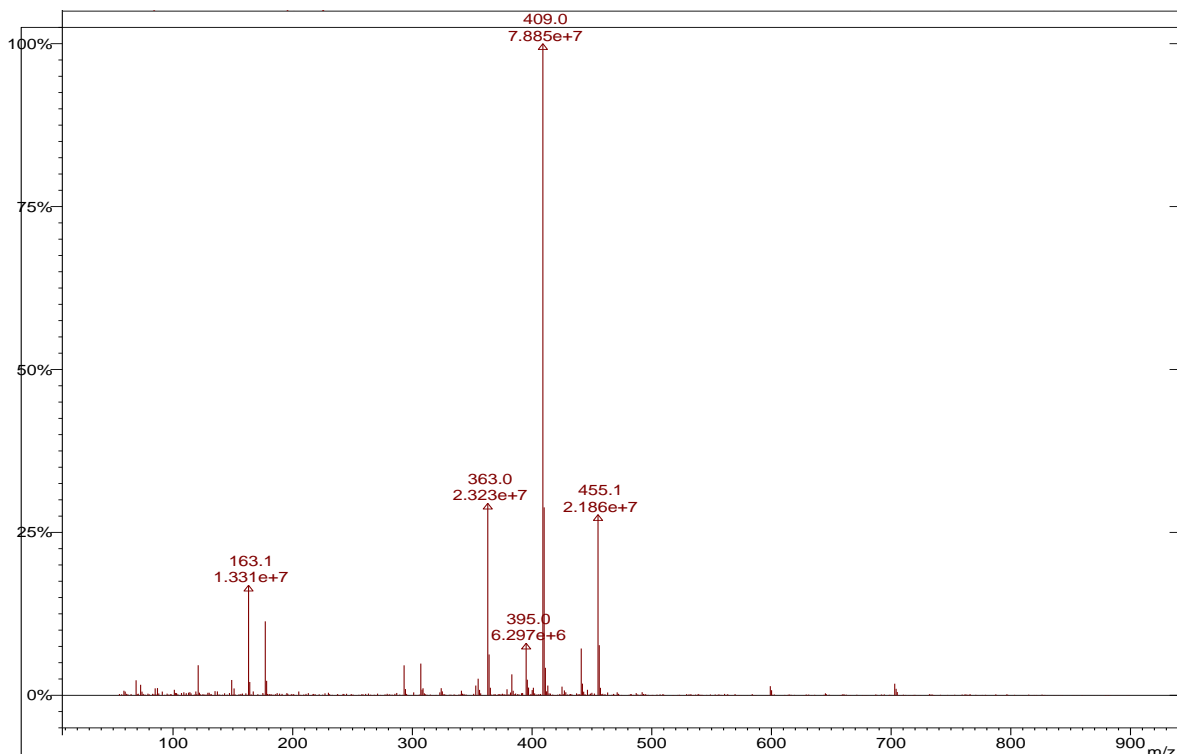
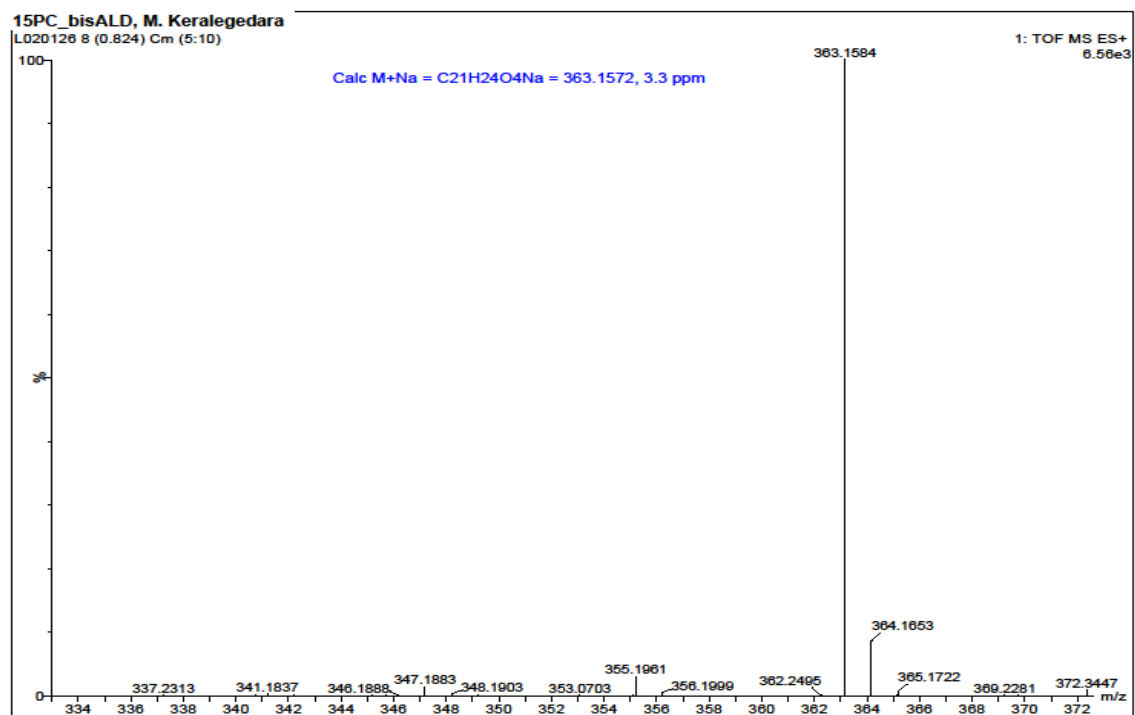


Figure 90. HRMS (top) and ESI-MS (bottom) data for compound **52**.

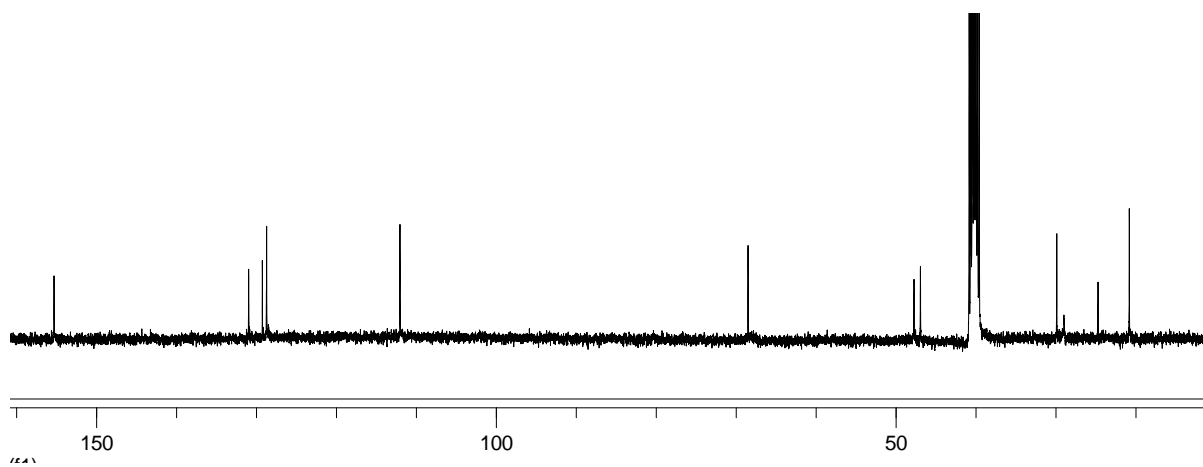
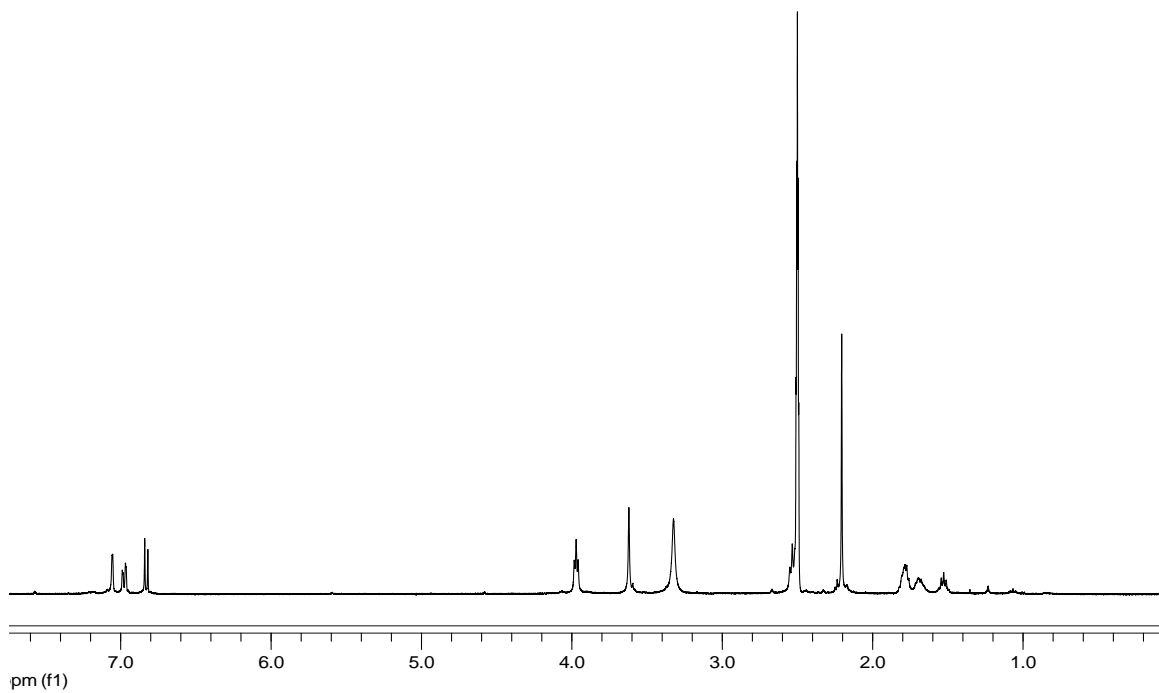


Figure 91. ^1H NMR (top) and ^{13}C NMR (bottom) data for compound **53**

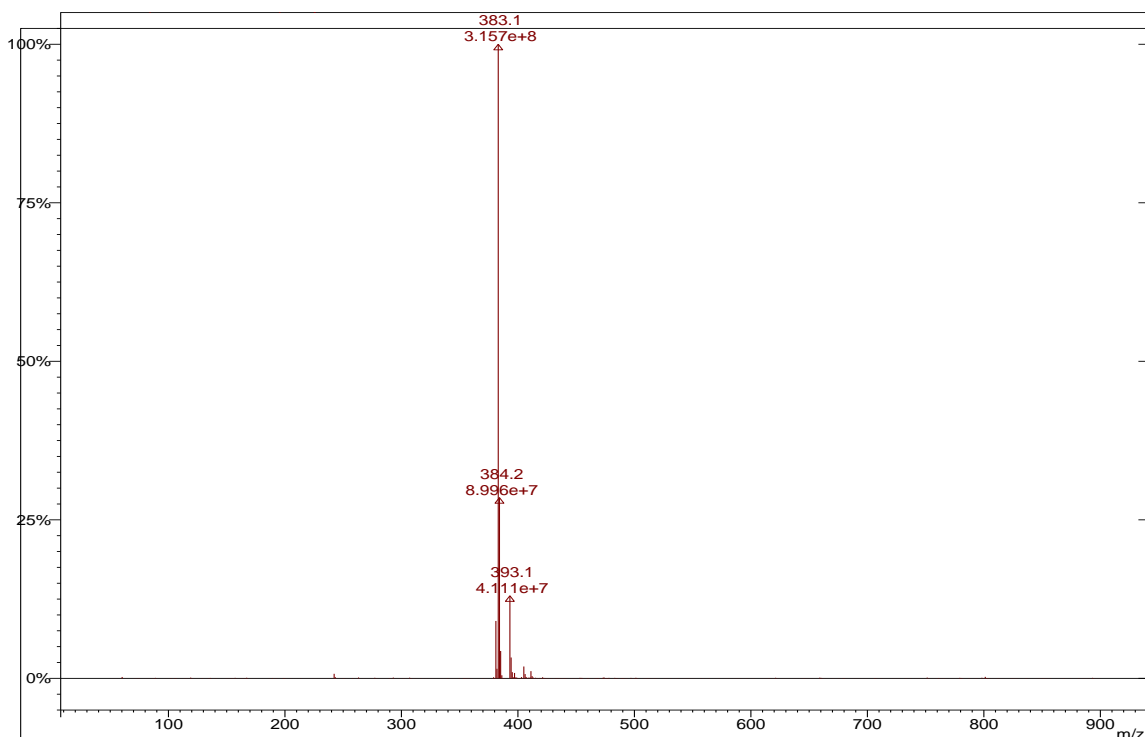
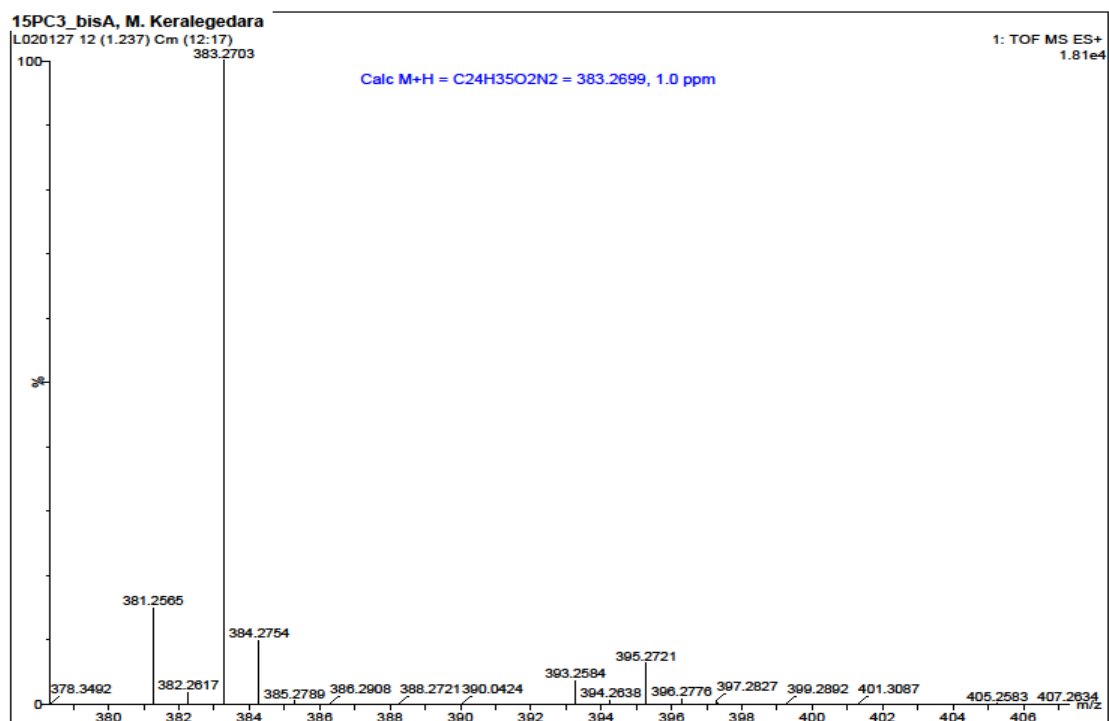


Figure 92. HRMS (top) and ESI-MS (bottom) data for compound **53**.

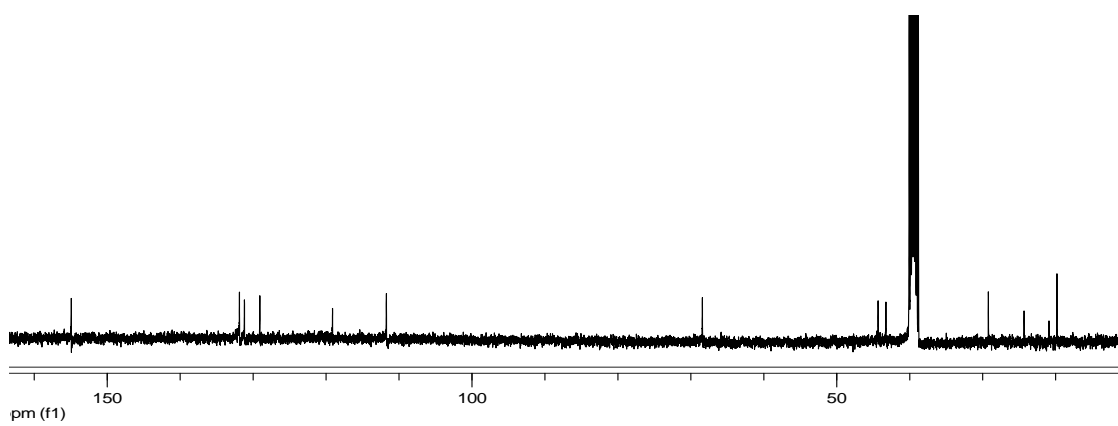
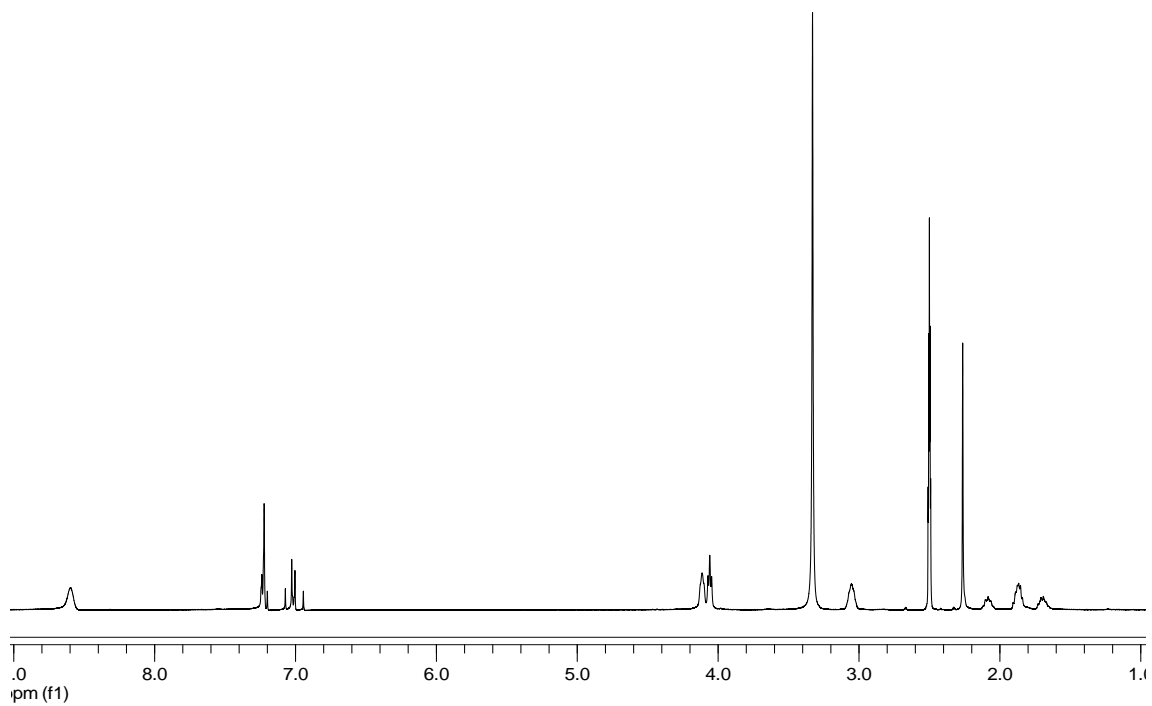


Figure 93. ^1H NMR (top) and ^{13}C NMR (bottom) data for compound **54**

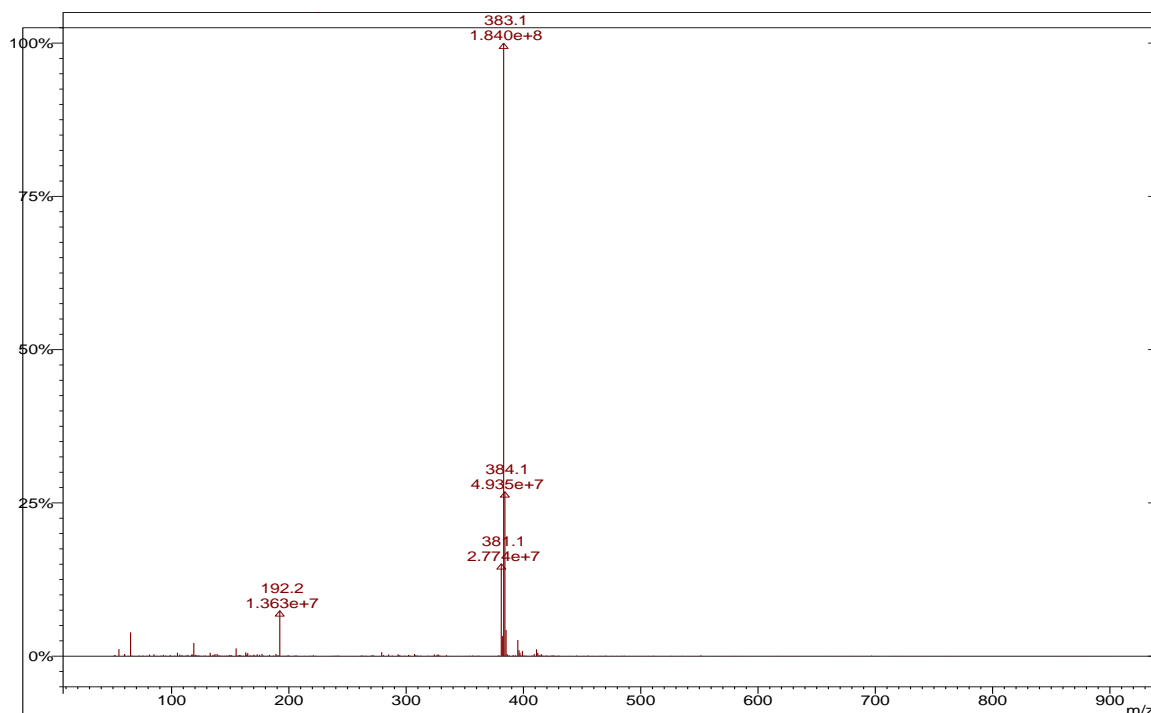
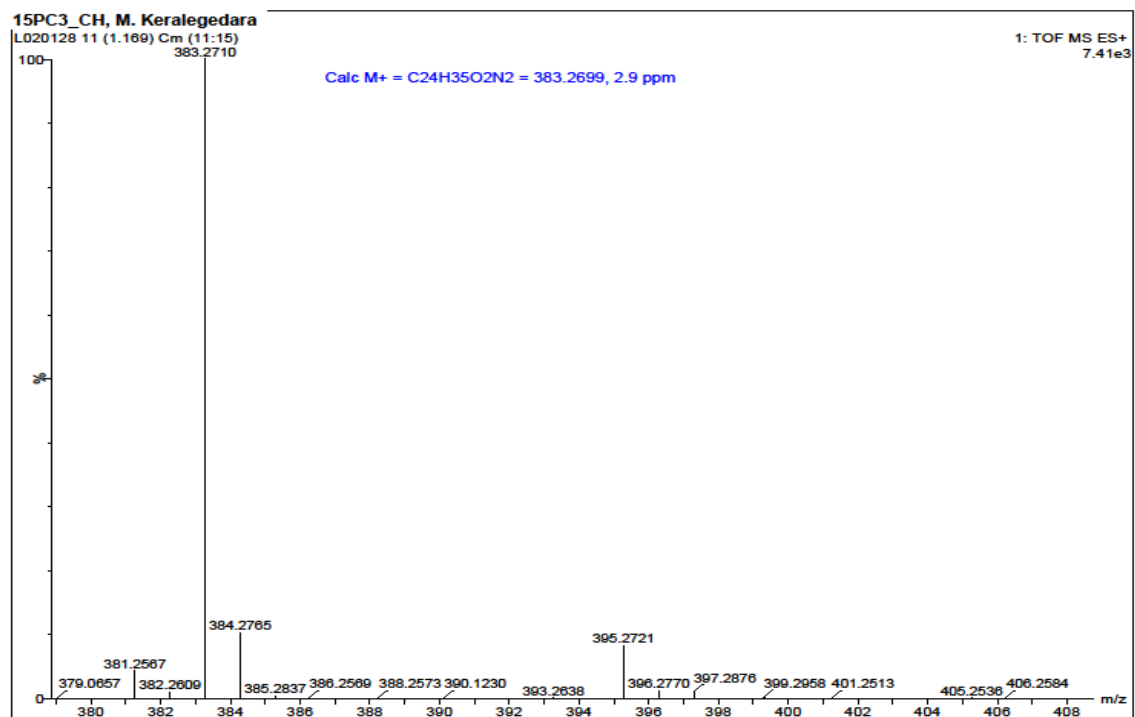


Figure 94. HRMS (top) and ESI-MS (bottom) data for compound 54.

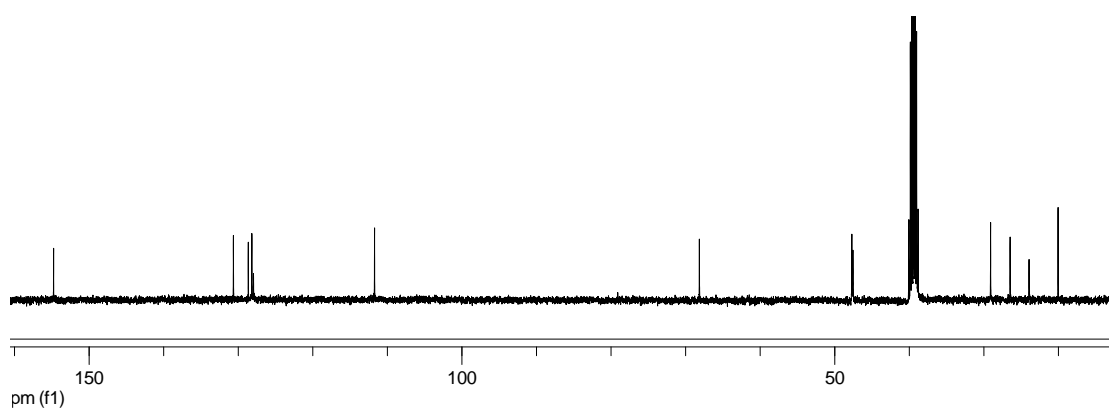
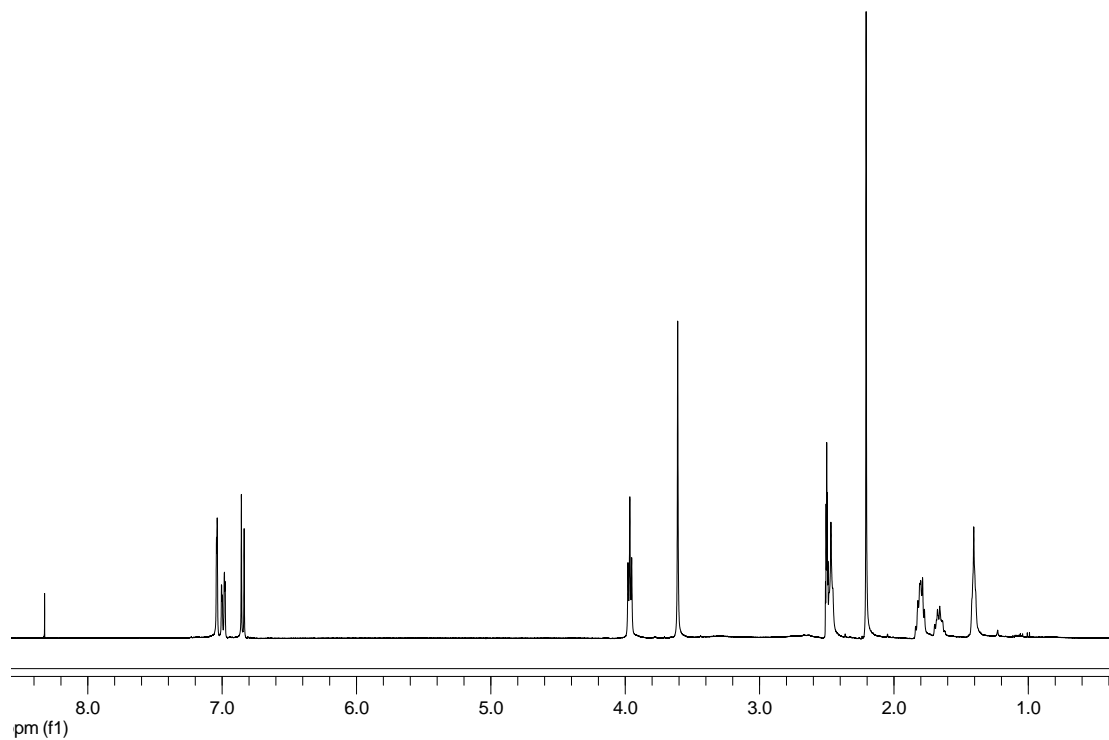


Figure 95. ^1H NMR (top) and ^{13}C NMR (bottom) data for compound **55**

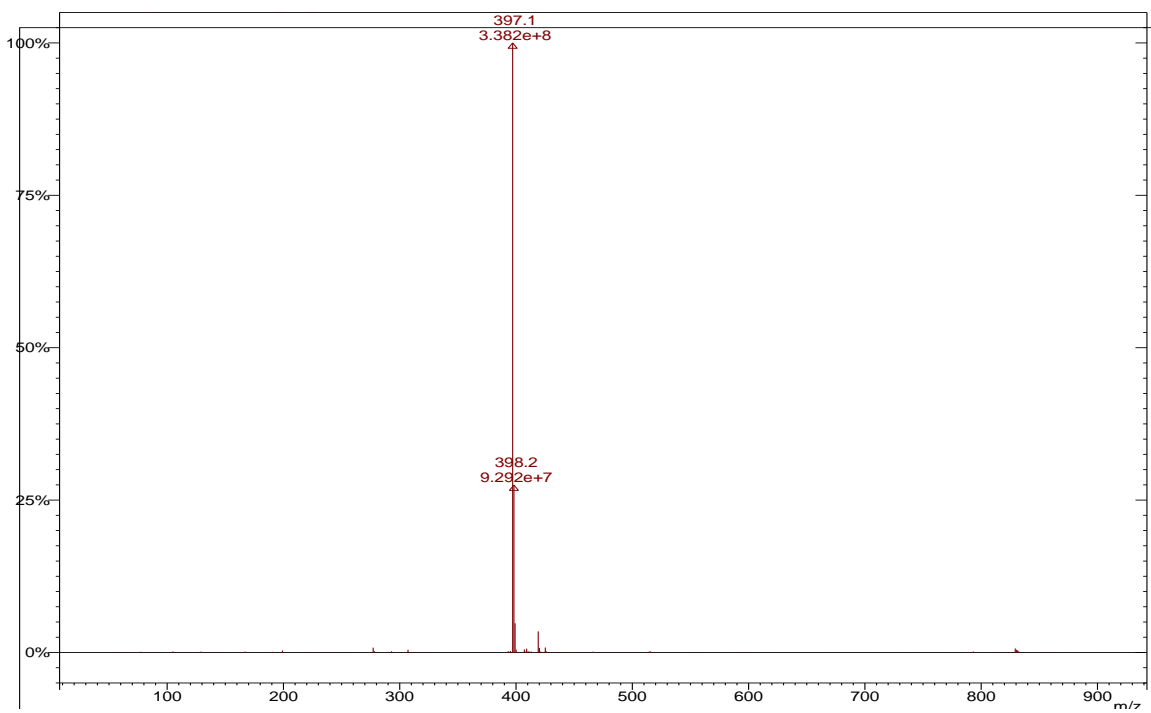
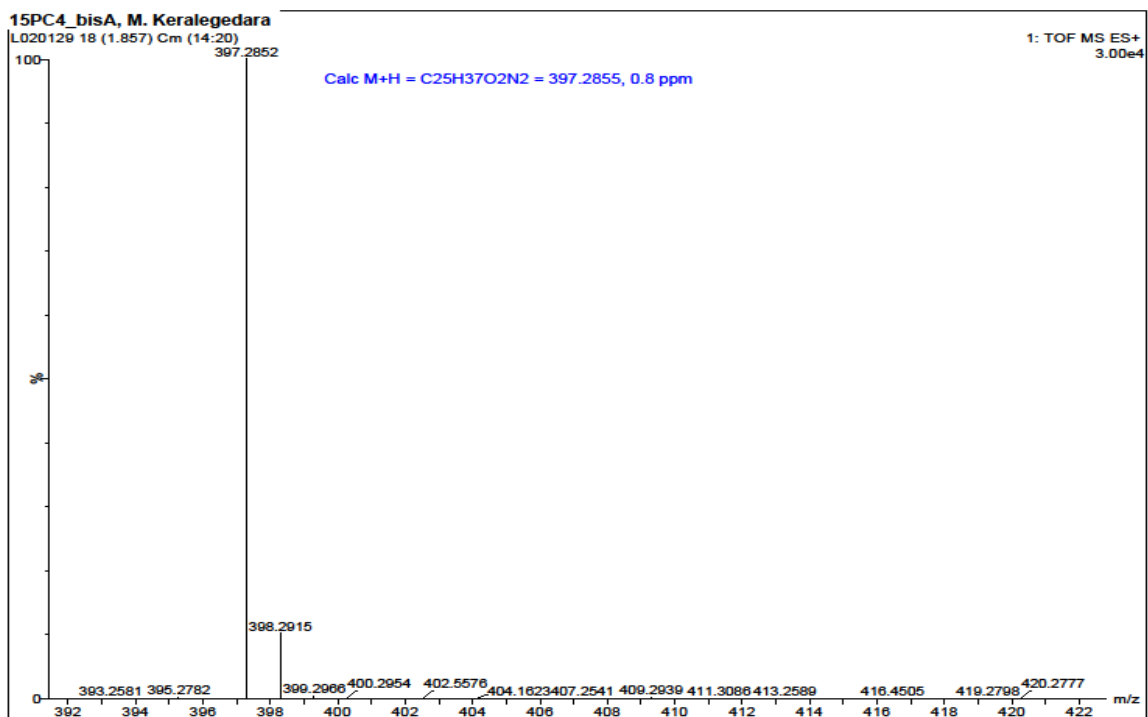


Figure 96. HRMS (top) and ESI-MS (bottom) data for compound **55**.

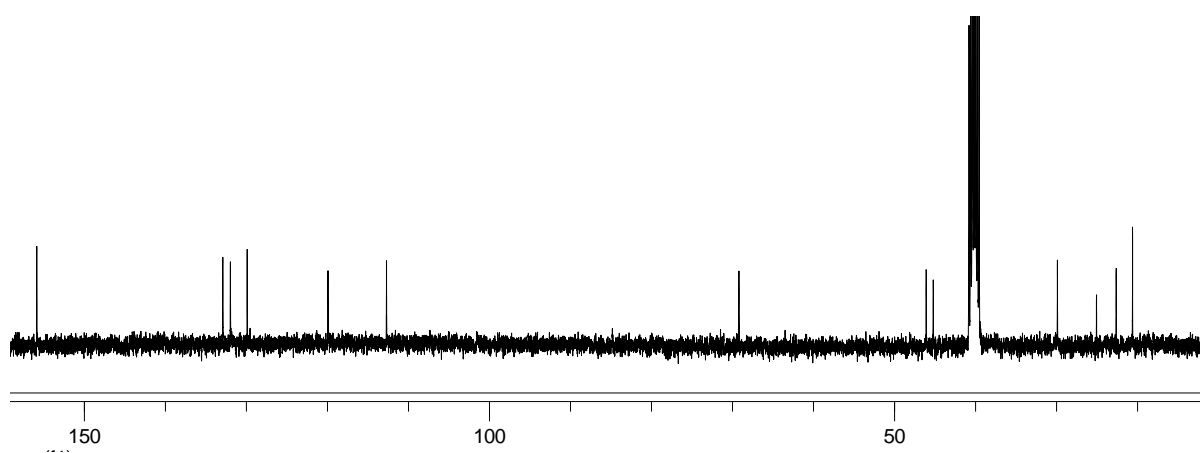
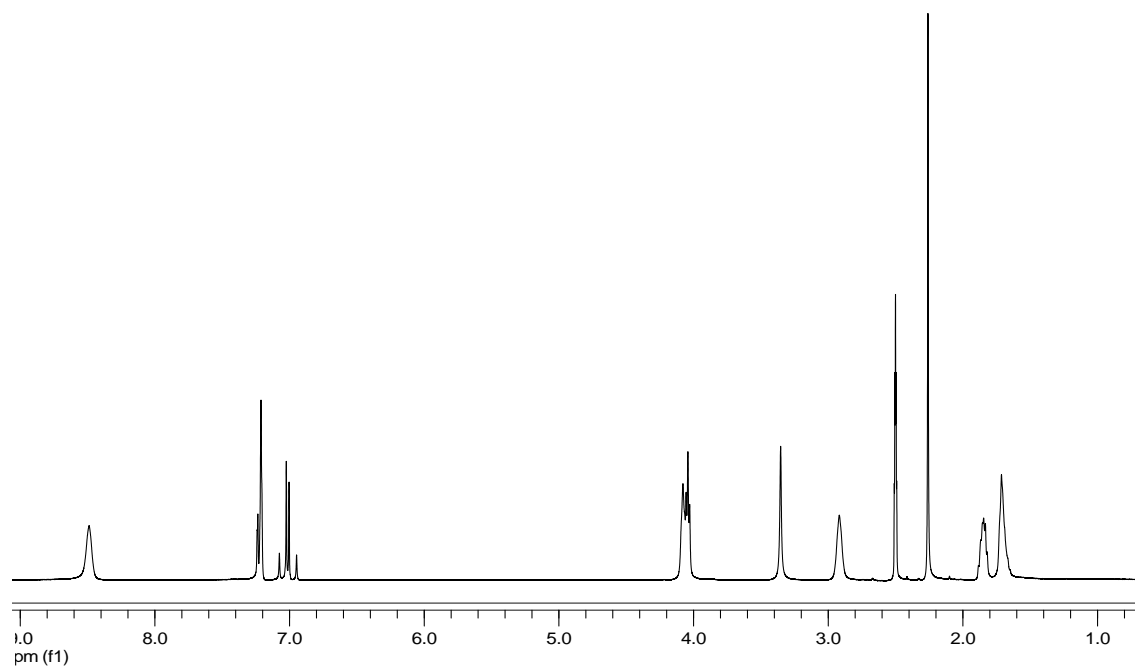


Figure 97. ^1H NMR (top) and ^{13}C NMR (bottom) data for compound **56**

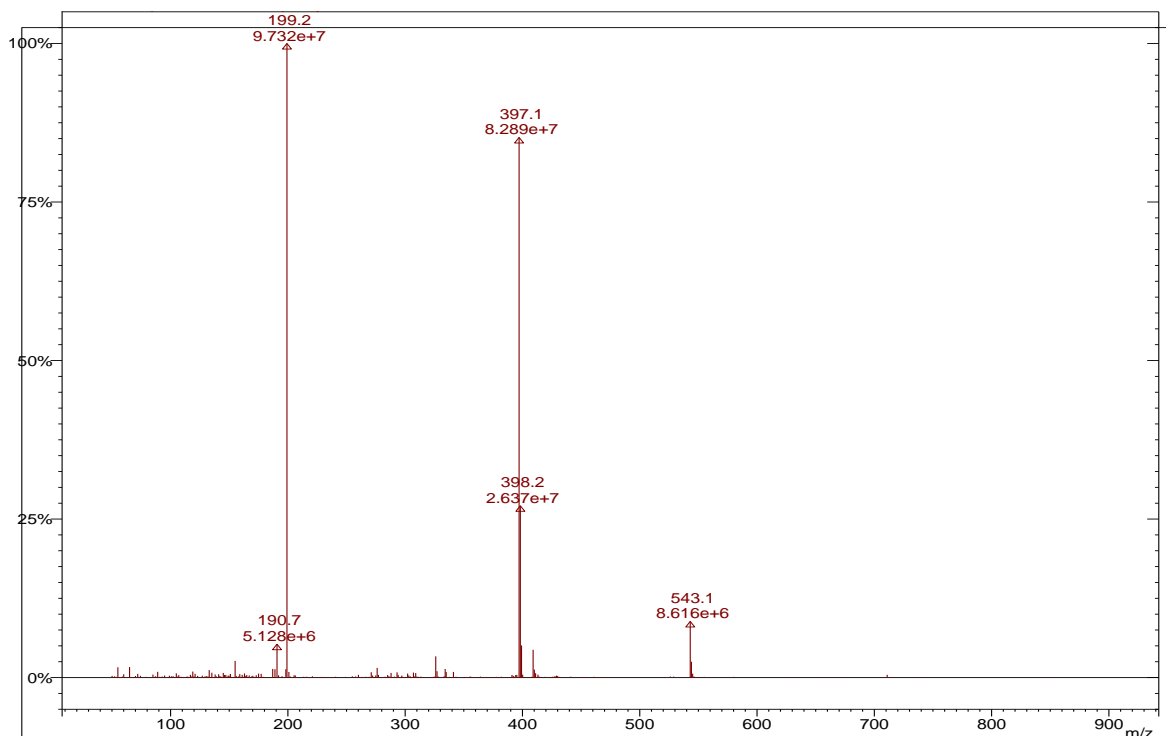
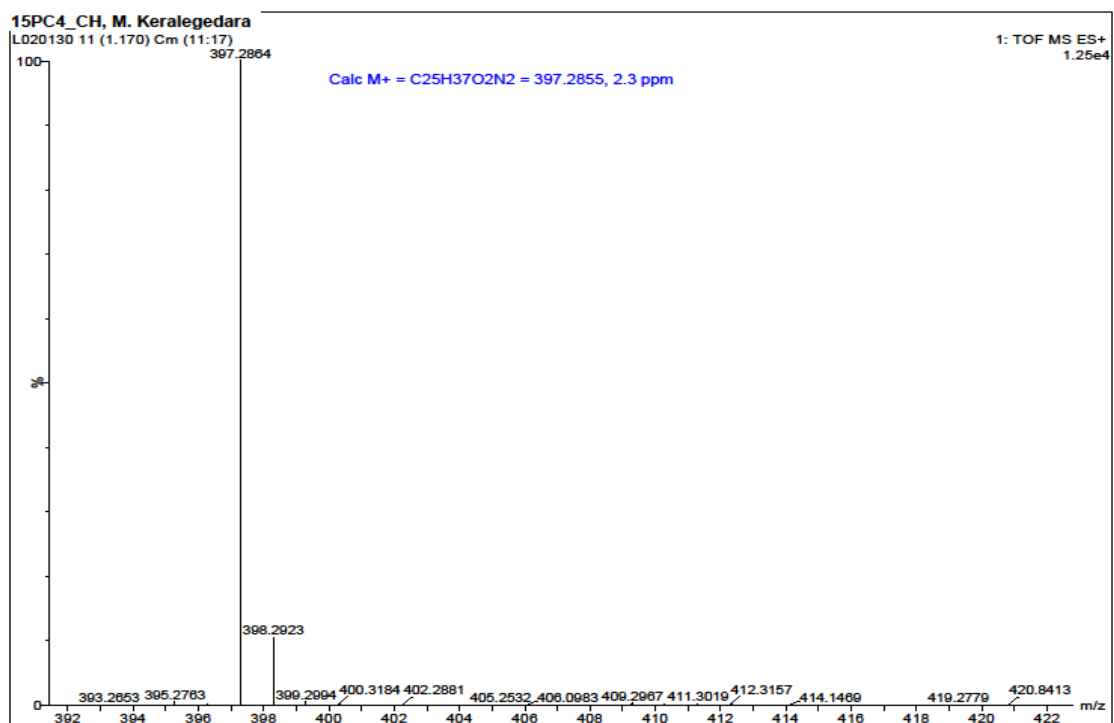


Figure 98. HRMS (top) and ESI-MS (bottom) data for compound **56**.

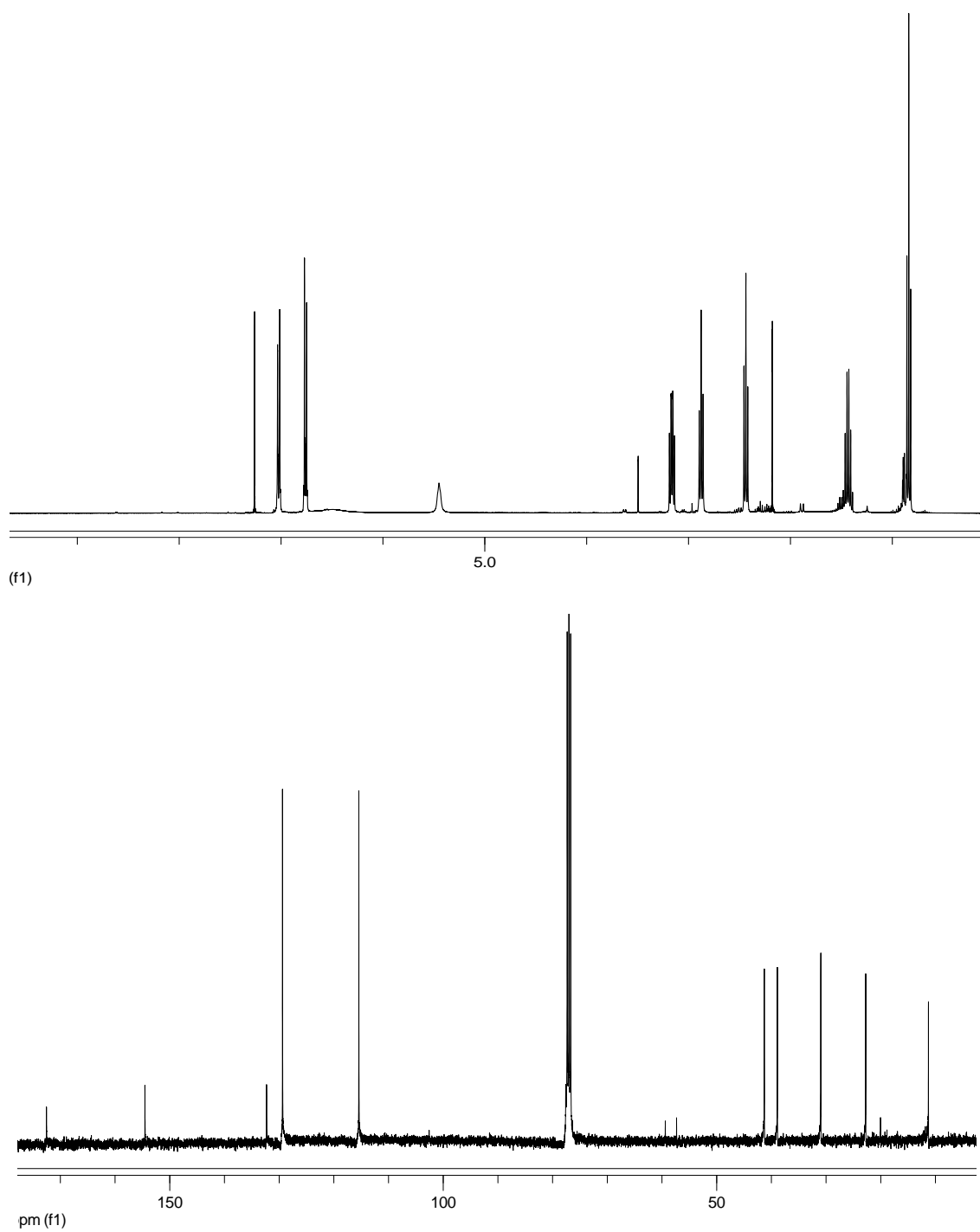


Figure 99. ^1H NMR (top) and ^{13}C NMR (bottom) data for compound **59**

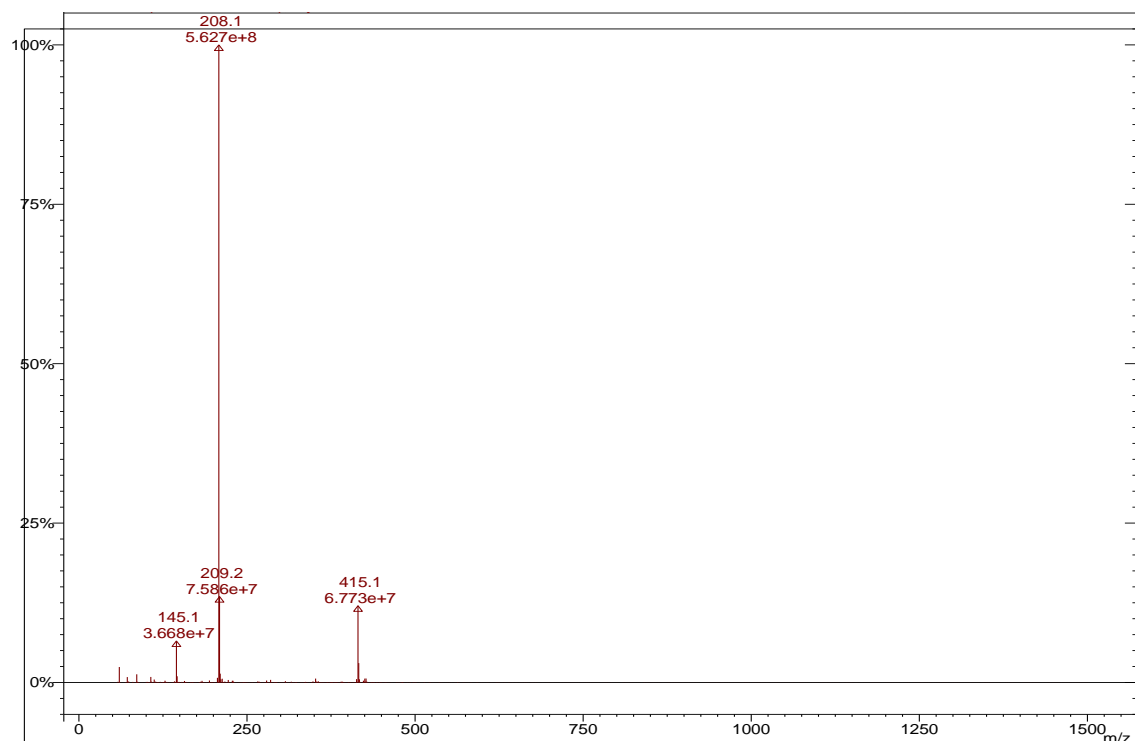
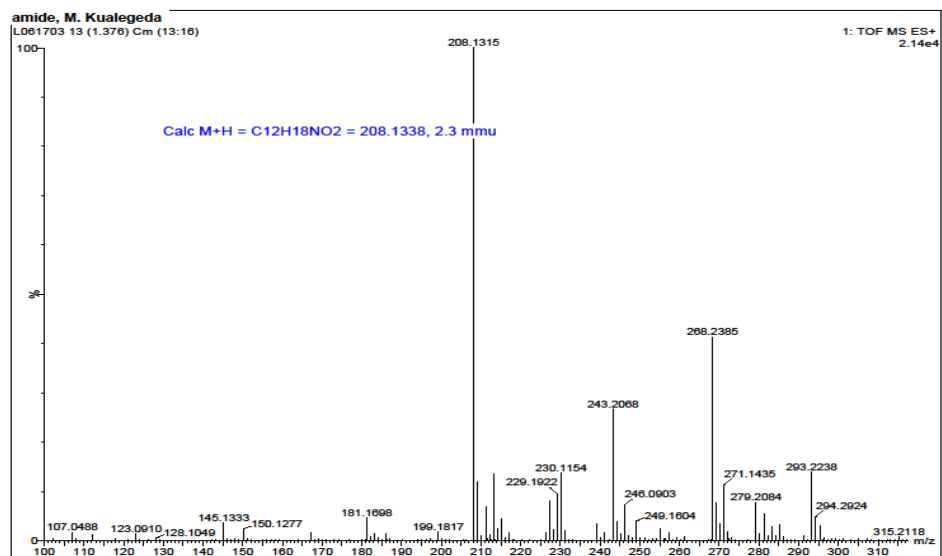


Figure 100. HRMS (top) and ESI-MS (bottom) data for compound **59**.

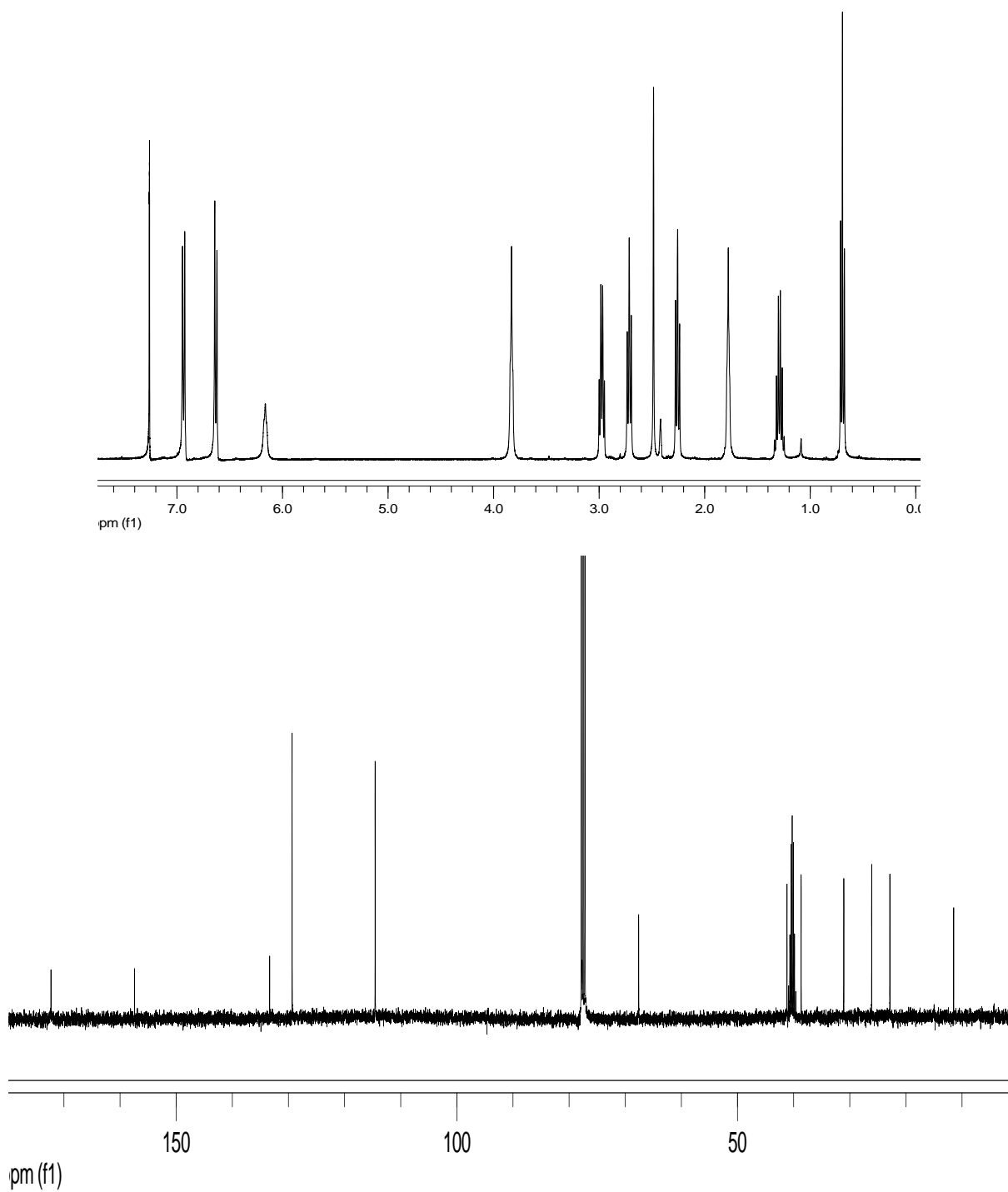


Figure 101. ^1H NMR (top) and ^{13}C NMR (bottom) data for compound **60**

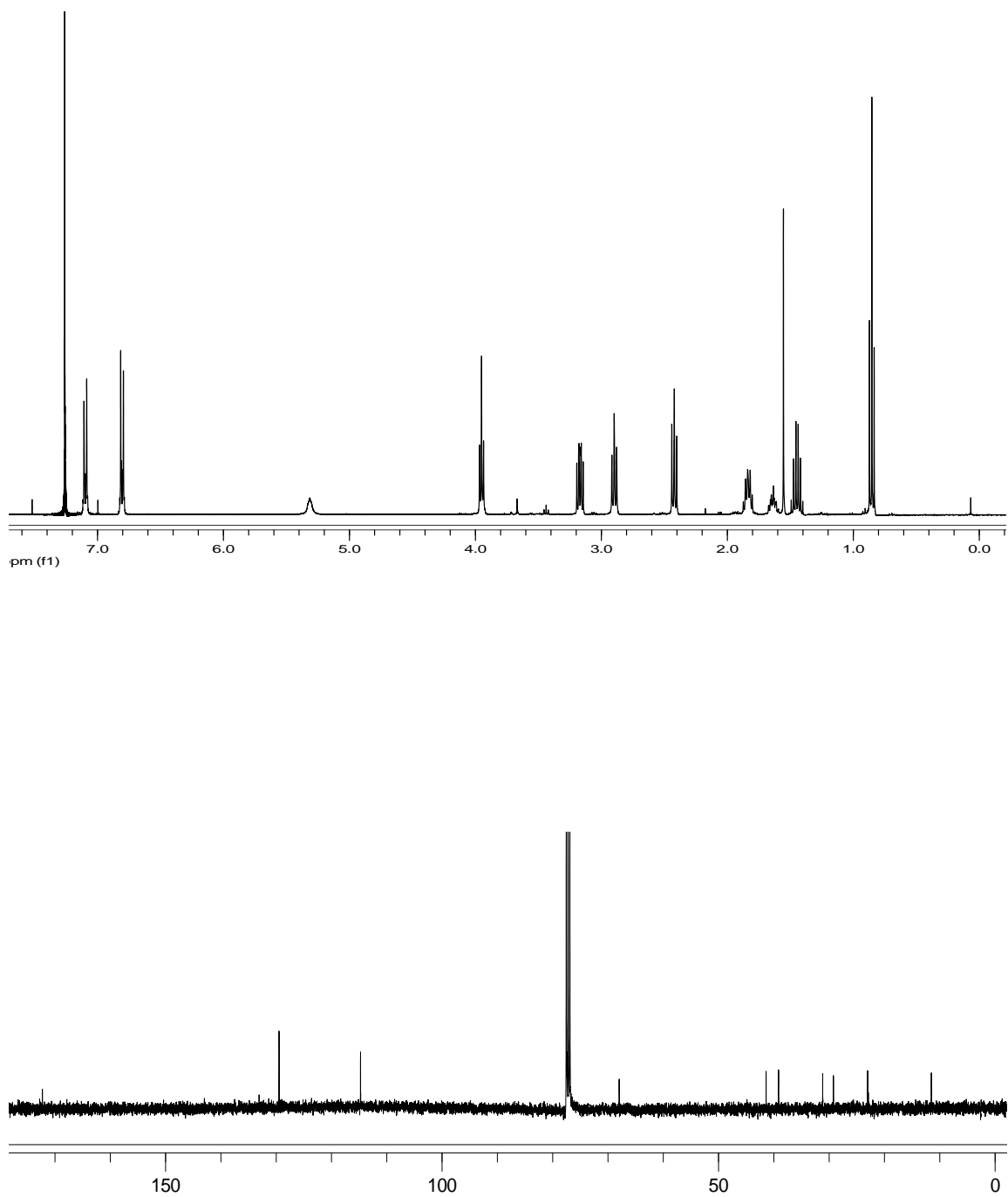


Figure 102. ^1H NMR (top) and ^{13}C NMR (bottom) data for compound **61**

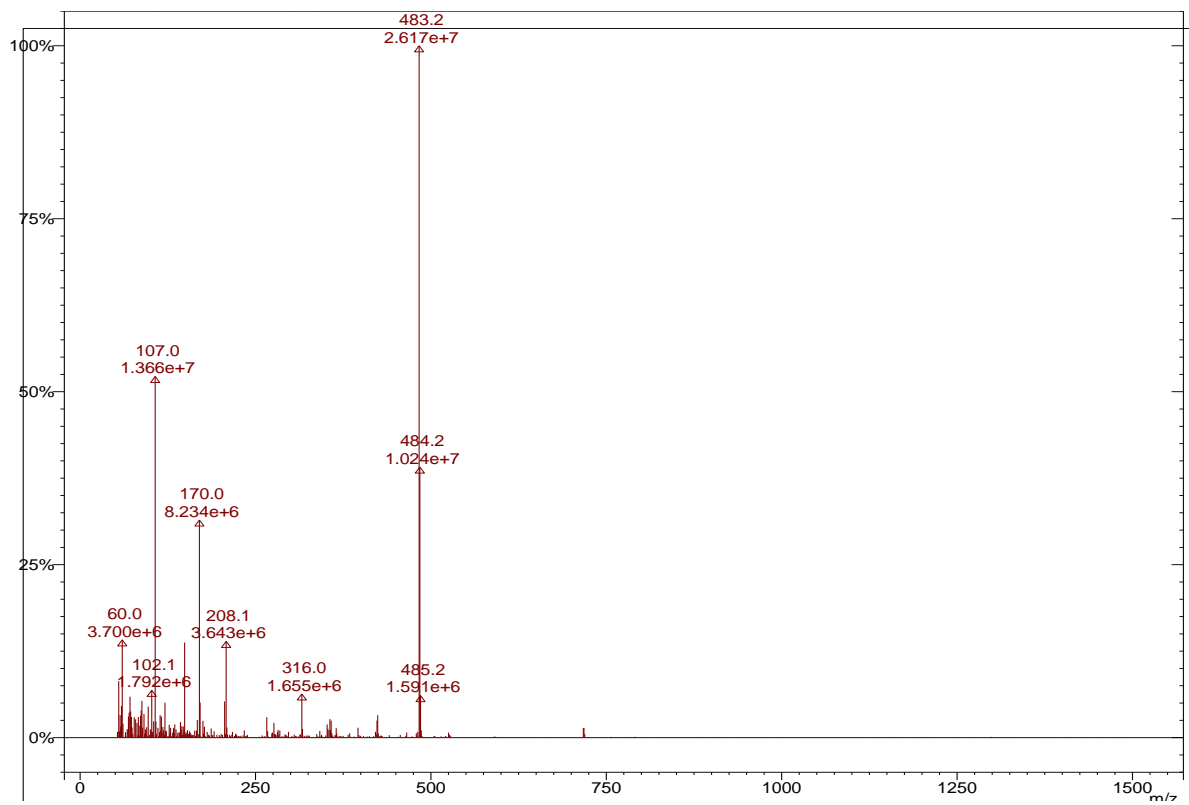


Figure 103. ESI-MS data for compound **61**.

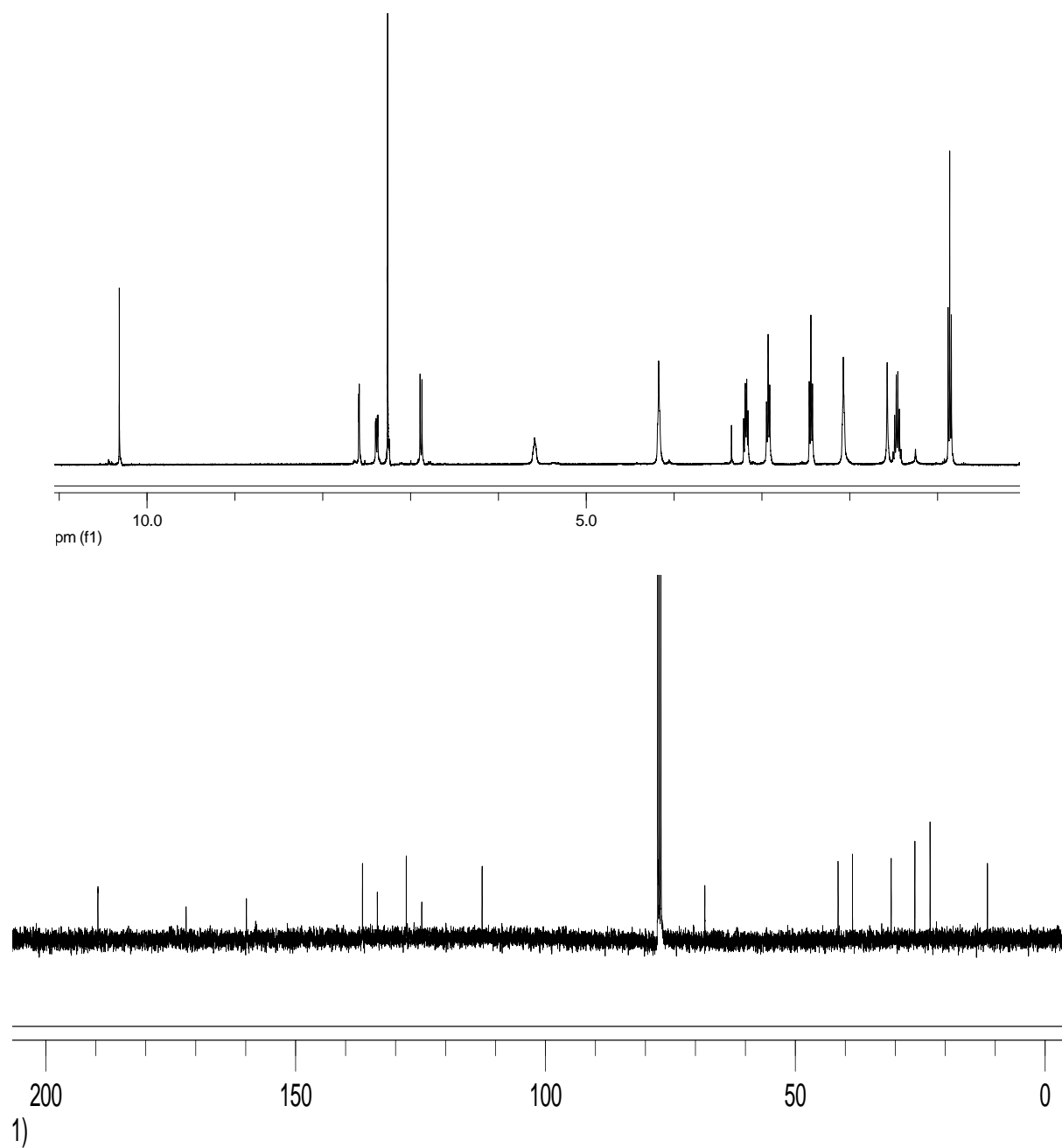


Figure 104. ^1H NMR (top) and ^{13}C NMR (bottom) data for compound **62**

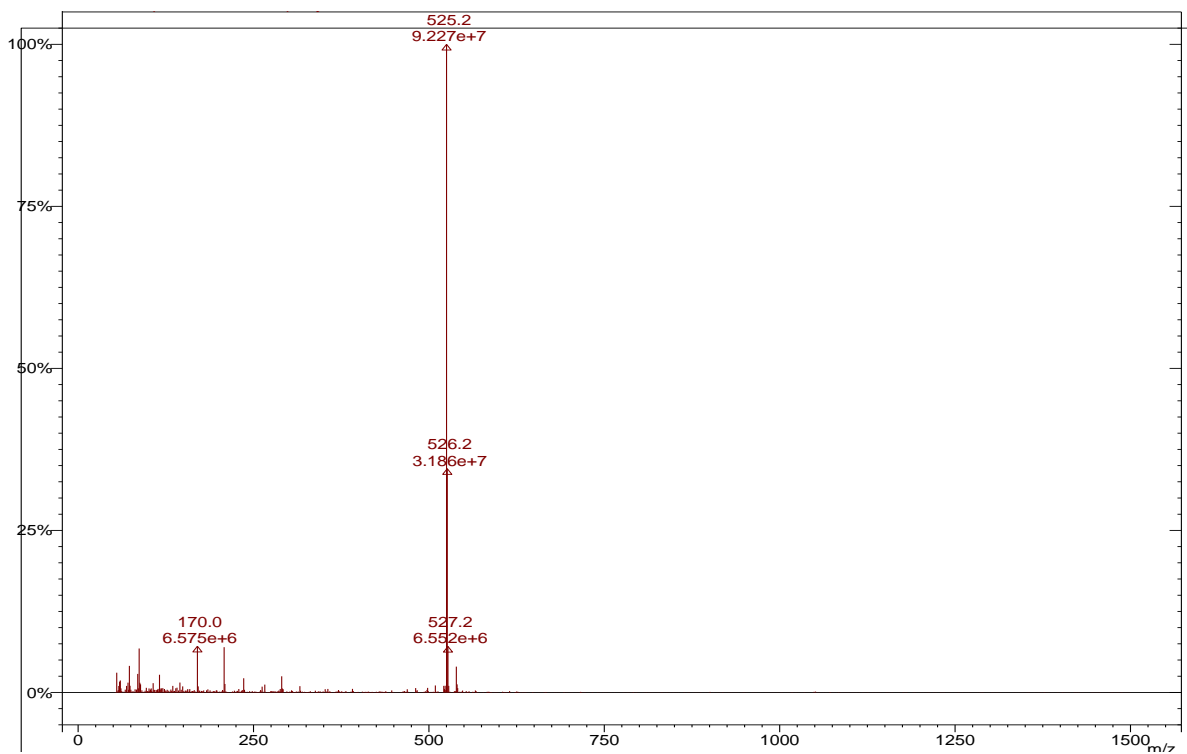
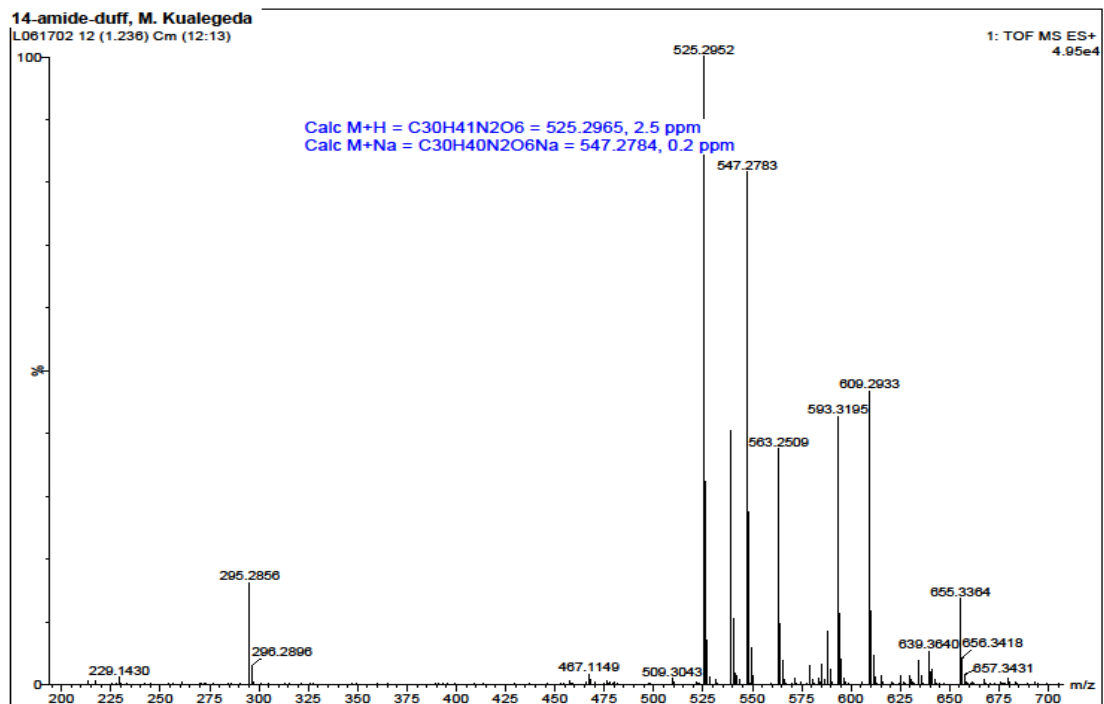


Figure 105. HRMS (top) and ESI-MS (bottom) data for compound **62**

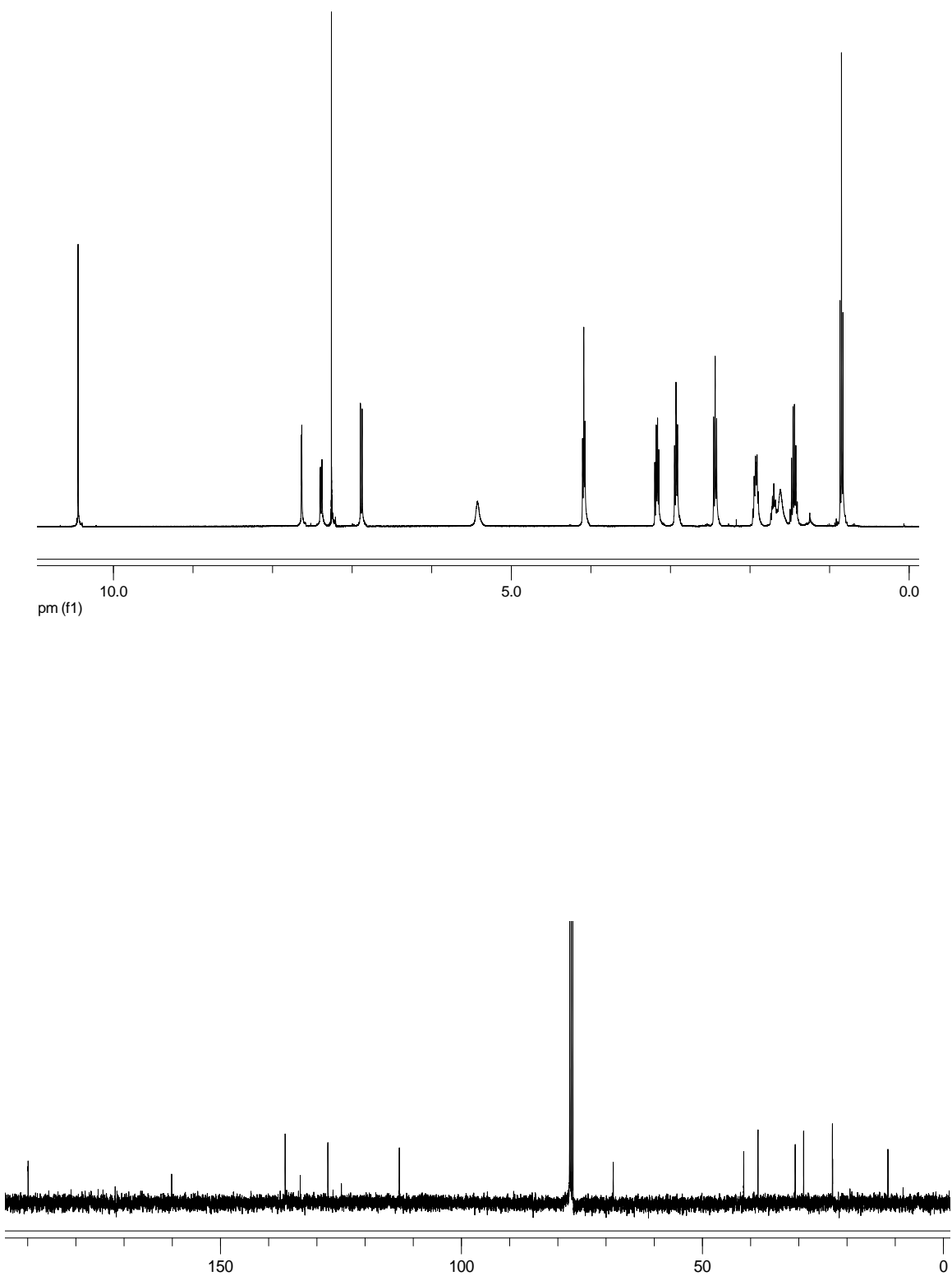


Figure 106. ^1H NMR (top) and ^{13}C NMR (bottom) data for compound **63**

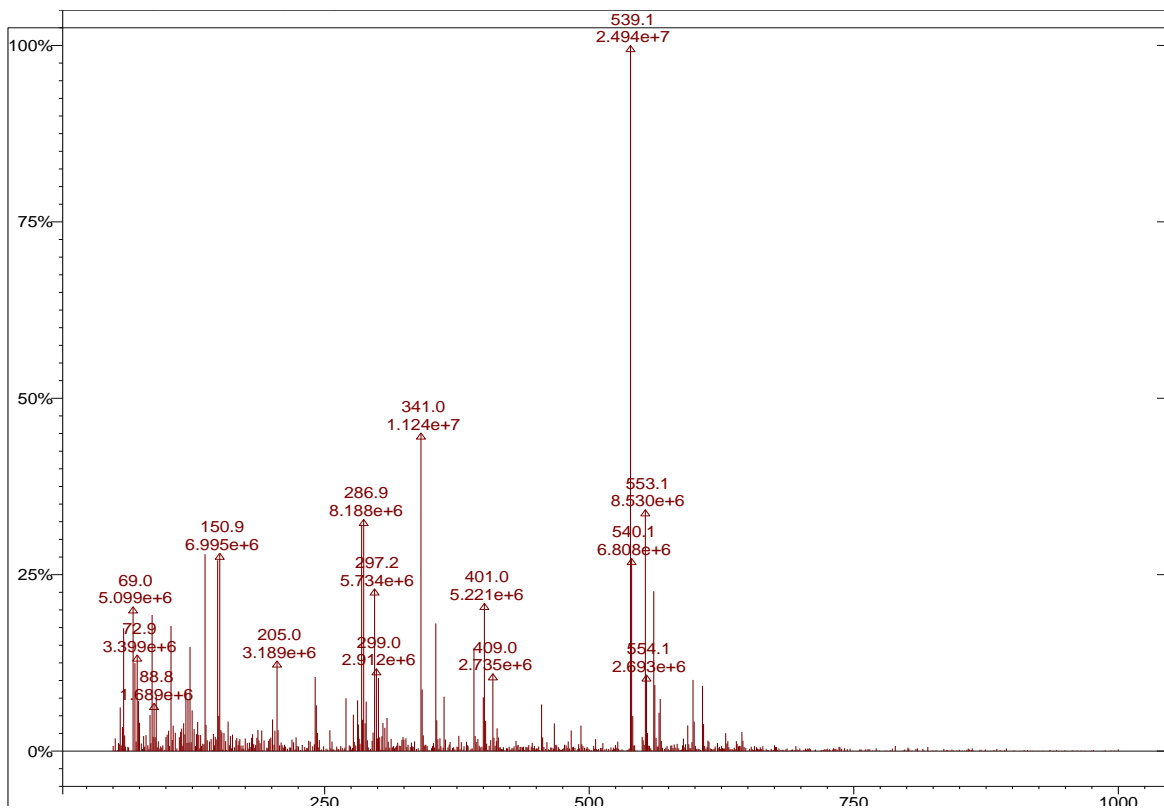


Figure 107. ESI-MS data for compound **63**.

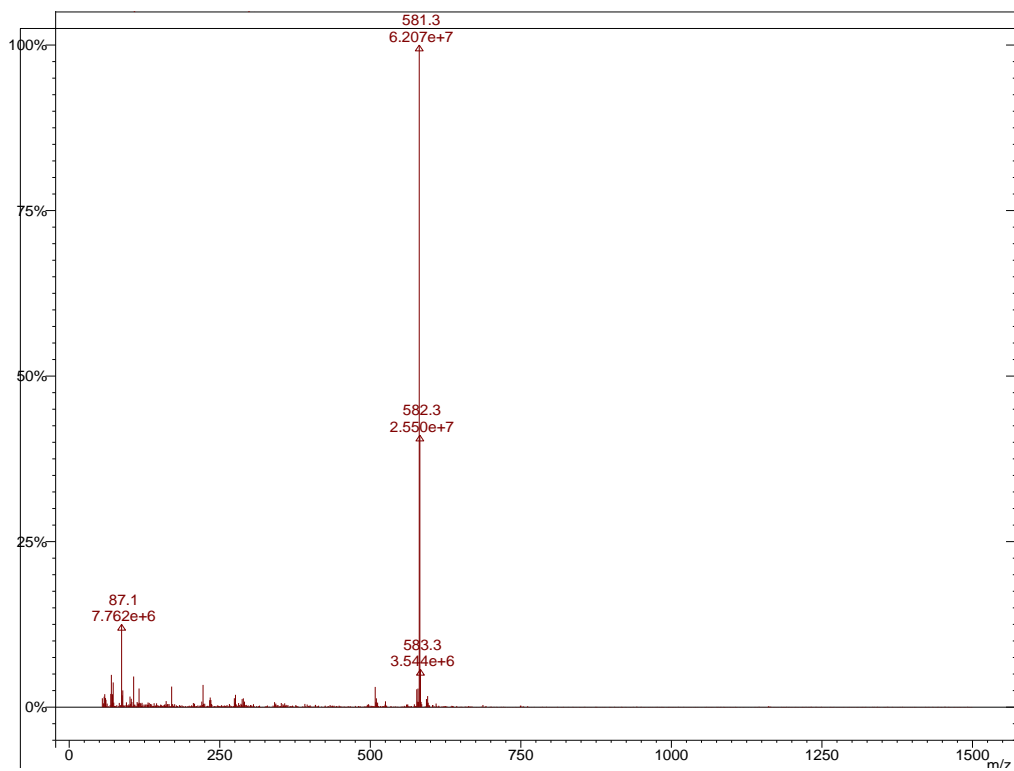
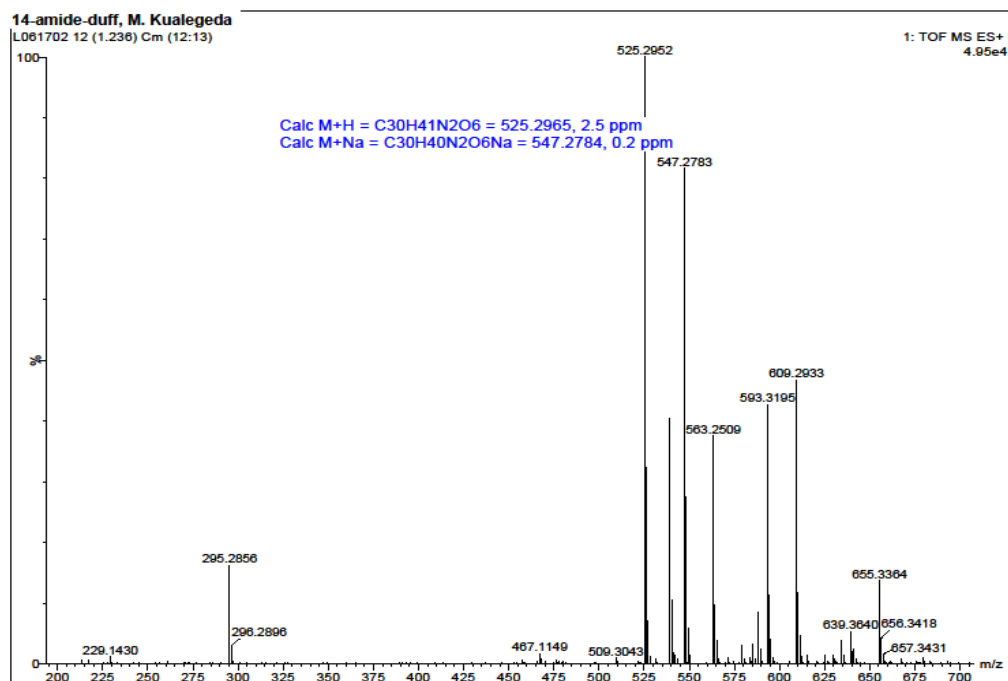


Figure 109. HRMS (top) and ESI-MS (bottom) data for compound **64**

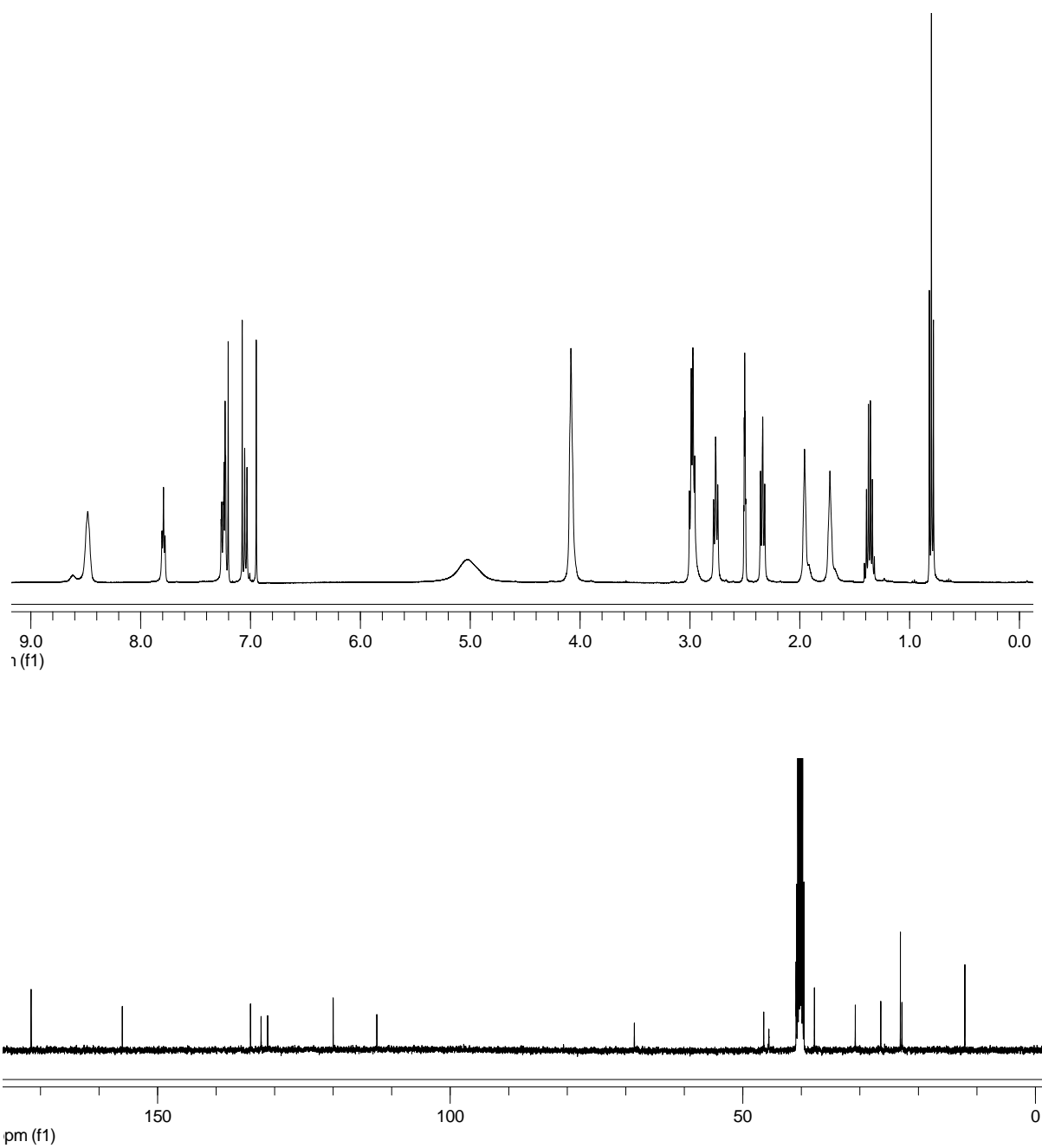


Figure 110. ^1H NMR (top) and ^{13}C NMR (bottom) data for compound **57a**

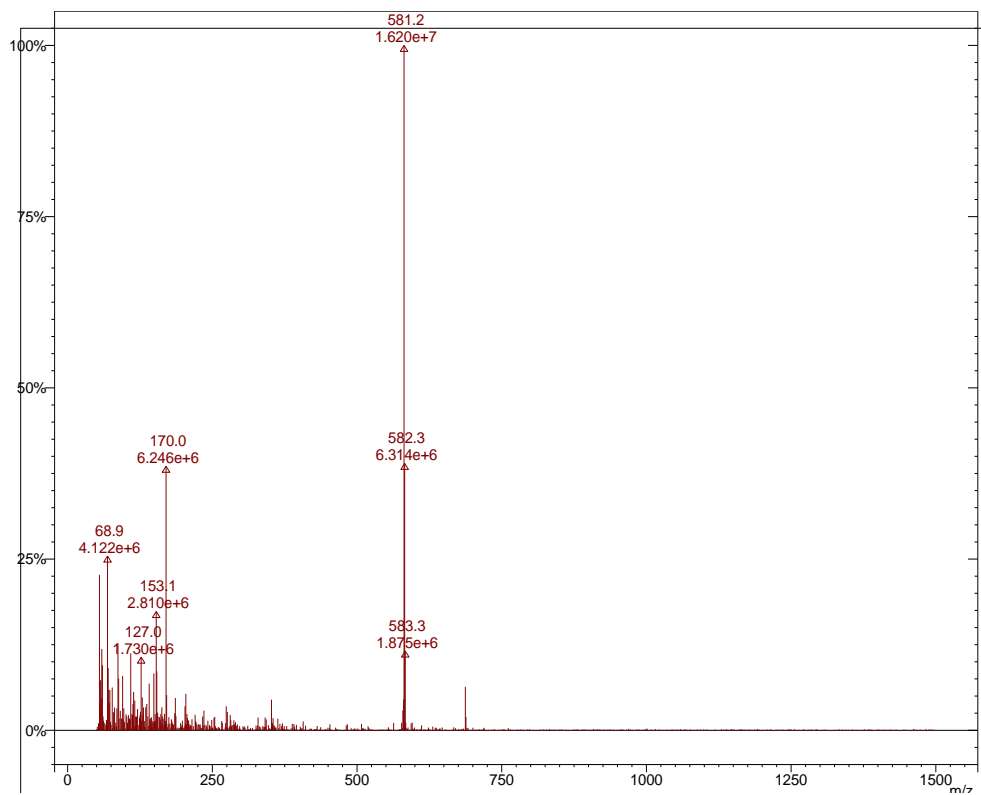


Figure 111. ESI-MS data for compound **57a**.

APPENDIX A (continued)

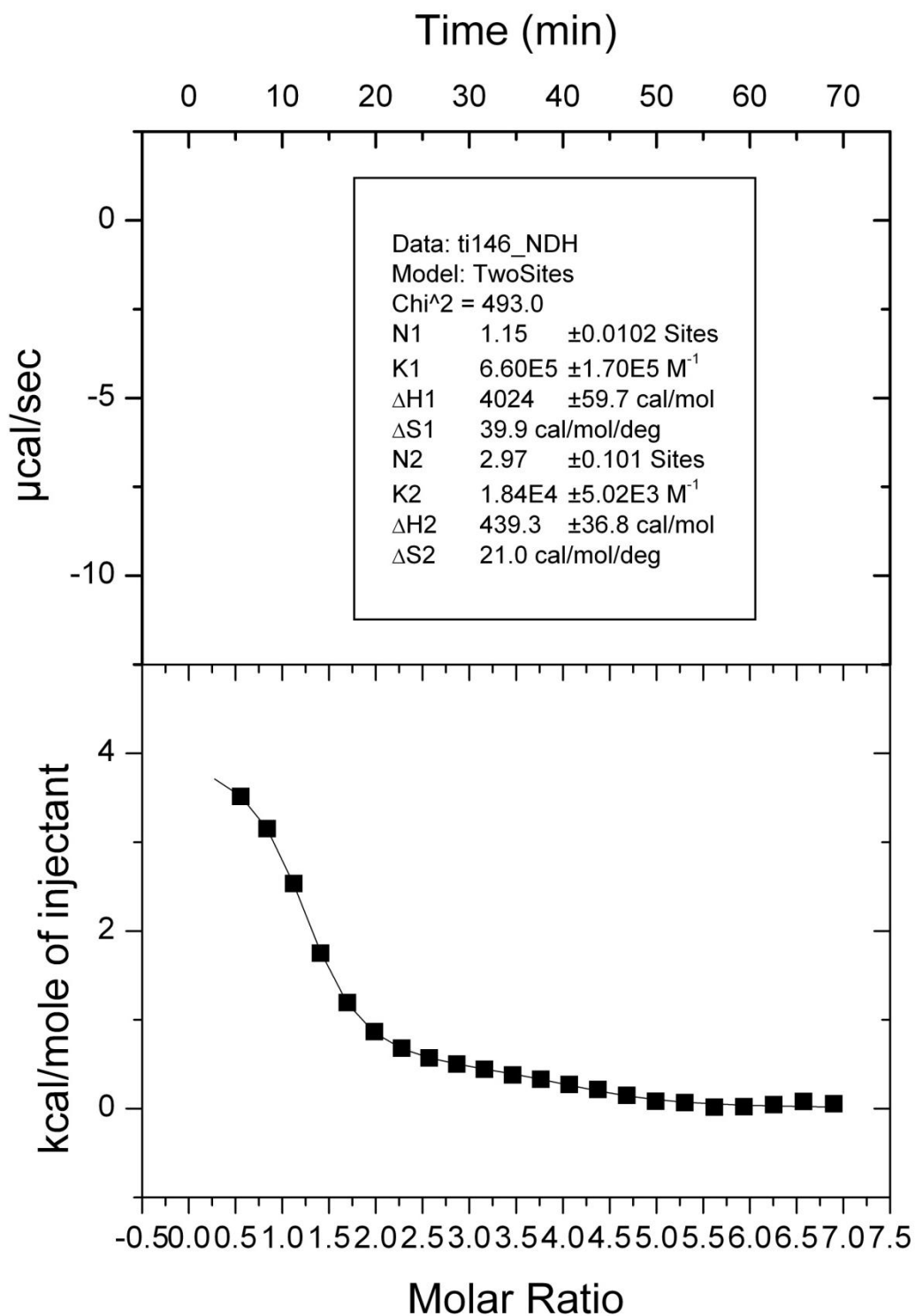


Figure 112. ITC data for compound **45** with dihydrogenphosphate

APPENDIX A (continued)

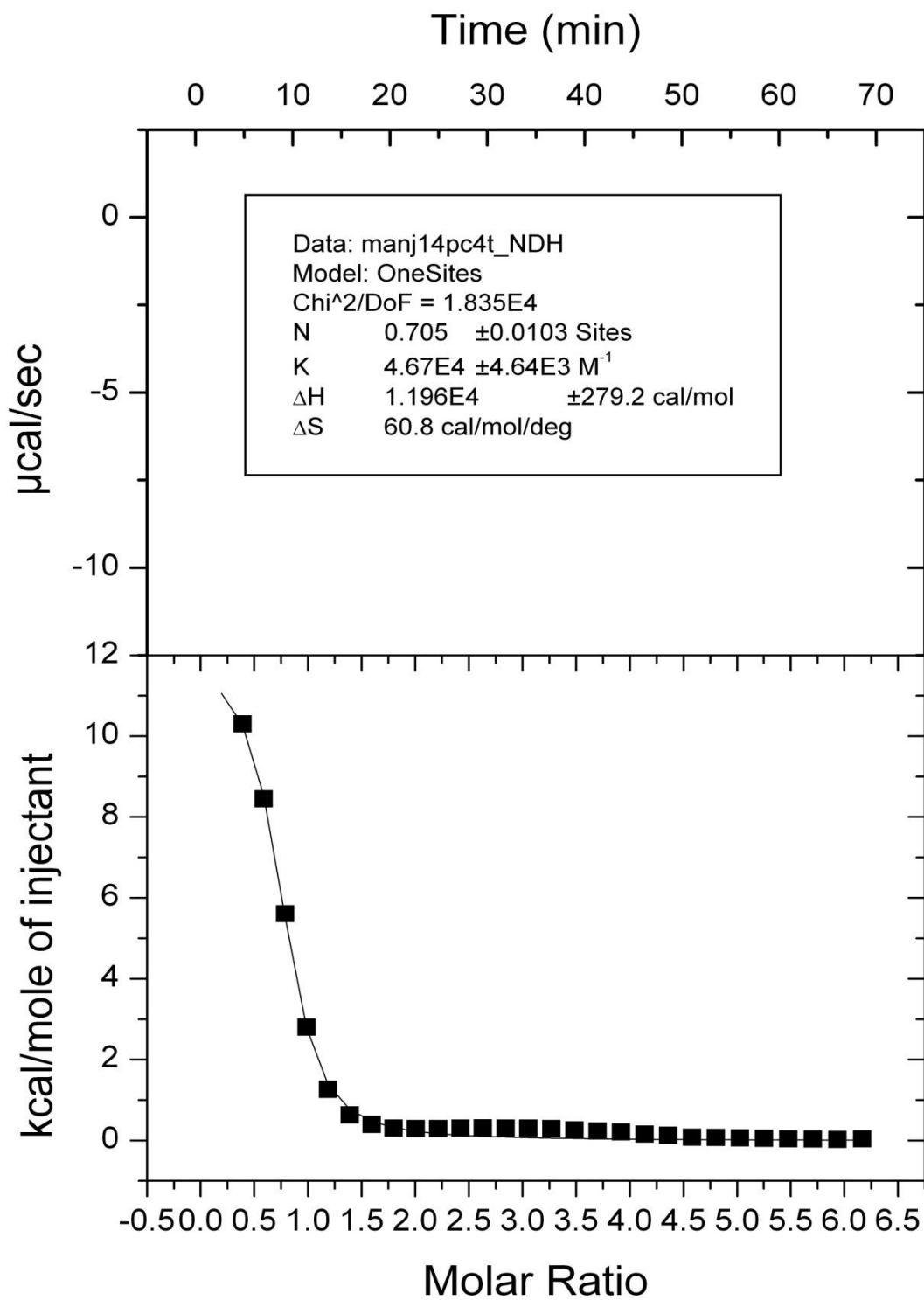


Figure 113. ITC data for compound **47** with dihydrogenphosphate

APPENDIX A (continued)

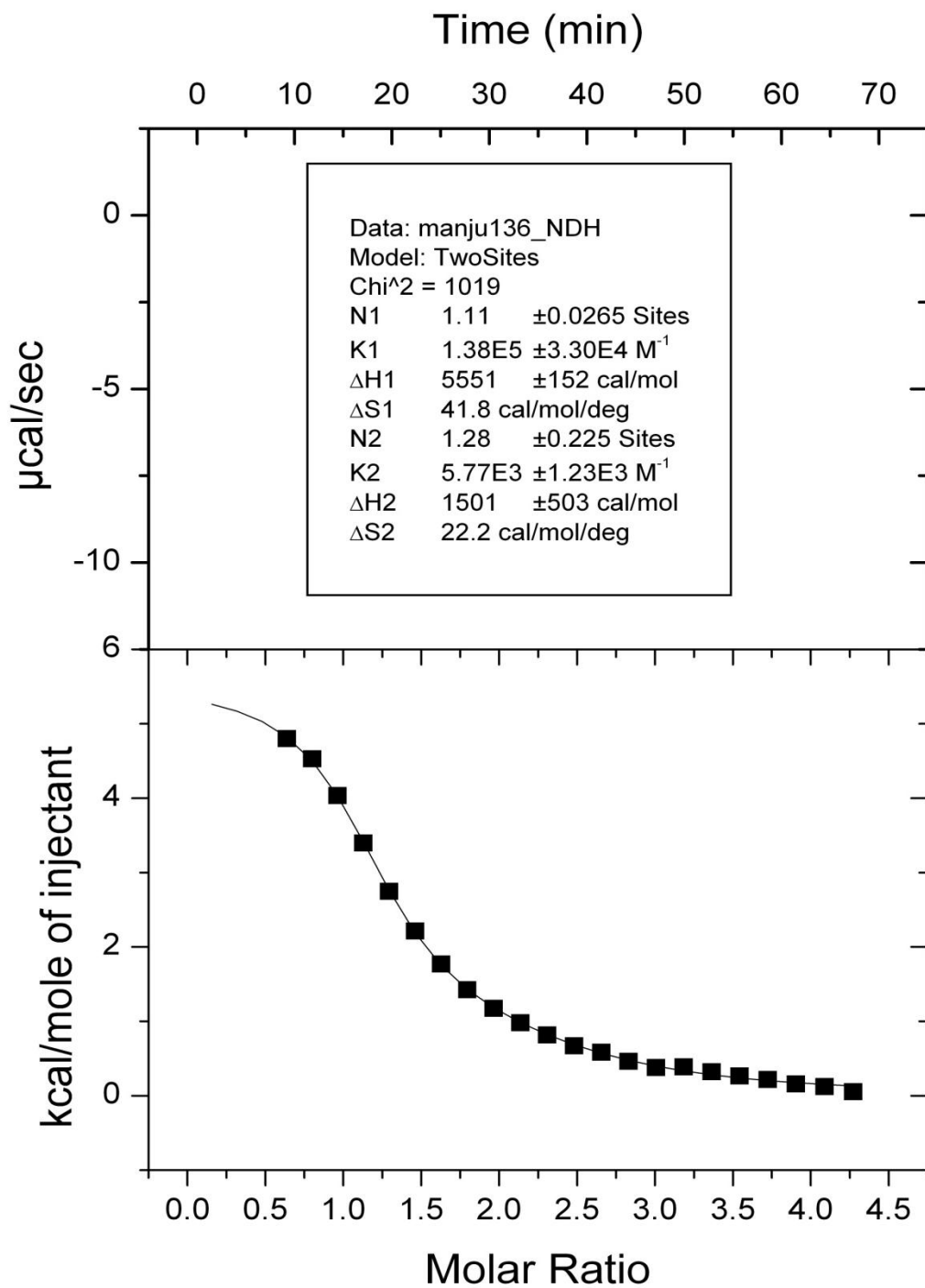


Figure 114. ITC data for compound **49** with dihydrogenphosphate

APPENDIX A (continued)

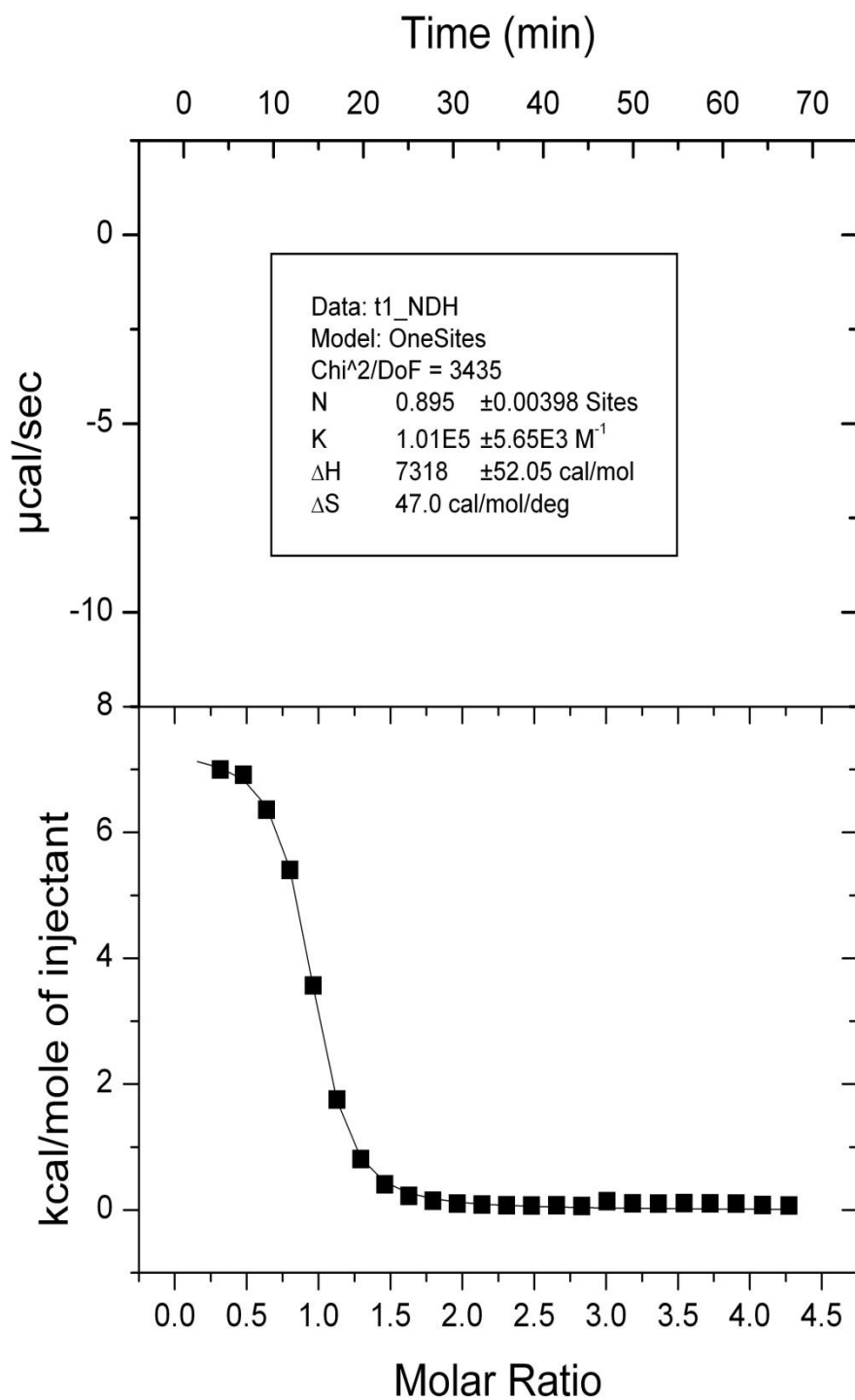


Figure 115. ITC data for compound **54** with dihydrogenphosphate

APPENDIX A (continued)

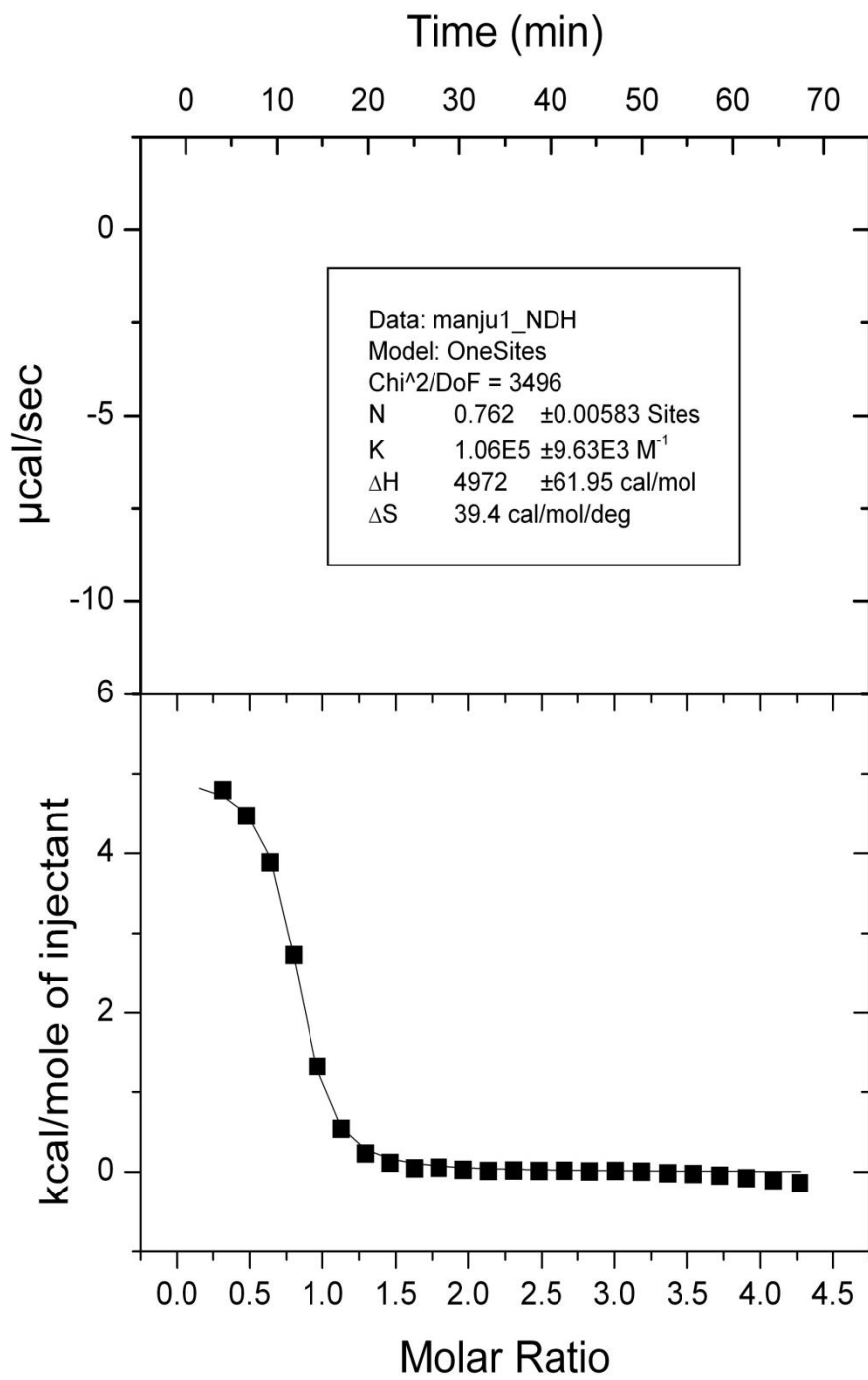


Figure 116. ITC data for compound **56** with dihydrogenphosphate

APPENDIX A (continued)

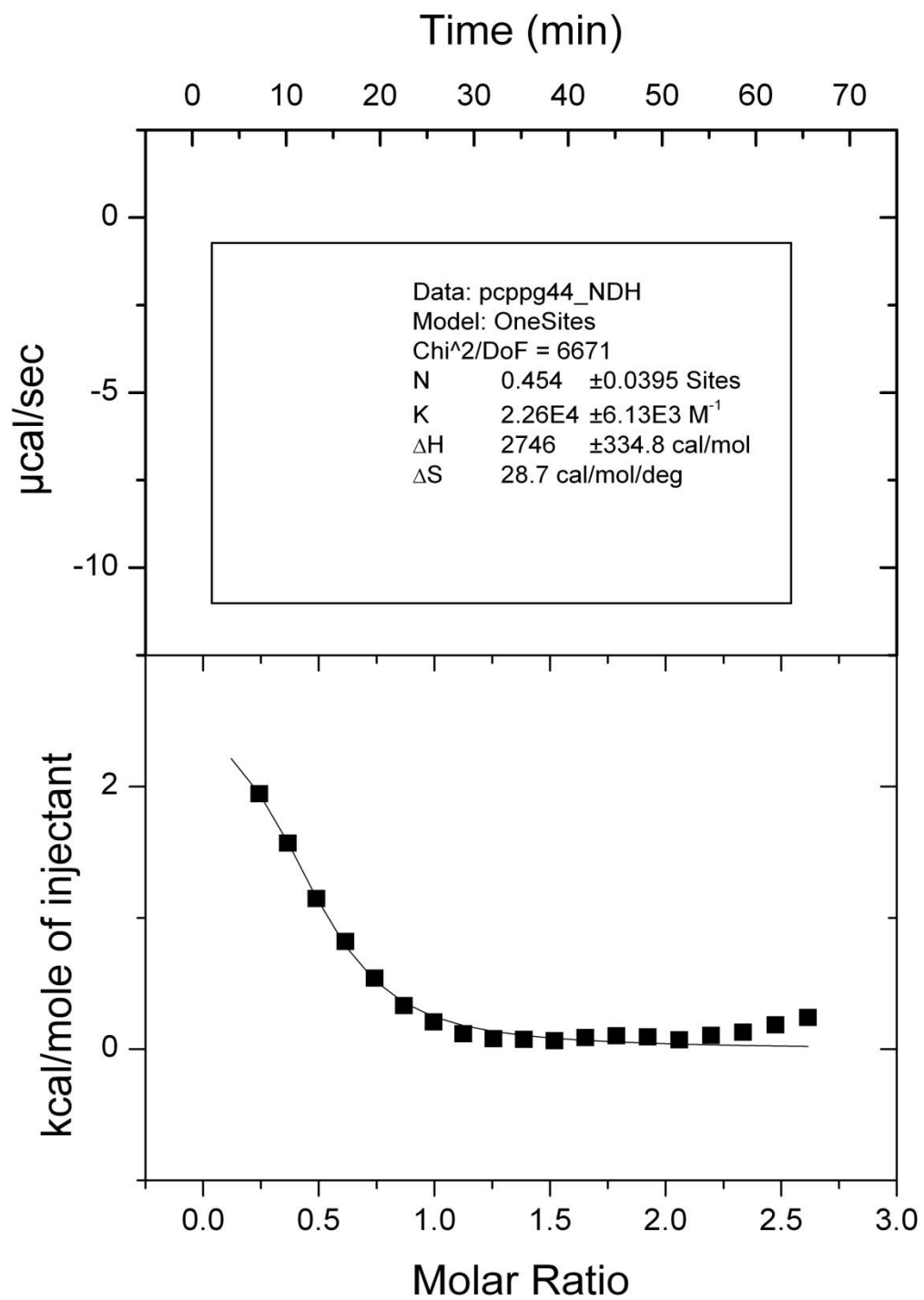


Figure 117. ITC data for compound **47** with PPG anion

APPENDIX A (continued)

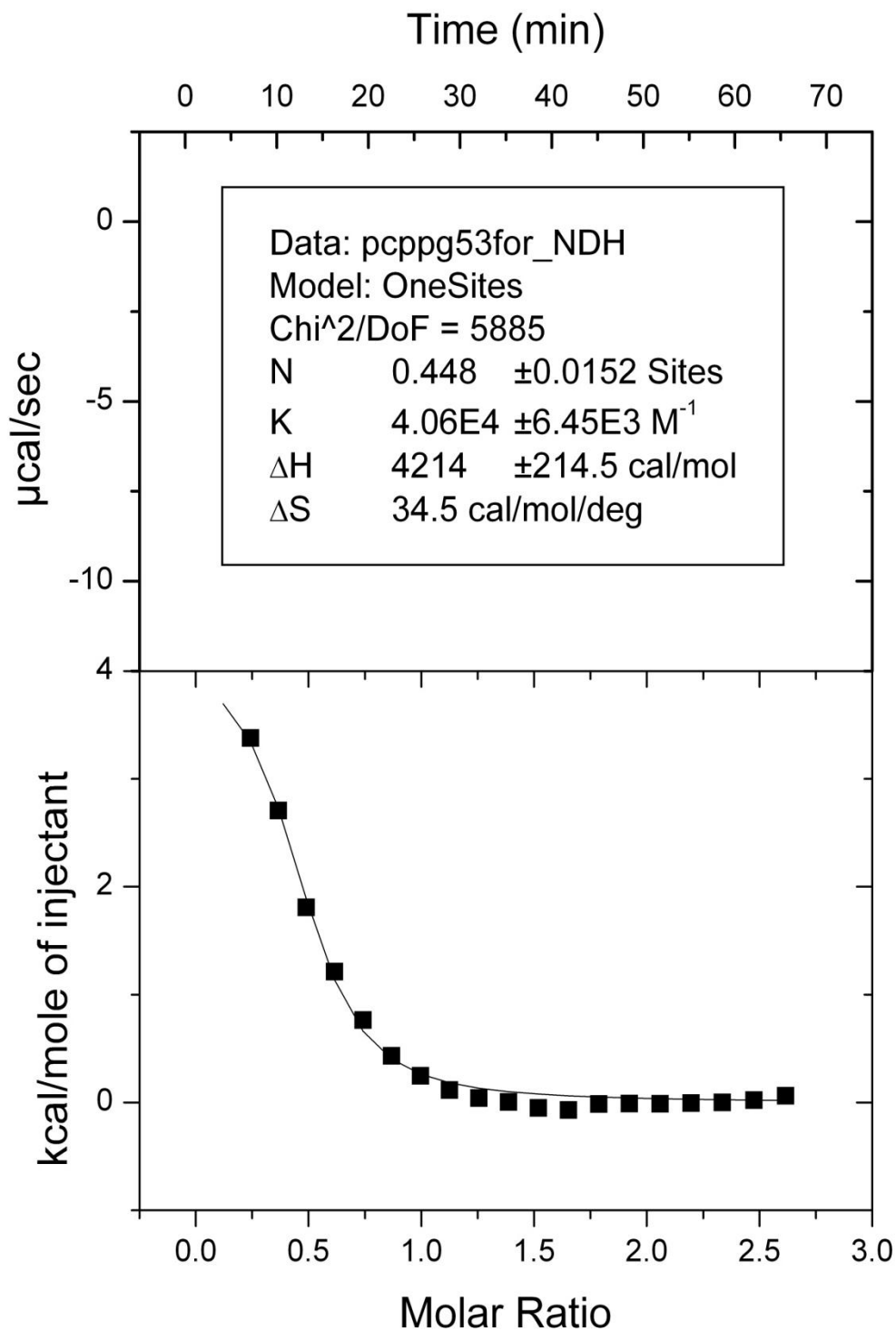


Figure 118. ITC data for compound **54** with PPG anion

APPENDIX A (continued)

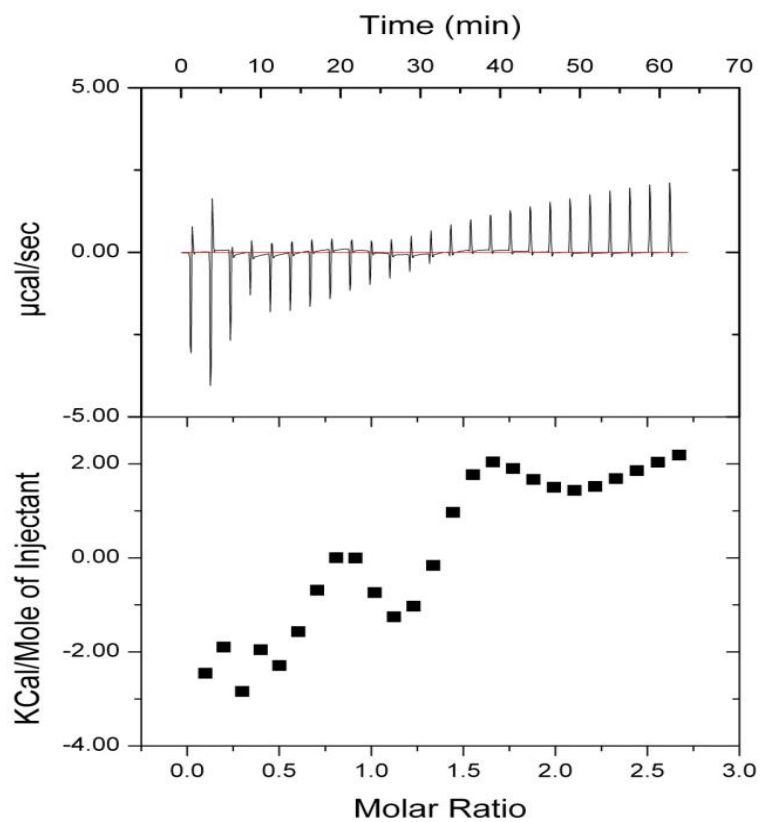


Figure 119. ITC data for compound **57a** with PPG anion

APPENDIX A (continued)

Crytallographic data

For the X-ray structures, crystals were selected under a polarizing microscope, affixed to a nylon cryoloop (Hampton Research) or glass filament using oil (Paratone-n, Exxon), and mounted in the cold stream of a Bruker Kappa – ApexII area detector diffractometer. The temperature at the crystal was maintained at 150 K using a Cryostream 700 EX low – temperature apparatus (Oxford Cryosystems). The unit cells were determined from the setting angles of the reflections collected in 36 frames of data. Data were measured using graphite mono-chromated molybdenum K_{α} radiation ($\lambda = 0.71073 \text{ \AA}$) collimated to a 0.6 mm diameter and a CCD detector at a distance of 50 mm from the crystal with a combination of phi and omega scans. A scan width of 0.5 degrees and scan time of 10 seconds were employed. Data collection, reduction, structure solution, and refinement were performed using the Bruker Apex2 suite (v2.0-2).¹ All available reflections to $2\theta_{\max} = 52^{\circ}$ were harvested and corrected for Lorentz and polarization factors with Bruker SAINT (v6.45).² Reflections were then corrected for absorption, interframe scaling, and other systematic errors with SADABS 2004/1.³ The structures were solved (direct methods) and refined (full – matrix least – squares against F^2) with the Bruker SHELXTL package (v6.14-1).⁴ All non – hydrogen atoms were refined using anisotropic thermal parameters. Hydrogen atoms were included at ideal positions and were not refined.

1. APEX2 User Manual, Bruker AXS, Madison (USA), **2005**.
2. SAINT Software Reference Manual, Verson 4, Bruker AXS, Madison (USA), **1994 – 1996**.
3. Sheldrick, G., SADABS (Version 2.03), University of Gottingen, Germany, **2002**.
4. SHELXTL, Reference Manual, Version 5.1, Bruker AXS, Madison (USA), **1997**.

APPENDIX A (continued)

TABLE 13.

CRYSTALLOGRAPHIC DATA TABLE

Compound	45-BF₄⁻ (Figure 18)	45-PF₆⁻ (Figure 19)	45-H₂PO₄⁻ (Figure 33)
Empirical formula	C ₂₆ H ₄₀ B ₂ F ₈ N ₂ O ₂	C ₂₆ H ₄₀ F ₁₂ N ₂ O ₂ P ₂	C ₂₇ H ₄₂ Cl ₃ N ₂ O ₁₀ P ₂
Formula weight	586.22	702.54	754.98
Temperature	150 K	150 K	150 K
Wavelength	0.71073 Å	0.71073 Å	0.71073 Å
Crystal system	Orthorhombic	Monoclinic	Monoclinic
Space group	Pbca	P2 ₁ /c	C2/c
Unit cell dimensions	a = 10.7360(11) Å	a = 10.272(8) Å	a = 30.780(3) Å
	b = 18.2224(18) Å	b = 34.671(16) Å	b = 12.9394(13) Å
	c = 29.732(3) Å	c = 8.925(3) Å	c = 23.090(4) Å
	α = 90°.	α = 90°.	α = 90°.
	β = 90°.	β = 96.19(5)°.	β = 130.712(5)°.
	γ = 90°.	γ = 90°.	γ = 90°.
Volume	5816.7(10) Å ³	3160.0 Å ³	6970.6(16) Å ³
Z	4	4	8
Density (calculated)	0.669 Mg/m ³	1.477 Mg/m ³	1.439/m ³
Absorption coefficient	0.059 mm ⁻¹	0.236 mm ⁻¹	0.469 mm ⁻¹
F(000)	1232	1456	3160
Crystal size	0.35 x 0.15 x 0.13 mm ³	0.124 x 0.134 x 0.256 mm ³	0.151 x 0.172 x 0.088467 mm ³
Theta range for data collection	2,34 to 26.00°.	2.08 to 26°.	3.06 to 26.00°.
Index ranges	-7<=h<=13, -22<=k<=20, -36<=l<=36	-12<=h<=12, -38<=k<=42, -11<=l<=11	-37<=h<=37, -15<=k<=15, -28<=l<=28
Reflections collected	40069	22667	105274
Independent reflections	5704 [R(int) = 0.2472]	6202 [R(int) = 0.2432]	6829 [R(int) = 0.1027]
Completeness to theta = 26.00°	99.7 %	99.8%	99.8 %
Data / restraints / parameters	5704 / 0 / 364	6202 / 0 / 436	6829 / 0 / 394
Goodness-of-fit on F ²	1.002	1.013	1.128
Final R indices [I>2sigma(I)]	R1 = 0.0613, wR2 = 0.1324	R1 = 0.0683, wR2 = 0.0602	R1 = 0.0828, wR2 = 0.1878
R indices (all data)	R1 = 0.2080, wR2 = 0.2084	R1 = 0.2847, wR2 = 0.0886	R1 = 0.1557, wR2 = 0.2482
Largest diff. peak and hole	0.294/ -0.285 e.Å ⁻³	0.254 / -0.273 e.Å ⁻³	0.703 / -0.821e.Å ⁻³